Biaryl ether formation on peptides to access bridged cyclopeptide natural product scaffolds

Zur Erlangung des akademischen Grades eines
Doktors der Naturwissenschaften
(Dr. rer. nat.)
von der Fakultät für Chemie
der Universität Dortmund
angenommene

DISSERTATION

von

D.E.A (M.Sc.)

Bahar Kilitoglu

aus Malkara/Türkei

Dekan: **Prof. Dr. Heinz Rehage**
1. Gutachter: **Prof. Dr. Herbert Waldmann**
2. Gutachter: **Prof. Dr. Martin Engelhard**

Tag der mündlichen Prüfung: 21.12.2009

Die vorliegende Arbeit wurde unter Anleitung von Dr. Hans-Dieter Arndt am Fachbereich Chemie der Technischen Universität Dortmund und am Max-Planck-Institut für molekulare Physiologie, Dortmund, in der Zeit von 1 November 2004 bis 31 Juni 2009 angefertigt.

Dedicated to my Joa, mom, dad and my brother

The important thing is not to stop questioning,
curiosity has its own reason for existing

Albert Einstein

Contents

1. Background & Objectives

Exploring nature as a source of novel agents is a validated approach for uncovering bioactive small molecules[1]. Innovative molecular entities inspired by bioactive natural product leads or by utilizing natural product scaffolds are a cornerstone of modern synthetic chemistry and chemical biology. Natural product serves several important purposes in chemistry and biology. On the one hand, synthetic and semi-synthetic natural product-derived molecules provide key tools to study biological processes and to discover or validate new biological modes of action. Therefore, syntheses of compounds collections based on natural products can be a good starting point to rationally explore the chemical space necessary to address biological targets.[2,3] On the other hand, natural product lead structures propel constant advancement of synthetic methods or strategies for making them accessible. Recent advancements in synthetic strategies on solid supports have allowed the generation of diverse natural product collections by giving access to diverse target structures in a parallel and automatized manner.[2] Using these methodologies, large peptide libraries can be readily assembled from amino acids (proteogenic and non proteogenic), to synthesize linear and cyclic peptides which may display a broad biological activity spectrum ranging from antibiotic[4] to antitumor[5] activity.

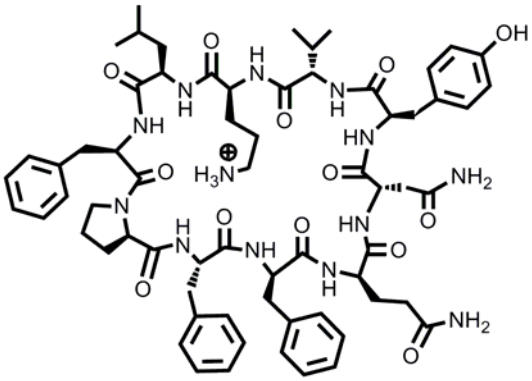

Tyrocidine A

Figure 1 Tyrocidine antibiotic drug.

Alternatively, integrated methods for accessing natural product derivatives have been also described. An example of a chemical biology strategy to obtain natural product based libraries was recently reported by Walsh *et al.*[6] for the synthesis of the non-ribosomal, cationic cyclopeptide tyrocidine A[a] and its analogs. Their biomimetic approach fostered linear solid phase peptide synthetic methodologies together with biosynthetic enzymes for macrocycle formation. Using this combination, a diverse natural product library of tyrocidine A analogs could be obtained and their antimicrobial activity was evaluated. Furthermore, apart from establishing new synthetic methodologies, total synthesis[7] and diverted total synthesis[8] provide also diverse structures based on natural products in order to elucidate mechanism of action and to find new drug candidates.

[a] Tyrocidine A has the sequence cyclo(DPheProPheDPheAsGlnTyrValOrnLeu) in which the ornithine (Orn) residue provides basic cationic side chain.

Peptides natural products (linear or cyclic peptides) form one major class of secondary metabolites together with carbohydrates (glycosides, polysaccharides, etc.), lipids (fatty acids, steroids, phospholipids, terpenoids), and nucleic acids (DNA, RNA, etc.). One representative example is cyclosporine,[9] a cyclic non-ribosomal peptide containing 11 amino acids isolated from a fungi in 1970, which is widely used as immunosuppressant drug to prevent organ rejection in transplant patients.

In contrast to linear peptides, cyclic peptides generally own privileged conformations that predispose the molecules to adopt a particular, well defined 3-dimensional structure. This offers advantages to identify or optimize biological activity in specific targets, for example by studying biomolecule-molecule interactions. Additionally, they are more resistant to proteases than their linear analogs, show increased serum stability and therefore improved pharmacokinetic properties. The combination of these factors makes cyclic peptides useful core structures and tools for drug discovery. Accordingly, cyclic peptides have been isolated or synthesized and tested as specific ion binders,[10] anticancer agents,[5] protease inhibitors,[11] antibiotics,[4] receptor antagonists[12] and artificial receptors.[13]

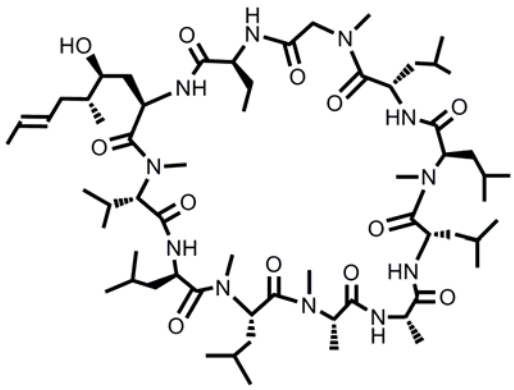

Cyclosporine

Figure 2 Cyclosporine (Sandimmune®) Immunosuppressant drug by Novartis.

Two biosynthetic pathways for obtaining cyclic peptide natural products have been described in microorganisms. One proceeds *via* multienzymes complexe (nonribosomal peptide synthesis, NRPS),[14] the other one uses the ribosome as a machinery to execute the production from a gene-encoded RNA template (Ribosomal protein synthesis- RPS).[15,16] Both are typically completed by post-assembly modifications where the cyclization may occur. Many bioactive natural products with a cyclopeptide structure contain additionally heterocyclic structures such as thiazoles, oxazoles, lactams as well as biaryl briged motives as one of the common features. (Scheme 1).

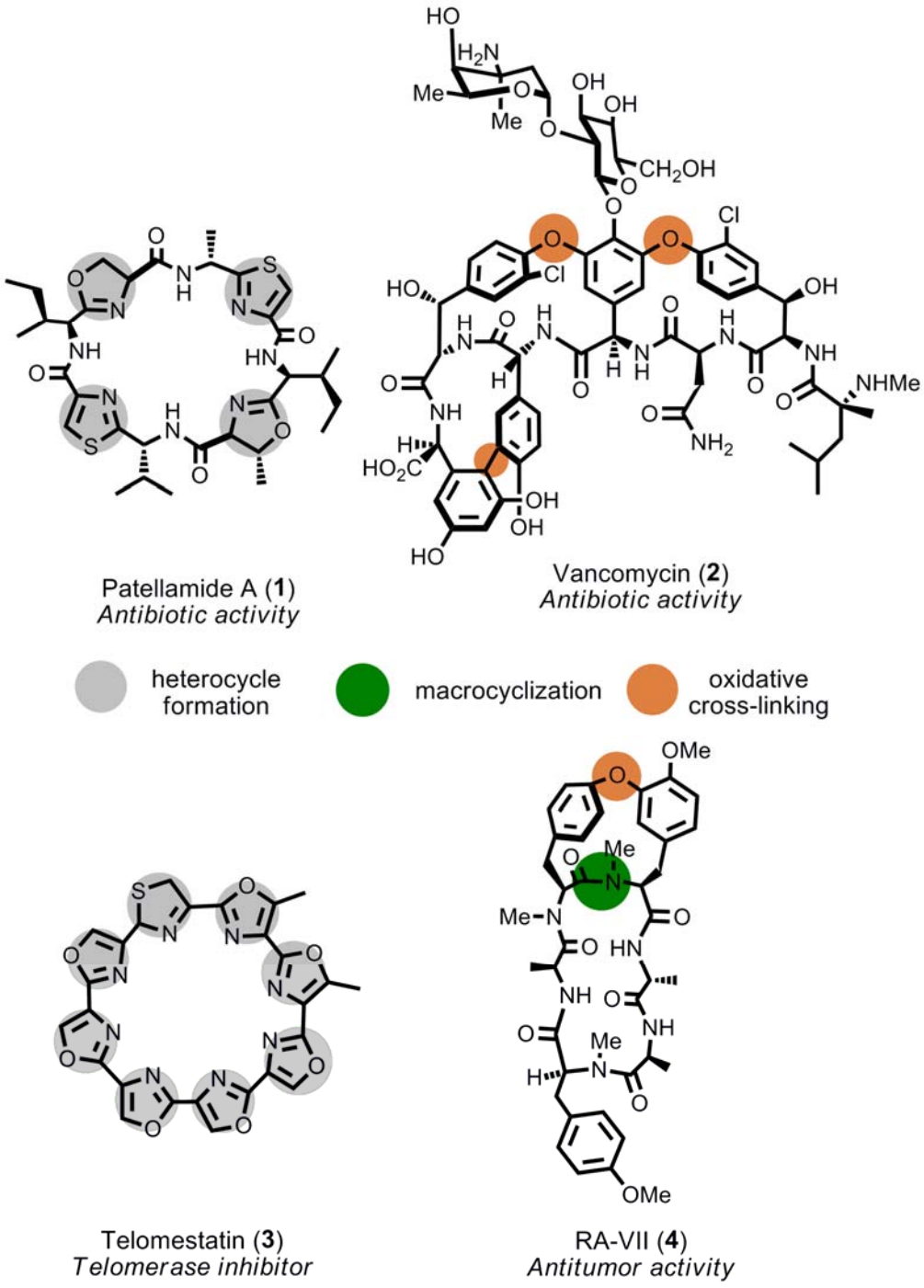

Scheme 1 A selection of ribosomally and non-ribosomally synthesized peptide natural products. Characteristic structural features confer rigidity to the peptide backbone.

These substructures produced in microorganisms such as bacteria, fungi, cyanobacteria or higher organisms such as plants or marine invertebrates are specific elements for molecular recognition and render the molecules more lipophilic and drug-like.

Selected structures of ribosomally and non-ribosomally synthesized natural products and their characteristic structural features are presented in Scheme 1. For example, patellamide A[17] (**1**) is a RPS product with antibiotic activity, the clinically used vancomycin[18] (**2**) is a NRPS natural product with strong antibiotic activity against gram positive bacteria. Telomestatin[19] (**3**), identified as a telomerase inhibitor, is possibly produced by RPS, however its biosynthesis is not yet documented.

Structural rigidity of the cyclic secondary metabolites is achieved by macrocyclization, heterocyclization or cross-linking, which endows the structure of a plain peptide backbone with a new level of uniqueness. It can be assumed that all these constrained rigid structures ensure the bioactivity by their specific interaction with the dedicated molecular target. This is the case for the lantibiotics,[20] peptide antibiotics containing polycylic thioether amino acids that have gain interest in food industry due to their possible use as a food preservative.

Another example of a cyclic peptide containing heterocyclic substructure is RA-VII (**4**) Scheme 1, which was extracted from the roots of the indian madder (*Rubia cordifolia).*[21] This plant has been used as remedy for regulation of high blood pressure in traditional medicine. RA-VII (**4**) is thought to be a NRPS product due to the presence of several *N*-methylated tyrosines, but the exact biosynthetic origin of the natural product is unclear to date. Recent developments in the cloning and sequencing of genes of higher organisms previously believed to produce marines natural products[17] indicate that at least some of the isolated secondary metabolites are not produced by higher organism but synthesized by symbiotic bacteria. The most important structure features of RA-VII (**4**) are two cyclization points together with a biaryl bridge motive that force a specific conformation and may have a critical role in the biological activity.[22] RA-VII (**4**) is a micromolar inhibitor of ribosome,[23] but further data on its mode of action is not available. Therefore, RA-VII (**4**) may be a highly promising lead scaffold to develop tool compounds to elucidate the ribosome function, and in extension for development of small molecules addressing RNA-protein complexes. Furthermore, its structural features should allow the development of innovative chemistry for making non-canonical cyclopeptide scaffolds accessible. Progresses toward these goals are described in the following chapters.

2. Introduction

Leading motif of this work was to develop a new synthetic strategy for bicyclic hexapeptide, RA-VII (**4**) which has gained increasing interest during the past decades as a potentially relevant molecule for cancer therapy.

2.1 Naturally occurring bicyclic peptides

Naturally occurred cyclic peptides possess diverse structural topologies ranging from monocyclic, over bicyclic to structurally complex polycyclic glycopeptide antibiotics. According to their cyclic core, they can be classified into several structural categories. Most of them can be seen in Scheme 2. Briefly a head-to-tail cyclized peptide may be further rigidified by cross-linking the backbone with an amide bond formation between carboxyl and amine groups to form structures of type **I**. Furthermore, an additional peptide sequence or a non-peptidic linker can connect the side chain to construct a linkage of type **II** or **III,** respectively. Alternatively, a disulfide bond between two Cys residues can create the bicyclic structure **IV**, or two head-to-tail cyclized peptides may be linked by an amide or disulfide bond (**V**). Additionally, two pairs of side-chain functionalities may be pairwise connected with amide or disulfide bonds (**VI**) or two side chain of cyclized monocyclic peptides can be connected by disulfide bridge **VII**.[24]

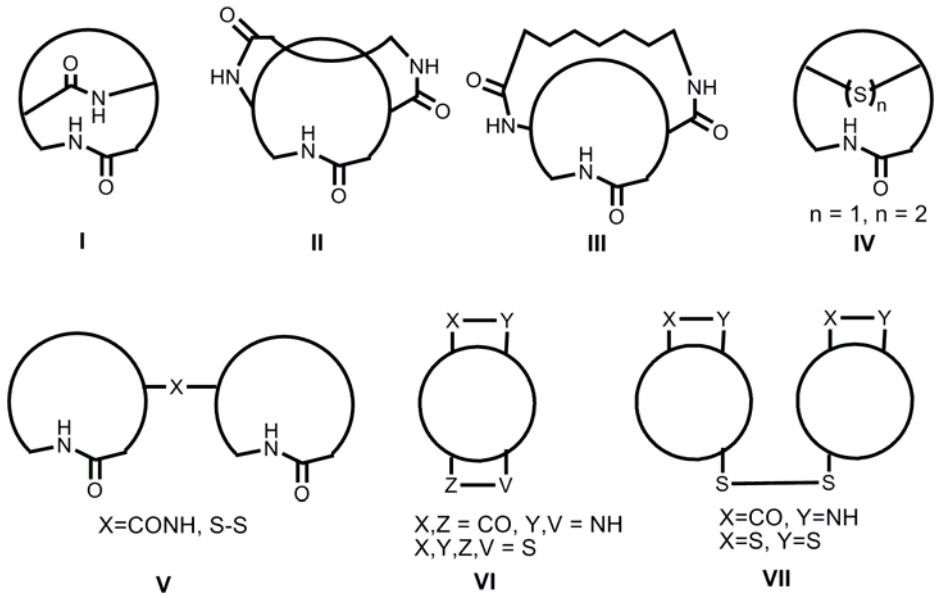

Scheme 2 Schematic presentation of different categories of natural and unnatural bicyclic structures with reported biological activity in the literature.

These macrocycles have characteristic feature such as limited conformational freedom which plays an important role on their biological activity. Furthermore, they pose a challenge for synthetic organic chemistry. Towards their synthesis advanced

levels of protecting group strategy are typically taken into account to ensure the desired regioselectivity of sequential cyclizations. Synthetic, semi-synthetic, or combined approaches can lead such type of structures. Apart from this cyclic core structure, additional linkages, such as biaryl or biaryl ether linkages, can be found in several naturally occurring bioactive compounds. One example of this is the antibiotic vancomycin (**2**), a privileged polycyclic glycopeptide that features a biaryl ether bridged structure. Vancomycin (**2**) targets bacterial cell wall biosynthesis in Gram positive bacteria and is usually considered as a drug of last resort. However, acquired resistance to vancomycin (**2**) due to a mutation on the target structure of the bacterial cell wall is a growing problem. Because of that, the interest on this antibiotic has increased in the last times and other antibiotics are needed to overcome bacterial resistance.

A member of the lantibiotic[20] class, ancovenine (**5**),[25] has been reported to be an inhibitor of the angiotensin converting enzyme and hence may be used for the treatment of hypertension.

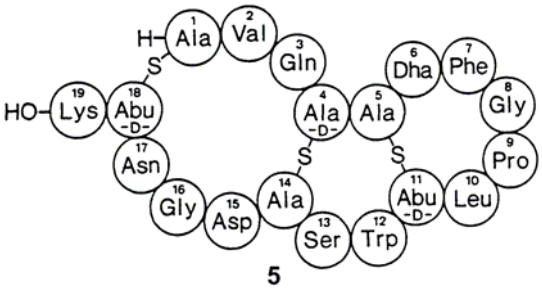

Figure 3 Ancovenine

In summary, cyclic peptide natural products are important bioactive sources. Their mode of action is linked to provide by specific interactions with their rigid features. Developing new synthetic methodologies for accessing such scaffolds as well as for studying their biological activity and their mode of action in more detail is an stimulating research field in chemical biology.

2.2 Biaryl ether containing cyclic natural products

2.2.1 Biaryl ethers and bioactivity

Biraryl ethers are privileged structures which are sometimes found in peptides and proteins. Typically two tyrosines joined by a biaryl ether bridge *via* phenolic oxidation give rise to an isodityrosine substructure.[26,27] In natural products, biaryl ether containing macrocycles contain isodityrosine substructures. Isodityrosine (**6**) as the smallest member of this class of natural products was isolated from plant[b] cell wall glycoprotein.[28] It was suggested that isodityrosine is an inter-polypeptide cross-link responsible for the hydrophobicity of this cell wall constituent.[29] Naturally occurring biarylethers show similar patterns containing *meta-para* or *para-meta* linkage between two tyrosines, with ensuing diverse biological activity. Relevant examples of biaryl ethers in biologically active natural products encompass bastadin 5 (**9**), which was isolated from marine sponges *Ianthella basta*[30-32] and is a potent Ca^{2+} channel receptor agonist (RyR1/FKBP12). It presents a *meta-para* substituted isodotyrosine. Piperazinomycin (**10**) isolated from *Streptoverticilium olivoreticuli* subsp. *neoenactius* is known as antimicrobial and antifungal agent and also presents an isodityrosine with *meta-para* substitution. OF4949-II (**8**) is an aminopeptidase B inhibitor[33] which has an isodityrosine containing *meta-para* substitution. It was isolated from the culture growth of the fungus *Penicilium rugulosum.* As another example, K-13 (**7**) was isolated from *micromonospova halophytica* subsp. *exilisia K-13*[34] and shows inhibitory effects on the angiotensin I converting enzyme (ACE). Contrary to the others, K-13 has a *para-meta* substitution (Scheme 3). Pharmacophore studies for K-13 (**7**) and OF4949-II (**8**) were undertaken by Boger *et al.*[35] All these cyclic 17-membered biaryl ether tripeptides contain the isodityrosine as their basic structural pharmacophore unit, but with a different substitution pattern (**7** and **8** dashed boxes in Scheme 3).

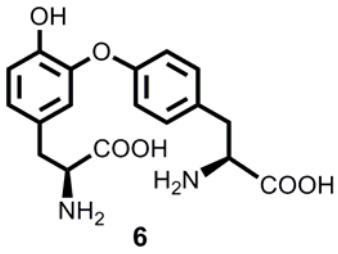

6

Figure 4 Isodityrosine

[b] Cell-suspension cultures of potato (*Solanum tuberosum*)

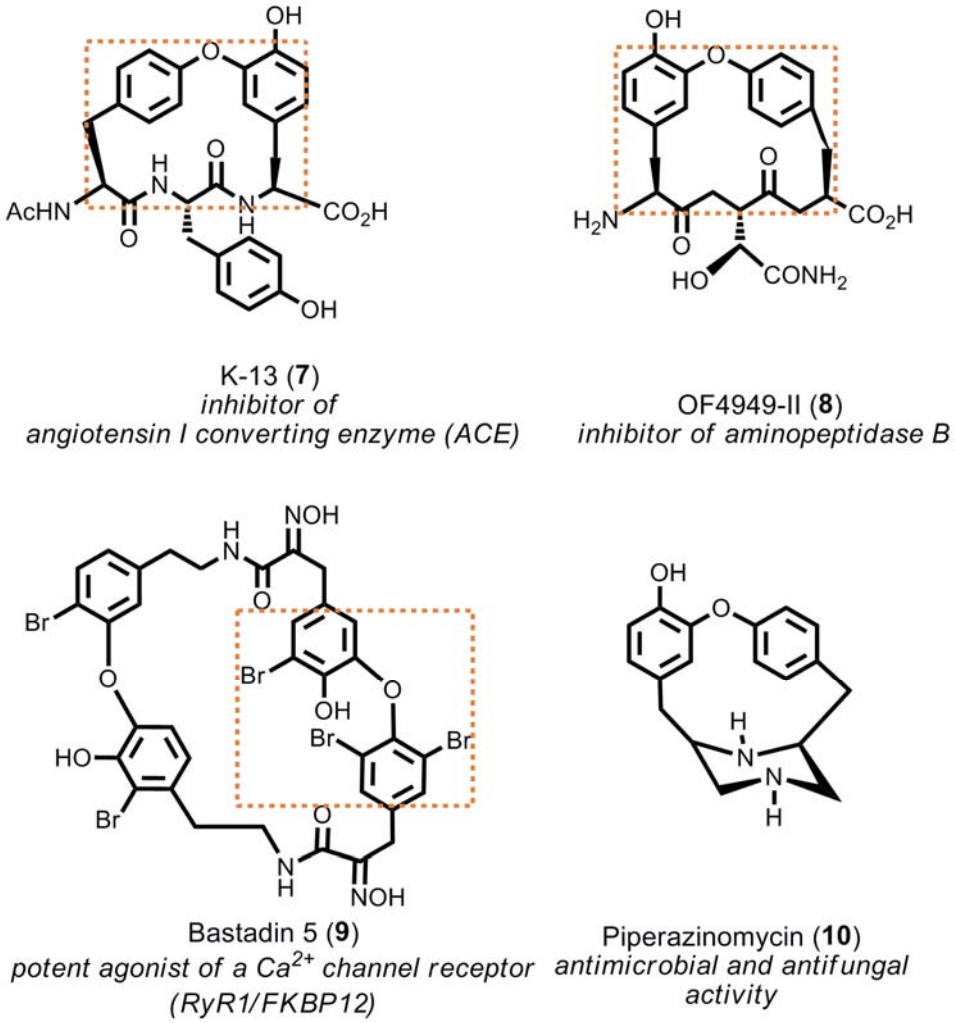

Scheme 3 Selected biaryl ether containing cyclic natural products. Dashed boxes illustrate suspected pharmachopore units.

The glycopeptides antibiotic vancomycin (**2**) also contains two *para-meta* biarylether subunits. Vancomycin (**2**) was shown to exert its main antibacterial effect through inhibition of cell wall cross-linking by binding to the D-Ala-D-Ala terminus of the peptidoglycan precursors through a network of five hydrogen bonds.[36] Several studies in the literature have documented structure activity relationship (SAR) studies data. Simplified analogs, where only one biaryl ether moiety was retained, showed decreased activity against both sensitive and resistant bacterial cell line.[18,37] It seems that despite the isodityrosines are not making a direct contact with the binding site, they donate molecular rigidity which most likely improves the interaction between D-Ala-D-Ala terminus of the peptidogylcan binding pocket and the glycopeptide. (Figure 5).

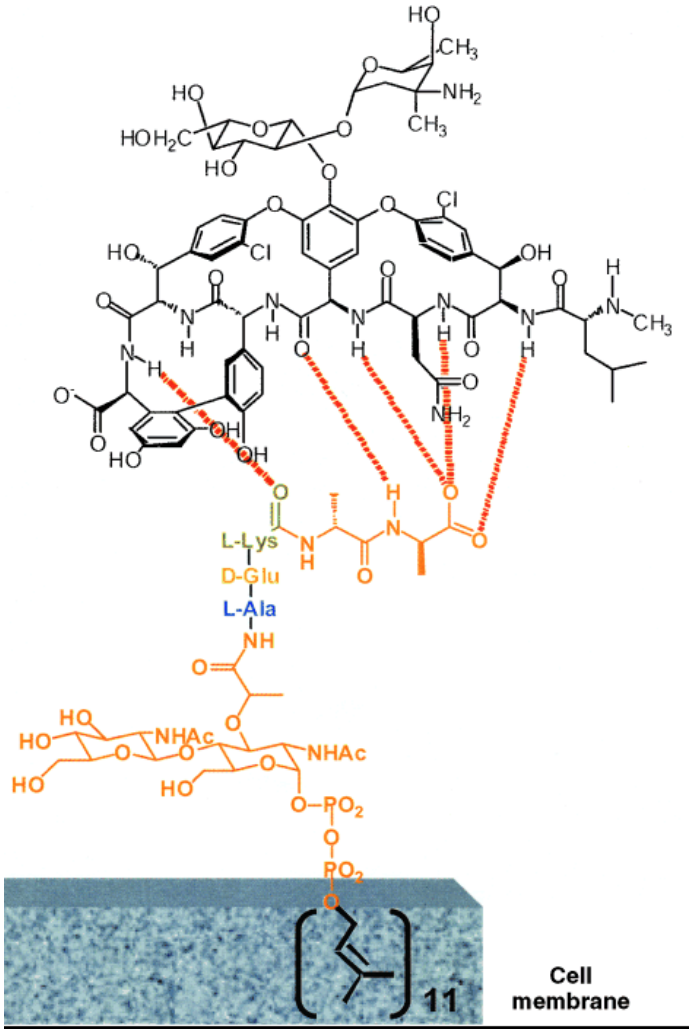

Figure 5 Hydrogen bonding in the interaction of vancomycin (**2**) with a cell wall biosynthesis intermediate. Picture from reference [38].

The marine natural product bastadin 5 (**9**) features two *para-meta* biaryl ether motifs in the structure. Due to their ability to interact with a Ca^{2+} channel receptor (RyR1), they are considered as useful chemical probes for studying signaling in neurons.[39] It was shown that the simplified cyclic analog **11** containing only one isodityrosine unit still retained activity.[40] Recently, another open chain analog **12** was demonstrated to mimic the effects of bastadins on Ca^{2+} channel regulators in cultured neurons.[39] Both studies indicated that the biaryl ether part (east or west) of the bastadin 5 (**9**) is responsible for the biological activity, which seems to be linked to the bromine substitution pattern in the aryl rings.

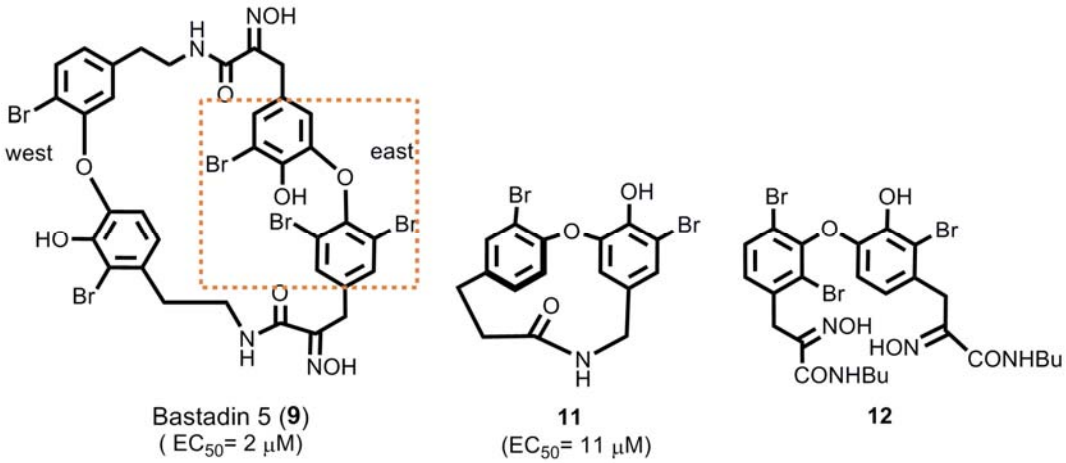

Scheme 4 Simplified bastadin derivatives

The plant natural product RA-VII (**4**) harbours a *para-meta* biaryl ether which was assigned as pharmacophore by Boger *et al.*[41] during an evaluation of synthesized partial structures. Compounds without the biaryl ether linkage showed a complete loss of cytotoxic effects on leukemia cells (L1210 cells, > 100 μg/mL) (**15** and **16**) while analogs containing the isodityrosine subunit retained some activity (10-50 μg/mL).

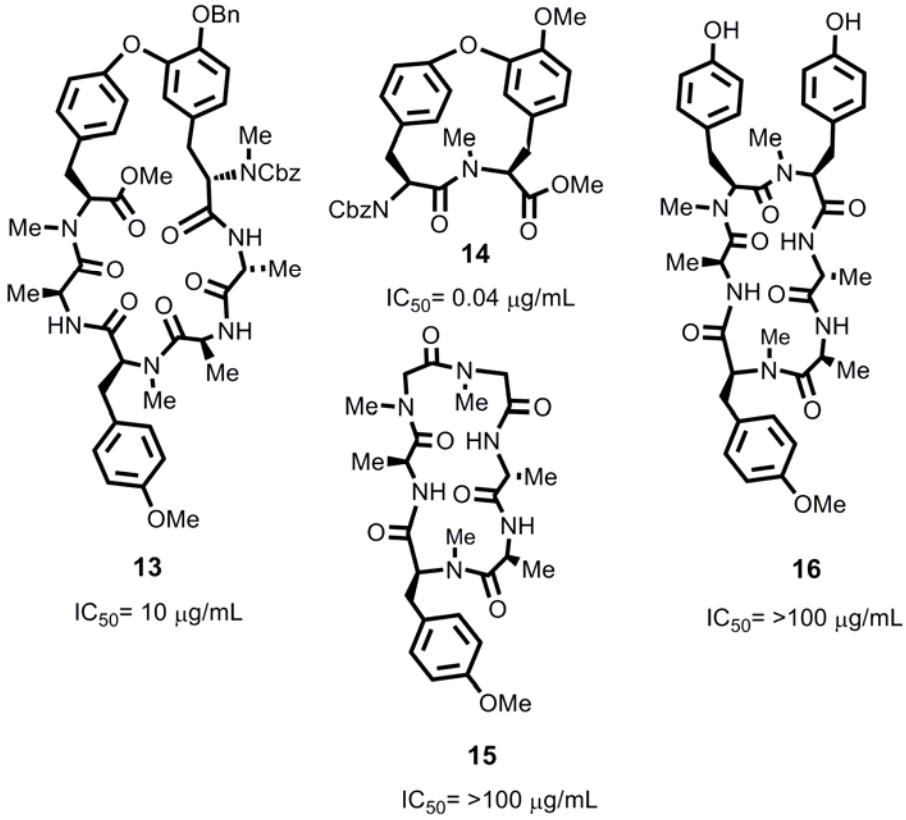

Figure 6 Simplified RA-VII (**4**) analogs and IC_{50} values in L1210 cells.

The cyclic isodityrosines **14**, showed improved activity (0.04 μg/mL) compare to the macrocyclic analog **13** (10 μg/mL) lacking transannular amide bond linkage. Furthermore, **16** lacking biaryl ether bridge and **15** lacking 14-member ring analogs were inactive up to >100 μg/mL concentration. These data indicate that the cyclic structure containing the biaryl ether bridge is very important for retaining biological activity. RA-VII (**4**) was the most potent compound in the series (IC_{50} = 0.002 μg/mL), showing the importance of the bicyclic structure.

Typically, biarylethers can rotate freely and show no stereoisomerism. However, when sterically demanding groups are present or when constrained rings are formed, they can exhibit atropisomerism just as biphenyls. This is the case in vancomycin where *ortho*-substituted biaryl ethers join a pair of hindered planar groups.[18,37] The identification and the synthesis of streochemically pure atropisomeric biaryl ethers is still a demanding field. The potential atropisomerism in poly-substituted acyclic biaryl ethers such as the ones belonging to the bastadin family (**9**) are not well understood. Clayden *et al.*[42] showed that highly substituted biaryl ethers can exhibit atropisomerism as soon as both rings are unsymetrically substituted and at least one of the *ortho*-substitute is bigger than *t*Bu. Furthermore, they showed that atropisomerism depends more on the substitution pattern than on the number of substituent present on the aryl rings. Recently, the same group was able to control the atropisomerism and enantioselectively synthesize a biaryl ether by incorporating *ortho* substitution with a chiral sulfoxide substituent.[43]

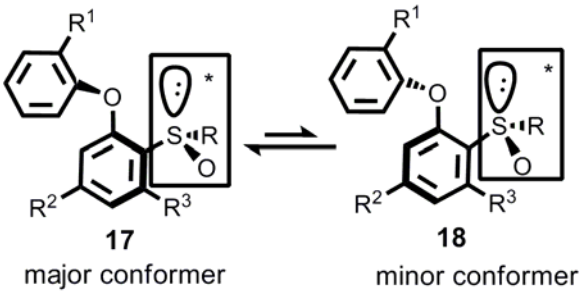

Scheme 5 A strategy employed by Clayden *et al.* for the synthesis of atropisomeric biaryl ethers under thermodynamic control.[43]

Introduction of a bulky alkyl sulfinyl substituent *ortho* to the C-O axis of a biaryl ether imposes a powerful conformational preference (Scheme 5). Further oxidation of the sulfoxide to a sulfone freezes the dynamic thermodynamic resolution of the atropisomeric ether towards the major conformer. This is the first enantioselective synthesis of an atropisomeric biaryl ether which is not part of a constrained macrocyclic ring.

2.2.2 Biosynthesis of biaryl ethers

In natural products, biaryl ethers are typically expected to be generated by oxidative coupling of phenols, catalyzed by heme proteins.[27,44] As an example for the biosynthesis of biaryl ethers, steps of the well-studied non ribosomal synthesis of vancomycin (**2**) are sketched in Scheme 6.[38] The reaction is carried out most probably by a radical mechanism and is catalyzed by three different oxidases (oxyA, oxyB, oxyC) each of which is responsible for one birarylether or biaryl cross linking event. The iron atom in the active site of each heme-based oxydase (**20**) is presumed to mediate the transfer of one electron from the two rings being cross-linked to the co-substrate O_2 for each generated cross link (**24**). The regio- and stereochemistry of the radical couplings are probably guided by the enzymatic binding pocket. The folding requirements of the linear peptide chain to initiate folding in the active site of the first heme protein oxydase is not known yet, but the chloro substituent on the *ortho* position may provide sufficient steric constraint for selecting one particular conformers. Cross coupling is initiated with one-electron oxidation of the electron-rich phenolic rings of **24**. Scheme 6 shows a possible route for formation of the aryl ether linkage (**26**).

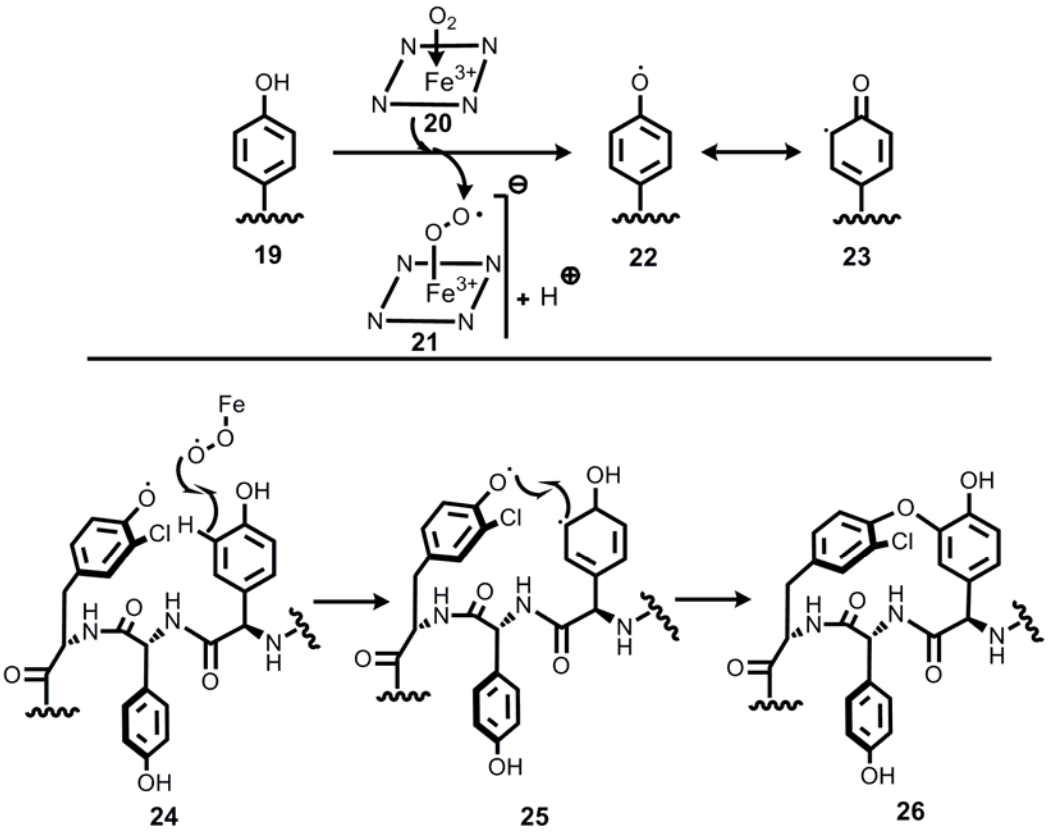

Scheme 6 Proposed biosynthesis of biaryl ether moiety in vancomycin biosynthesis.[38]

2.2.3 Chemical synthesis of biaryl ethers

2.2.3.1 Introduction

Biaryl ethers are an important class of organic compounds in life science and in polymer industry, and therefore several synthetic methods leading to these structures have been developed.[26-29] However, most of them are using harsh conditions such as tempratures > 100 °C in the presence of a strong base that may not be compatible with every substrate. Thus sensitive target molecules can be hard to synthesize. Both the synthesis of highly functionalized biaryl ethers and the large scale preparation of polymers for the industrial application remains a challenging task.

The condensation between phenols and aryl halides suffers from poor nucleophilicity of phenoxides and low reactivity of aryl halides. Therefore, the electronic properties of the substrates and different substitution patterns have a high impact on the ease of preparation of biaryl ethers.

In general, potential synthetic access to biaryls can be summarized as in Figure 7. The substitution pattern of both coupling partners play a vital role on the reactivity. Increasing the nucleophilicity of the phenol **29** and generating a mild but efficient activation for the coupling partner **28** (aryl halides, boronic acids etc.) needs to be investigated. Furthermore alternatives to high temperatures and long reaction times should be found. Mild conditions are necessary in order to prevent racemization of acidic α–CH protons in amino acids. Typically, each substrate class requires extra optimization due to electronic effects of aromatic substitutions.

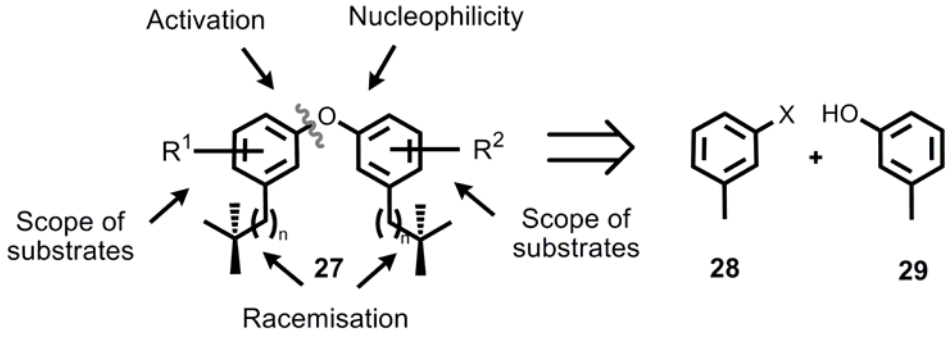

Figure 7 Important issues for the synthesis of biaryl ethers.

A number of approaches for the synthesis of biaryl ethers require special activation of the substrates. The poor reactivity of the coupling partner towards nucleophilic attack can be increased by introducing activating groups such as thioamides, NO_2, triazines

or quinones as substituents. Another possibility is using metal-aryl complexes or Cu or Pd catalyzed biaryl ether formation. Furthermore radical initiators, such as dications can also induce the transformation.[45] Some representative examples for the synthesis of biaryl ethers used in natural product synthesis or in industrial applications will be explained in more detail.

2.2.3.2 Nucleophilic aromatic substitution

Sodium phenoxides are typically sufficient as a nucleophile to react with activated aryl halides (*para*-phenyl carbonyl, phenylquinoxaline).[46] The method was applied for the biaryl ether linked polymer synthesis. Preparation of poly(arylethers)[46] **32** was achieved by refluxing aryl fluoride **31** and sodium phenoxides **30** in *N*-methyl-2-pyrrolidinone (NMP) The reaction proceed to the product by activation of both coupling partners by a *para*-carbonyl group. However removal of the phenacyl activating group by additional reaction steps renders this method less efficient.

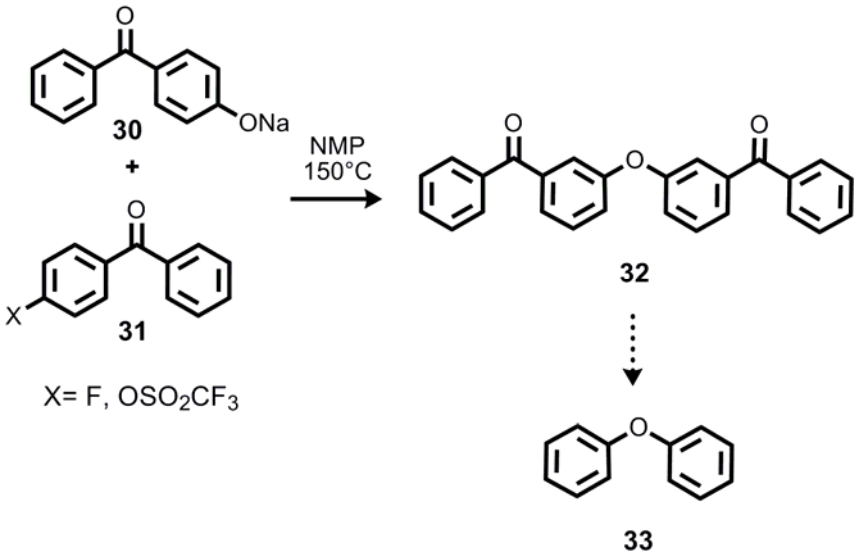

Scheme 7 Biaryl ether formation with *para*-phenylcarbonyl-activated phenoxylate and aryl fluoride/ aryl triflate.

A particularly popular method makes use of the *ortho*-activation of aryl halides by nitro groups or triazines. The metal free synthesis of biaryl ethers has been studied by Eicher and *al.*[47] Aryl-halides are activated by the *ortho*-nitro group **34** towards nucleophilic attack of phenoxides **35** in the presence of base and at elevated temperatures. (Scheme 8)

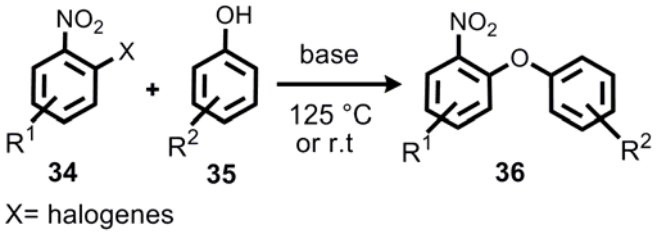

Scheme 8 Biaryl ethers by *ortho*-activation with NO_2 *via* S_NAr reactions.

Later on, this method has been applied to the synthesis of cyclic biaryl ethers.[48,49] By activating the phenol as phenoxide, the cross coupling was achieved under milder conditions. However, it requires subsequent reduction of the nitro group and deamination in order to remove the auxiliary group, unless it is present in the final product (**36**) (Scheme 8). The approach used by Nicolaou *et al.*[49] was similarly based on the activation of aryl halides. In this case a triazene-substituted aryl halide **37** was employed. The triazene was placed on the *ortho* position of the leaving group as a potential "electron sink". Phenol **35** is activated through coordination to Cu(I) to form a complex with aryl halide **39**. Further elimination of the leaving halogen atom **X** afforded biaryl ethers **38** in the presence of K_2CO_3 and $CuBrxMe_2S$ at 80°C in good yields[49] (Scheme 9). In following steps the triazene can be converted to phenols under acidic conditions. In a recalcitrant case, stepwise conversion had to be applied. First the triazene was reduced to the aniline by Raney Ni. Then diazotation followed by treatment with Cu(I)/Cu(II) and water gave the phenol **40**.[49]

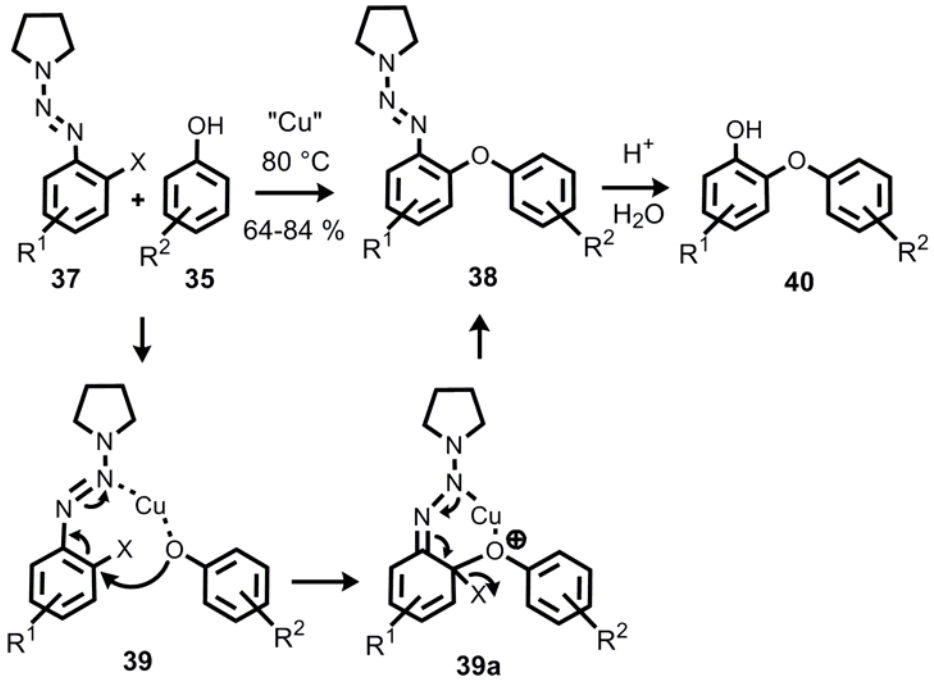

Scheme 9 Biaryl ethers by *ortho*-activation with triazene *via* SnAr.

Furthermore, iodinium salts[50] or benzoquinone salts[51] can also be coupled with phenoxide under high temperature to synthesize biaryl ethers. In general, aromatic substitution mediated by activating groups may be often an advantageous approach. In cases of differently functionalized molecules it may be necessary to explore other methods. For example, removal of an activating NO_2 group under the reductive conditions does not tolerate amine functionalities, but metal mediated methods do. A typical application of the method is presented in Scheme 10. Chloroarenes can be activated through the formation of aryl-metal π complexes (Mn, Fe, Ru) (**41**) with react with the phenol **42** at low temperature.[52]

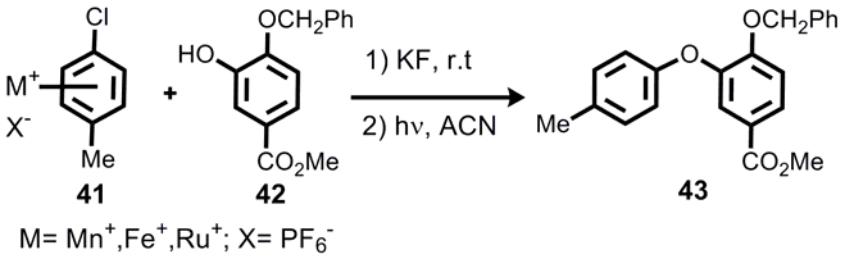

Scheme 10 Biaryl ethers by activated chloroarenes using metal π complexes.

2.2.3.3 Metal mediated cross coupling

The classical arylation method is a condensation of phenols or amines **45** with aryl halides (**44**) in the presence of powdered copper salts, which was discovered by Fritz Ullmann in the early 1900s.[53] It was a follow up discovery after the finding of the Ullman reaction between two aryl halides to form biaryls.[54] This reaction requires high temperature as a result of poor nucleophilicity of the phenoxides and low reactivity of aryl halides involved. The mechanism of this reaction remains unclarified to the date

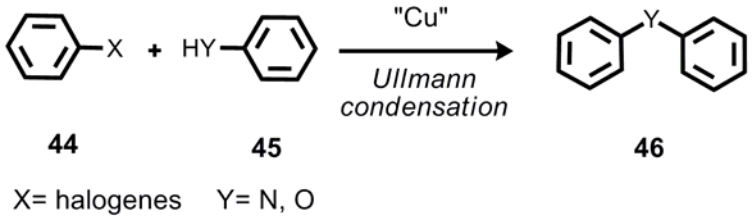

Scheme 11 Ullmann condensation for the synthesis of biaryl amines and biaryl ethers.

The Ullmann condensation was applied to total synthesis of natural products, however sensitive functional groups and stereogenic centers suffered under the harsh reaction conditions.[55,56] Improved synthesis in terms of substrate scope were achieved by Mann and Hartwig[57] and Buchwald *et al.*[58] Furthermore, the catalytically driven cross couplings mediated by Pd(0) were investigated by both groups. The cross coupling conditions achieve leaving group activation (**47**) by palladium-catalysis. Electron deficient aryl bromides react with the *in situ* generated complex of phenoxide and 1-1´-diphenylphosphanyl-ferrocene-Pd(0) afford the biaryl ether (**49**) as a cross coupling product. Later, Buchwald *et al.*[58] published an activation of phenol by cesium carbonate, which coupled with arylhalides in the presence of catalytic amount of Cu(I). A cuprate-like intermediate $[(ArO)_2Cu]^-Cs^+$ has been proposed to be the reactive species in this case. Although these methods improved biaryl ether synthesis in terms of reactivity of the substrates, the reactions still needed relatively high temperature, strongly basic conditions and long reaction times.

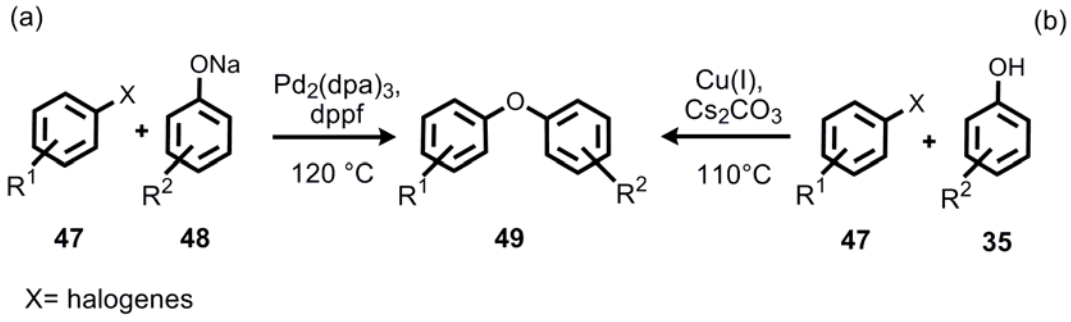

Scheme 12 Metal catalyzed biaryl ether synthesis.

In the late 90s, reports from the research groups of Chan *et al*.[59], Evans *et al.*[60] and Lam *et al*.[61] introduced a new form of copper-mediated heteroatom arylation for C-N and C-O bond formation. These groups showed that boronic acids (**51**) and phenols or amines (**50**) can form biaryl ethers (**52**) or amines in the presence of Cu(II) salts under oxidative atmosphere. This method applied tertiary amines as weak base, and no elevated temperatures were required. However the disadvantages of the method were long reaction times and stability issues of the costly boronic acids.

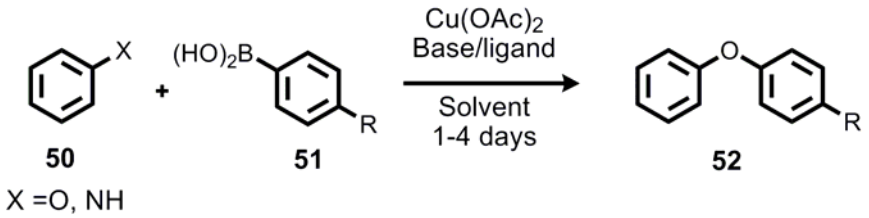

Scheme 13 *Chan-Evans-Lam* cross coupling.

The method found several applications in biaryl ether containing natural product synthesis.[62-64] An elegant example was reported by Decicco *et al.*[65] for the synthesis of macrocyclic biaryl ether as hydroxamic inhibitors of collaginases 1 and gelatinases A and B. In both cases, *Chan-Evans-Lam* conditions were the key step of the synthetic strategy which stages the intramolecular macrocyclization between boronic acid and phenol. A collection of macrocycles (**54**) was prepared effectively in a short synthetic route (6 steps) from boronic acid (**53**). The *ortho* hydroxy substituted boronic acids did not yield cyclic biaryl ether products under the reaction conditions. The reaction was found to proceed under sufficiently mild conditions to accommodate the chemical functionalities commonly present in peptidomimetics.

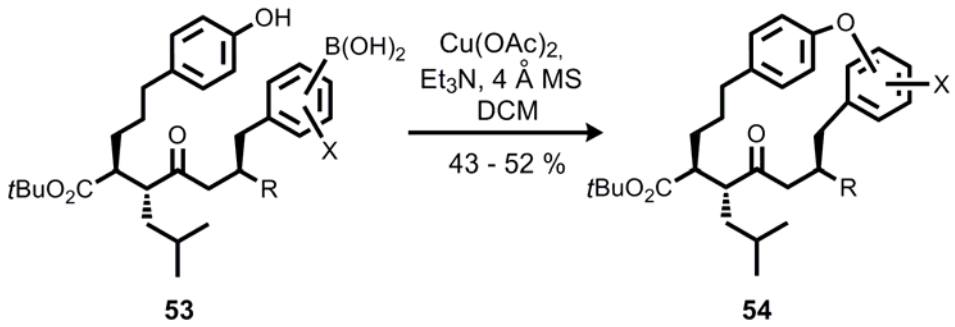

Scheme 14 Preparation of macrocyclic hydroxamic inhibitors of collaginases 1 and gelatinases A and B by *Chan-Evans-Lam* cross coupling.[65]

Milestones of the cross coupling reactions for the biaryl ether synthesis were highlighted in this section. Generally the reactivity can be increased by using the electronic effects of *ortho*-substitution or by forming a metal-aryl complex. This allows the nucleophilic aromatic addition or oxidative couplings between aryl halides and phenols which can also be facilitated by Pd(0) or Cu(I) catalysis according to Hartwig and Buchwald. On the other hand, in the case of *Chan-Evans-Lam* coupling, reactivity is only limited by boronic acids and the substitution pattern. For example, *ortho*-substituted electron rich substrates are barely tolerated.

2.2.4 Biaryl ethers by copper mediated cross couplings

2.2.4.1 Introduction

Since the term of “cross-coupling” has been often used in the last chapter, a definition might be beneficial. This term is generically used to denote a σ-bond metathesis reaction between nucleophilic and electrophilic reagents, and can be regarded as a generalization of nucleophilic substitution *via* intermediate catalyst-bound substrates (see Equation 1). Many cross couplings take place in the presence of transition metal catalysts such as copper or palladium salts.

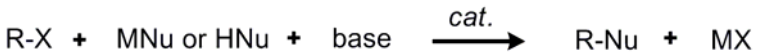

X= Cl, Br; R=aromatics, aliphatics; Nu= OH, NH, $B(OH)_2$, SnR_3

Equation 1 Generalization of cross-coupling reactions in the presence of a catalyst.

Typically, in a cross coupling reaction, the metal ion participates in successive oxidative addition, transmetallation, and reductive elimination reactions. However, details such as ligand effects needs to be taken into account. It has been observed that copper can take part in cross coupling chemistry in a comparable way to palladium. A well defined understanding of the catalytical species is missing in this case, unlike palladium-assisted chemistry. Major difference is the easy accessibility of copper for four oxidation states ranging from 0 to +3, while palladium[c] has three stable oxidation states[66] (0, +2, +4).[67-69] For copper it is unknown in which order the oxidation and transmetalation steps occur and it may be highly dependent on the substrates.[69] Two possible cycles (A or B) are shown in Scheme 15. Typically, the order of the intermediates are varied by the participation of substrates. Cycle A represents the oxidative addition of RX followed by an addition of nucleophile which undergoes reductive elimination to release the cross coupling product and copper species. Cycle B is initiated by an addition of nucleophile first, followed by an oxidative addition of RX and release of the cross coupling product by reductive elimination. The catalyst is regenerated at the reductive elimination step categorized as compound CuX (**59**), which may bear different ligands than the compound CuY (**55**) which is entering the catalytic cycle. Therefore the regenerated oxidation state does not necessarily resemble the reactive form of the catalyst which initiated the cycle. This may or may

[c] Albeit under current discussion the uneven oxidation states of palladium remain to be unambiguously identified as relevant in Pd mediated chemistry.

not undergo a ligand exchange to form the active species to enter the catalytic turn. Activation or deactivation of the copper species involved remains poorly understood.

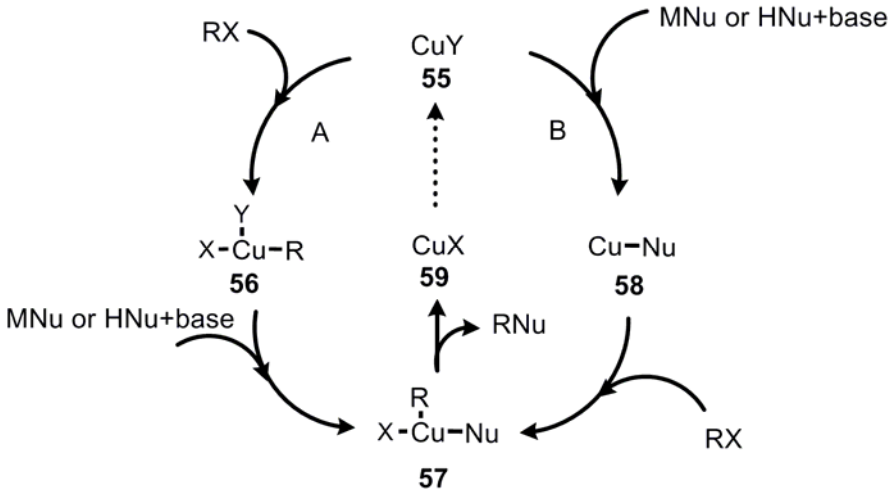

Scheme 15 Approximate scheme of catalytic cycle of Copper.

It is important to note that many hypotheses on catalytic cycles driven by Cu-ions are based on analogy to Pd(0), and not on actual mechanistic studies (Scheme 15). In addition, copper is known to potentially take part in redox single electron transfer processes, leaving the possibility for a free radical mechanism as an alternative. Mechanistic proposals in the literature fall back on from the studies of Lockhart[70] (Scheme 16), and Barton *et al.*[71] (Scheme 17). As the copper(II) catalyzed arylations have been mainly investigated for synthetic purposes, only a few number of mechanistic studies tried to elucidate the nature of the active copper intermediates. These studies can be categorized by the aryl donors, hypervalent or low valent organometalic reagents and the amount of copper catalyst which will be discussed separately in the following paragraphs.

2.2.4.2 Reactions with electron-deficient organometalic reagents and catalytic copper salt

In the course of identifying the active copper species, a hypervalent copper (III) as an intermediate was proposed to be the active species for the reaction by two possible pathway by Lockhart.[70] In case of electron-deficient organometalic reagents (Bi^{5+}, I^{3+}, Pb^{4+}, Sb^{5+}) as aryl donors, the active Cu(I) complex can be generated in the early stages of the reaction through the reduction of the original copper(II) diacetate by a

nucleophilic component. Pathway **a** in Scheme 16 corresponds to a formal nucleophilic displacement on the aromatic carbon by Cu(I), This can be initiated by oxidative addition of diphenyliodonium salt (**61**) to Cu(I). Subsequent loss of iodobenzene (**63**) leads to a phenyl copper(III) intermediate (**64**), which can give phenyl ether (**65**) and benzene (**66**) in the presence of methanol. Pathway **b** illustrates an inner sphere electron transfer resulting in a copper-complexed diphenyliodine radical (**62**), similar to the electron transfer complex proposed in the reaction of a diazonium salt with copper[70]. Subsequent intramolecular migration of a phenyl group to copper would produce the Cu(III) intermediate (**64**) from which the phenyl ether is formed (**65**). Lockhart showed that Cu(I) starts the catalytic cycle, and his experiments suggested intermediacy of phenylcopper(III) species **64** which can react with available nucleophiles to afford aryl ethers. Benzene (**66**) was detected as minor product, which was assumed to be the dematellation product formed from water traces under the oxidative conditions.

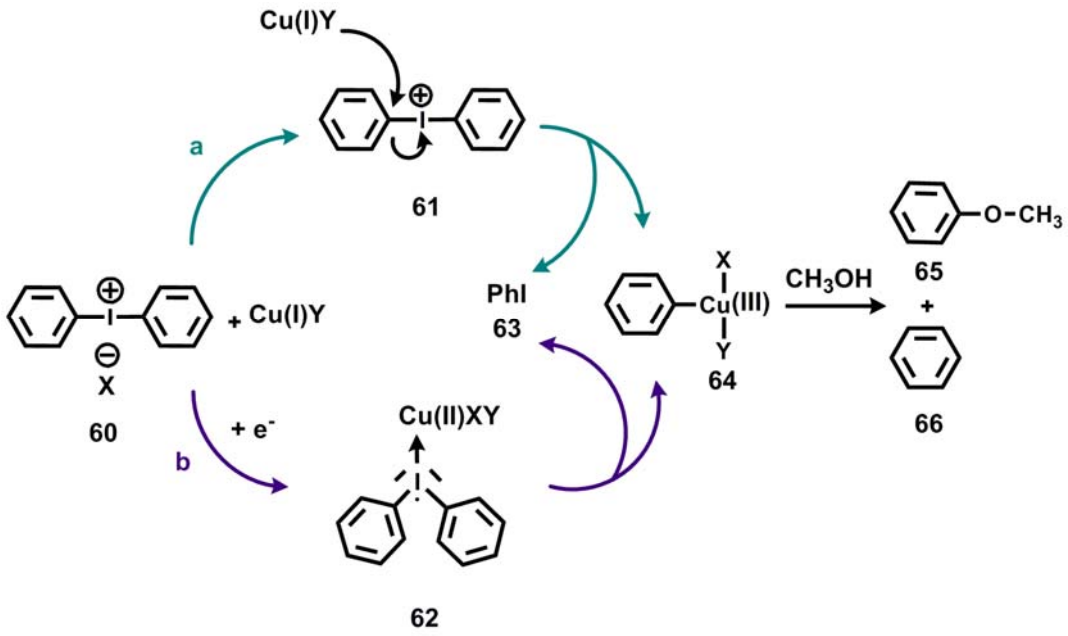

Scheme 16 An early example of hypervalent Cu(III) species: Mechanism of copper-catalyzed reactions of diphenyliodonium salts.

2.2.4.3 Reactions with electron rich organometalics reagent and stoichiometric copper salt

In the case of electron rich organometalic reagents (such as organoboron or organotin reagents) and stoichiometric amount of copper(II) salts, different mechanisms were proposed for *O*- and *N*-arylations. In general the copper(II) complexes (**69** and **74**) are expected to form copper(III) intermediates in the presence of oxygen, which then undergo reductive elimination to give cross coupled products (**71** and **76**). Evans *et al.*[60] proposed a mechanism for the arylation of phenols by transmetallation followed by coordination of the phenol to afford copper(II) complex (**69**). Reductive elimination then leads to biaryl ether **71**. The postulated mechanism for the arylation of amines by Lam *et al.* [72] involves a similar coordination of the substrate to Cu (II) (**73**) followed by a transmetallation to obtain copper(II) salts (**74**). Product **76** can be formed after the reductive elimination of copper complexes (**74** or **75**). This mechanism was suggested by the observations that the same yield of cross coupling product was obtained when boronic acid was added after the formation of the aryl-copper(II) complex (**73**). However, the single-electron oxidation from Cu(II) to Cu(III) by O_2 remains to be demonstrated.

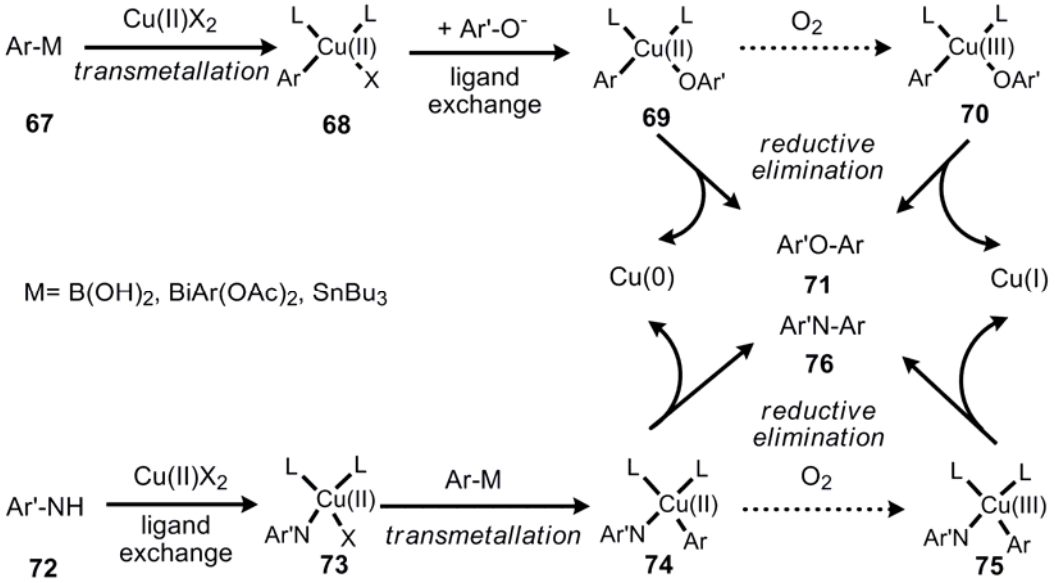

Scheme 17 Proposed mechanisms for the *O*- and *N*-arylations with low-valent organometallic reagent by stoichiometric Copper (II) salt.[60,72]

2.2.4.4 Reactions with aryl halide and pseudohalides (I, Br, OTf) and catalytic copper salt (Ullman-type condensations)

This type of copper catalyzed reactions are sometimes called Ullmann condensations.[53,54] In the Ullman-type condensation, phenol **78** is coupled to an aryl halide or pseudoarylhalide **77** in the presence of a catalytic amount of copper salt to form biaryl ethers **79**. For this transformation, Evans *et al.*[60] suggested a mechanism initiated by an oxidative addition of aryl halide to Cu(I) species to yield Cu(III) complex **80** which follows a subsequent addition of the aryl alcohol **78** to form **81** as an active species. In that stage, the oxidation state of the intermediates remains an unresolved issue. Plausible aryl copper phenoxide intermediates **82** could also be formed by a single electron transfer in the presense of oxygen. Therefore the Cu(III) and Cu(II) species could both undergo reductive elimination to yield the biaryl ether **79** while liberating Cu(I) and/or Cu(0). Cu(III) complex formation still remains to be clearly demonstrated for such type of arylations.

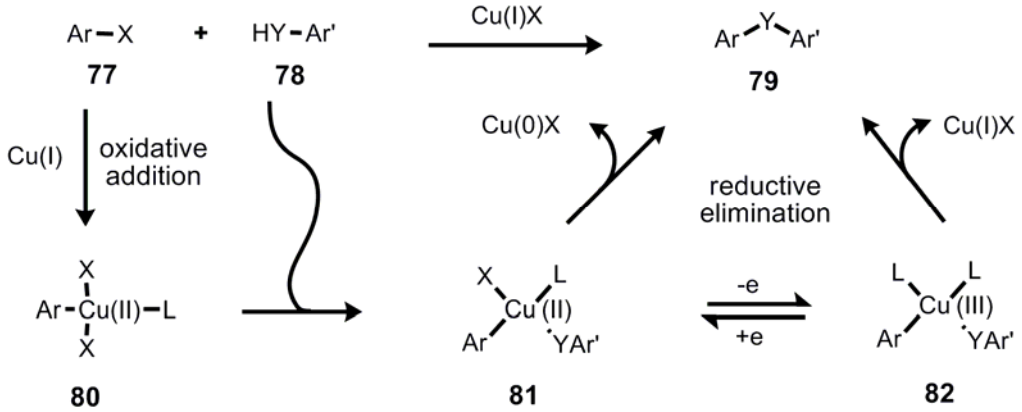

Scheme 18 Plausible mechanism for the copper-catalyzed Ullmann condensation. X= I, Br, OTf; Y= OH, NH, SH.

2.2.4.5 Reactions of electron rich organometallic reagents in the presence of catalytic copper salt with reoxidant

The cross couplings in the presence of catalytic amount of copper(II) species is an important step for a further application. In the recent literature phenols[73] and amines[74] were successfully coupled with boronic acids in the presence of catalytic amount of copper salts. Notably, O_2 is necessary to drive these reactions and the initial oxidation state of the copper salt applied has no influence. The mechanism of this reaction was subject of considerable speculation. In the most advanced work, Collmann *et al.*[75] have proposed catalytic Cu(II)-dioxygene complexes for the coupling of imidazole with

aryl boronic acids. However their proposal suffers from improper electron counts. Here, based on this rough proposal,[75] a refined catalytic cycle is tentatively proposed for cross couplings between phenol/amine **83** and boronic acid **84** (Scheme 19).

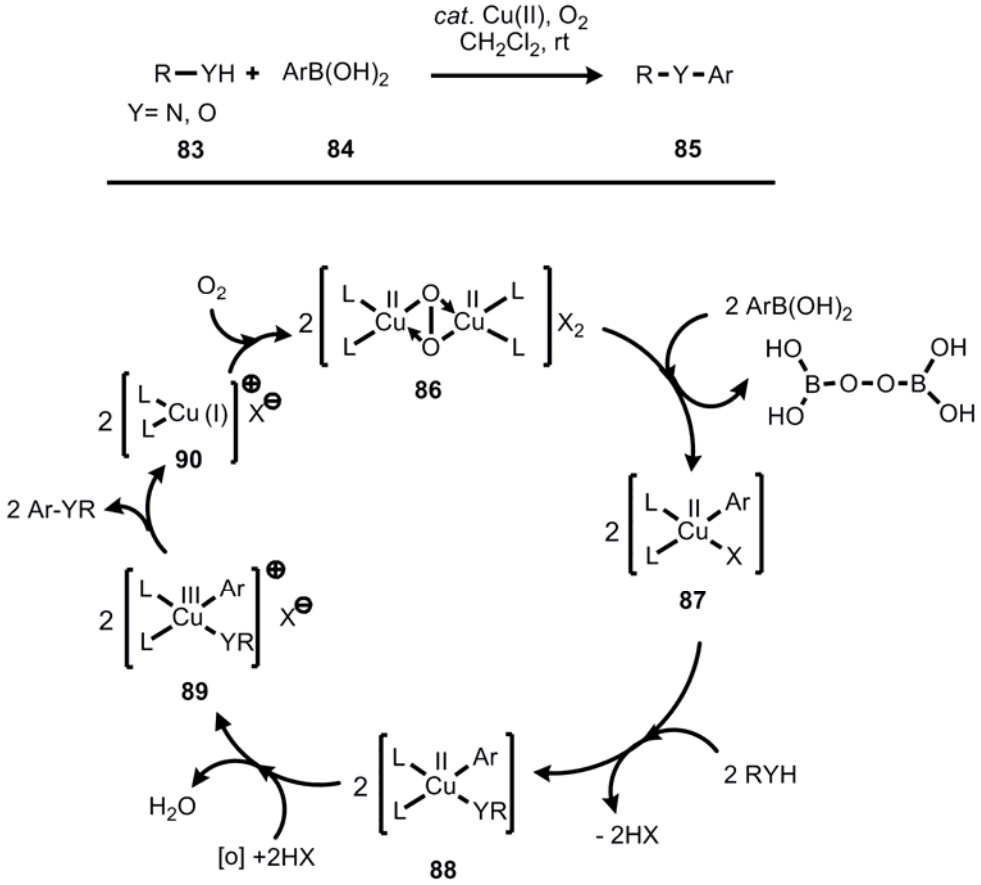

Scheme 19 Mechanistic hypothesis of the *N*- *O*-arylation reactions with arylboronic acid, catalytic copper salt.

Collmann assumed that Cu(II)-peroxo complexes must be involved, because these are well documented products of Cu(I)-oxidation by dioxygen.[76] However, if **86** would react with boronic acid **84**, perborates should be formed, given the high oxophilicity of boron. Furthermore, 2 equivalents of intermediate **87** should be liberated. Ligand exchange with nucleophile **83** would lead to intermediate **88**, which could then become oxidized to the Cu(III)-species **89**. This oxidation could be mediated by O_2, but the perborate produced in the first step might even be a better oxidant for this purpose. **89** would then quickly undergo reductive elimination to liberate the product **85** and intermediate Cu(I)-complex **90**, which should become swiftly reoxidized to **86** by dioxygen.

Overall, this proposal integrates the findings of Collmann with a proper electron balance and other mechanistically relevant indications from the literature.[60] Future

research must be dedicated to the nature of the intermediates involved, and to the potential occurrence of other oxidants than O_2.

3. Biaryl ether containing cyclic natural product: RA-VII

3.1 Therapeutic promise of RA-VII

Several different RA alkaloids have been described, which share a common macrocyclic core structure and the presence of a biaryl ether subunit. RA alkaloids, including RA-VII (**4**) were isolated together from the methanolic extracts of the dried root of *Rubia cordifolia* by Itokowa *et al.* in 1983.[21] Their bicyclic structures consist of two L-alanines, one D-alanine and two (*O,N)*-methyl L-tyrosines, and one *N*-methyl L-tyrosine. The RA alkaloids mainly differ in the substitution present at one of the phenolic alcohols and in one of the aminoacids residues that can be alanine, serine, threonine, or glutamic acid (**96**-**102**). Additionally, bouvardin (**91** and **92**) derivatives carry an extra hydroxyl group at one β-carbon. They all have interesting biological activity. Among the close family members, RA-VII (**4**) is the most potent antitumor agent. This drew attention from several research groups with respect to an analogy to studies of structurally similar known antiproliferative agent bouvardin[77] (**91**). RA-VII (**4**) showed similar high antitumor and antineoplastic activity.

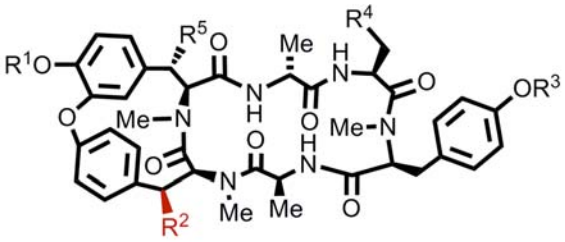

RA alkaloids

	R^1	R^2	R^3	R^4	R^5	
4	Me	H	Me	H	H	RA-VII
91	H	OH	Me	H	H	Bouvardin
92	Me	OH	Me	H	H	*O*-methyl bouvardin
93	H	H	Me	H	H	Deoxybouvardin (RA -V)
94	H	H	Me	OH	H	RA-I
95	Me	H	H	H	H	RA-II
96	Me	H	Me	OH	H	RA-III
97	Me	H	Me	H	OH	RA-IV
98	Me	H	Me	(OH)Me	H	RA-VIII
99	Me	H	Me	CH_2CO_2H	H	RA-X
100	H	H	Me	CH_2CO_2H	H	RA-XI
101	β-D-glucose	H	Me	H	H	RA-XII
102	β-D-glucose	H	Me	CH_2CO_2H	H	RA-XIII

Scheme 20 Alkaloids isolated from *Rubia cordifolia L. (Rubiaceae)*

In 1986,[78] RA-VII (**4**) was shown to be active against 148 human specimens of various malignant tumors in a clonogenic assay. From the results of a study using a human lung cancer cell line (PC-6), RA-VII (**4**) appeared to possess time-dependent

antitumor activity. It showed almost the same activity like four standard anticancer drugs (adriamycin, mitomycin C, cisplatin, vinblastine), but the activity spectrum of RA-VII (**4**) appeared to be different. RA-VII (**4**) entered phase I study in 1993[79,80] as a promising antitumor drug. Later, RA-VII (**4**) was shown to have also significant antitumor activity against leukeumia and colon tumors in mouse models for leucocytosis.[81,82] However, the mechanism of action remained unclear. First results in this direction were presented at 1995 by Toogood *et al.,* who showed that RA-VII (**4**) can act as an inhibitor of eukaryotic protein synthesis.[23] The results obtained in *in vitro* biochemical assays showed that unlike bouvardin, RA-VII (**4**) has no effect upon aminoacyl-*t*RNA binding, but it interacts directly with the 80S ribosome and inhibits the peptide bond formation. Another interesting study on potential modes of action of RA-VII (**4**) was reported by Wakita *et al.*[83] Their results indicate that RA-VII (**4**) reduces cyclin D1 level independent of protein synthesis in DLD-1 colon cancer cells. These researches concluded that RA-VII (**4**) might actively promote the degradation process of cyclin D1 *via* the ubiquitin-proteasome pathway. Additionally, ongoing biological evaluation of RA-VII (**4**) showed influences on the actin cytoskeleton. It induces the G2 arrest through the inhibition of cytokinesis.[84] However, the effect of RA-VII (**4**) on cyclin D1 degradation and actin filament modulation seems to be much weaker than its ribosome inhibition ability.

RA-VII (**4**) is fairly rigid, but can exist in different conformations mainly due to its *N*-methylated amide bonds. It has been shown that RA-VII (**4**) can adopt three major conformers (**4**, **4a** and **4b**, Figure 8)[d] in deuterated DMSO-d_6.[85-87] In general they differ by the configuration of amide bonds. The junction between Tyr^5 and Tyr^6 conserves its *cis* configuration, while the more flexible amide bond between Tyr^3 and Ala^4 can adopt a *trans* or *cis* conformation. [85-87] In $CDCl_3$ solution only conformers **4** and **4a** were observed. Besides making characterization difficult, the presence of conformeric mixtures makes it challenging to design a productive synthetic strategy for the active conformation. Furthermore, the active conformation ultimately responsible for the biological activity remains to be elucidated.

[d] Elucidated by NMR spectroscopy (500 MHz) at 30°C.

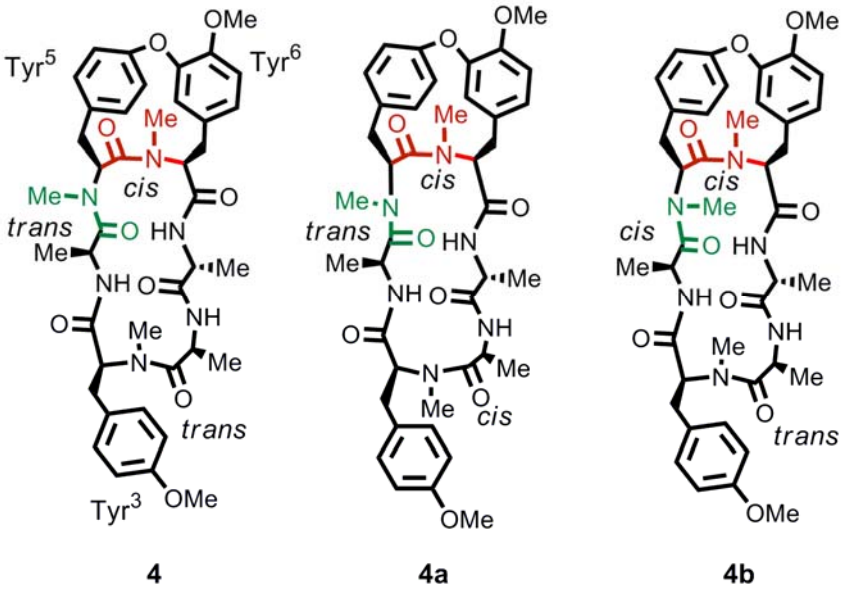

Figure 8 RA-VII conformers in solution.

In order to track the interesting biological profile of RA-VII (**4**) and to make simplified and/ or functionalize modified analogs accessible, synthetic access is necessary. This will be especially important, as the natural product itself does not carry any functional groups suitable for functionalization. Apart from the interest in synthesizing modified analogs of RA-VII (**4**), the total synthesis of this natural product has also interest itself. Previously reported total synthesis strategies for RA-VII (**4**) will be discussed in the following chapter.

3.2 Previous total synthesis strategies of RA-VII

Synthetic design inspired by nature might be a good starting point to design a total synthesis of RA-VII (**4**). However, many biosynthetic pathways to bicyclic natural products containing biarylethers are unknown, including the biosynthesis of RA-VII. RA alkaloids are known to be isolated from plant roots, however the biosynthesis of such natural products in higher organisms are not yet well understood. Recent reports show that natural products originating from plants or animals may be produced not by the plant/animal itself but by a microbial symbiont.[17] One can only speculate that the RA alkaloids are secondary metabolite products. Further inspection shows that RA-VII (**4**) contains several *N*-methylations and a D- amino acid which is a strong indication for a non ribosomal biosynthesis. Therefore here a plausible biosynthetic precursor, **105** is proposed as an analogy of vancomycin (**2**) biosynthesis, using non-ribosomal

peptide synthase. Following this line of thought, a “biomimetic” cyclopeptide precursor (**105**) could be investigated, where a late stage oxidation would define the biaryl ether bond to complete a total synthesis of RA-VII (**4**).

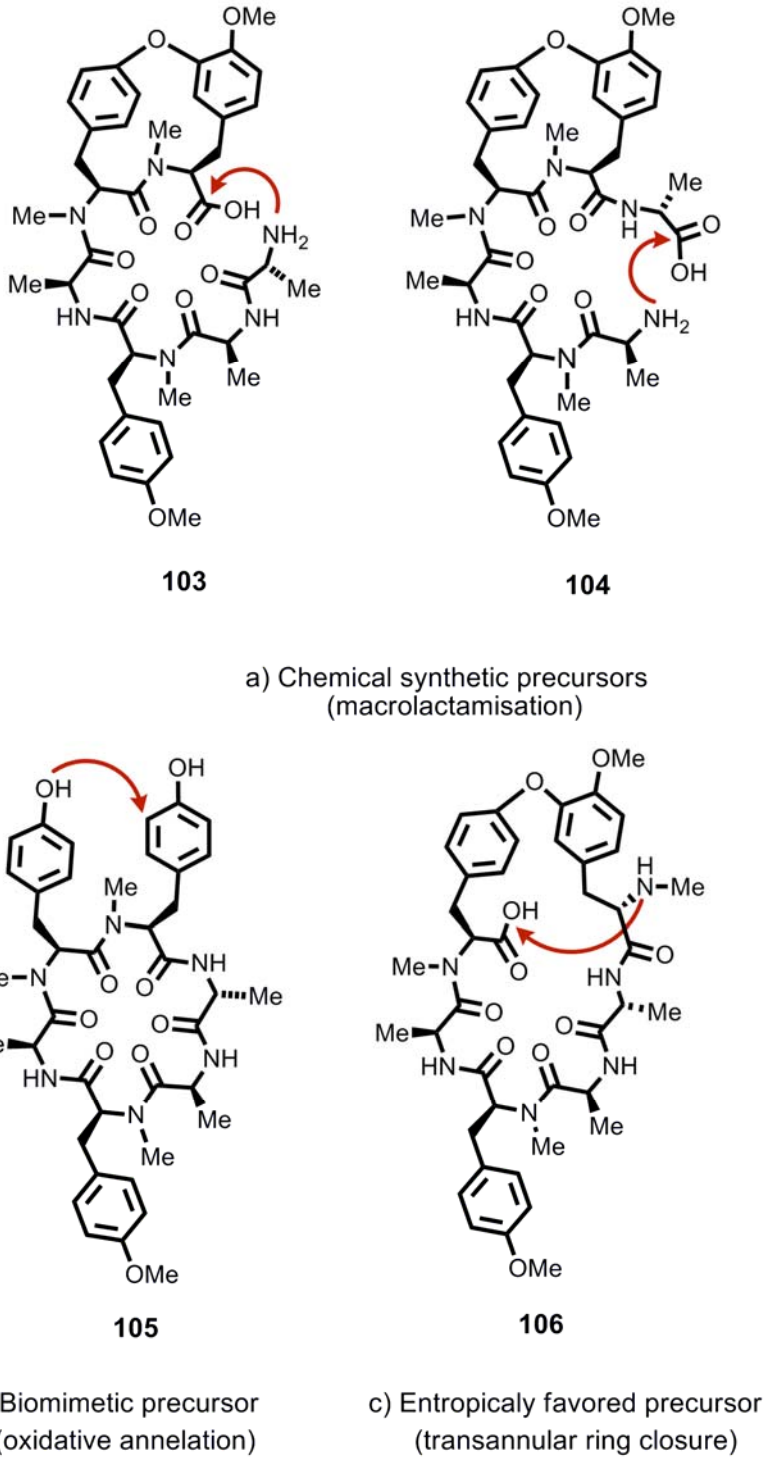

Scheme 21 Plausible precursors for the synthesis of RA-VII (**4**).

Alternatively, two distinct synthetic strategies can be discussed where precursors containing a biaryl ether bond could be used. Either, the strained 14-membered ring could be already installed and the cyclopeptide be set up in the last step (**103** or **104**). On the other hand the 14-membered ring could potentially be installed lastly by transannular ring closure (**106**), thereby profiting from preorganization and supportive transition state entropy (Scheme 21).

The synthetic strategies pursued so far by several research groups are summarized in Scheme 22 and will be discussed shortly. Bond disconnection (**a**) focused on ring closure of more flexible cyclic petide moiety of RA-VII (**4**), (**b**) involves the biaryl ether formation as discussed in the section 2.2.2 as the last step, while strategy (**c**) involves transannular macrolactamization to obtain the bicyclic structure in the last step. Itokowa *et al.* and Boger *et al.* reported to be successful using strategy **(a)** while Zhu *et al.* were only successful using strategy (**d**). However, the synthetic strategies applied either suffered from epimerization or lack reproducibility and limited amount of material produced. Additionally, many studies have unclear structure determination (*vide infra*). A straightforward, versatile synthesis of RA-VII (**4**), ultimately involving for example solid phase peptide synthesis to facilitate the assembly of RA-VII (**4**) analogs has not been realized.

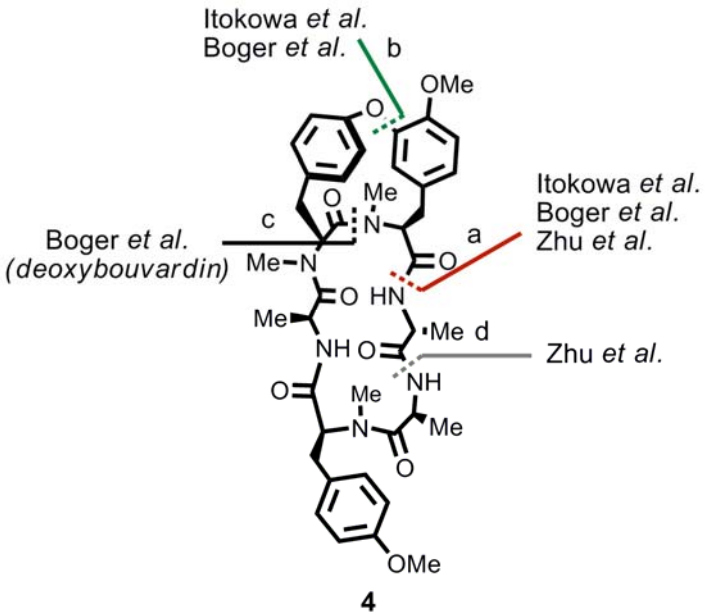

Scheme 22 Retrosynthetic strategies have been studied by independent research groups up to today towards the bicyclic structure of RA-VII (**4**).

3.2.1 Total synthesis approach by Itokawa *et al.*

The first attempted total synthesis of RA-VII (**4**) by Itokawa *et al.* was inspired by anticipating how nature might synthesize such type of structures using strategy (**b,** Scheme 22),[88] which is based on the formation of the biaryl ether linkage at the last step. Unfortunately, the cyclic hexapeptide precursor could not be converted to the target structure by oxidative coupling with thallium(III) trinitrate (TTN). Their next attempt, using approach **a** (Scheme 21) is shown in Scheme 23. Regioselective oxidative conditions developed by Yamamura *et al.* [89] were used to construct the highly strained 14-membered ring. Therefore **110** was oxidized by TTN[90] to form cycloisodityrosine **107** and then coupled to tetrapetide **108** in order to obtain RA-VII (**4**) by macrolactamization mediated by diiphenyle phosphonyl azide (DPPA).[91] This strategy afforded the desired final compound RA-VII (**4**), albeit in very low yield (< 1 % over all.)

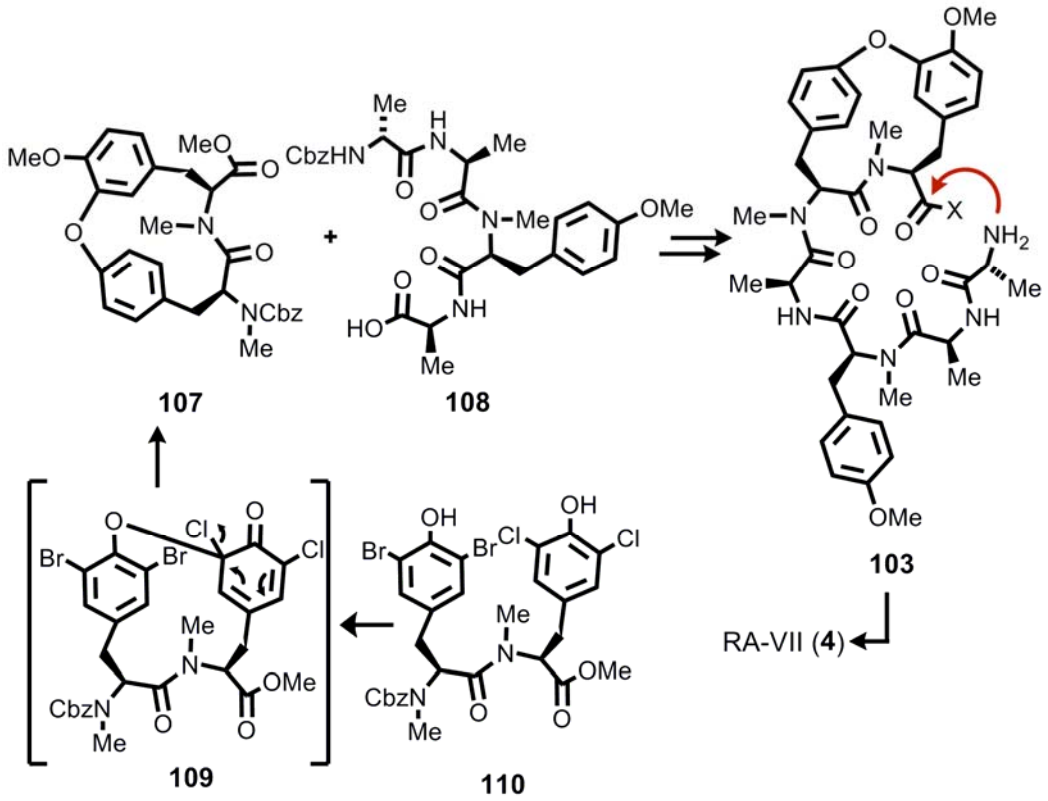

Scheme 23 Synthetic strategy for the total synthesis of RA-VII (**4**) by Itokowa *et al.*

3.2.2 Total synthesis approach by Boger *et al.*

Boger *et al.* put efforts[92-95] in creating a viable synthetic strategy to obtain RA-VII (**4**) and deoxybouvardin (**93**). Connecting the tetrapeptide to the cycloisodityrosine was the only method to obtain the bicyclic structure for these researches as well (Scheme 24). Brief studies on strategy (**c,** Scheme 22) and (**b,** Scheme 22) were less promising according to their accounts.[89] Initially, it was necessary to construct the cycloisodityrosine structure (**107**). Intramolecular Ullmann-type condensation conditions with C^1-O^2 bond formation proved synthetically viable for the direct formation of 14-membered biaryl ethers. However, considerable epimerization was detected under these conditions.[59-62] Eventually, S_NAr reactions were investigated in order to obtain stereoisomerically pure cycloisodityrosine.[94] The precursor **112** was used to afford cycloisodityrosine (**107**) which gave partial epimerization on the C^9 carbon of cycloiosdityrosine residue and afforded a mixture of the isomers (**9*S, 12S***) and (**9*R, 12S***) isomer. They later found that thermodynamically favored cycloisodityrosine **114** is the non-natural epimers compare to the natural epimer **113** due to the electronic effect of nitro group. (Scheme 24) This shows that cycloisodityrosine **107** is therefore strained and prone to epimerization. First, this epimerization went unnoticed,[96] and the group published the total synthesis of the "right" epimer of RA-VII (**4**) by macrolactamization. In later work they made the case that epimerization of the C^9 center must have had occurred, to fully revert it back to the "natural" configuration.[41] Albeit not being absolutely impossible, a successful total synthesis using correct epimer **107** was never published, so the remaining consistency was not fully resolved.

RA-VII (**4**) contains *cis* conformation in biarylether linkage which has already been discussed. The Boger group documentedl[97] that **107** that possesed *trans* configuration in solution, but in the final product it is *cis* configured. This suggests that the preorganized cyclic 14-membered ring induces ring strain leading to sensitivity of the particular C^9 center. It also may explain the low yield of cyclizations for the macrolactamization which may need a slow trans/cis interconversion of this central amide bond to proceed.

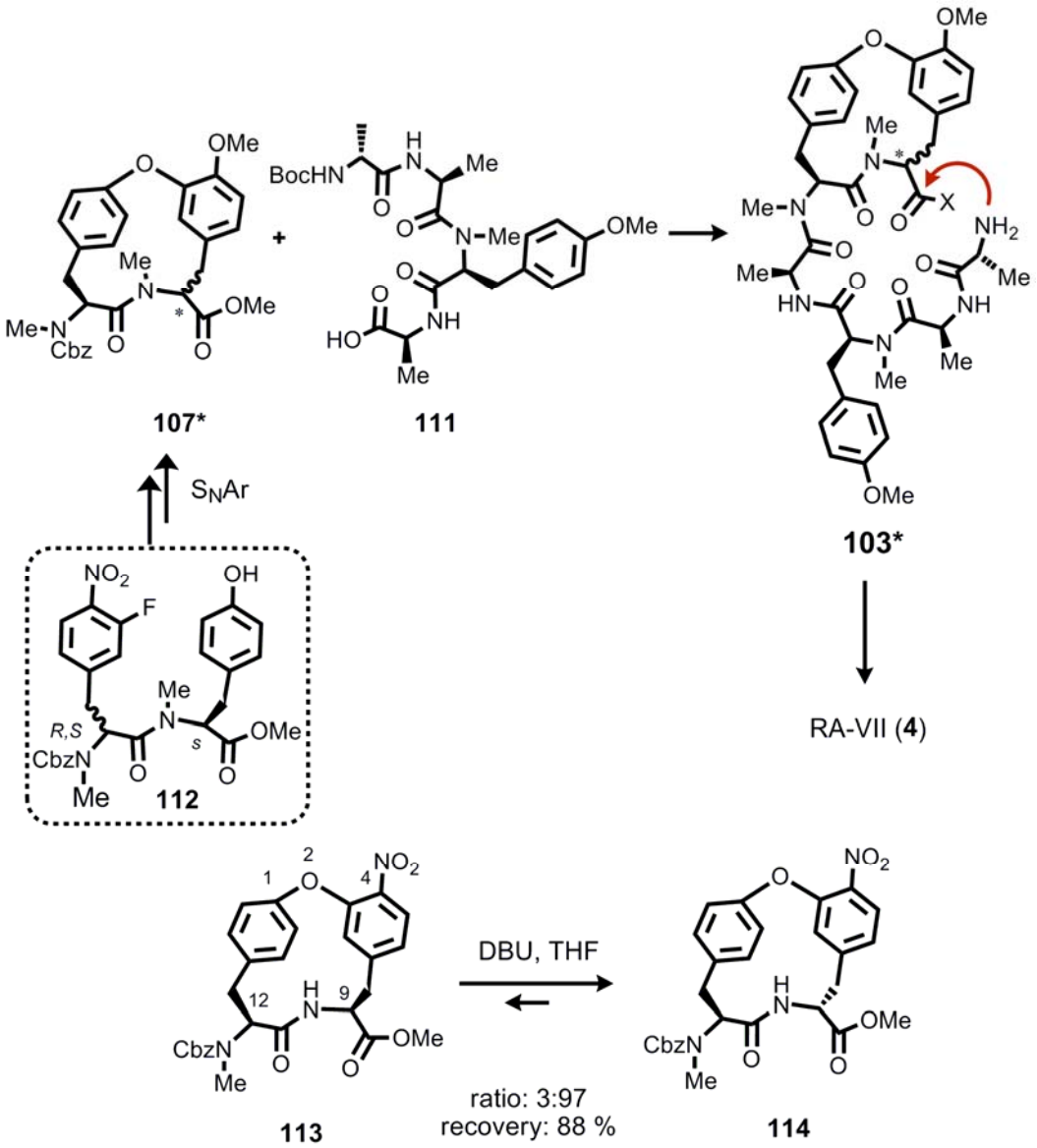

Scheme 24 Synthetic efforts for the total synthesis of RA-VII by Boger *et al.* and epimerization sensitive cycloisodityrosine **107**.

3.2.3 Total synthesis approach by *Zhu et al.*

Being aware of the work of the Boger group, Zhu *et al.*[48] designed the total synthesis strategy following the route **d** (Scheme 22) to allow for more effective macrolactam formation (Scheme 25). A racemization free synthesis for the cycloisodityrosine unit was also required. Their assumption was that acidity of C^9 increases by the *para* placement of the NO_2 substituent (Scheme 25). Therefore, in their precursor design, they placed the NO_2 group on the *meta*-position to reduce the deactivating effect on

the 4-position. Pure cycloisodityrosine by S_NAr was synthesized in 70 % yield and allowed to study the macrolactamization. For their efforts, using the correct epimer of the cycloisodityrosine, [2+4] segment coupling strategy between **117** and **111** as reported by Boger *et al*. and Itokawa *et al.* failed. However, a [3+3] segment coupling, where the fragments **115** and **116** were assembled gave RA-VII (**4**) in the presence of DPPA in 20 % macrolactamization yield.

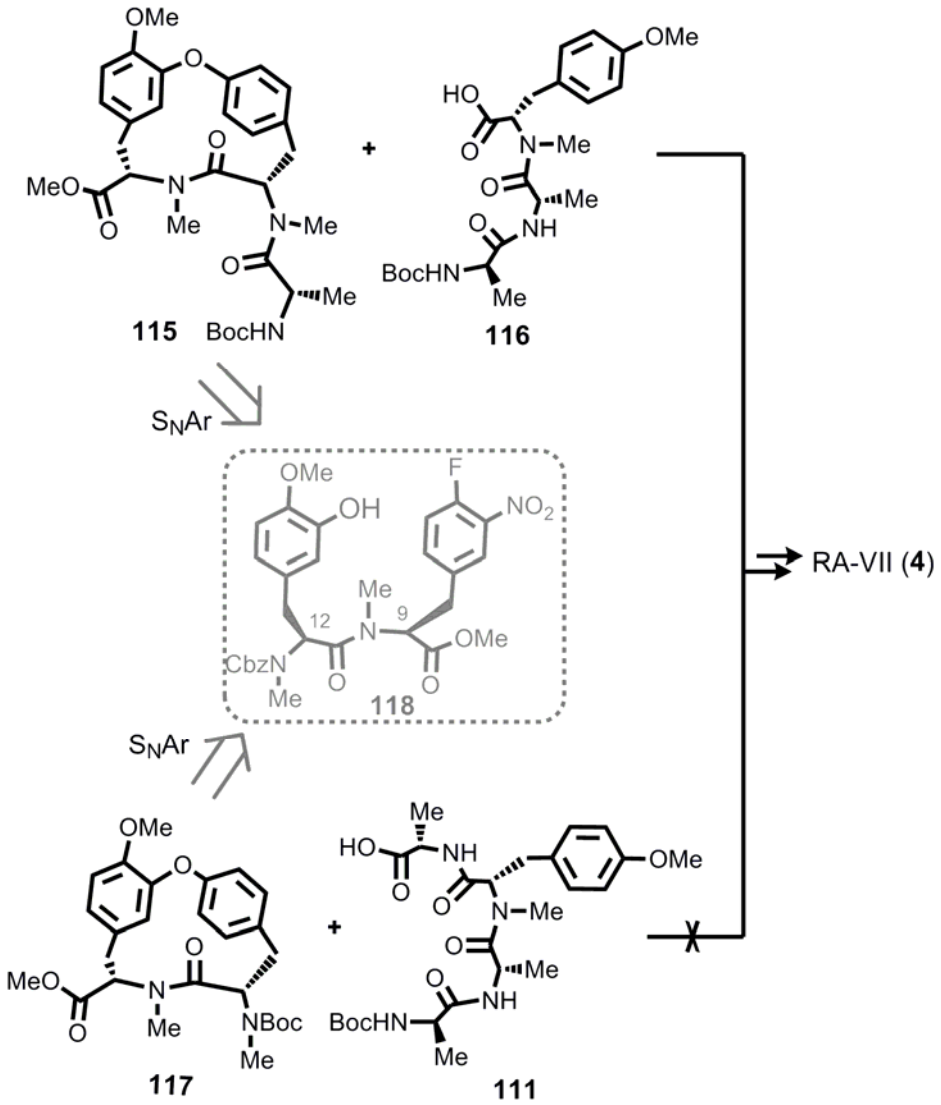

Scheme 25 Synthetic strategy for the total synthesis of RA-VII by Zhu *et al.*

Different synthetic strategies for obtaining RA-VII (**4**) have been reviewed in this section. However, these previous synthesis either suffered from epimerization or lack of reproducibility. Unfortunately, the reports do not fully support each other. Itokowa *et al.*[88] and Boger *et al.*[90] reported to be successful using strategy (**c**) while Zhu *et al.*[48]

were only successful using strategy (**d**). Additionally, some of the studies suffer from not fully clarified structure determination. Therefore, a new synthesis towards RA-VII (**4**) should follow a different design. In addition, the establishment of solid phase peptide synthesis methodologies would be really valuable because it would give access to the synthesis of RA-VII analogs using unified technology.

4. Aim of the project

Previously reported syntheses for RA-VII (**4**) either suffered from epimerization or lacked reproducibility. Furthermore, due to its unclear biogenesis and its lack of functional groups for derivatization, synthetic access to RA-VII (**4**) and its analogs is vital to study the bioactivity of this highly promising molecule in more detail. This thesis therefore aimed at scouting a potentially highly versatile transannular disconnection towards the synthesis of RA-VII (**4**). Ultimately, it should involve solid phase peptide synthesis technology for facilitating its assembly.

4.1 Retrosynthetic consideration

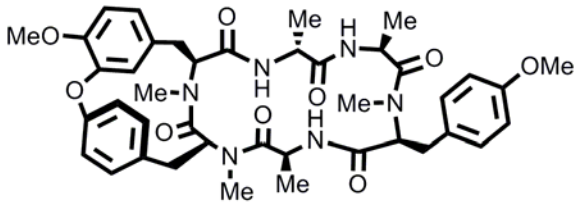

RA-VII (**4**)

Figure 9 RA-VII structure.

The peptide sequence of RA-VII (**4**) consists only of tyrosine and alanine amino acids. Three L-tyrosines are *N*-methylated, two of which are *O*-methylated as well. One of the alanine residues is D configurated. Previous syntheses have concentrated on annelating macrolactam formations in completing the bicyclic scaffold. As discussed before, these roads were apparently (4 successful in completion, but with modest efficiency (see chapter 3.2). It thus seemed to investigate a transannular ring closure step in more detail (**4** ⇒ **119**). Such a strategy would potentially benefit from preorganization and favorable entropy. Furthermore, the strained *cis*-configured transannular amide bond would not be a prerequisite to reach the transition state for ring closure.

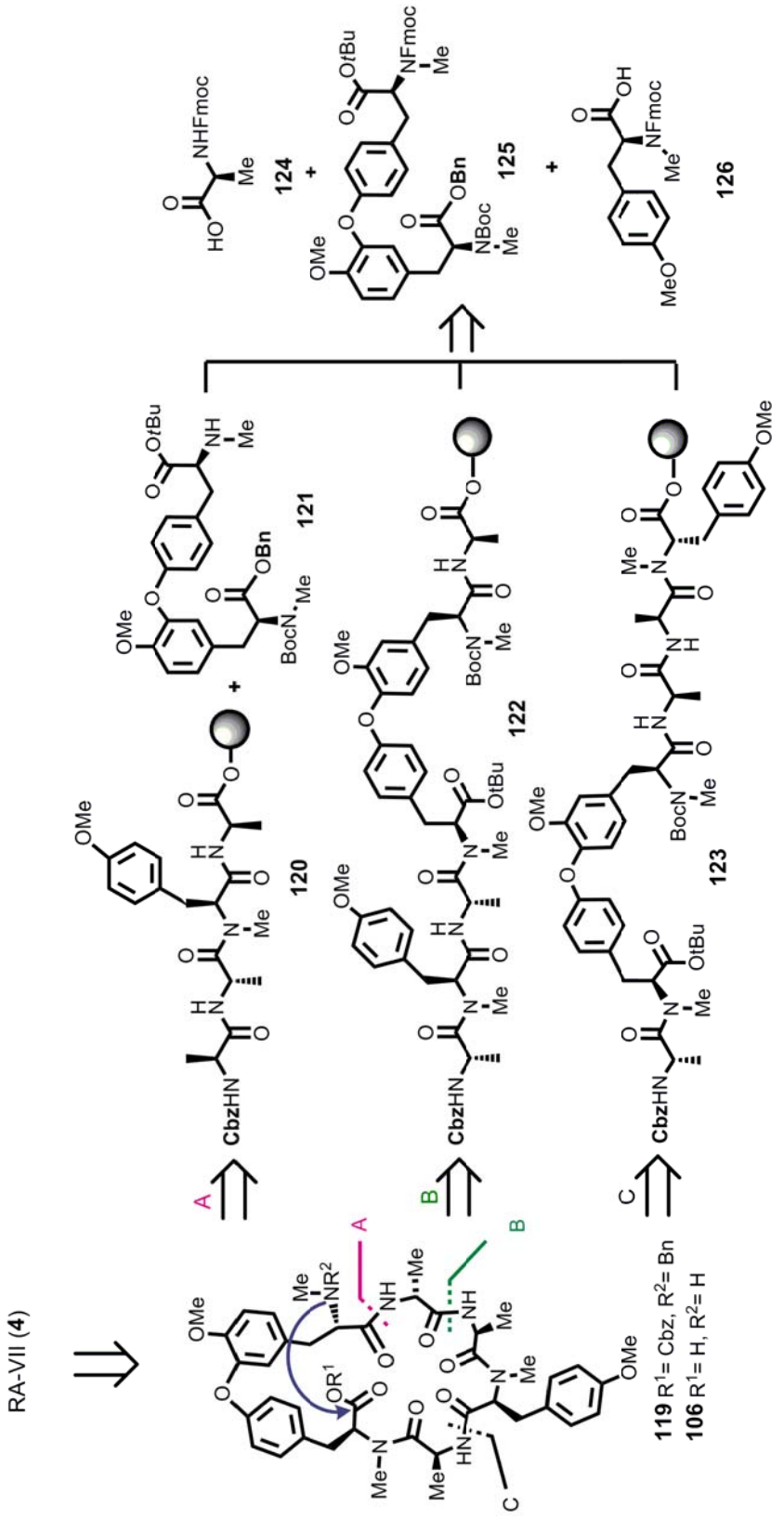

Scheme 26 Retrosynthetic analysis of RA-VII (**4**).

Lastly, the target molecule synthesis could be simplified to synthesizing a medium ring-size cylopeptide. The structural variation should thus be easily achieved, once a method for transannular bond formation has been found. Solid supported synthesis would be easily applied to realize flexibility, time economy and variation in the synthesis of analog libraries. For macrolactamization of **119** different sites would be available. For **119** only disconnections containing at primary amine residues were selected for investigation, as they were expected to be the most productive macrolactamization sites (A, B, C, Scheme 26). This macrolactamization then would be followed by the transannular macrolactamization to complete the synthesis. By variation of cyclic hexapeptide **119**, this strategy could in extension result in a unified approach to obtain RA-VII (**4**) derivatives.

The three strategic disconnections (A, B, C, Scheme 26) forming closure lead to three linear peptides. The first approach to consider is to build the linear tetrapeptide **120** on solid support, followed by coupling to the isodityrosine **121**. The second approach is full linear peptide synthesis of the hexapeptide on solid support to afford the linear precusors **122** and **123** using different coupling sequences. The two possible synthetic approaches, linear solid phase and [4+2] segment coupling require differently functionalized isodityrosine building blocks, such as **121** or **125**. In general, all building blocks (**124**, **125**, **126**) can be designed to have orthogonal deprotection when its necessary. Bn and Cbz, were chosen to mask the macrolactamization sites leading to **119**. Additionally, acid sensitive protecting groups *t*Bu and Boc were selected for a late deprotection (**106**) to orthogonally protect the functional groups involved in transannular macrolactam formation. The isodityrosine building block **127** was designed to carry orthogonal protecting groups (Scheme 27). Fully protected **125** then can be converted by basic removal of Fmoc group to building block **121** and by hydrogenation[98] to building block **127.** Disconnection of building block **125** by a *Chan-Evans-Lam* Cu(II)-mediated oxidative coupling leads to two building blocks, boronic acid **128** and phenol **129**. Additionally, Fmoc protected *N*- and *O*- methylated tyrosine carboxylic acid **126** (Scheme 26) would be needed as the third tyrosine building block. All these building blocks should be accessible from L-tyrosine. **126**, and **129** mainly necessitate protecting group introduction, where for **128** also the *meta*-positioned boronic acid has to be introduced. This functional should be available by Miyaura-borylation[99] of 3-iodo-tyrosine **130**, which is accessible from L-tyrosine (**132**) by hydroxy directed iodination.[100] A further challenge was posed by the *N*-methyl goups, which are difficult to introduce.[101] In all cases, means of introducing the *N*-methyl group without racemisation must be found.

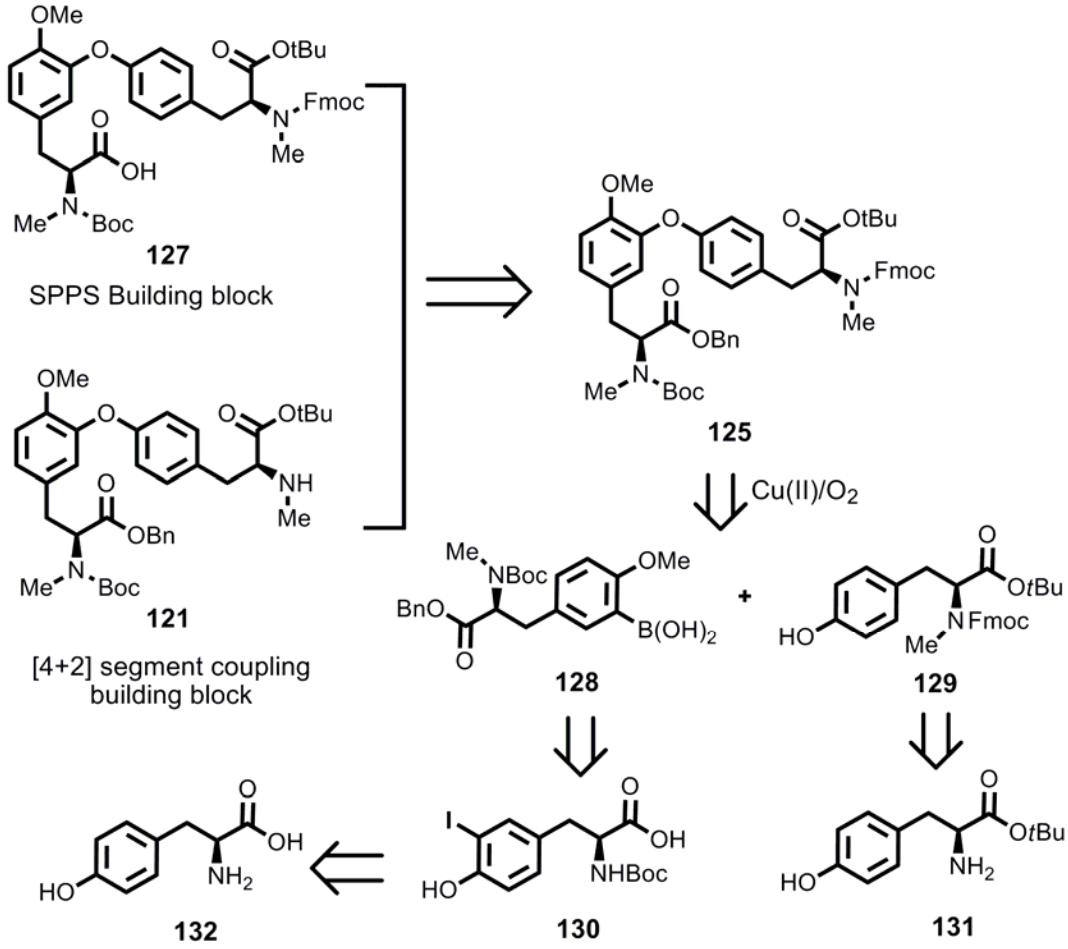

Scheme 27 Retrosynthetic scheme for the preparation of isodityrosine building blocks by **105** and **104**.

4.2 Modelling of RA-VII and minimized energies of the precursors

From the preceding studies by other groups it was clear that a flexible synthesis for providing such bicyclic peptides as RA-VII had not been realized. To facilitate the synthesis of analogs by a general strategy would be highly useful. In this regard, macrocycle **106** deemed most attractive, as it would allow varying the sequence easily. Of course, disconnecting the *cis*-configured *N*-substituted transannular amide would lead to a rather challenging bond construction in the forward sense, but reagents to construct such hindered peptide bonds have been reported. On the other hand, previous attempts of closing the apparently simpler cyclopeptide ring at the end of the synthesis were not really reproducible.

RA-VII (**4**) and its precursors **106** and **133** were subjected to molecular modelling experiments in order to identify potential problems which might arise from the uncommon structural features and unanticipated energy bariers. As already discussed in the previous chapter, a X-ray crystal[97] structure of **107** (Scheme 24) corresponding to the isodityrosine segment in the dashed box in Scheme 28 was reported. It possessed *trans* conformation on amide bond which highlights the fact that the preorganized cyclic 14-membered ring in the final product might be even more strained due to the *cis* configuration on final compound (**4**). Therefore, the potential precursors were studied in comparison.

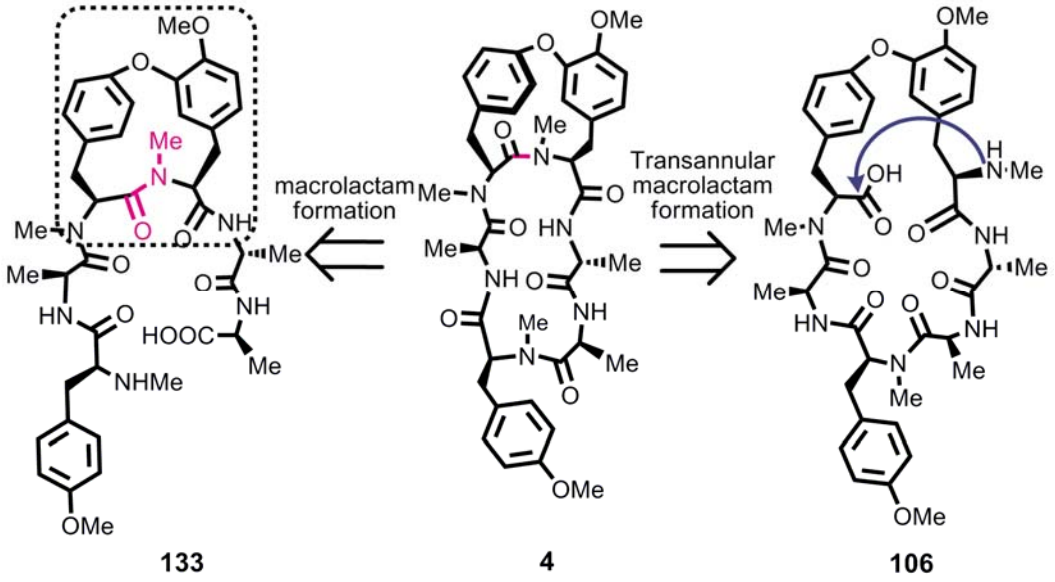

Scheme 28 Selected precursors of RA-VII (**4**) for the molecular modelling calculation.

A full conformational search was performed[e] for the structures **4**, **106** and **133**. The results showed a weak difference in global energy (1.9 kcal/mol) for both monocyclic precursors (**106** and **133**). The amount of different conformations in a global minimum frame was calculated (1 kcal, 2 kcal, 3 kcal, 5 kcal and 10 kcal). The numbers in the brackets (Scheme 29) gives the number of conformers within an energy window of 10 kcal/mol. The cyclic precursor **106** was calculated to have a significant higher number of conformers then **133**. It could be argued that this extra flexibility increases the chance of reaching the thermodynamically favored transition state, indicating that **106** could be a better precursor then **133** for the last ring forming reaction. On the other hand, it can be anticipated from the minimized energy values (kcal/mol) that **86** and **133** are similar precursors in terms of reactivity. Despite of all the uncertainty

[e] Molecular modelling calculation was performed by Dr. Stefan Wetzel.

associated with molecular mechanics calculations and energetics, these results gave confidence to study the transannular macrolactamization, as once tried by Boger *et al.*, in more detail.

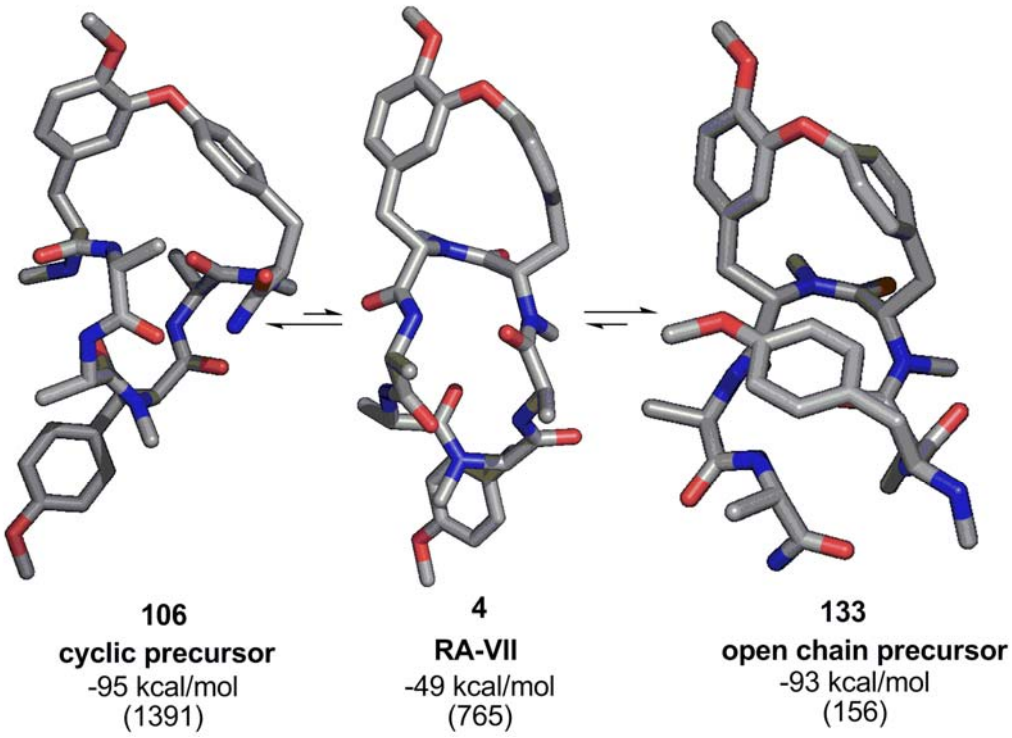

Scheme 29 Global minimum energies (kcal /mol) of cyclic precursor, RA-VII (**4**) and open chain precursor and number of conformers with in 10 kcal/mol (in the brackets).

5. Results and Discussion

5.1 O-Arylations of tyrosine derivatives

The *Chan-Evans-Lam* cross coupling is one of the most powerful methods known to synthesize highly functionalized biaryl ethers. This coupling allows the introduction of a biaryl motif into complicated structures using mild reaction conditions, making it the most promissing approach for the sensitive substrates used in this project. For our study towards the synthesis of RA-VII (**4**), biaryl ether moieties needed to be introduced on tyrosines in the most effective manner. The *Chan-Evans-Lam* coupling conditions were therefore studied in detail. Sensitive substrates such as α amino acids for the phenol component only have weak precedent in the literature.[60] On the other hand, typical cross couplings with boronic acids are limited by their instability of the substrates. In the course of this work slow release of boronates[102] has been reported to control boronic acid hydrolysis which allows some access to couplings of the unstable boronic acids such as heteroatom containing aromatic boronic acids. However, this method has not yet found its applications for biaryl ether synthesis. In this section, the scope of the coupling substrates (the boronic acids and the phenols) and limitations and optimization of the *Chan-Evans-Lam* reaction conditions to the biaryl ethers were investigated.

5.1.1 Optimization of Chan-Evans-Lam cross couplings

In the beginning *Chan-Evans-Lam* were investigated using model substrates, which were subjected to the original literature reaction conditions[60] in order to explore the limitations. The simple aryl boronic acid **134a** (3 equiv.) coupled to *para*-methyl phenol **135** (1 equiv.) in the presence of a stoichiometric amount of $Cu(OAc)_2$, 5 equivalents of pyridine and powdered 4 Å MS in dichloromethane under oxygen (1 atm.) to give the cross coupling product **136** with 75 % yield. However, the electron rich *ortho*-methoxy substituted boronic acid **134b** reacted with *para*-methyl phenol **135** under the same conditions resulted in a poor 21 % yield (Scheme 30).

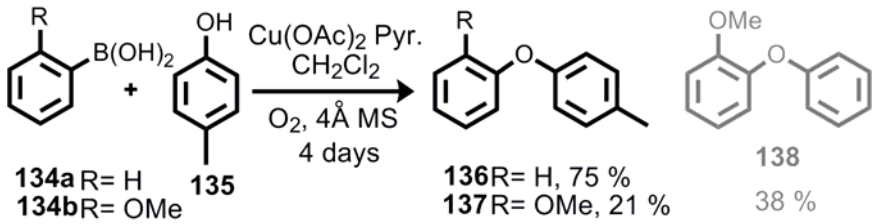

Scheme 30 *ortho*-methoxy boronic acid under the cross coupling conditions.

It was found that the reactivity difference between the two boronic acids **134a** and **134b** can be explained by the dissimilar stabilities of the boronic acid. The electron rich *ortho*-methoxy substituted boronic acid was prone to hydrolysis or decomposition under the oxidative reaction conditions (Figure 10). After stirring for 4 days under the reaction conditions, the by-products **139** and **140** were observed by GCMS monitoring[60]. Additionally, less apparent homo coupling by-product **138** was isolated in 38 % yield, which appears to have originated from the cross coupling between *ortho*-methoxy boronic acid **134b** and phenol **141** (Scheme 30).

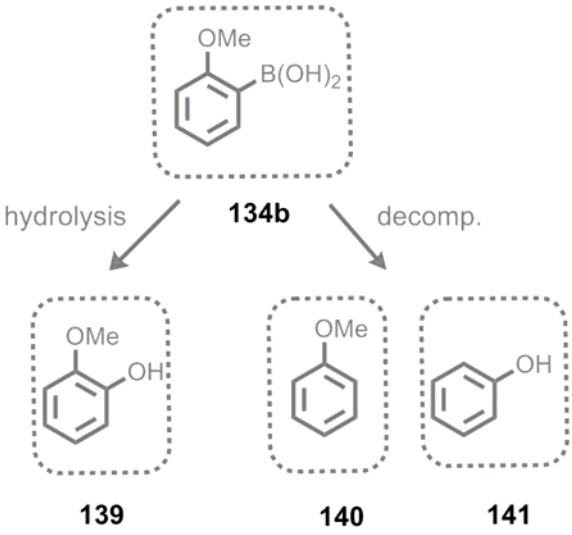

Figure 10 Boronic acid decompositions.

The cause of these side reactions and resulting diminished yields are not fully clear, but are probably related to competitive arylation of water and hydrogen peroxide potentially formed by reduction of O_2, and/or subsequent competition with *para*-methyl phenol (**135**). To solve this problem, molecular sieves were added[60] as a scavanger for H_2O and H_2O_2. This may also lead to boroxine formation.[103] We found the optimal amount of powdered 4 Å MS to be 800 mg/0.5 mmol boronic acid. This partially suppressed the partial decomposition pathways and formation of **138** and it increased the yield of **137** from 21 % to 40 %.

In order to enlarge the scope of the reaction for further applications, for example on isodityrosine **125** synthesis, sensitive α-amino acids were studied for *O*-arylations. Fmoc-protected amino acids and peptides were preferantially investigated to test for compatibility with typical Fmoc solid phase synthesis substrates. Reported conditions for the arylations of phenols with boronic acids feature stoichiometric $Cu(OAc)_2$, a tertiary amine base, molecular sieves, an O_2-containing atmosphere, and an excess of boronic acid (typically 3 equiv.).[59,60,72] In initial studies for tyrosine derivatives, these parameters were checked with compound **142** and phenyl boronic acid

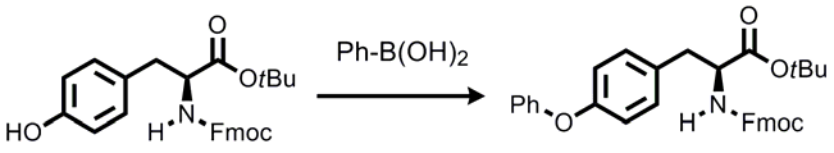

142 **143a**

Scheme 32 Fmoc-Tyr-O*t*Bu and phenyl boronic acid were used for the further optimization of *Chan-Evans-Lam* coupling as model substrates. **142** (1 equiv.), $Cu(OAc)_2$ (20 mmol %), pyridine (5 equiv.), 4 Å MS, $ClCH_2CH_2Cl$/DMF 19:1, slow addition of $Ph(BOH)_2$ (1.4 equiv., 16h), 5 % of DMF was added to the solvent.

Pyridine as a base was found to be superior over aliphatic tertiary amines such as triethyl amine (NEt_3) or *N,N*-disopropylethyl amine ($EtN(iPr)_2$). Furthermore, no reaction was observed in the presence of 2,6-lutidine, nor in the presence of dimethylaminopyridine DMAP[104]. Only the degradation of starting material was observed in this case and no conversion to the desired product occured. Delightfully, the reaction tolerated reducing the amount of $Cu(OAc)_2$ to catalytic amounts, which had no precedent[105] in the literature with α-amino acids substrates. Using an oxygen atmosphere as an oxidant and activated molecular sieves was mandatory for the success of this transformation. In our observations, chlorinated solvents gave best results, but the addition of DMF was tolerated to enhance substrate solubility. The large excess of boronic acid was deemed most critical for further applications on complex substrates. It was found that low addition of the boronic acid to the catalyst with a syringe pump allowed to achieve high conversions with only a slight excess of arylating reagent. These optimized conditions were then tested on a range of boronic acids. All reactions were run at room temperature. Increasing the tempreature did not improve the conversion towards the desired product, but increased competing the hydrolysis of boronic acid.

A panel of commercially available boronic acids was studied next (Scheme 33). Both electron-rich (**143b** and **143d**) as well as electron-poor boronic acids (**143c**) could be reacted under these conditions. However, in general they were found to be less efficient than the parent compound $PhB(OH)_2$. Steric hindrance was tolerated only for electron-poor substrates (cmp. **143c** (88 %) with **143e** (29 %) and **143f** (n.d)). Heterocyclic boronic acids (**143g** and **143h**) seemed to be unstable under the reaction conditions. Slow addition of the boronic acids resulted in a significant increase in yield for all the boronic acids tested except for the very stable phenyl boronic acid (**143a**), indicating the importance of the slow addition of the sensitive boronic acids.

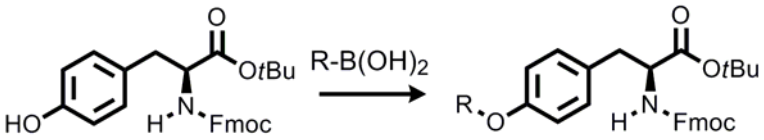

142 **143a**

entry	R	yield of **143** (%)[b]	conv. (%)
a	Ph	82 (80)[c]	>99
b	2-$MeOC_6H_4$	93 (45)[c]	41
c	2,4,6 $(F_3C)C_6H_2$	88 (40)[c]	40
d	4-PhC_6H_4	83 (38)[c]	72
e	1-naphtyl	29 (10)[c]	38
f	2,4,6-$Me_3C_6H_2$	n.d	<5
g	3-pyridyl	n.d	<5
h	2-benzothiophenyl	n.d	<5

Scheme 33 Arylation with boronic acids: **142** (1 equiv.), $Cu(OAc)_2$ (20 mmol %), pyridine (5 equiv.), 4 Å MS, DCE, slow addition of $R(BOH)_2$ (1.4 equiv., 16h), 5 % of DMF was added to the solvent, [b] based on recovered **142.** [c] yields without slow addition of syringe pump.

The scope of the phenols used in this reaction was also investigated. Coupling was performed using phenyl boronic acid and utilized the optimized *Chan-Evans-Lam* cross coupling conditions. Starting from commercially available tyrosine *tert* butyl ester (**144c**), tyrosine derivatives **142, 144a, 144b** were prepared. The detailed synthesis of **144a** and **144b** will be presented in the next chapter (5.2.2.3).

The substrate **142** was prepared by the treatment of tyrosine *tert* butyl ester (**144c**) with Fmoc-OSu and DIPEA in dichloromethane/methanol. After recrystalization, **142** was obtained in 92 % yield.

With $PhB(OH)_2$ as the reagent, the tyrosines **142** and **129** were cleanly arylated in very good yields of 82 % and 95 % respectively. The free amines **144a** and **144b** were also found to react, albeit with lower efficiency. The secondary amine **144a** afforded the desired product **145** with a 63 % yield. However, in the case of the primary amine **131,** an aryl transfer to the nitrogen was observed in favor of *O*-arylation, indicating a delicate balance of nucleophilicity and steric factors. The carboxylic acid **144b** remained unreactive.

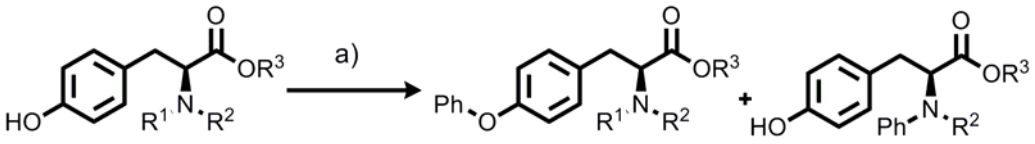

144 **145** **146**

Phenol	R^1	R^2	R^3	yield of **145** %	yield of **146** %	conv. (%)
142	H	Fmoc	*t*-Bu	82	-	>99
129	Me	Fmoc	*t*-Bu	95	-	>99
144a	H	Me	*t*-Bu	63[b]	-	64
131	H	H	*t*-Bu	-	55[b]	80
144b	H	Fmoc	H	-	-	<1

Scheme 34 Chemoselectivity of the arylation of tyrosines: a) Phenol (1 equiv.), $Cu(OAc)_2$ (20 mmol %), pyridine (5 equiv.), 4 Å MS, ClC_2H_4Cl, slow addition of $Ph(BOH)_2$ (1.4 equiv., 16h). [b]Based on recovered phenol-

To take this methodology one step further, short peptides were prepared on suitable solid phase linkers. **147a** was prepared on Wang resin and after acidic cleavage the free acid was obtained in 81 % yield. The tripeptide allyl ester **147c** was prepared by treatment of **147a** with allyl bromide in the presence of $NaHCO_3$ in DMF, which gave **147c** in 43 % yield. **147b** was prepared on a Rink amide linker and after acidic cleavage with TFA/Et_3SiH/H_2O (95:2.5:2.5) the *C*-terminal tripeptide amide **147b** was obtained in a 85 % yield.

The tyrosine containing peptides **147a**-**c** were then used (Scheme 35) for the investigation of backbone modification of short peptides. The substrates were dissolved in dichloroethane/DMF 1:1 as a reaction medium to ensure solubility of all components. In contrast to the previously investigated carboxylic acid **144b**, peptide **147a** underwent clean *O*-arylation at the tyrosine residue (**148**), albeit at a slow reaction rate. For the less acidic C-terminal amide **147b**, selective conversion to the C-terminal amide **149** with no reaction on phenol could be achieved. Increasing the amounts of reagent and catalyst led to the formation of the doubly arylated product **150**, however in a low isolated yield (18%).

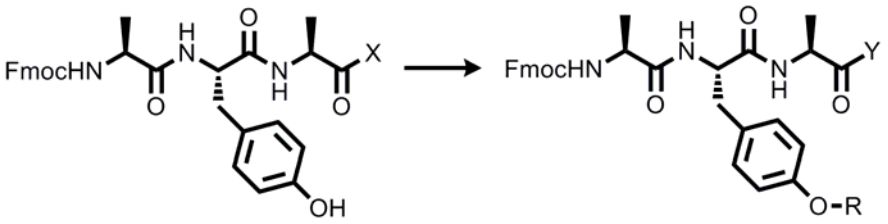

147

148 (Y=X, R=Ph)
149 (Y=NHPh, R=H)
150 (Y=NHPh, R=Ph)

147	X	yield of **148** (%)	yield of **149** (%)	yield of **150** (%)	conv. (%)
147a	OH	50	-	-	80
147b	NH_2	traces	68	18	44
147c	OAll	60	-	-	>99

Scheme 35 Arylation of tyrosine containing peptides. **147** (1 equiv.), $Cu(OAc)_2$ (20 mmol %), pyridine (5 equiv.), 4 Å MS, DCE-DMF (10:1), slow addition of $Ph(BOH)_2$ (1.4 equiv., 16h).

In contrast, ester **147c** could be cleanly transformed to the biaryl ether derivative **148,** clearly demonstrating the importance of an inert *C*-terminal functionality for this transformation.

The reaction conditions were applied next to the peptide **151** containing multiple tyrosine residues in order to study if multiple backbone modifications can be executed in parallel. The same conditions as in the case of tripeptides **147** (Scheme 36) were used including the DMF addition to insure adequate solubility. Similarly to **147c**, Peptide **151** underwent *O*-arylation at the tyrosine residue (**152a**) in the presence of 1.4 equiv. of phenyl boronic acid, albeit at slow reaction rate. Increasing the amount of boronic acid to 2.8 equiv and catalyst to 40 mmol % led to the formation of the doubly arylated product **152b** in a 44 % yield. The overall conversion reached 90 % when 5 equivalents of boronic acid and a stoichiometric amount of $Cu(OAc)_2$ was used. However, mono **152a** (31 %), double **152b** (44 %) and triple arylated peptides **152c** (22 %) were isolated in parallel. Mono and double arylated products were isolated as regioisomeric mixtures which could not be separated.

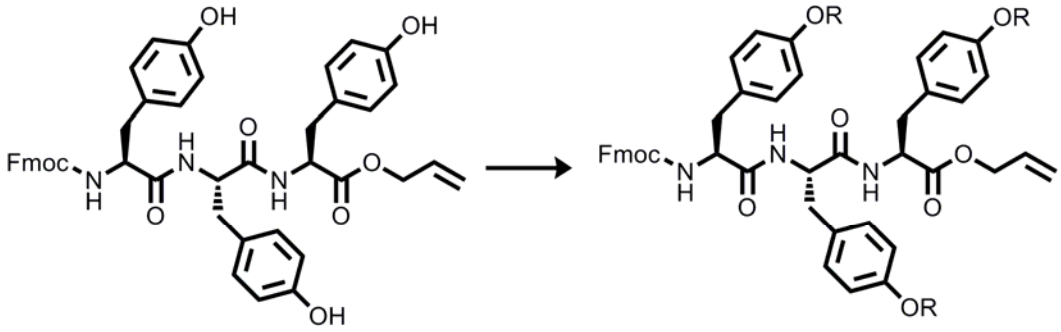

Scheme 36 Arylation of tyrosine containing peptides. **151** (1 equiv.), $Cu(OAc)_2$ (1 equi.v), pyridine (5 equiv.), 4 Å MS, DCE-DMF (10:1), slow addition of $Ph(BOH)_2$ (5 equiv., 16h), 3 days, rt.

The reactivity of the longer chain peptide esters (**153** and **155**) was generally similar to the peptides shown above, but in these cases pronounced cleavage of the *N*-terminal Fmoc group was observed. Free serine in peptide **155** was not tolerated and led to the formation of a variety of truncated products, many of them indicating a cleavage of the *N*-terminal serine residue. In contrast, the hydrophobic peptide **153** gave the backbone modified peptide **154** in a yield of 56% after complete Fmoc removal. From this data it can be reasoned that in contrast to a primary amide, sterically less accessible secondary amide bonds are well tolerated, allowing peptides to be used as substrates. A competitive coordination of the peptide backbone to the catalytically active species might account in these cases, for reduced conversions and the partial cleavage of the Fmoc group, since this was only observed for the longer chain peptides **153** and **155**.

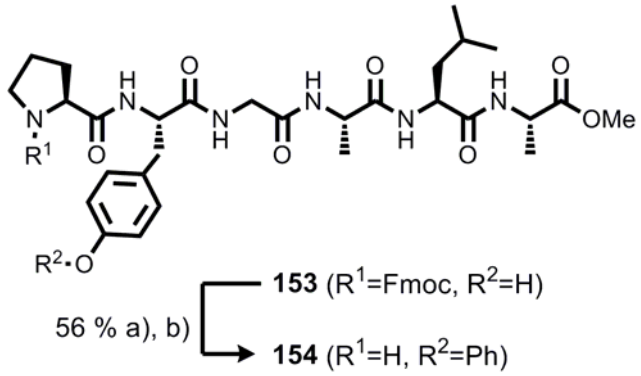

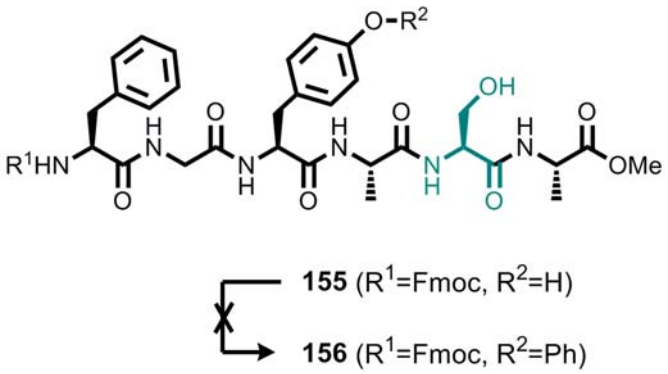

Scheme 37 Arylation of hexapeptide side chains: Reagents conditions: a) $Cu(OAc)_2$ (1 equiv.), pyridine (5 equiv.), 4 Å MS, O_2 (1 atm), DCE-DMF (1:1), slow addition of $PhB(OH)_2$ (2 equiv., 48 h), b) $HNEt_2$-CH_2Cl_2 (1:1), 30 min.

5.1.2 Conclusions

The *Chan-Evans-Lam* cross coupling conditions were optimized using α amino acids as the phenol containing substrates. It was found, that slow addition of the boronic acids greatly enhanced the yields and reaction efficiency. Electron rich boronic acids were able to give the cross coupling products in reasonable to good yields. It has been shown that sterically hindered boronic acids tolerated the optimized reaction conditions only if they were electron poor. Heterocyclic boronic acids were found to be unstable.

Reactivity of the tyrosine *t*Bu esters studied followed the substitution of amine groups present; tertiary carbamates > secondary carbamates > secondary amines. In the case of primary amines, the nucleophilicity of the amine was found to favor arylation of the amine rather than of the phenol in an oxidative copper(II) environment. Overall nucleophilicity and steric factors need to be carefully adjusted to achieve optimal results. The tyrosine derivative containing a free carboxylic acid generally remained unreactive, except in the tripeptide (**147a**), which was able to react with phenyl boronic acid to yield the backbone modified tripeptide. The reactivity of tripeptide **147** was dependent on the functionality of the C terminus. The tripeptide containing the allyl ester (**147c**) was arylated smoothly, while the arylation of amide-containing tripeptide (**147b**) was unclean. This later problem may be caused by the tendency of amides to strongly bind to copper ions.

Post-translational modifications of peptide backbones in biological settings may result in multiple functionalizations. Therefore, the *Chan-Evans-Lam* method was tested to investigate the possibility of multiple arylations using the tripeptide allyl ester **151.** The

efforts towards the fully arylated product **152c** were unsuccessful and a mixture of products such as mono-, di- and tri- arylated tripeptides were isolated. All these results indicated that the *Evan-Chan-Lam* coupling can be used to site-specifically modify complex peptide substrates, but side chains and terminal functionality prone to intract with the copper catalyst should be avoided, even in a strongly competitive solvent (DMF).

5.2 RA-VII synthesis

5.2.1 Building block synthesis

The structure of RA-VII (**4**) contains three *N*-methylated tyrosine derivatives which had to be prepared. Two of these tyrosine building blocks (**128** and **126**) were *O*-methylated on the phenol, while the third derivative carried a free phenol (**129**) which should be further cross coupled with the boronic acid derived tyrosine (**128**) to afford **125**. Furthermore, the isodityrosine building blocks should be prepared by selective deprotection of **125** to afford amine **121** and carboxylic acid **127**. Two racemization-free *N*-methylated amino acid preparation methods have been investigated in this work. The synthesis of all three tyrosine building blocks were designed based on the shortest sequence and most efficient approach.

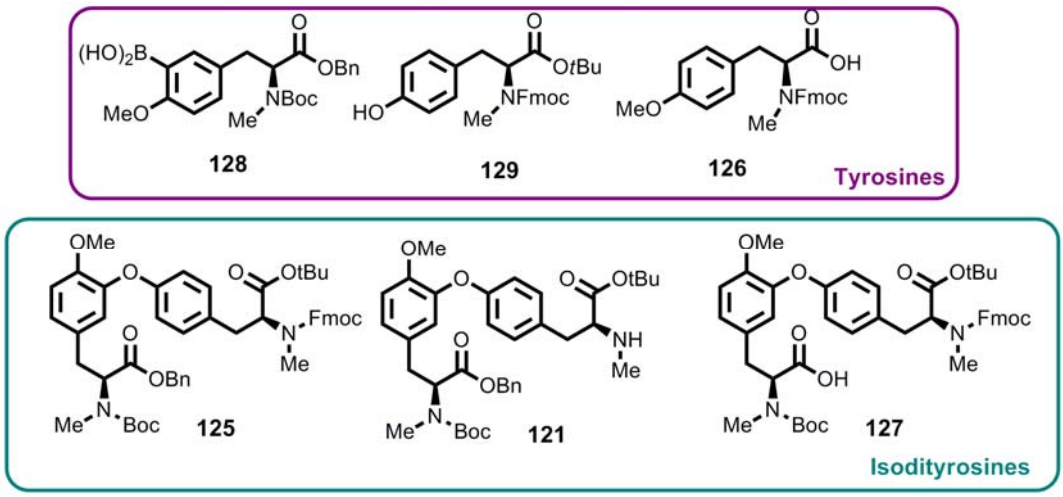

Figure 11 Required tyrosine building blocks for the synthesis of RA-VII (**4**). First generation: tyrosine monomers. Second generation: Isodityrosines.

5.2.2 Tyrosine building blocks

5.2.2.1 *L*-*N*Me-Tyr-(*O*Me)-OH building block (126)

The multi-gram scale preparation of tyrosine building block **126** was realized in a 7 step procedure in 66 % overall yield (see Scheme 38). Starting from commercially available L-tyrosine **132**, initial regioselective benzyl ester formation was achieved through a toluene sulfonic acid salt with 80 % yield.[106] In the beginning of the synthesis sequence amine protection by Cbz was introduced because the base labile

Fmoc necessary for the solid phase strategy would not withstand the reaction conditions for alkylations. Hence, it should be introduced at the later stage. After the Cbz protection of the free amine (87 % yield), methylation of phenol **158** was performed in the presence of MeI and gave the desired product **159** in 80 % yield. The *N*-Cbz and benzyl ester groups were quantitatively deprotected in one pot by hydrogenation over 2h to give amino acid **160**. Building block **126** required the amine functionality to be Fmoc protected for further reactions. As such, the resulting free amine **160** was protected in 60 % yield using FmocOSu.

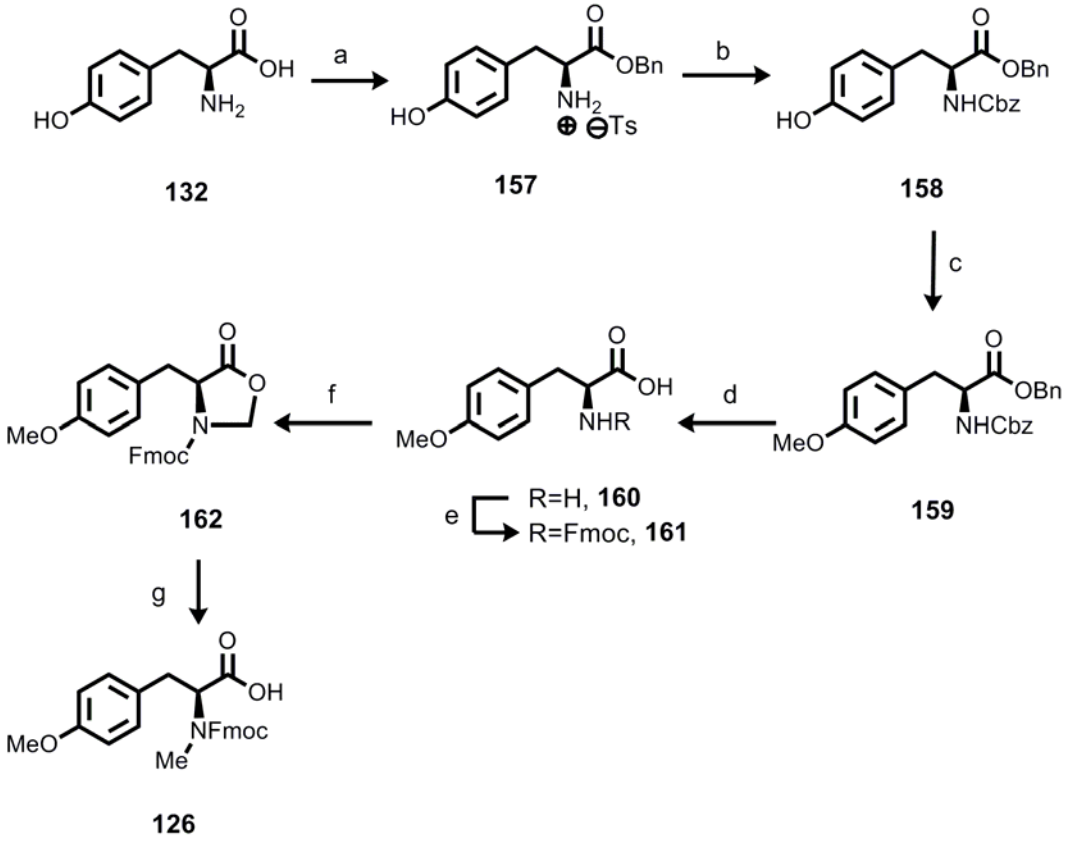

Scheme 38: Synthesis of tyrosine building block **126** for the tetrapeptide unit of RA-VII. a) BnOH, p-TSA, TsCl, reflux, 5h, 80 %; b) Cbz-Cl, Et_3N, MeOH, 0°C – rt, 2h, 87 %; c) K_2CO_3, MeI, DMF, rt, 16h, 80 %; d) H_2 Pd/C, MeOH/HCOOH, rt, 2h, quant. e) FmocOSu, CH_2Cl_2, 0°C - rt, 5 h, 60 %; f) $(CH_2O)_n$, toluene, reflux, 16h, 78 %; g) Et_3SiH, TFA/CH_2Cl_2 1:1, rt, 16h, 79 %.

To introduce the *N*-methyl group with little or no racemization, the method from Freidinger[107] was explored. Formation of a oxazolidinone-5-one was achieved by a condensation with paraformaldehyde in the presence of pyridine paratoluene sulfonic acid, resulting in the cyclic **162** in 70 % yield.

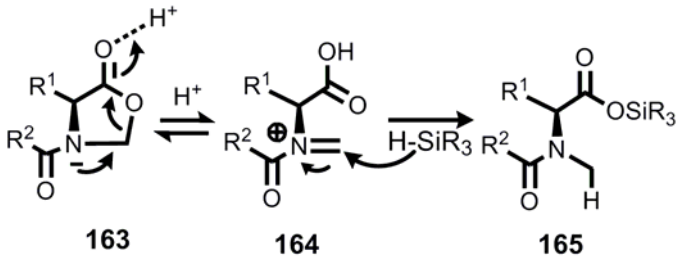

Figure 12 Mechanism for *N*-methylation by reductive cleavage of an oxazolidinone.

Then, the oxazolidine-5-one ring (**162**) was opened under the acidic conditions to an *N*-acyl imminium ion (**164**) and reduced *in situ* with silane to install the *N*-methyl functionality (**126**) in 79 % yield.[108]

In summary, the tyrosine building block **126** was conveniently *O*- and *N*- methylated and Fmoc protected from tyrosine in reasonably high yields. It is an important building block required for the solid phase synthesis of the target tetrapeptides and hexapeptides. Multi gram synthesis of **126** was achieved with this method. In order to find the optimal separation conditions **126** was partially racemized by treatment with excess potassium *tert* butoxide in DMF at 60°C to yield a mixture of *R* and *S* enantiomers of **126** (data not shown). This sample used as a reference for the enantiomeric purity determination of **126** by chiral HPLC (97:3, 94 % ee).

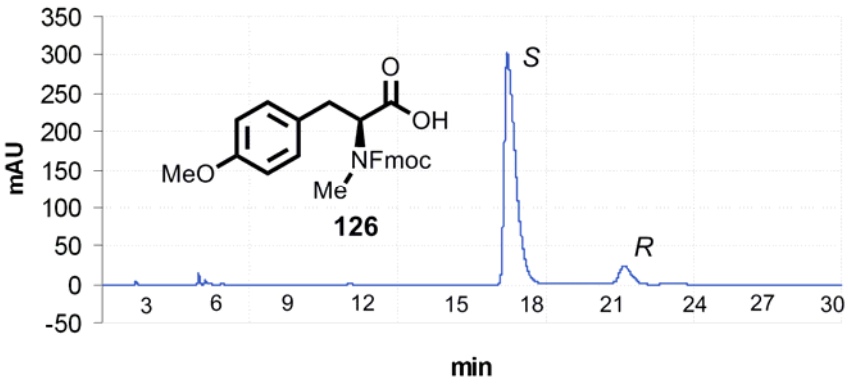

Figure 13 Enantiomeric excess determination of **126** by chiral HPLC. IC-(250 x 4.6 mm): 10% CH_2Cl_2 + 2% EtOH, 90% *i*-Hexane (30 min.).

5.2.2.2 *Boronic acid building block*

The biaryl ether moiety is a key unit for the total synthesis of RA-VII (**4**). Our methodological study had shown that *Chan-Evans-Lam* coupling should allow smooth synthesis of isodityrosine **125** under mild conditions.

This method, however, is limited by the preparation of an appropriate boronic acid building block. Therefore a method to produce enantiomerically pure boronic acid **128** on a multi-gram scale through a 7 step synthesis (Scheme 39) was developed.

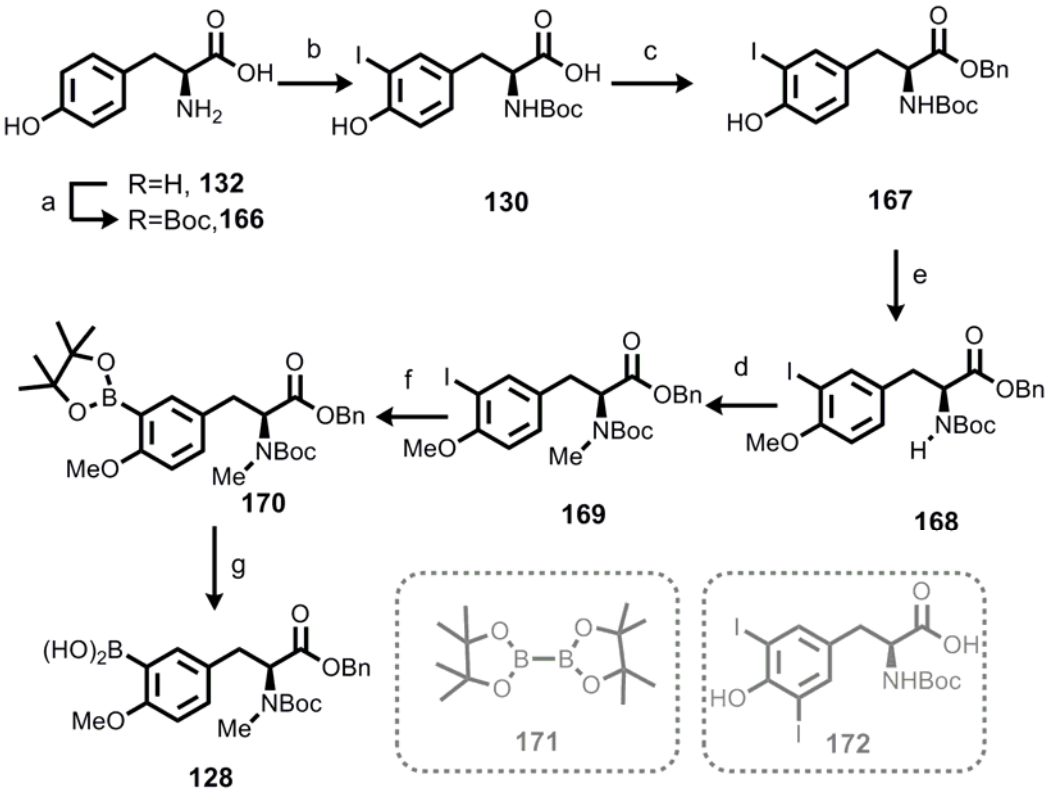

Scheme 39 : Synthesis of boronic acid coupling partner **128** for *Chan-Evans-Lam* cross coupling a) Boc_2O, 2 M aq. Na_2CO_3, THF, RT, 3 h, 90 %; b) I_2, NH_4OH, 95 % EtOH, 0°C, 1h, 63 %; c) BnBr, DIPEA, acetone, rfx, 16 h, 72 %; d) MeI, Na_2CO_3, acetone, rfx, 16 h, 92 %; e) MeI, Ag_2O, DMF, 35°C, 8h, 72 %; f) 1.1 eq. **171**, 113,3 % mol $PdCl_2$(dppf), KOAc, DMF, 80°C, 16 h, quant.; g) $NaIO_4$, acetone/NH_4OAc, RT, 36 h, 71 %.

First, tyrosine was *N*-Boc-protected under standard conditions in high yield (90 %) to give *N*-Boc-tyrosine **139**, which was iodinated at the *ortho* position uder the action of iodine and aqueous ammonia. This gave the functionalized tyrosine **130** in a 63 % yield on large scale, with only little of the bis-*iodo*-compound **172** being formed. Iodination of L-tyrosine **132** itself was also investigated, however, the desired

compound was difficult to separate by column chromatography from the doubly iodinated side product. Selective benzyl ester formation was achieved in the presence of benzyl bromide and DIPEA in 72 % yield and the resulting tyrosine benzyl ester **167** was subsequently methylated at the phenol oxygen to give **168** in 92 % yield.

Early in the course of our synthesis, we found that **168** has poor reactivity towards *N*-methylation and many known literature procedures[109] for the alkylation of the carbamates were unsuccessful. For example base mediated allylations led to excessive over reaction, ester cleavage, and recemisation. The method[108] of *N*-alkylation with MeI *via* Ag_2OxH_2O activation was therefore investigated as an alternative method to synthesize the substrate **169**.

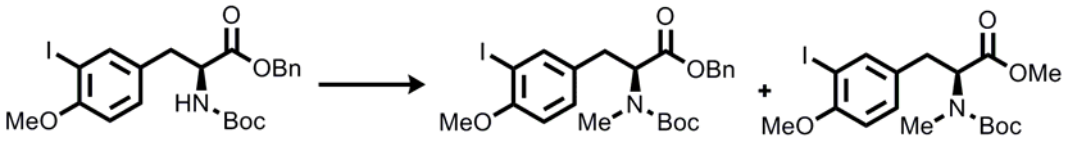

Entry	scale (mmol)	Ag_2OxH_2O (equiv.)	T (°C)	t (h)	**169** (%)	**173** (%)	conv. (%)
1	2	0.5	r.t	16	n.d	2	50
2	2	1	32	16	n.d	2	80
3	2	2.4	45	16	40	58	> 99
4	**2**	**2.4**	**45**	**8**	**90**	**7**	**> 99**
5	20	2.4	45	8	68	25	> 99
6	**45**	**2.4**	**45**	**5**	**72**	**15**	**> 99**

Scheme 40: Optimization of the *N*-Alkylation of **168**. These reactions were carried out in DMF under argon and in darkness.

Preliminar studies showed successful conversion to methylated tyrosine **169** using this method. However, since the R_f values of the substrate **168** and the product **169** were identical in normal phase TLC conditions, the reaction had to be optimized up to full conversion in order to isolate the pure desired compound **169.** The starting material consumption could be improved from 50 % (Scheme 40, entry 1 and 2) to >99 % (Scheme 40, entry 3 and 4) by increasing the amount of Ag_2O (excess) used and warming the reaction to 45°C. Together with desired **169**, side product **173** was

also produced in a 1:1 ratio (Scheme 40, entry 3). The reaction time was decreased to 6 h, which reduced the side product formation on a 2 mmol scale (entry 7). Unfortunately, this trend did not transfer to reaction scale-up (20 mmol) and the 1:1 ratio was again found on this scale (entry 5). Better conditions for synthesis were found using an excess of MeI in the presence of 2.4 equiv. of Ag_2O in DMF at 45°C for 5 h (entry 6). The formation of **173** was significantly decreased (21 %) but could not be eliminated. Freshly prepared Ag_2OxH_2O was vital for the full conversion of **168,** however, it did not prevent the formation of the side product **173**. The desired product **169** seemed to be prone to transesterification under the reaction conditions, resulting in the formation of the side product. Longer reaction times increased the formation of the side product **173**, minimizing the amount of product **169** isolated.

A plausible mechanism for the activation of this type of unreactive carbamate by silver oxide is shown in Scheme 41. Both carbonyl groups many weakly coordinate to the Ag_2O x H_2O solid surface to the carbonyl (**174**), which shields the carbonyl oxygen and serves to bring the MeI and the amine of the carbamate into proximity. Spontaneous attack of carbamate nitrogen on strongly coordinated MeI releases the Ag^+ complex by *N*-methylating the carbamate. However further direct attack of carbonyl to activated MeI may result in oxonium ion **175** which after attack of any nucleophile on the benzylic carbon will produce a net transesterification and afford methyl ester **173** as a side product.

The benzyl ester functionality also played a considerable role in initiating side product formation as sterically hindered *t*Bu-ester types did not undergo transesterification under the same reaction conditions (*vide infra*). Furthermore, the strong dependency of side product formation on the scale indicates that surface effects on the inorganic salt contribute to the facility of this side reaction.

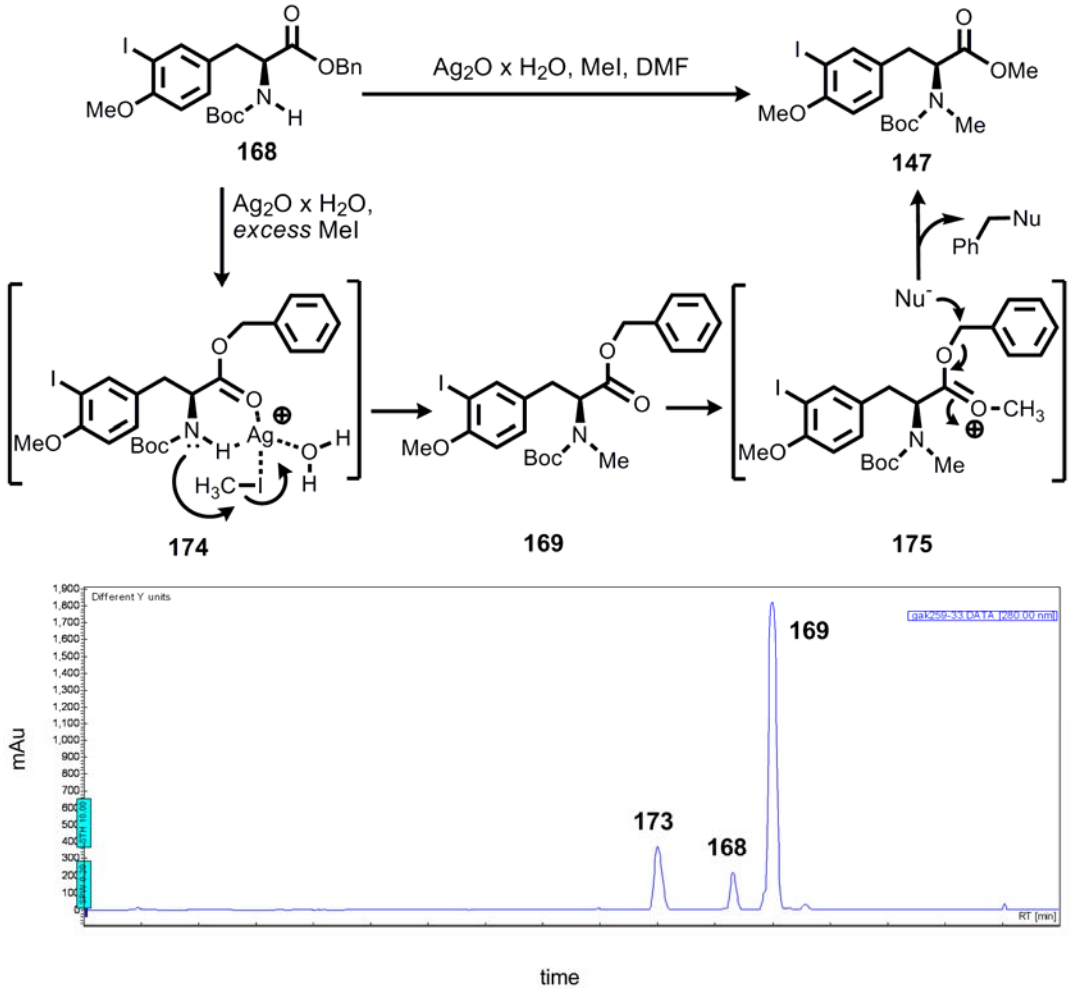

Scheme 41: Plausible mechanism for the formation of the *N*-methylation product (**169**) *via* *N*-activation of carbamate by silver oxide and further reaction to form side product **173** and the high performance liquid chromatography (HPLC) trace of the reaction mixture.

The procedure could be conducted on preparative scale (45 mmol) with good efficiency and delivered enantiomerically pure *N*-methylated tyrosine derivative **169**. The enantiomeric purity was determined by chiral HPLC (Method-RP-Ch-1, see 8.1). In order to find the optimal separation conditions of the two enantiomers, **169** was racemized by treatment with excess potassium *tert*-butoxide in DMF at 60°C to yield a 1: 1 mixture of *R* and *S* enantiomers (**150**). After optimizing the chiral HPLC column conditions for the racemic mixture, untreated **169** was injected and showed and exceptional purity of > 98 % ee (Figure 14).

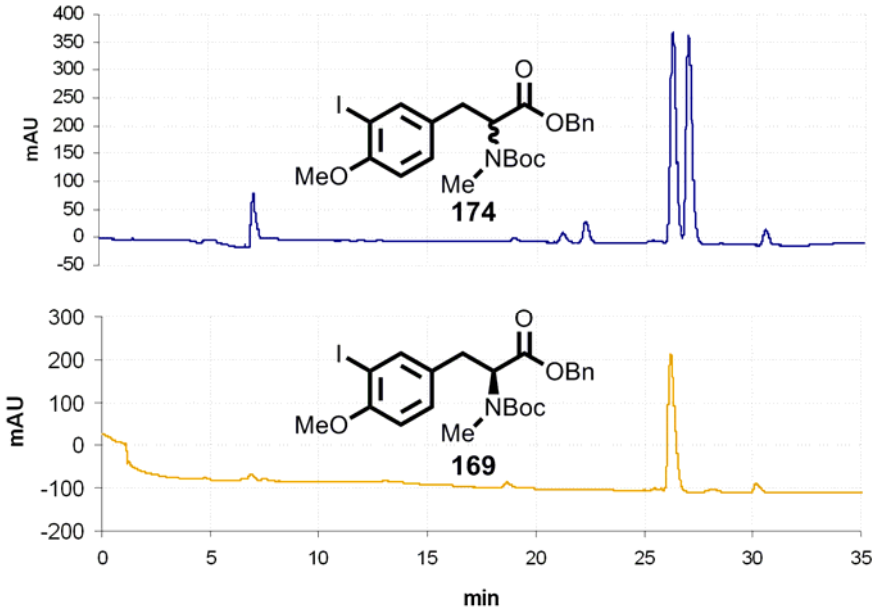

Figure 14 Determination of excess enatiomeric of **169** by chiral HPLC. Conditions are given in section 8.

After the successful preparation of enantiomerically pure **169**, boronic ester **170** was synthesized by the treatment of **169** with bis pinacol boronate (**171**) in the presence of Pd(0) and KOAc in DMSO.[110] The material such obtained was used directly in the next step.

A general catalytic cycle for Pd(0) mediated transmetalation to boron is shown in Scheme 42.[110] It initiates with the oxidative addition of **175** to coordinatively unsaturated Pd(0), follows by ligand exchange with KOAc. Transmetallation occurs by the addition of bis pinacol boronate (**171**) and product **176** is liberated by reductive elimination of the Pd(II) complex **182**.

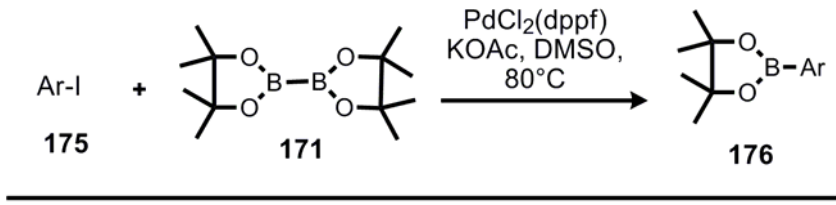

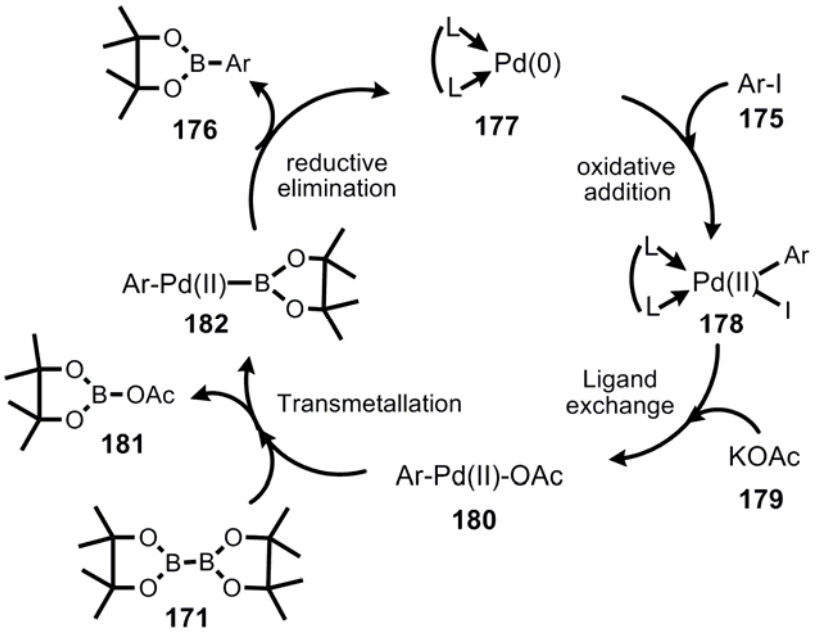

Scheme 42 Mechanism of Pd(0) catalyzed cross couplings with alkoxyboron[110].

Boronates can be readily hydrolyzed under acidic conditions (pH=3). However, simple hydrolytic procedures[111] only gave conversions of around 20 % for the synthesis of **128**, presumably because the acid mediated equilibrium favors the starting boronate ester.

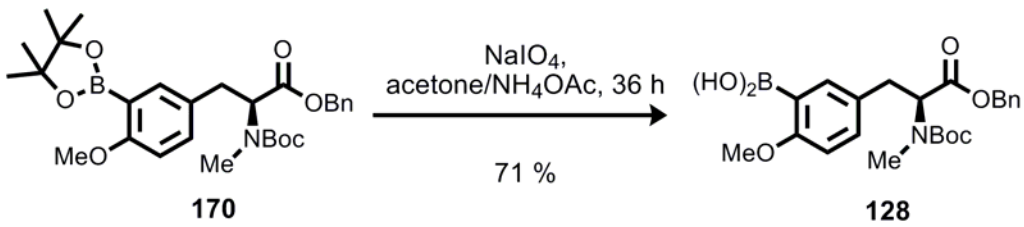

Scheme 43 Boronic ester hydrolysis under acid media.

Oxidative hydrolysis of the boronate **170** in neutral media was then investigated. Boronate **170** gave the boronic acid **128** a 71 % yield in two steps. This method[112] allows for the separation of the diol side product (**184**) from the desired product **128** *via* oxidative cleavage in the presence of sodium peridodate. Sodium periodate is an electrophilic oxidant reacting with the cleaved diol to produce 2 mol equivalents of acetone, which do not interfere with the reaction anymore.

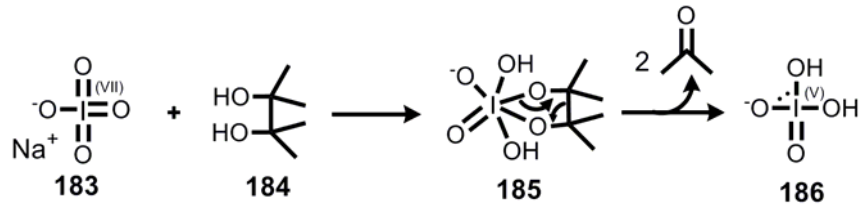

Scheme 44 Oxidative removal of diol **184** from the equilibrium during boronic ester hydrolysis.[112]

5.2.2.3 Phenol building block (129)

For the synthesis of isodityrosine phenol **129** was required. This could be prepared in 5 consecutive steps on a multi-gram scale. Commercially available tyrosine *tert*-butyl ester (**131**) was first amine-protected as a benzylcarbamate group to give compound **187** in 95 % yield after recrystalization.

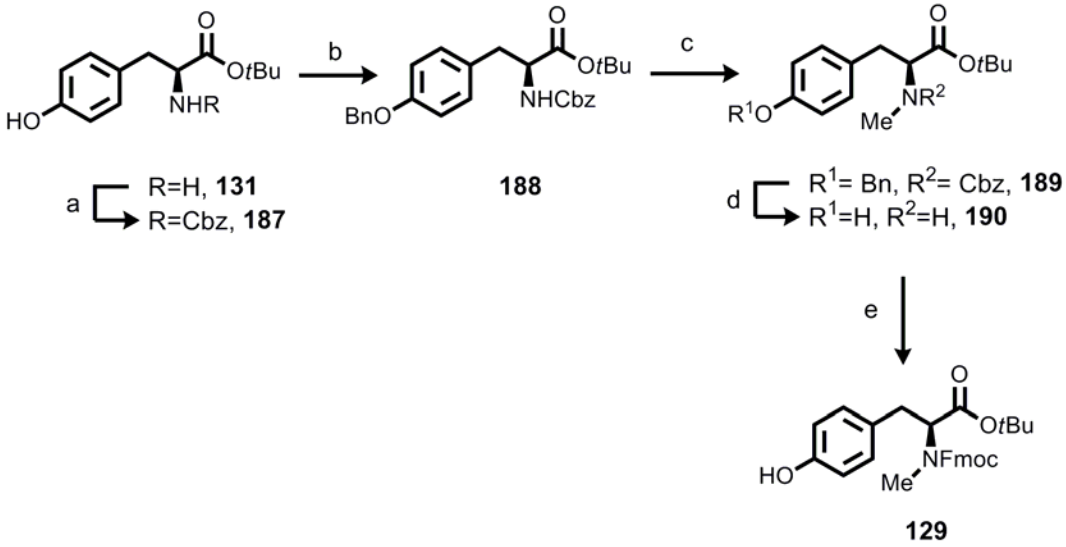

Scheme 45 Synthesis of phenol coupling partner **129** for modified *Chan-Evans-Lam* cross coupling**,** a) Cbz-Cl, Et_3N, dioxane/H_2O, rt, 16h, 95 %; b) BnBr, Na_2CO_3,DMF, RT, 16h, 96 %; c) Ag_2O, DMF, RT, 5h, 94 %, > 98 % ee; d) 10% Pd/C, H_2, MeOH/HCOOH, RT, 16h, quant.; e) Fmoc-OSu, DIPEA, DCM, 0°C→RT, 4h, 77 %.

Treatment of **187** with benzyl bromide in the presence of an inorganic base afforded transiently protected phenol **188** in 96 % yield. Successive *N*-methylation with MeI in DMF in the presence of Ag_2O x H_2O as previously established gave compound **189** in 94 % yield with >98 % enantiomeric excess. In this case the transesterification by-

product, which was mentioned in Section 5.2.2.2, was not observed. This may be due to steric hindrance as the carbonyl moiety is considerably more hindered in the *tert* butyl ester than in the benzyl ester case. (Figure 15).

Enantiomeric purity was again verified by chiral HPLC. To find the optimal separation again both enantiomers were needed. For this purpose **189** was partially racemized by treatment of excess potassium *tert* butoxide in DMF at 60°C to yield a (uneven) mixture of *R* and *S* enantiomers. After optimizing the chiral HPLC column conditions for the racemic mixture of **192** enantiomers, building block **189** was injected and an excellent purity of > 98 % ee was found for **189**. (Figure 16).

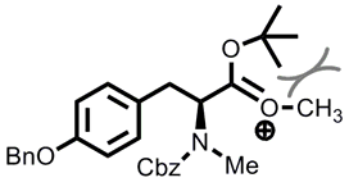

191

Figure 15 Intermediate for the sterically hindered ester.

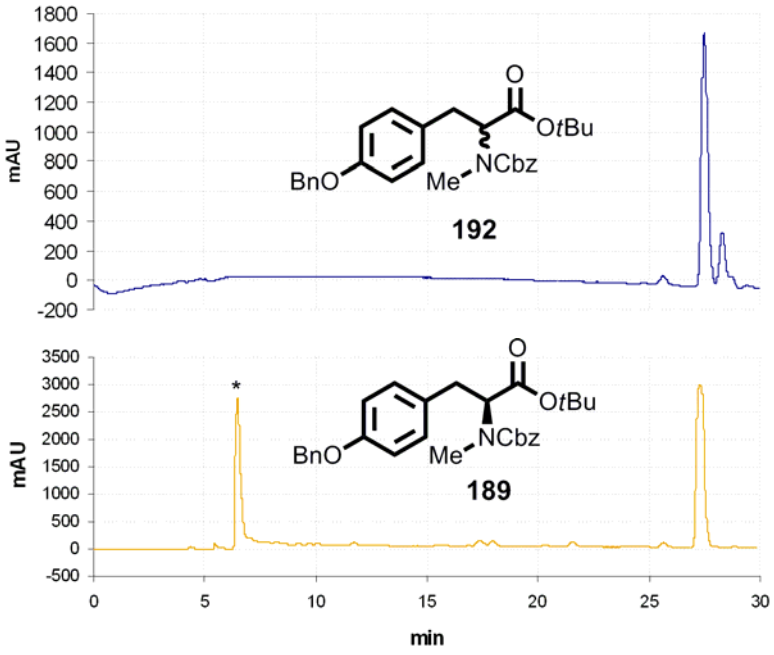

Figure 16 Determination of enantiomeric excess of **189** by chiral HPLC. Top: partially racemized compound **192** (L, D epimers). Bottom: enantiomerically pure L configured **189.** Conditions are given in chapter 5. (Method-RP-Ch-2). *Observed impurity which could not be suppressed under the chiral HPLC conditions.

5.2.3 Isodityrosine building blocks

5.2.3.1 Modified *Chan-Evans-Lam* cross coupling

Having established initial conditions of the *Chan-Evans-Lam* cross coupling with the model substrates (chapter 5.1), and being aware of the limitations of this method, the synthesis of the isodityrosine building block **125** was investigated. Initially, the reported *Cham-Evans-Lam* cross coupling method utilizing boronic acid **128** (3 equiv.), 1 equiv of phenol (**129** or **190**), 10 mmol % $Cu(OAc)_2$, 5 equiv. pyridine and powdered 4 Å MS under oxygen (1 atm.) was studied. Where phenol **129** would lead to the fully protected building block **125**, **190** would be an ideal starting material to afford **121** which can then be used for the further synthesis of RA-VII by [4+2] segment coupling (see section 5.2.5.1)

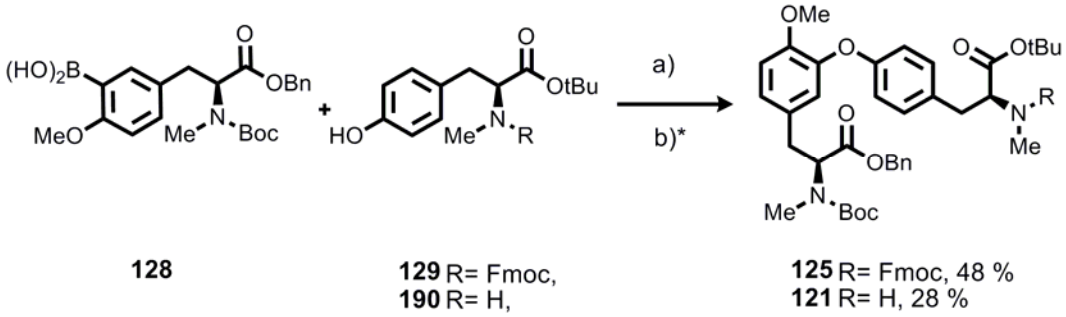

Scheme 46 Modified *Chan-Evans-Lam* cross coupling for biaryl ether subunit of RA-VII (**4**) a) **128** (3 equiv.), **129** or **190** (1 equiv), $Cu(OAc)_2$ (10 mol %), pyridine, powdered 4 Å MS, dichloroethane; b) TBDMSCl, imidazole, dimethyl formamide, rt, then column chromatography. *the second step was applied only for **125**.

The reaction proceeded when the secondary amine containing phenol **190** was coupled with boronic acid **128**, giving rise to a modest 28 % yield of the desired isodityrosine **121**. Fmoc-protected tyrosinyl phenol **129**, however, gave the desired isodityrosine **125** in much better yield (48 %). Even though the boronic acid was used in excess, full conversion of the phenol to the isodityrosine was impossible with these conditions. Since the separation of **125** from starting material **129** was extremely difficult, an additional step was applied in order to obtain pure isodityrosine. The unconsumed phenol **129** was silylated by TBDMSCl and removed by a short filtration over silica gel to afford pure **125**. The phenol **129** was then recovered by the treatment of silylated phenol **193** with TBAF in 20 % yield. (two steps).

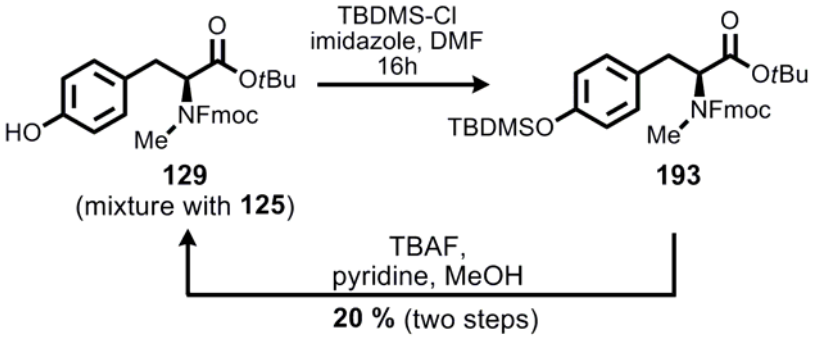

Scheme 47 A solution for the purification problem of **125**, Unconsumed phenol **129** was removed from biaryl ether **125** by the treatment of TBDMSCl.

A possible explanation for the modest efficiency for the coupling of **190** can be the chelating effect (ligand effect) of a secondary amine to the Cu(II) catalyst. However, the *ortho*-methoxy substituted boronic acid showed better efficiency (Scheme 46) than expected from the model trials (Scheme 30), indicating that this reaction is strongly substrate dependent on the boronic acid side. Using tyrosine amino acids as the phenol coupling partner gave results matching well with the previous results. Boronic acid decomposition could not be avoided completely, but it was evident from HPLC that isodityrosine formation was slightly faster than arylation by H_2O.

The low conversion due to decomposition of the boronic acid to the corresponding demetalation product or the *ortho*-hydroxy derivative had to be improved. Furthermore, saving the precious boronic acid building block (**128**) was vital to arrive at an overall effective and economic synthesis. To minimize boronic acid decomposition under these oxidative conditions, the slow addition of boronic acid was studied (table 6). Addition of boronic acid in one hour by syringe pump gave about 55 % conversion in regard to phenol consumption and 55 % yield of the desired isodityrosine **125**. (Scheme 48, Entry 1). Interestingly, slow addition of the boronic acid over 16h resulted in almost complete suppression of boronic acid decomposition and side product formation and resulted in full consumption of phenol **129**, allowing the extra purification step to be removed (entry 3). Long reaction times had no further effect. Reaction efficiency was further improved using pure oxygen (1 atm.) as atmosphere together with rigorous stirring in an oversized flask. Taking the long reaction time into account, dichloroethane was the choice of solvent for practical reasons to keep the reaction concentration stable.

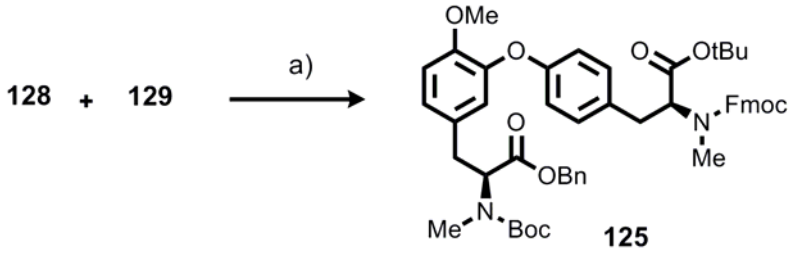

entry	conditions	yield (%)	conv. to **125** (%)
1	1h addition time	55	55
2	5h addition time	63	65
3	16h addition time	92	99
4	36h addition time	90	99

Scheme 48 Synthesis of fully protected isodityrosine **125** by modified Chan-Evans-Lam coupling. a) 1.4 equiv. **128**, 1 equiv. **129**, $Cu(OAc)_2$ (10 mol %), pyridine (5 equiv.), powdered 4 Å MS (1.6 g/ 1 mmol **128**), dichloroethane

The reaction procedure was optimized with a 16 h slow addition of boronic acid to the reaction mixture which led to the formation of **125** in 92% yield. (Scheme 48). Notably, only catalytic amount of Cu(II) (10 mol %) had to be used. Orthogonally protected isodityrosine **125** can be manipulated in order to obtain functional building blocks for the synthesis of RA-VII (**4**).

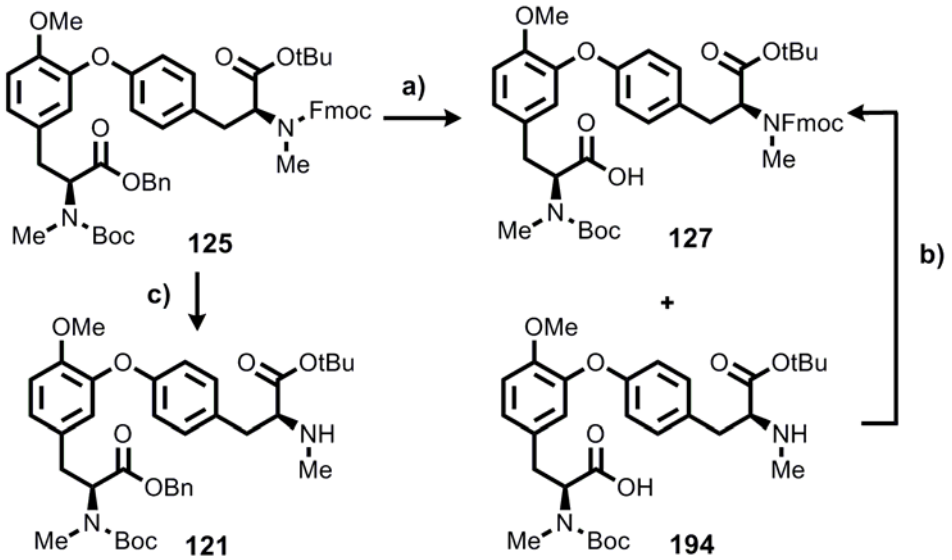

Scheme 49 Selective deprotection of Isodityrosine **125** to isodityrosine amine **121** and isodityrosine carboxylic acid **127**, a) Pd/C, H_2, MeOH, 5 min., b) Fmoc-OSu, Et_3N, DCM, 1h, 90 % (two steps); c) Et_2NH/DCM, 0°C - rt, 8h, 84 %.

The first building block **127** (terminal free acid isodiytrosine) was prepared by hydrogenation of **125** with Pd/C under H_2 in a reasonable yield of 64 %. Partial Fmoc deprotection was evident and accounted for 30 % of material (**194**). The Fmoc-deprotected fraction was easily reprotected *in situ* using Fmoc-OSu and Et_3N. The amine **121** will be a crucial segment for the linear hexapeptide construction. It was prepared by the orthogonal deprotection of the Fmoc group of **125** in Et_2NH/DCM to yield the *N*-terminal free isodityrosine **121** in 84 % yield.

5.2.4 Tetrapeptide preparation

Tetrapeptide **197** is a subunit of the RA-VII (**4**) structure. An efficient synthesis was required to have enough material continue the full synthesis of RA-VII (**4**) by following the fragment coupling approach (method a, Scheme 26). A challange was the coupling of this short peptide sequence to building block **126,** which requires special activation methods for the secondary amine of **126**.

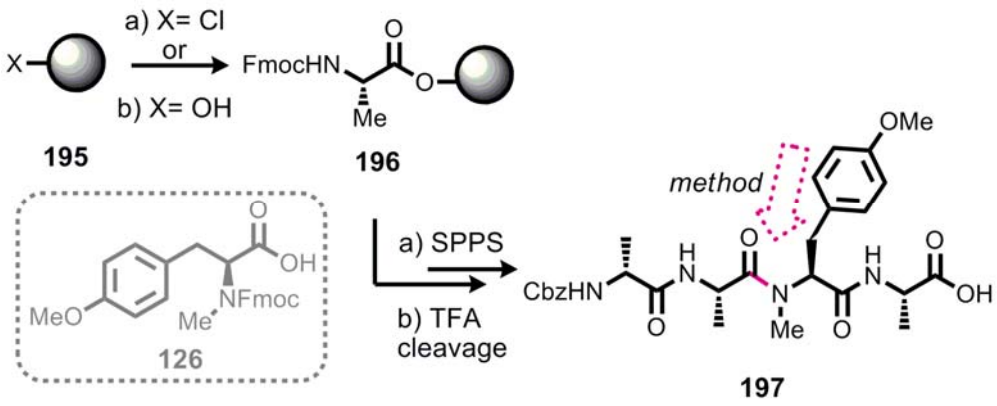

Scheme 50 Preparation tetrapeptide **197** on solid support

The tetrapeptide sequence consists of two L-alanine amino acids, one D-alanine amino acid and one *O*- and *N*- methylated L-tyrosine building block **126.** The tetrapeptide assembly was studied on three different solid supports utilizing three types of methods, in order to identify an efficient coupling between the solid support anchored secondary amine derived from **126** and L-alanine.

Initially solid phase linkers were investigated by using standard peptide coupling conditions with HOBt/HBTU (GP5) (Scheme 51, entry 1). All three solid support linkers afforded similar yields (37 – 40 %), but up to 10 % epimerization was observed during the loading of the first amino acid to Wang and Sasrin resin The solid supports require strong activation (such as DIC, DMAP) in order to link the first amino acid to the hydroxyl resin by an ester bond. The 2-Cl trityl linker did not necessitate any

carboxylic acid activation, and no epimerization was observed in this case. In order to improve the yields, different methods were investigated for secondary amide bond coupling (Scheme 51). Using O-(7-Azabenzotriazol-1-yl)-1,1,3,3-tetramethyluronium hexafluorophosphate (HATU)[113]/ 1-hydroxy-7-azabenzotriazole (HOAt)[114] (method B) was more efficient (58 - 75 %) than O-(benzotriazol-1-yl)-1,1,3,3-tetramethyluronium hexafluorophosphate (HBTU)/1-hydroxybenzotriazole (HOBt) (method A) (37 - 40 %) or bis-triphosgene (BTC)[115] (method C) (56 – 65 %). However taking coupling rates[f] into account, BTC proved to be a faster coupling reagent and led to complete coupling, while method B required double coupling.

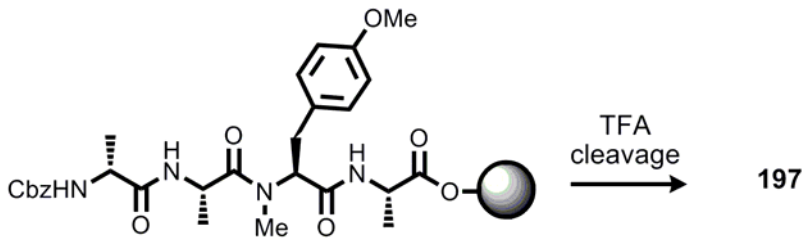

120

entry	method	yields (%)		
		Wang resin (0.62- 0.55 mmo/g)	Sasrin* (0.45 - 0.57 mmol/g)	2-Cl-trityl resin (0.55 mmol/g)
1	Method A	40 %	37 %	38 %
2	Method B	**75 %**	58 %	**65 %**
3	Method C	65 %	56 %	62 %

Scheme 51 a) Table: Optimization of tetrapeptide formation on the solid support yields after the cleavage. *Sasrin (Bachem) or HMPB-BHA (Novabiochem) (0.45 -0.57 mmol/g) was used; HOBt/HBTU (**GP5**) was used for the primary amine couplings. For the secondary amine coupling: Method 1: HOBt/HBTU, double coupling 2 x 8h (**GP5**), Method 2: HATU/HOAt, double coupling 2 x 3h (**GP6**), Method 3: Bis-triphosgene, 90 min. (**GP7**). General methods (GP) (see section 8.5).

BTC[115] is a mild coupling reagent that is believed to convert carboxylic acids into the active mixed anhydride **203**. The *in situ* formed phosgene **201** may also activate the carboxylic acid through acyl chloride **202** formation, thereby allowing two activation modes by intermediate **200** and/or **202** for this reaction and thus rendering this a

[f] Coupling rates are monitored by HPLC on a sample obtained from a test cleavage from the solid support.

powerful method. Activation is achieved in the presence of mild bases such as 2,4,6-collidine, which enables sterically hindered couplings to be performed without epimerization. However, because BTC reacts with DMF the reaction had to be executed in THF as solvent. This doubled solvent changes from DMF to THF and back render the synthesis labor intensive and inappropriate for automation, which disfavored this method.

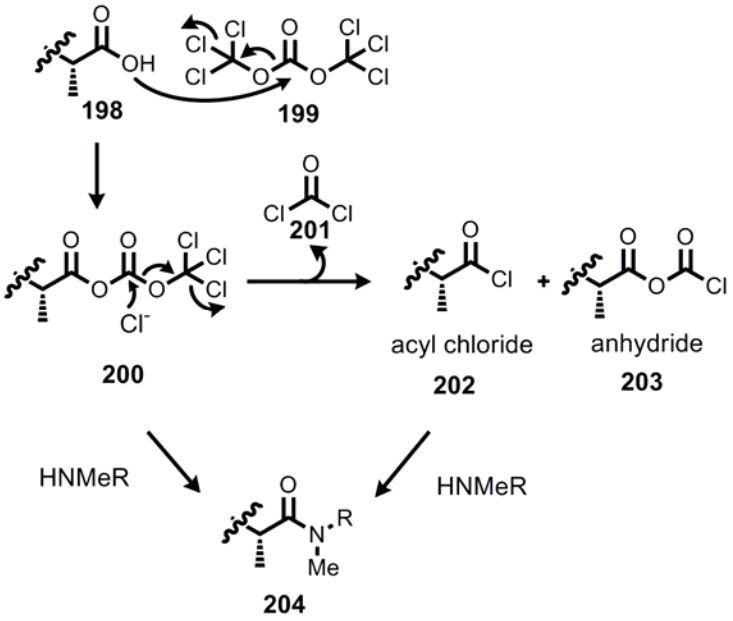

Scheme 52 BTC activation of a carboxylic acid for peptide couplings.[116]

Finally, tetrapeptide preparation was optimized by using standard solid phase peptide coupling method HOBt/HBTU (method A) for the primary amine peptide couplings and HATU/HOAt (method B) for the secondary amine couplings on 2-Cl trityl chloride resin. In this fashion the tetrapeptide could be isolated in 65 % yield without any epimerization.

5.2.5 Assembly of the hexapeptide

Proper choice in ring disconnection sites is critical for the success of the peptide macrocyclization reaction. A poor choice of cyclization site may result in slow reaction rates and low yields, possibly accompanied with various side reactions such as epimerization of the C-terminal residue, dimerization, and oligomerization.[117] Three amide bond ring disconnection sites resulting from the coupling of a carboxylic acid and primary amine were studied. Two approaches were investigated in order to find the most efficient way to assemble the hexapeptide. The first, through [4+2] segment coupling, required an efficient method to form the amide bond between amine **121**

and carboxylic acid **197**. The second approach was designed fully assembly of the linear peptide on solid phase. The optimization steps of this two approaches are described in the following paragraphs.

5.2.5.1 Approach I: [4+2] Segment coupling

Hexapeptide sequence **I** features a coupling between the L-Tyr^{6} carboxylic acid and the D-Ala^{1} amine, which had been used as ring closure site for macrolactamizations.[118]

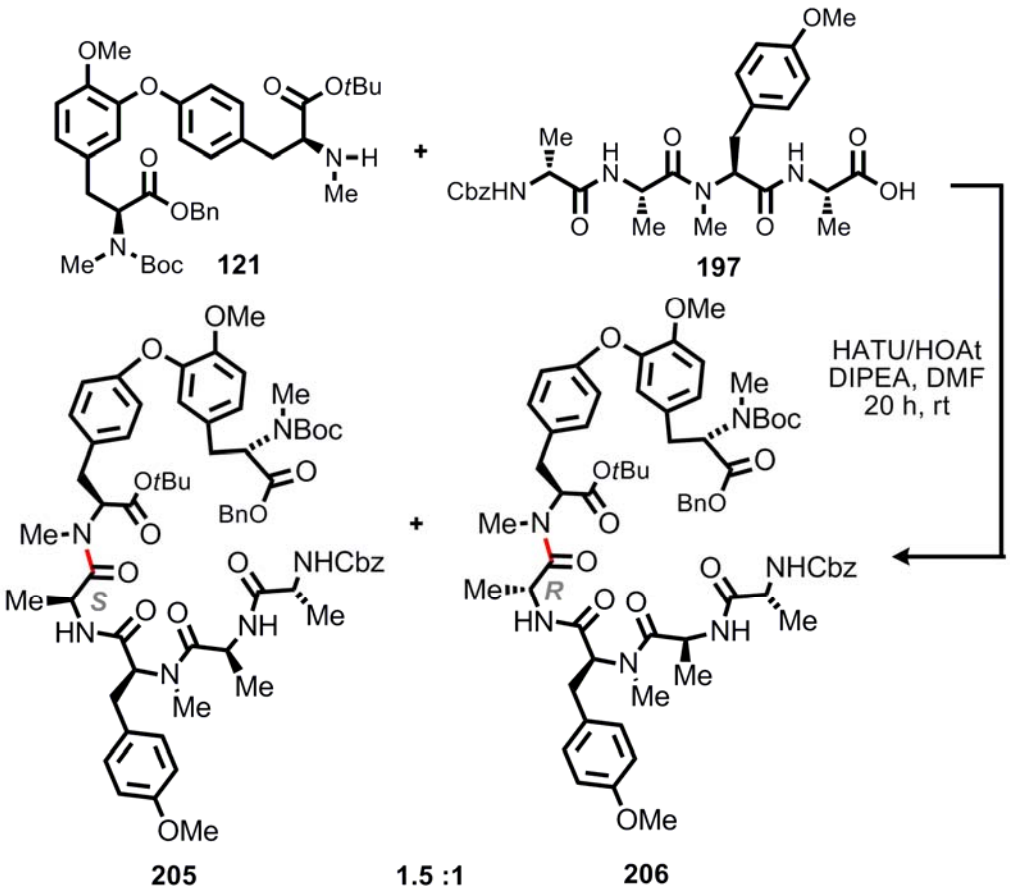

Scheme 53 [4+2] Segment coupling under HATU/HOAt coupling conditions afforded two epimers (1.5:1).

Hexapeptide assembly was achieved by the [4+2] segment coupling between isodityrosine **121** and tetrapeptide **197**. The secondary isodityrosine amine **121** (1 equiv.) and carboxylic acid tetrapeptide **197** (1.2 equiv.) were subjected to a coupling with HATU/HOAt in the presence of DIPEA in DMF. Under these conditions, strong epimerization at the α carbon of the C-terminal tetrapeptide was observed. This problem is well known in the literature with fragment coupling approaches and is caused by competitive deprotonation of the strongly activated active ester and

oxazolone formation during peptide coupling. A formation of the enolate leads to the loss of stereochemistry on the α-carbon. To prove the proposed epimerization at this position, the respective epimer (**207**) of the tetrapeptide was synthesized and subjected to the same reaction conditions. HPLC monitoring of the reaction between amine **121** and tetrapeptides **197** and **207** clearly proved the epimerization of the tetrapeptide under these reaction conditions. Additionally, different reactivity was observed for the two diastereomers of tetrapeptide by performing fragment coupling reactions in parallel with HPLC monitoring (Figure 17). During the fragment coupling with amine **121**, the ***R*** diastereomer **207** was consumed sightly faster than the ***S*** diastereomer **197** converted to hexapeptide **205** and **206** in a 2:3 diastreomeric mixture. (upper trace: starting materials 4:1, product ratio 3:2, lower trace: starting materias 1:1, product: 2:3 ratio).

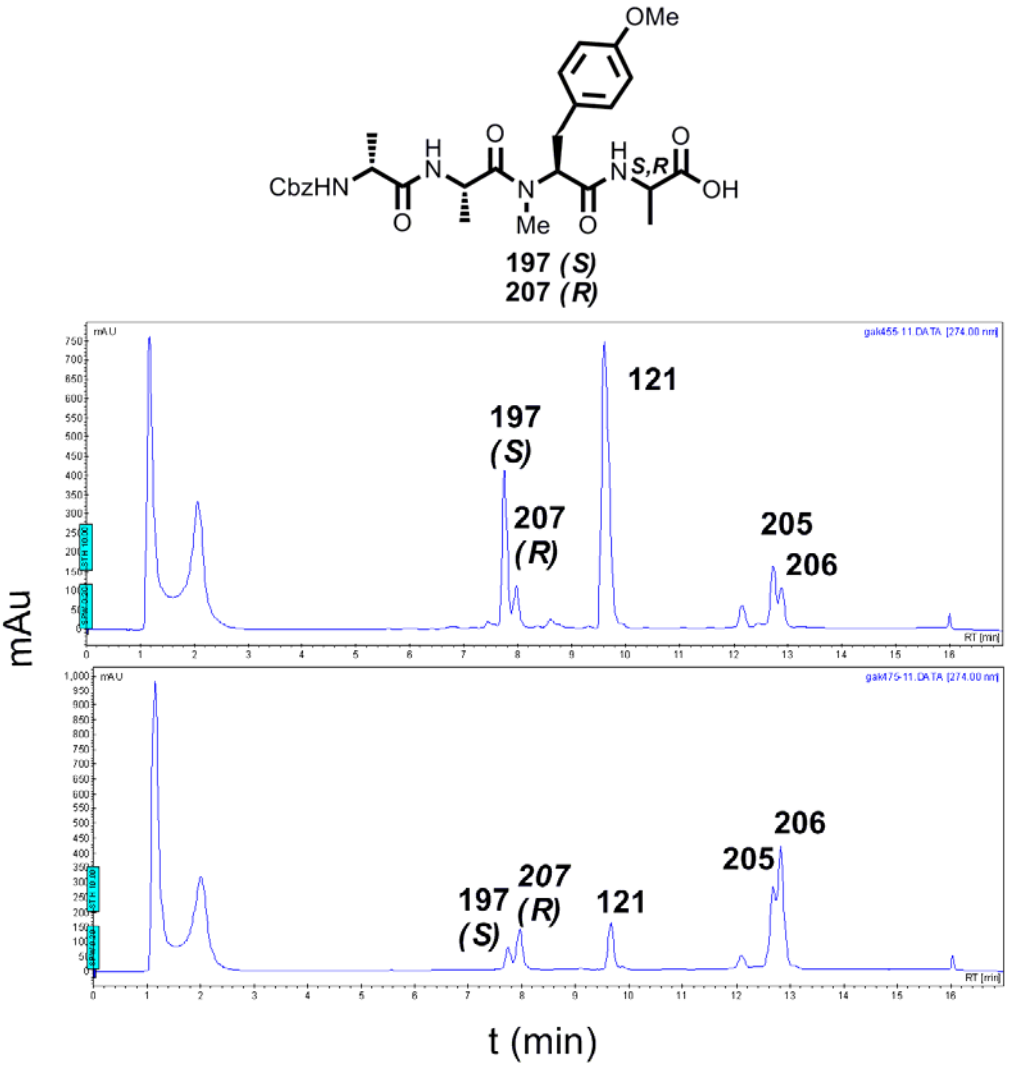

Figure 17 HPLC monitoring of the reaction mixture for [4+2] segment coupling. Upper chromatogram reaction mixture of **197** and **121**, lower chromatogram presents the reaction mixture of **207** and **121**.

The [4+2] segment coupling was then studied under various carboxylic acid activation conditions, in order to suppress the racemisation of the α-carbon of the C-terminus tetrapeptide. Aminium salt, HATU with or without HOAt (entry 1 and entry 2, Scheme 54) resulted in the formation of the hexapeptide in a similar ratio of diastereomeric mixtures (1.5:1 and 1.3:1, respectively). In both cases, recovery of the isodityrosine amine was possible (20 - 25%). The use of carbodiimides such as EDC-Cl gave similar results (entry 3). The mechanism of activation for these reagents involves the formation of the HOAt active ester intermediate, which reacts smoothly with the amine, but with undesired loss of stereochemical purity.

The organophosphorus based reagent 3-(diethoxyphosphoryloxy)-1,2,3-benzotriazin-4(3H)-one (DEPBT)[119] (**208**) was tested as well. In the presence of $NaHCO_3$ in CH_2Cl_2, DMF or THF it yielded the desired compound **205** in 38% yield, but only in 70 - 80% purity. A reagent derived side reaction[120] occurred. A phosphoric ester was formed that was difficult to remove. The alternative phosphonium based coupling reagent, bromotri(pyrrolidino)phosphonium hexa-fluorophosphate (Pybrop) was investigated as well. Despite its frequent application[121,122] for the coupling of secondary amines, in our work it did not afford the desired product **205**, but resulted in decomposition. During these invesigations it was observed that the activated carboxyl intermediate was stable in the presence of a tertiary amine for a short time (up to 60 min.). If this intermediate would quickly react with the secondary amine, isodityrosine **121**, within this period, epimerization could be suppressed. To shorten the reaction times, the coupling reagent HATU in the presence of Cs_2CO_3 was investigated under microwave heating (150 W, 70°C, 20 min.) and the resulting ratio of enantiomers was determined by (HPLC).

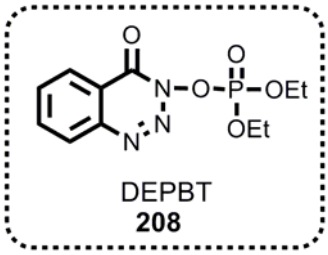

DEPBT
208

This resulted in the formation of **205** in a 38 % yield, and without detectable epimerisation. Isodityrosine **121**, however, was not stable and partially decomposed under the microwave conditions, hence it was impossible to recover the precious amine from the crude mixture.

121 + **197** —*conditions*→ **205** + **206**

Entry	*Conditions*	**121** (equiv.)	**178** (equiv.)	yields of **205** (%)	yields of **206** (%)	yields of **121** (%)
1	**HATU/HOAt DIPEA or NMM, DMF**	**1.2**	**1**	**45**	**30**	**25**
2	HATU, sym-collidine, DMF	1	1	40	30	20
3	EDC-Cl/HOAt, sym-collidine, DMF,	1	1	35	28	20
4	DEPBT, $NaHCO_3$ DCM/DMF or THF	1	1	38	n.d	35
5	**HATU/HOAt, Cs_2CO_3, MW, DCM**	**1**	**1**	**35**	**n.d**	**-**

Scheme 54 [4+2] segment coupling between amine **121** and carboxylic acid **197.** Reactions were performed at room temperature for 20h or microwave heating (150 W, 70°C, 20 min.)

In summary, hexapeptide **205** was successfully prepared by [4+2] segment coupling. The use of HATU/HOAt as coupling reagents in the presence of DIPEA in DMF clearly gave in hexapeptide **205** (45 %) and its epimer **206** (30 %). The diastereomers could be separated by silica gel chromatography and the unreacted amine isodityrosine **121** could be recovered making this method preparatively useful. Alternatively, using microwave irradiation (150 W, 70°C, 20 min.), **205** could be synthesized with 35 % yield as the single product without any detectable epimerization. However, in this case the precious building block amine isodiyrosine **121** could not be recovered.

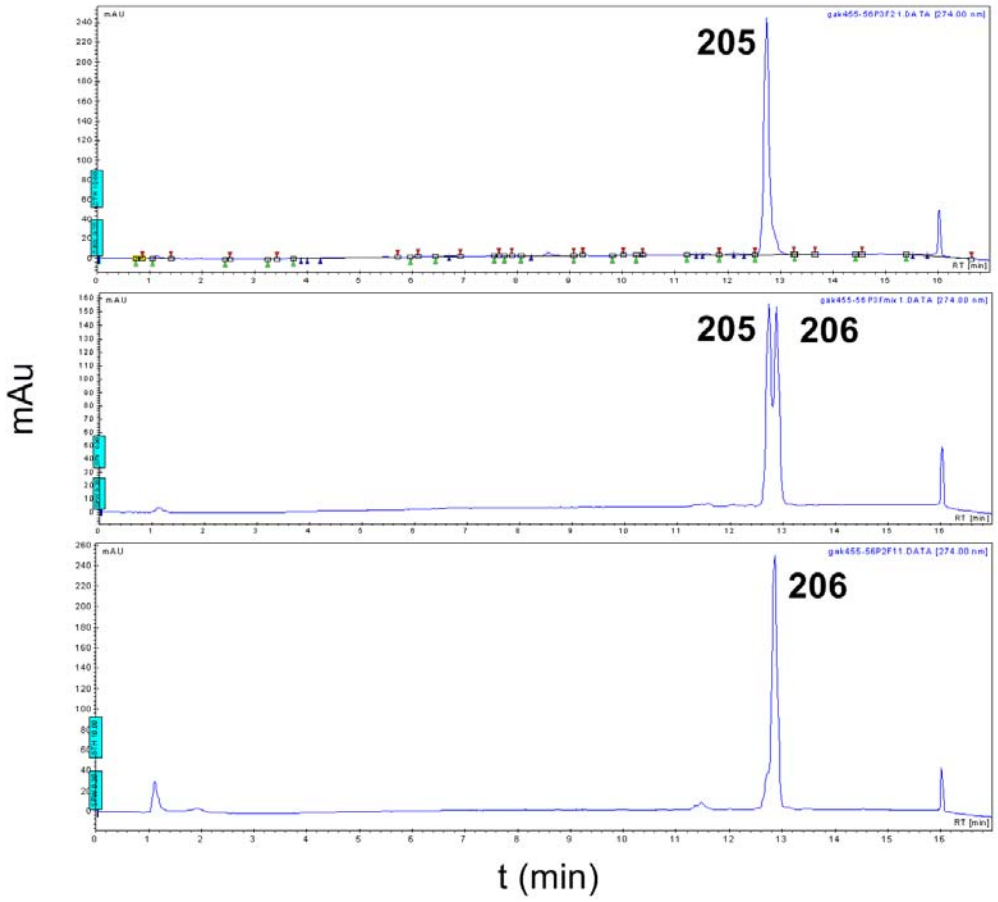

Figure 18 HPLC chromatogram of linear hexapeptides **205**, **206** and mixtures. A) Natural epimer of linear hexapeptide **205**, B) Mixture of isomers **205** with **206**, C) Unnatural epimer of linear hexapeptide **206**.

5.2.5.2 Approach II: Linear solid phase peptide synthesis (SPPS)

To investigate alternative ring closure strategies, hexapeptide sequences **211** and **213** were prepared on 2-Cl-trityl resin using standard peptide coupling conditions by loading of Fmoc-L-Ala-OH (0.35 mmol/g) and building block **126** (0.40 mmol/g) on 2-Cl-Trityl resin, respectively. However, the loading of the biaryl ether building block **127** for the synthesis of **205** was inefficient (0.15 mmol/g for 1.5 equiv. **125**) and could not be improved. Therefore, linear hexapeptide **205** had to be synthesized by segment couplings in solution as described before.

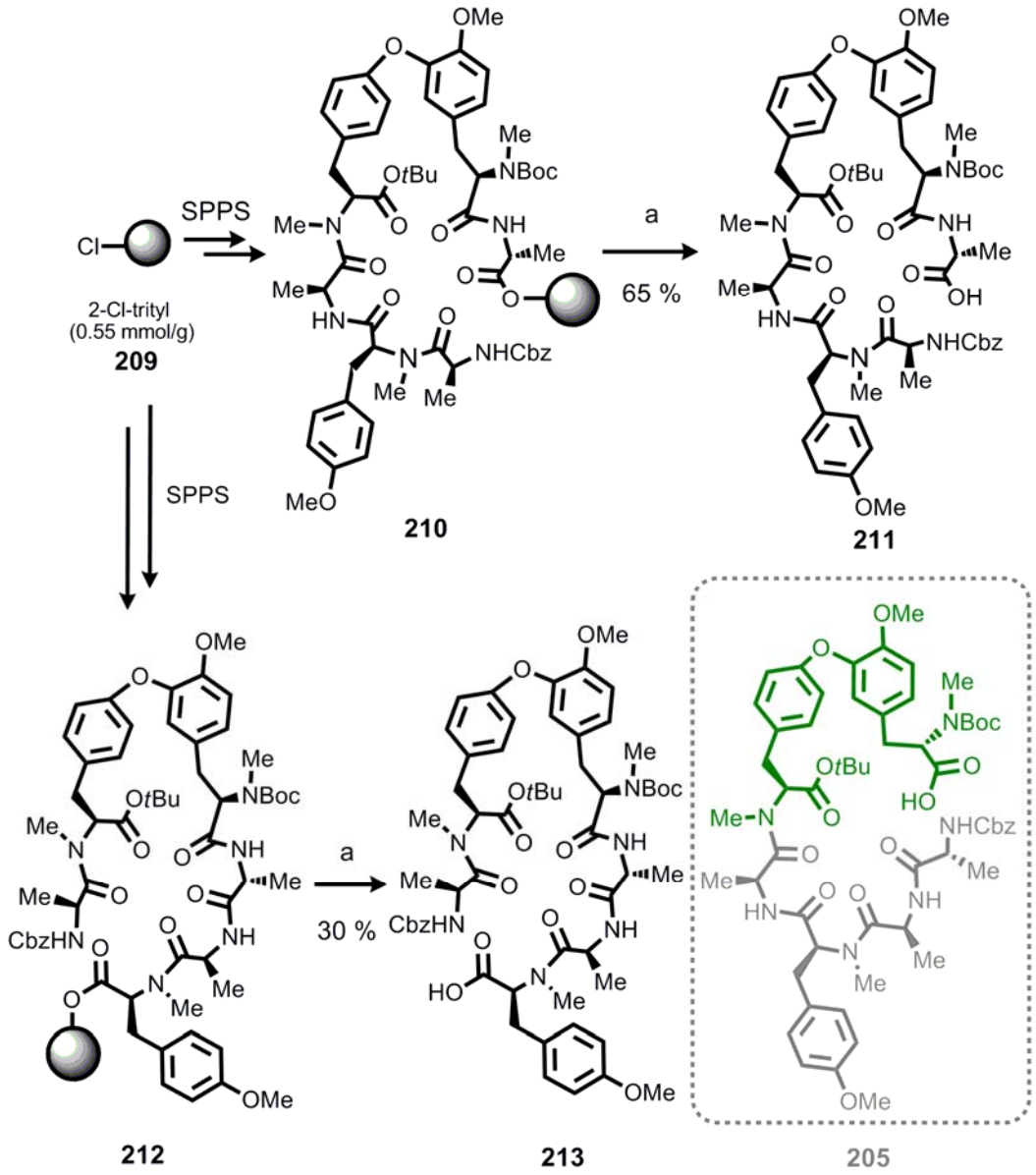

Scheme 55 The synthesis of linear hexapeptides on solid support. Highlighted in green in the structure of **205** is the building block **127**. a) TFA/DCM/Et_3SiH 2:94:4.

Initially, the resin was loaded with Fmoc protected alanine to 0.4 mmol/g with respect to the initial resin loading. All primary amines were coupled with HOBt/HBTU (0.4 M) solution in DMF and all secondary amines were coupled with HATU/HOAt (0.4 M) solution in DMF. For the secondary amines, double coupling was necessary, but truncated tripeptide **214** after the coupling of L-Ala to the hindered amine of isodityrosine was still always observed (~10%). Therefore, the procedure was optimized using a capping step with acylation of the uncoupled amines with acetic anhydride in dichloromethane in order to facilitate the purification.

A mild acidic treatment (TFA/DCM/Et_3SiH 2:94:4) of the resin released the peptides with good yields of 65 % and 40 %, respectively. The preparation of hexapeptide **211** using an automated microwave peptide synthesizer[g] was performed as well and resulted in a promising and straight forward preparation (60% yield with >80 % purity). As the hexapeptides cleaved from the solid support with 5% TFA showed partial Cbz deprotection, the cleavage procedure was optimized and 2% TFA together with 4% Et_3SiH as a scavenger in dichloromethane was used.

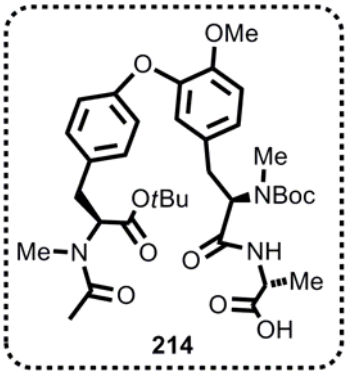

Scheme 56 Isolated side product after the cleavage.

In summary, linear hexapeptides **211** and **213** were prepared on solid support with an efficiency which could not be achieved by the preparation of **205** in solution due to epimerization. Solid supported peptide synthesis (approach II) was the most powerful method to prepare biaryl containing hexapeptides.

5.2.6 Macrolactamization

5.2.6.1 Natural linear precursors of RA-VII

Macrocyclization to yield the biaryl cyclopeptide **119** was addressed next. In general, the results of the peptide cyclization are strongly influenced by the conformation of the linear peptide precursors in solution.[117] Therefore, three different linear precursors (**205, 211, 213**) which were synthesized in the previous chapter, were investigated as precursors for the synthesis of **119**. Furthermore, all of them should lead to the same compound, thereby cross indicating potentially occurring epimerization during macrolactamization, which are otherwise very difficulty to detect by NMR due to the multi conformational behaviour and slow exchange of *N*-methylated peptides. The order of assembly was varied to investigate the highest yielding conditions for this ring closures. Cyclization of the linear sequences can be achieved through the coupling of the free carboxylic acid and primary amine. For **205,** this is between the carboxylic acid of L-Tyr^6 and amine D-Ala^1, for **211**, between the carboxylic acid of D-Ala^1 and the amine L-Ala^2 and for **213**, between the carboxylic acid of L-Tyr^3 and the amine L-Ala^4 Scheme 57.

[g] Discover (CEM) technology MW conditions per coupling: power = 18 watt, T = 75 °C for each coupling 300 s.

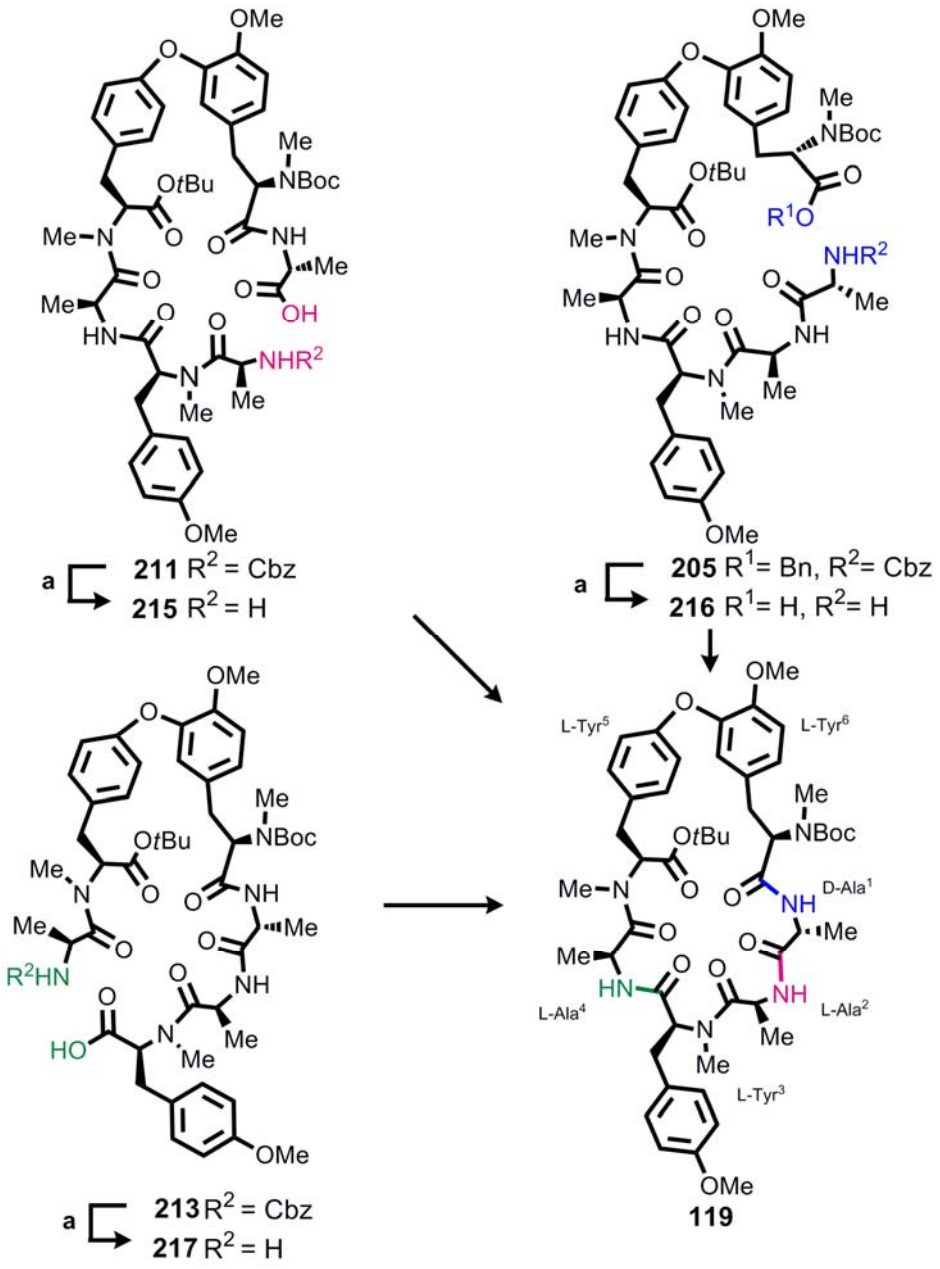

Scheme 57 Variation of cyclization sites on hexapeptides synthesized then cleaved from the solid support. a) H_2, Pd/C, MEOH/HCOOH, quant.

Prior to cyclization, the benzyl and Cbz protecting groups were removed by hydrogenation, which liberated the free carboxylic acid and free amine for all three precursors in 3 hours quantitatively. The deprotected linear hexapeptides **215**, **216** and **217** were then subjected in high dilution to various macrolactamization conditions. Scheme 58 summarizes the results of coupling conditions for the cyclization of each of these linear sequences (**215**, **216**, **217**) to achieve the same macrocycle **119**. Activated aromatic esters are known to be prone to react with nucleophiles, especially

amines, under mild conditions with reduced racemization.[123] Therefore our initial study was focused on aminium, phosphonium and orgona phosphorus based coupling reagents such as HATU[114] (method I), DEPBT[119] (method II) and pentafluorophenyl diphenyl phosphonate (FDPP)[124] (method III) to form the active esters. Furthermore, diphenylphosphoryl azide (DPPA)[91] (method IV) was also used to form the acyl azide intermediate, which is able to react with amines at low temperatures.[93] (Scheme 58).

entry	methods	cyclization yields **119** (%)		
		prec. **216**	prec. **215**	prec. **217**
1	I	40	26	18
2	II	15	10	-
3	III	13	10	-
4	IV	10	5	-

Scheme 58 Cyclizations of various precursors (prec.) of linear hexapeptides (**215**, **216**, **216**) under several coupling conditions. Method I: HATU/HOAt, DIPEA, DMF, RT, 28 h; Method II: DEPBT, $NaHCO_3$, THF, RT, 16 h; Method III: FDPP, DIPEA, DMF, RT, 16h; Method IV: DPPA, $NaHCO_3$, DMF, RT, 16h. * Yield after prep HPLC.

The best results were obtained for all three precursors using the HATU/HOAt coupling conditions (Scheme 58, entries 1 and 2). Replacement of DIPEA with *N*-methyl morpholine (NMM) and 2,6-collidine gave comparable results for the cyclization of **216** (Scheme 58, entry 1). The efficiency of HATU/HOAt activation may be due to coordination of HOAt to the amine proton, which causes an intramolecular base catalysis **222.**[125]

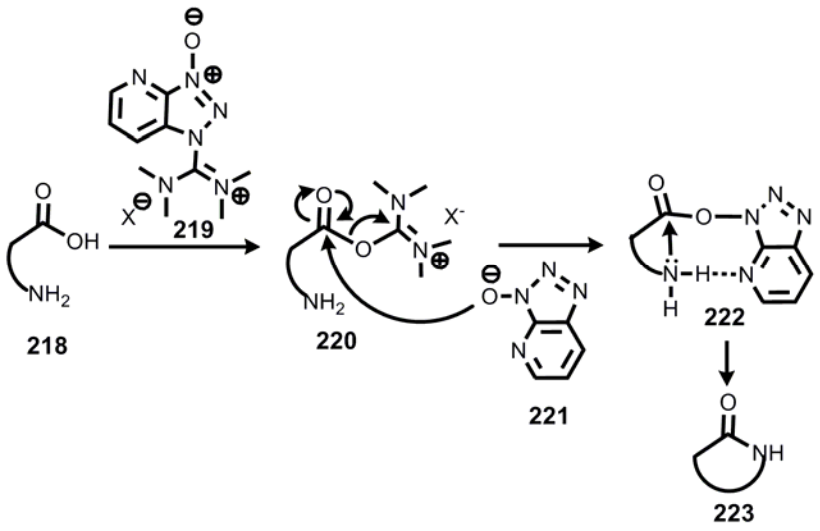

Figure 19 Plausible mechanism for HATU/HOAt mediated peptide cyclizations.

Organaphosphorus based coupling reagents were also investigated for the ring closure reaction condition. These reagents offer different of activations for example active esters (**202** and **200**) or acyl azide formation **204** in order to form the desired macrocycle **198**. (Scheme 59).

Use of the coupling reagents DEPBT and FDPP gave the desired macrolactamization product but in a lower yield than the HATU/HOAt coupling reagents. In both cases, the yield of **216** was slightly better than that for **215** (Scheme 58, entries 3 and 4).

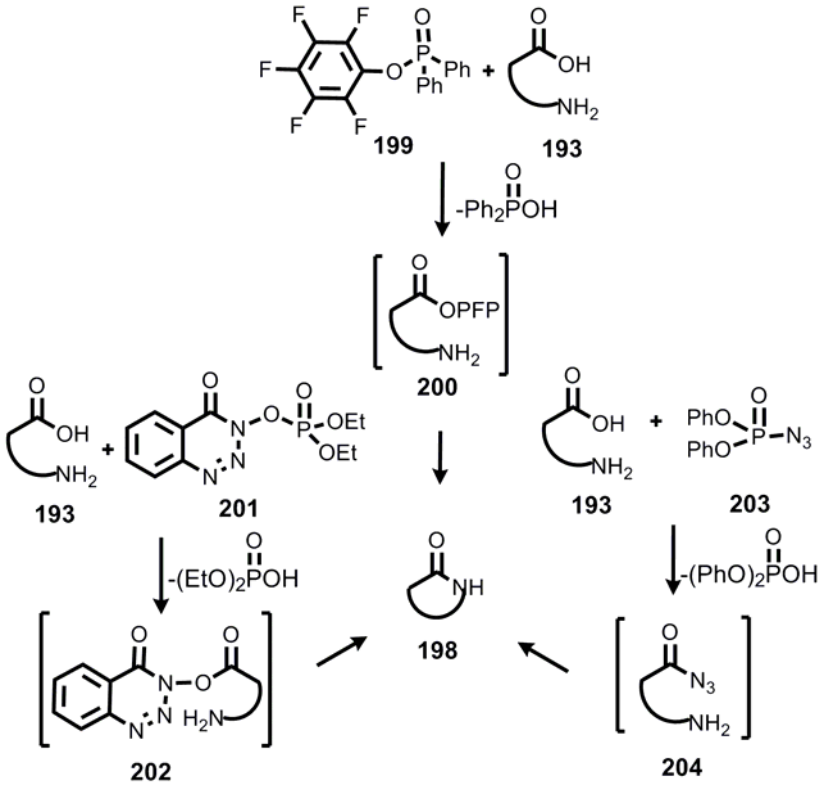

Scheme 59 Organophosphorus based coupling reagents for macrolactamization.

The use of DPPA for both hexapeptides **216** and **215** resulted in poor conversion. Apparently, long reaction times, even at 0°C, led to the formation of different side products (Scheme 60). The formation of the isocyanate by Curtius Rearrangement,[91] result the isocyanate **230** which can be converted to carbamic acid **231** by attack of water. Furthermore, the azide can be hydrolyzed to yield acid **218**. Alternatively, the side product urethane **232** can be observed by decomposition of DMF.

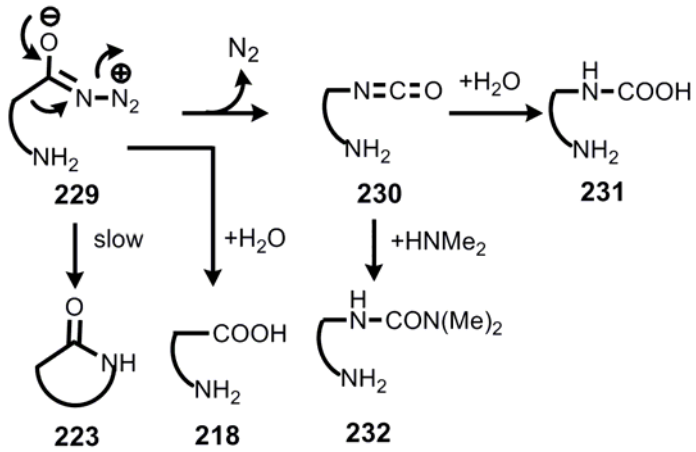

Scheme 60 Typical **s**ide reaction during the DPPA coupling by Curtius Rearrangement.

HATU proved to have the greatest efficiency of the coupling reagents investigated for the macrolactamization of all three sequences (entry 1 and 2, Scheme 58). Among the studied natural linear precursors (**215**, **216**, **216**), the optimal cyclization site was the site between L-Tyr^6 and D-Ala^1 (**216**). Ring closure between D-Ala^1 and L-Ala^2 was only slightly less effective, but L-Ala^2 and L-Tyr^3 seemed to be suited less well.

In line with our results, other groups had reported high efficiency of HOAt esters for macrocyclizations. For example, bismacrocyclization on each end of the linear precursor was simultaneously achieved by the use of HATU/HOAt/DIPEA by Danishefsky[126,127] Low yields may be reasoned by steric hindrance of the active esters, which may be more susceptible to attack by other smaller nucleophiles that are also available in the reaction mixture (for eg. water). Furthermore, favorable or unfavorable preorganisation of the open chain precursor influence ring closure efficiency. Apparently, despite of the non-natural biarylether linkage, cyclization sites proximal to the L-/D- stereochemical alternation in the chain are more effective, in line with literature precedence.[128]

5.2.6.2 Chelating effects on macrolactamization of linear hexapeptide 215

It has been reported that RA-VII (**4**) forms complexes with LiCl and that the equilibrium of stable conformers was strongly affected by LiCl.[95] In supramolecular chemistry, ion effects are well investigated and have been used effectively to promote difficult ring closures, such as very large macrocycles and crown ethers.[129,130] However in peptide chemistry this effect is not well studied. Therefore, having

established an efficient preparation method for **215** by solid phase peptide synthesis (yield of pure hexapeptide 65 % after the cleavage from the 2-Cl-Trityl resin), the macrolactamization of **215** was further investigated with templation[131] to improve the yield of macrocyclization product **119**. It was reasoned that chelation by cations could bring the carbonyls of the hexapeptide together. The amine and active ester would be brought in closer proximity and should therefore react more readily and specifically. (Scheme 61).

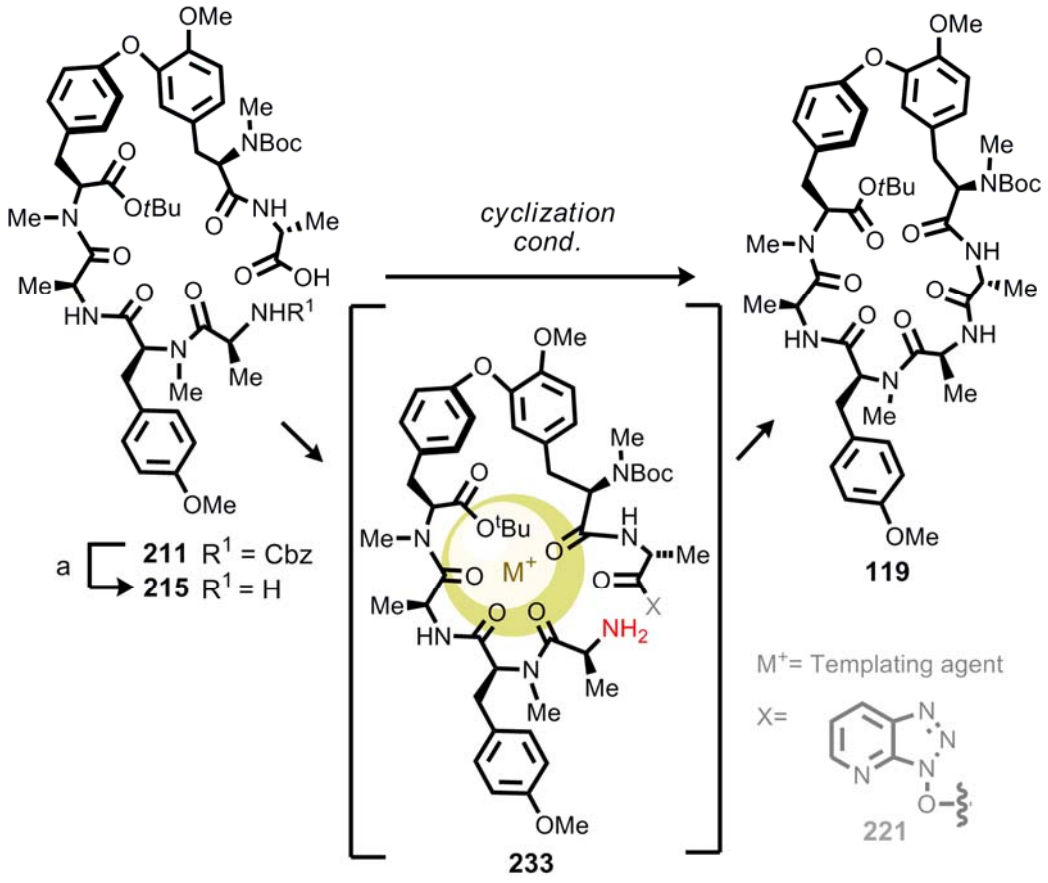

Scheme 61 Macrolactamization of **215** in the presence of potassium hexaphosphate as templating reagent. a) H_2, Pd/C MeOH/HCOOH, 1h, quant.

The previous found ”best” reagent combination was therefore studied in the presence of inorganic cations for cyclization efficiency. For best results typically an inert anion ion has to be employed. Potassium hexafluoro phosphate has been reported as templating reagent for these type of cyclization reactions.[129] On the other hand, Cs^+-salts are frequently used effectively, but it was speculated that the effect of Cs^+-salts is not always directly related to specific templation.[132]

The linear precursor **215** was subjected to cyclization conditions in the presence of K^+ and/or Cs^+ cations. In Scheme 62, various methods and the ion effect of the KPF_6 and $CsCO_3$ salts are summarized to form HOAt ester **233**. Utilizing HATU in 10 % DMF in DCM (to improve the solubility of **215** and Cs_2CO_3) did not increase the yield of product **119**, (comparison Scheme 62, entry 1 and entry 2). Difficulties from the transformation to **119** arose in the presence of KPF_6, whereby the transformation appeared to be blocked. The use of base was investigated by changing Cs_2CO_3 to K_2CO_3. Unfortunately, in CH_2Cl_2, DMF or MeCN, only traces of product could be detected (Scheme 62, entry 3). EDC-Cl/HOAt in the presence of K_2CO_3 leads to the desired **119** in poor 5 % yield (entry 4). PyBrop, on the other hand, was found to significantly increase this yield (31%) in the presence of Cs_2CO_3 in acetonitrile (entry 5). The PyBrop/HOAt in the presence of combination of two potassium salts, K_2CO_3 and KPF_6, afforded macrocycle **119** with a similar yield (35 %, entry 7), whilst the Cs_2CO_3 and KPF_6 combination resulted in a lower yield of 19% (entry 6). Furthermore, synthesized other linear sequence **216** was also subjected to the macrolactamization conditions in the presence of Cs_2CO_3. The yields were similar (38 %) to the yields were obtained under the previously discussed conditions (section 5.2.6.1).

215 —*cyclization cond.*→ **119**

Entry	Coupling reagents	Base	Solvent	**119** yield %
1	HATU/HOAt	DIPEA	DMF	26
2	HATU/HOAt	Cs_2CO_3	CH_2Cl_2/DMF	23
3	HATU/HOAt	Cs_2CO_3/KPF_6	CH_2Cl_2/DMF	-
4	HATU/HOAt	K_2CO_3	DMF or MeCN	-
5	EDC-Cl/HOAt	K_2CO_3	MeCN	5
6	**PyBrop/HOAt**	**Cs_2CO_3**	**MeCN**	**33**
7	PyBrop/HOAt	Cs_2CO_3/KPF_6	MeCN	19
8	**PyBrop/HOAt**	**K_2CO_3/KPF_6**	**MeCN**	**35**

Scheme 62 Representative results for the templated macrolactamization of **215** to **119**.

These results show the dependency of cyclization behaviour on the activation of carboxylic acid residue. We can conclude that using a template reagent made a difference by varying the method of HOAt ester formation, and the addition of K^+ or Cs^+ salts led over 50% improvement in terms of yield compared to the original conditions. Future research must focus on further improving this method by using other templating reagents for example Cu(I), Cu(II), Sc(IIII), Ca(II), Ba(II), or other metal salts.

5.2.6.3 Unnatural linear precursors of RA-VII

The hexapeptide **206,** an epimer of **205**, was isolated as a side product from the [4+2] segment coupling reaction. This was also subjected to cyclization after deprotection by hydrogenation. Under the standard macrolactamization conditions, in high dilution with HATU/HOAt, the cyclization of **234** resulted in two macrolactamization product **235** and **236** in combined 40 % yield.

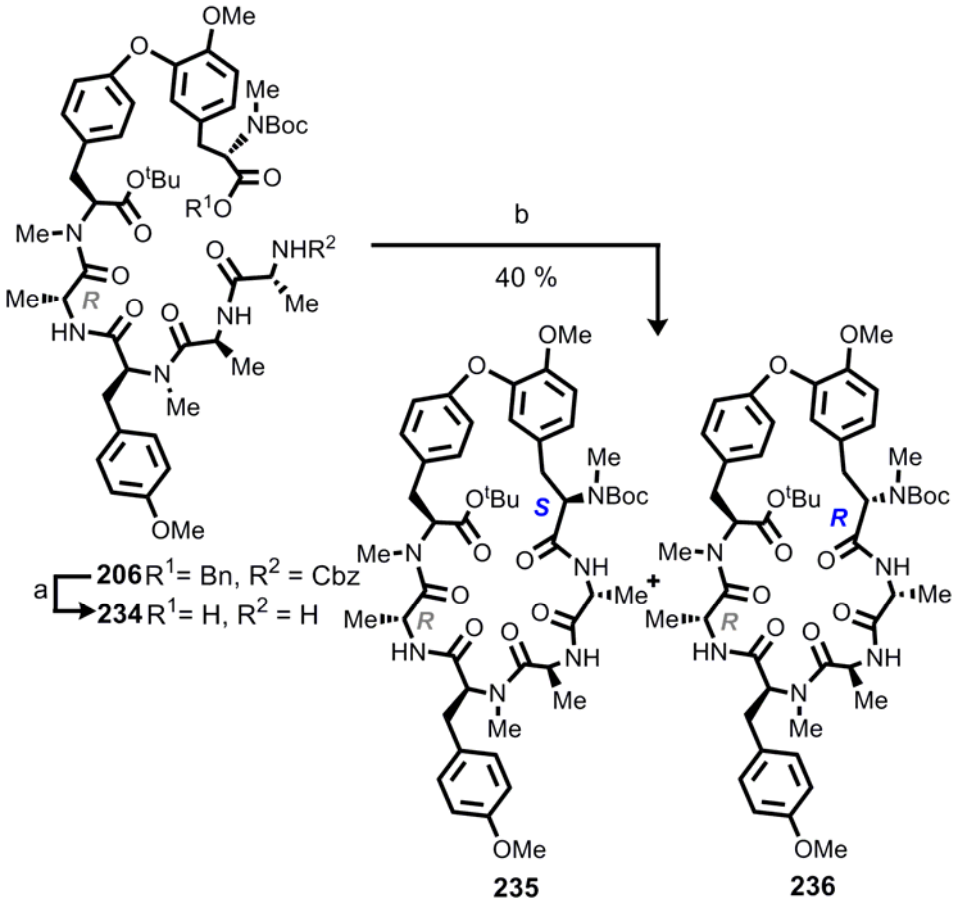

Scheme 63 Macrolactamization of the unnatural **234** epimer. a) H_2, Pd/C, MeOH/HCOOH, 3 h, quant; b) HATU/HOAt, DIPEA, DMF, 20 h, high dilution c= 5 μM.

HPLC monitoring of the reaction mixture showed that macrolactamization occurs cleanly between the carboxylic acid of the L-Tyr[6] and the amine of the D-Ala[1], however, after 10h linear **234** epimerized under the reaction conditions and the epimer **234*** formed. Unlike the natural precursor **215**, **216**, **217**, unnatural precursor **234** formed epimers under the cyclization conditions, indicating a considerable sensitivity of substrates dependent on stereochemistry.

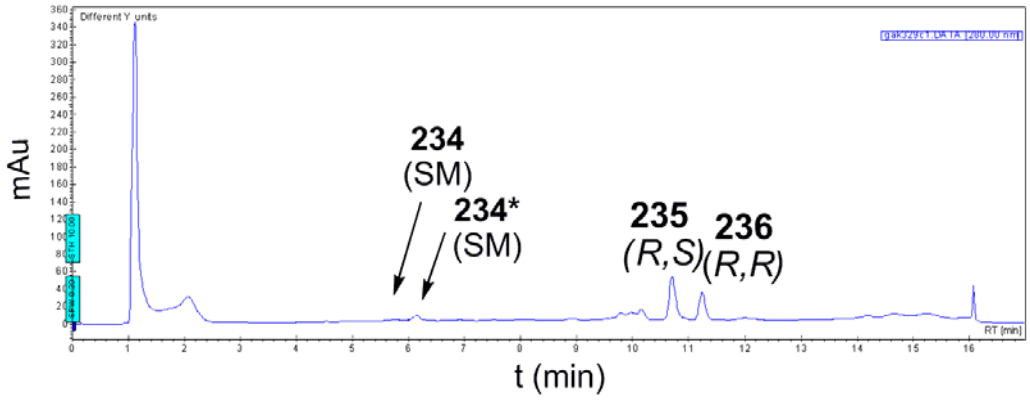

Figure 20 HPLC monitoring of the reaction mixture for the macrolactamization of **234.** Under the macrolactamization conditions after 10h cyclic epimers **235** and **236** was observed.

The separation of the two diastereomers **235** and **236** proved to be quite difficult, and purification on silica gel lead to only low isolated yields and purity of products. Therefore, these epimers were separated by preparative HPLC which resulted in isolation of each pure epimer in low yield (*R,S:* 6.2 % and *R,R:* 12 %).

In summary, linear hexapeptides **205**, **211**, **213** and **206** were successfully synthesized and characterized. They were deprotected and subjected to various conditions to optimize their cyclization. For all four linear precursors, the HATU/HOAt coupling conditions proved to be the best coupling reagents for the macrolactamizations. The template-promoting reagent KPF_6 was found to further improve macrolactamization yields, under certain conditions. In the case of **206**, unavoidable epimerization was observed. HPLC traces of three different stereoismers of hexapeptide macrocycle are shown in Figure 21.

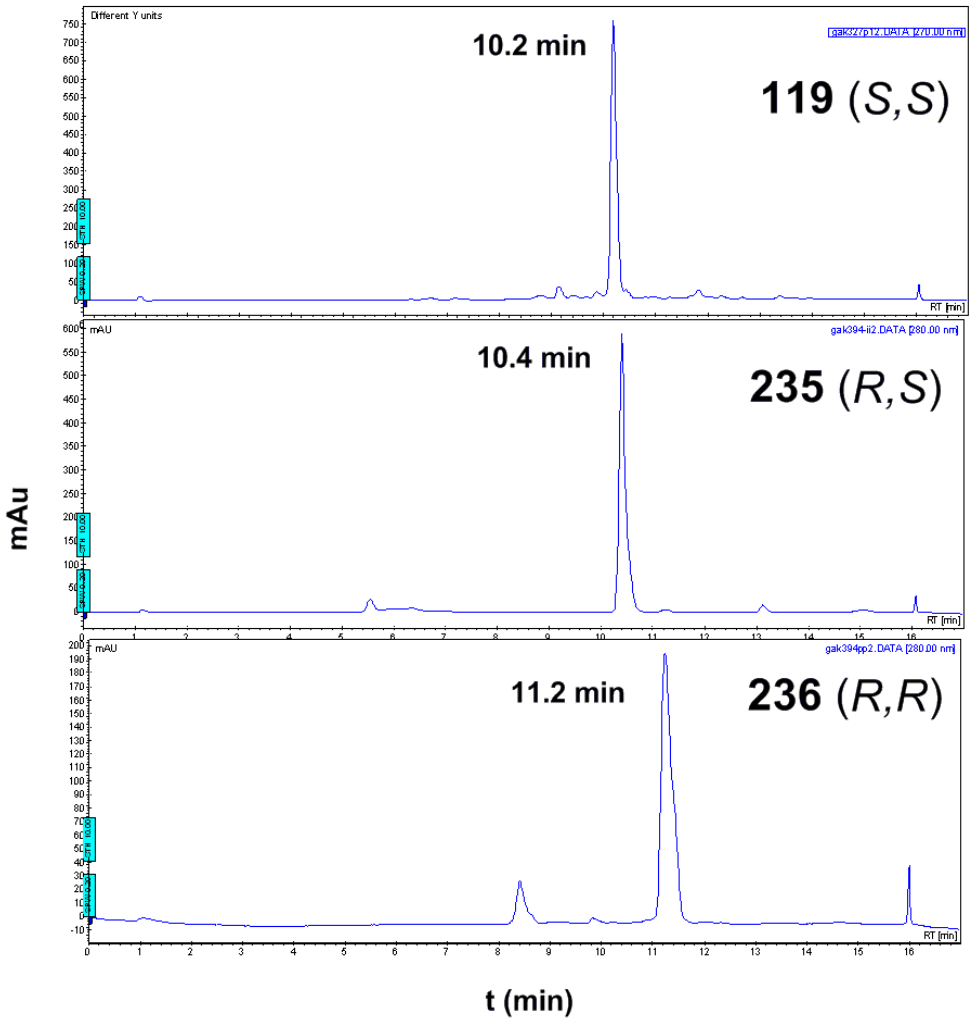

Figure 21 HPLC traces of natural **119** and unnatural (**235, 236**) cyclic precursors. (for the HPLC condition, See 8.1, method A)

5.2.7 Transannular macrolactamization

In the initial planning, it was envisioned that a transannular macrolactamization would lead to the target structures, where the amide bond formed last should obtain the *cis* configuration.[87] In order to study the influence of stereochemistry, transannular macrolactamization was studied on synthesized natural and natural cyclic precursors (**119**, **236** and **235**). The natural macrocyclic epimer **119** was expected to lead to RA-VII, whereas **235** and **236** would deliver stereoisomers which would be interesting compounds for biological testing as well. After successful removal of the acid sensitive protecting groups of **119** (*t*Bu and Boc), precursor **106** was subjected to several transannular macrolactamization conditions

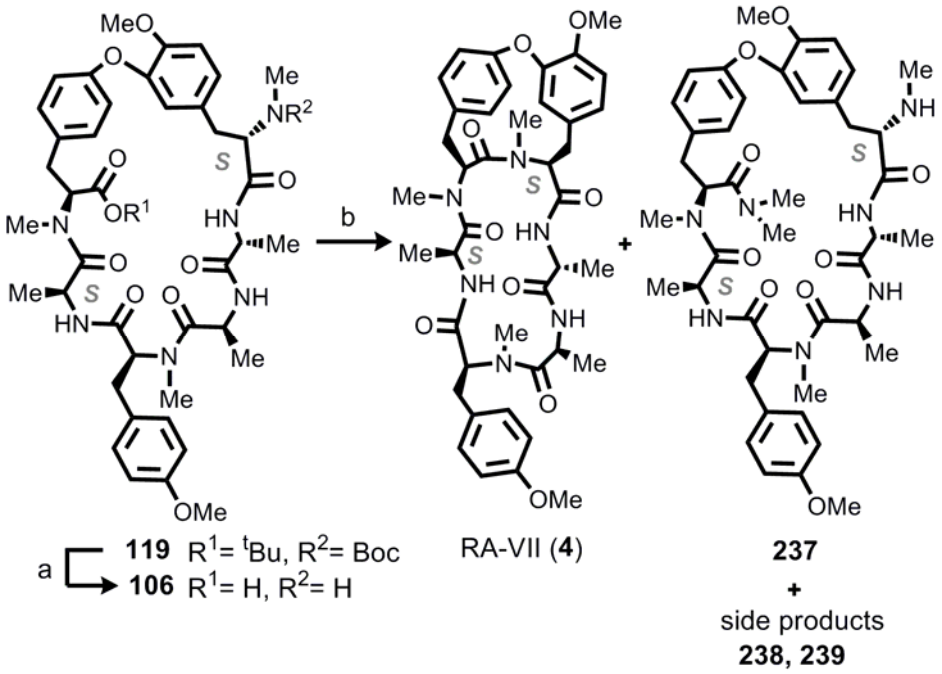

Scheme 64 Transannular macrolactamization for the natural epimer **119**. a) 50 % TFA, DCM, 1h, rt; b) HATU/HOAt, DIPEA, DMF. (yields are compiled in Scheme 65)

In the experiments, HOAt active ester formation from **106** induced by HATU did not lead to the formation of the target molecule. Instead formation of dimeric molecules was observed, as evidenced by HPLC-MS. Two distinguished dimers were identified by HRMS analysis and MS-MS experiments were used to chracterized their structures (vide infra). Furthermore, dimetylamine adducts **237** and **238** were found, which were probably formed by slow decomposition of the DMF solvent (to $HNMe_2$).

In order to characterize the dimers, **238** and **239** were subjected to LCMS with electrospray ionization (ESI) and tandem Ms_2 experiments. The dimers were ionized and the ionized fragments passed trough ion traps. ESI Ms^2 and Ms^3 (MS-MS-MS) experiments were measured using an ionization power of cid 35.00. Characteristic fragments from both **238** and **239** were identified from the Ms^2 and Ms^3 experiments. These included fragment **f1**, the fragment resulting from the cleavage of dimethylformamide from the dimer and fragments **f2** and **f3**, which are cyclic monomers derived from the cleavage of the amide bond between the dimer. Ms^2 experiments performed on fragment **f2** gave three further fragments whilst Ms^2 experiments on fragment **f2** displayed no further fragmentation (at cid 35.00). Characterization of dimer **238** by MS^2 experiments did not result in any fragmentation, indicating the tricyclic structure.

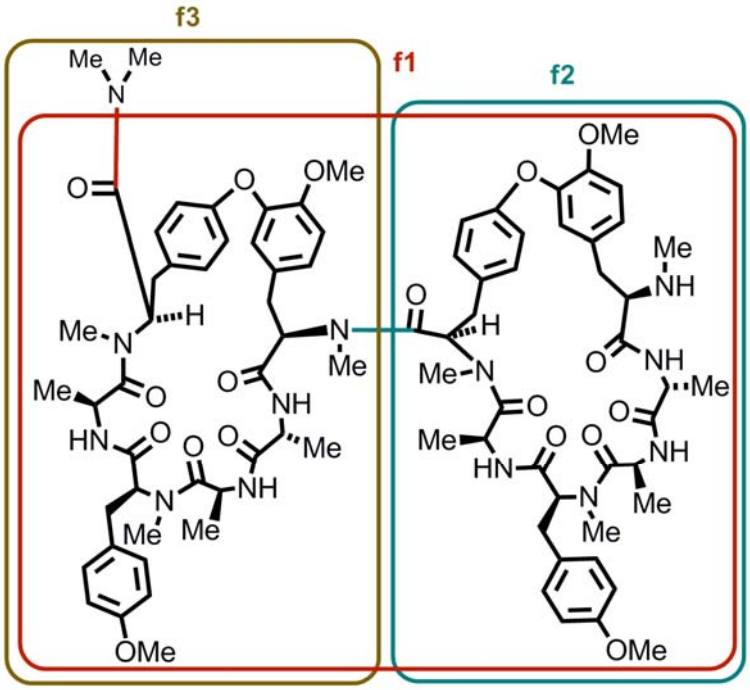

238

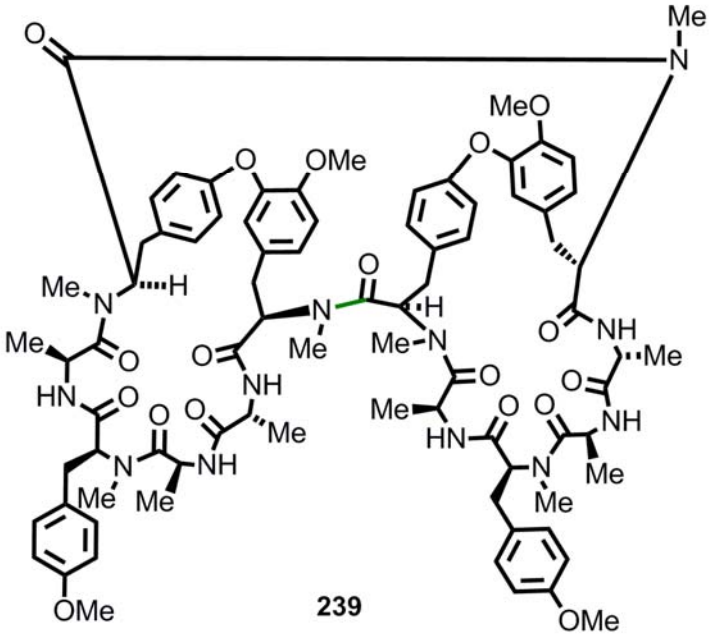

239

Figure 22 Indentified dimers **238** and **239** produced from **106** under transannular macrolactamization conditions. Fragments (**f1**, **f2**, **f3**) resulting from MS-MS experiments are shown in boxes.

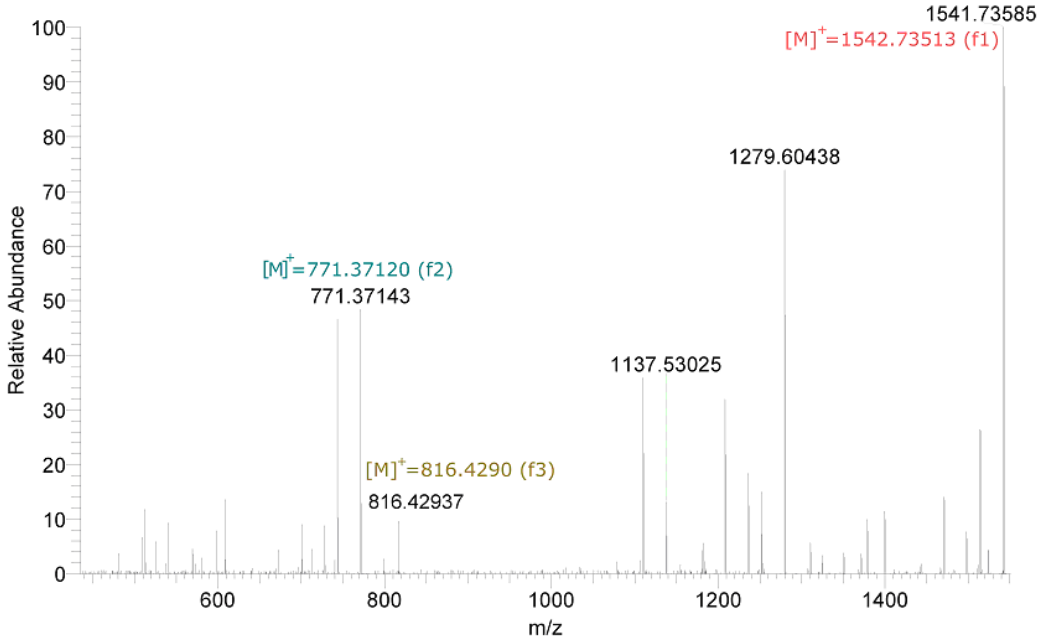

Spectrum 1 Identified fragments of **238** (**f1**, **f2**, **f3**) resulting from MS-MS experiment.

The transannular macrolactamization was studied using several other coupling reagents. Activation as active esters, acid fluorides, acyl azides and acyl chlorides were investigated. The results of these studies are summarized in Scheme 65. HATU, EDC-Cl and Pybrop were used to generate the HOAt ester. The carbodimide and phosphonium based reagents, however, gave neither conversion to the desired product (**4**) nor any dimer formation (entry 6 and entry 7). Although the active ester formation was monitored by TLC, only **106** could be re-isolated from the reaction mixture. This may be due to hydrolysis of the HOAt ester to the carboxylic acid (Scheme 65).

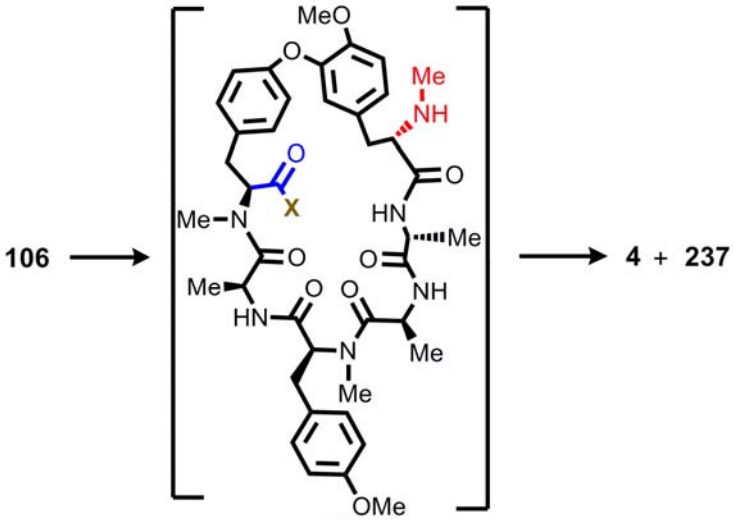

Entry	Coupling reagents	Base	X	Solvent	yields of **4** (**237**)	comments
1	HATU/HOAt	DIPEA	AE	DMF or DCM/DMF	- (30 %)	dimers (**238**, **239**)
2	DAST	DIPEA	Acid fluoride	DCM	-	SM, decomposition
3	DAST/ Zn dust	-	Acid fluoride	DCM	-	SM, no conversion
4	DPPA	$NaHCO_3$	Azide	DMF	- (20 %)	curtius rearrangement
5	Bop-Cl	Et_3N	AE	DCM	-	SM, n.d
6	EDC-Cl/HOAt	DIPEA	AE	DCM	-	SM, no conversion
7	PyBrop/HOAt	Cs_2CO_3/KPF_6	AE	DCM	-	SM, dimers (**238**, **239**)
8	DEPBT	Cs_2CO_3/KPF_6	AE	THF/DCM/MeCN	-	SM, decomposition

Scheme 65 Conditions for transannular macrolactamization.

Using DEPBT for the activation of the carboxylic acid resulted in the decomposition of the starting material, probably due to the highly reactive phosphorous-based side reagent. At this stage, it was tested if steric incompetence could be reason why the active esters would not ring close with the secondary amine function of **240**. DPPA was therefore used as a coupling reagent to form the sterically unhindered acyl azide[123] (entry 4). However, under these reaction conditions, the dimethyamine-derived by-product (**238**) was the major product isolated (20 %). The solvent was therefore changed to dichloromethane, which resulted in the formation of urethane (**232,** Scheme 60) and also hydrolyzed side products (**218** and **231**, Scheme 60) by the Curtius rearrangement.

Acid fluorides were tested next, and DAST was used as a fluorinating reagent in order to facilitate the attack of the secondary amine to the acyl fluoride to allow the transannular macrolactamization. DAST has been shown to be an effective coupling reagent without the use of any accompanying base.[133,134] However, for our substrate, we could only observe reactivity by addition of Hünig's base (DIPEA), which resulted in the formation of the diethylamide side product (see compound **251**, Scheme 66). Addition of Zn-dust [135] (Scheme 65, entry 3) to neutralize the reaction media by capturing the produced HF, did not afford any of the desired transannular macrolactamization product (**4**).

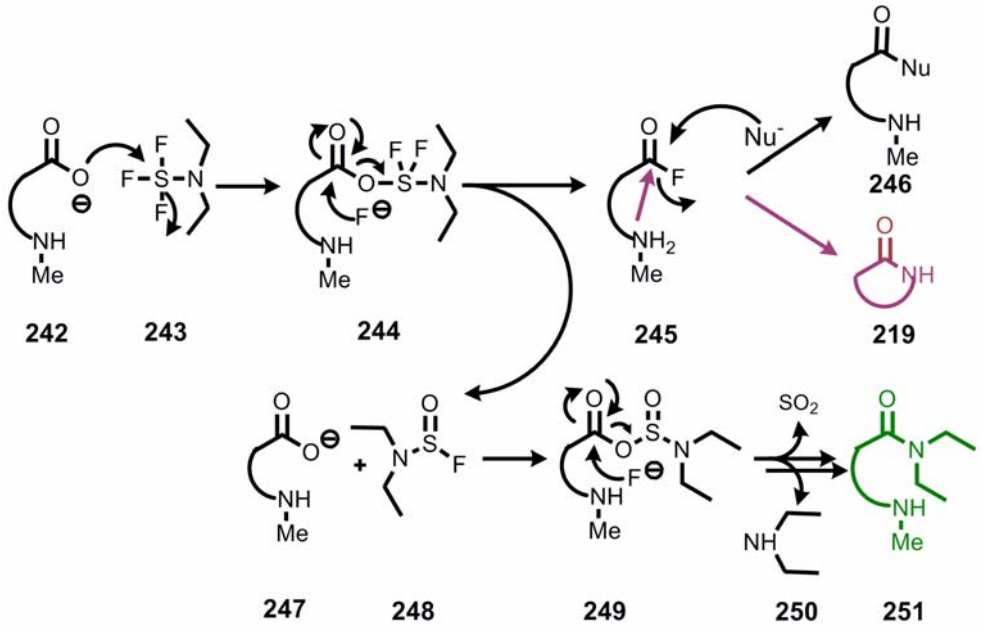

Scheme 66 Activation of carboxylic acid by DAST and plausible side product pathways.

Unfortunately, the desired transannular macrolactamization product (**4**) could not be formed from the cyclic precursor **106** using the previously described methods. To test if it was a problem of general reactivity or of unfavorable conformational preorganization, we tested the diasteroisomers **235** and **236** as well.

A mixture of cyclic hexapeptides **235** and **236** was treated with 50 % TFA in DCM for 1h to deprotect the acid labile groups prior to being subjected to the HATU/HOAt conditions in the presence of DIPEA in DMF. In this case, cyclic epimers of RA-VII (**4**) (**252** and **253**) could be obtained by transannular macrolactamization, albeit in low yield (Scheme 67). [D-Ala-4]RA-VII **252** and [D-Ala-4][D-Tyr-6]RA-VII **253** were isolated via preparative HPLC in yields of 2 % and 3 % respectively. Unfortunately, due to the low amounts and conformeric mixture in the solution,[56, 89-91] these epimers could not be fully characterized by NMR.

Nevertheless, this result conclusively showed that transannular lactam formation can indeed be used to successfully form the strained 14-membered cyloisodityrosine ring.[93] To the best of our knowledge, this is the first example of a transannular macrolactamization toward RA-VII (**4**) in the literature. Although this transformation occurs in a low yield and the reaction conditions need to be improved, it carries the promis that RA-VII (**4**) and/or its analogs can be obtained by a transannular macrolactamization based strategy. Studies towards this goal must be subject of future works.

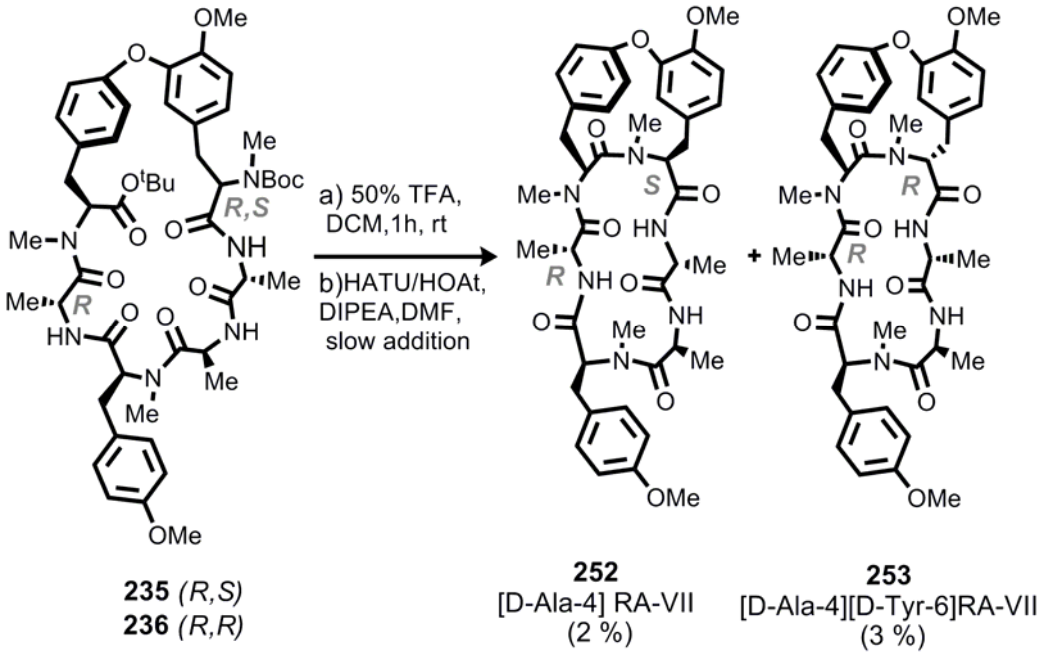

Scheme 67 Synthesis of [D-Ala-4]RA-VII (**252**) and [D-Ala-4][D-Tyr-6]RA-VII (**253**) *via* transannular macrolactamization.

Previous studies on conformational analysis of RA-VII (**4**)[55, 86-88] have shown two conformers in $CDCl_3$ and three conformers in DMSO-d_6. RA-VII (**4**) and epimeric analogs [D-Ala-4]RA-VII (**252)** and [D-Ala-4][D-Tyr-6]RA-VII (**253**) were therefore subjected to molecular modelling experiment in order to elucidate the optimal conformers. This should lead to insight in the reactivity differences of RA-VII and its epimers. Molecular modellings were performed by using the software, Maestro 7.5, MacroModel 9.1 and energy minimization of the optimal confermers were calculated by OPLS2005. [h]

For RA-VII (**4**) the minimum energy conformer features *trans-trans-trans-trans-cis-trans* (*t, t, t, t, c, t)* amide bond configutraions between D–Ala^1/Ala^2, Ala^2/Tyr^3, Tyr^3/Ala^4, Ala^4/Tyr^5, Tyr^5/Tyr^6, Tyr^6/D–Ala^1, which fully corresponded to the experimental data provided by NMR in the literature.[86] In parallel to this experiment, the conformations of epimeric analogs [D-Ala-4]RA-VII (**252)** and [D-Ala-4][D-Tyr-6]RA-VII (**253**) at the global energy minimum were evaluated. According to these calculations they possess (*t, t, t, t, c, t) and* (*t, c, t, t, t, t)* amide bond configurations, respectively (Figure 23)

[h] Molecular modelling calculations were performed by Dr. Stefan Wetzel.

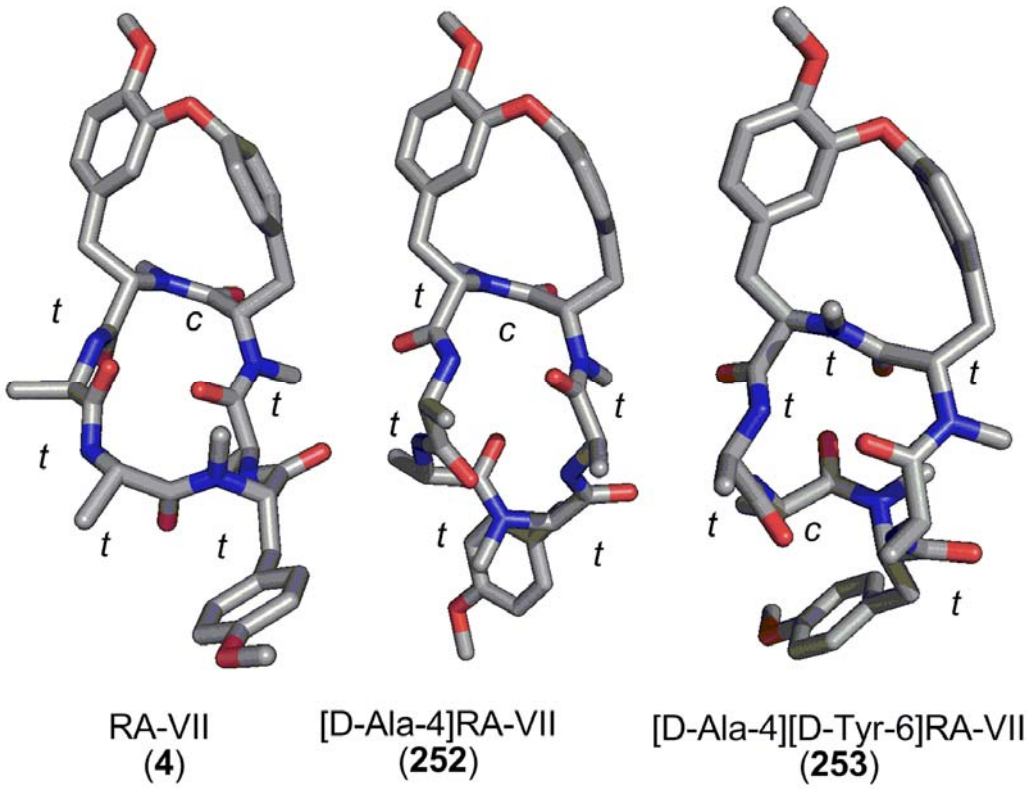

Figure 23 Minimized energy conformational search of **4**, **252**, **253** was done by molecular modelling (OPLS 2006).

Overlayed structures of RA-VII (**4**) and analogs [D-Ala-4]RA-VII (**252)** and [D-Ala-4][D-Tyr-6]RA-VII (**253**) are shown in Figure 24. The shape of the cyclic isodityrosine unit is conserved with the exception of **253.** Due to the *trans* amide bond between Tyr^5/Tyr^6 the OMe of Tyr^6 points the other direction than in **4** and **252**. The tetrapeptide part seems to be more flexible and in this motive a difference is seen for Tyr^3. In **252**, it points upward from the upper cycloisodityrosine part, but it is directed in an opposite direction **4** and **253** keeps the alignment quite similar way.

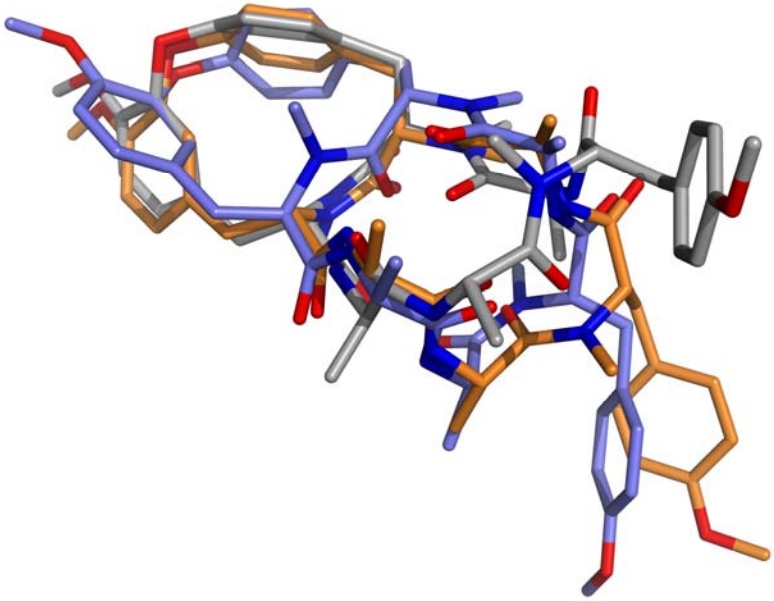

Figure 24 Overlay of minimized structures of RA-VII (**4**), [D-Ala-4]RA-VII (**252**) and [D-Ala-4][D-Tyr-6]RA-VII (**253**) as obtained from molecular modelling calculation (OPLS 2006). Orange: RA-VII (**4**); grey: **252** and blue **253**.

By taking a closer look at the modelling data, a difference in the population of conformational states could be deduced for **4** and **252**. The *trans* isomer of **252** was apparently disfavored by 10 kcal, while the *trans* isomer of **4** is more disfavored. Occurrence began at 20 kcal differences only. This could be a possible explanation for the observed difference in the success of the cyclization reaction for **4**, **252** and **253**. It implicates that **4** is more strained than in **252** and **253** with respect to the central amide bond.

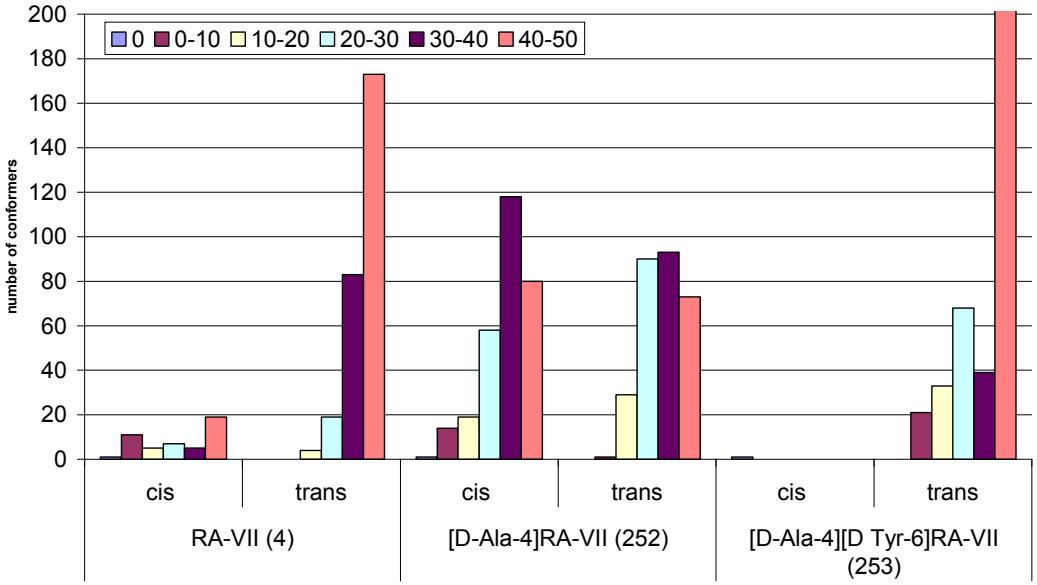

Graphic 1 Population states at different energies between the minimized conformers.

Eventually, the formation of the *cis* amide bond for the 14-member ring junction (Tyr^5/Tyr^6) may require more energy input than the studied reaction conditions offered. The epimeric analogs, which have more tendencies towards the *trans* amide bond are seen also to undergo a transannular macrolactamization more easily. This could indicate that the ability of populating a *trans*-configured transannular amide bond at least supports the intended reaction pathway. Future reaction design should take this parameter into account.

Previously it was reported that simplified analogs of RA-VII (**4**) retained the biological activities[41]. Therefore we considered to test the cyclic epimers (**119**, **235** and **236**) various biological purposes. Cytotoxity, antitumor activity and microbial activity have been evaluated. The cytotoxic evaluation of simplified acyclic analogs of RA-VII (**4**) and deoxybouvardin (0.002 μg/mL) in L1210 cells *in vitro* still showed detectable activity (10 μM). RA-VII (**4**) is known as nM range eukaryotic protein synthesis inhibitor.[23] The eukaryotic ribosome is believed to be the molecular taget of the RA-VII (**4**) as an anticancer agent. Up to date neither RA-VII nor the simplified analogs were studied on prokaryotic systems. Therefore simplified analogs were tested in available bacterial coupled transcription and translation inhibition assay.

RA-VII (**4**) has also inhibitory effects such as cell growth inhibition of cancer cells and cytokinesis inhibition by binding to actin[84]. Available cell proliferation assay on MCF-7 breast cancer cells were carried out for the simplified analogs of RA-VII (**4**).

The WST assay was used to measure the cytoxicity of the (**119**, **235** and **236**). Unfortunately, they did not show any inhibitory effect in L1210 leukemia cells and MCF-7 breast cancer cells up to 10μM concentration. Furthermore, non of the simplified RA-VII (**4**) analogs showed any inhibitory effect on bacterial protein synthesis up to 40 μM. The fully developed bicyclic scaffold hence seems to be important for biological activity.

6. Conclusion

This work explored a novel strategy to synthesize the bicyclic hexapeptide natural product RA-VII, which has gained increasing interest a mode of action which needs to be further clarified as promising anticancer agent.

Towards the total synthesis of RA-VII, the synthesis of tyrosine and isodityrosine building blocks was established on multi gram scale. The isodityrosine derivatives were synthesized by modified *Chan-Evans-Lam* cross coupling protocol. Isodityrosine **125** was synthesized in very good yield (90 %). Analogs **121** and **127** were prepared by orthogonal deprotection strategy in order to obtain either the unprotected *N* terminus or *C* terminus, respectively.

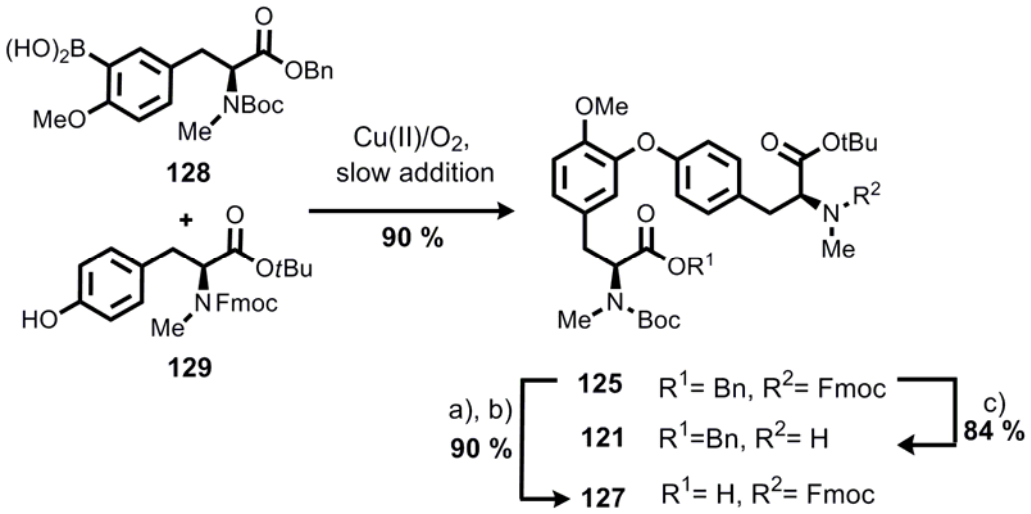

Scheme 68 Optimized *Chan-Evans-Lam* cross coupling protocol for the boronic acid **128** and phenol **129**. Isodityrosine building blocks (**121** and **127**) via orthogonal protecting group protection.

This allowed to explore versatile routes to investigate different hexapeptide assembly strategies. Solid phase peptide synthesis methods were established to couple the building blocks towards the linear hexapeptides. This has been achieved with two different sequences of linear precursor (**211** and **213**) of RA-VII with very good yields (30-65 % overall). Alternatively, a fragment coupling approach to synthesize hexapeptide was utilized to afford linear hexapeptide natural precursors **205** (45%) and epimer **206** (30%). These advancements gave the opportunity to study the best cyclization site for macrolactamization of the entire RA-VII (**4**) structure.

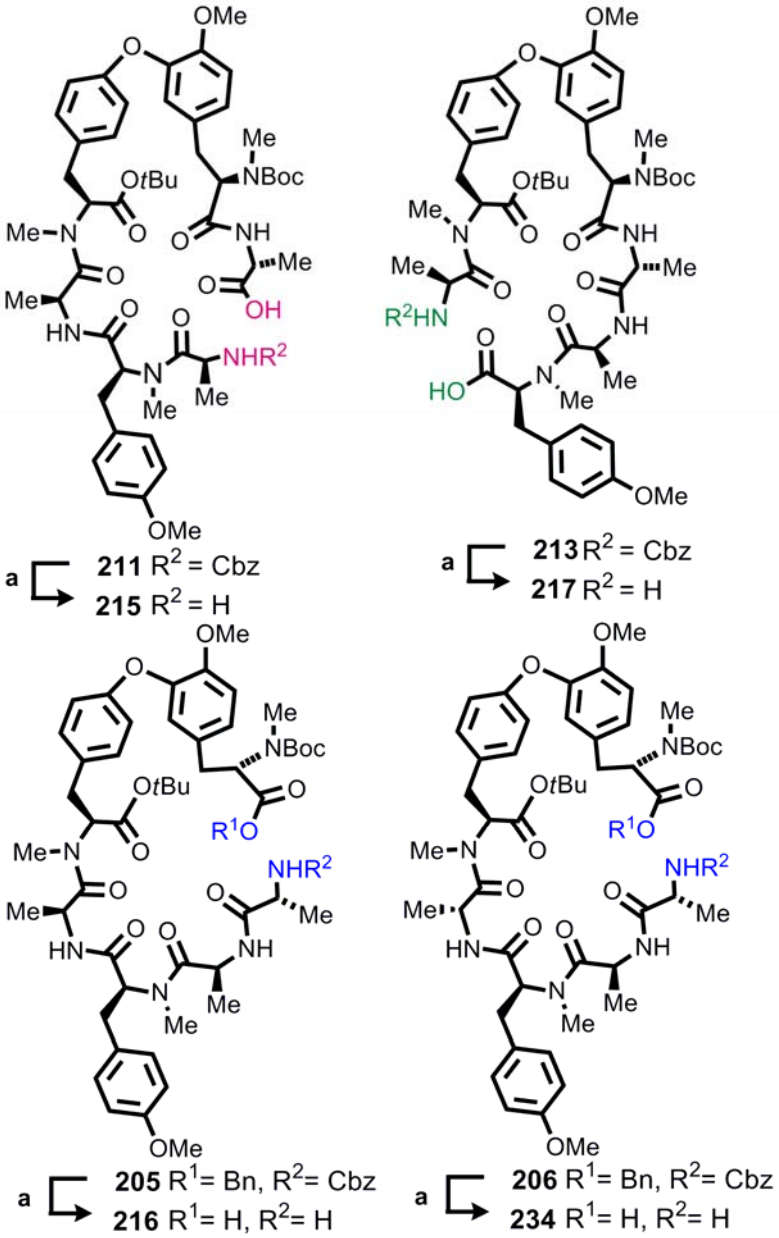

Scheme 69 Synthesized linear hexapeptide precusors. a) H_2, Pd/C, MeOH.

Productivity of the solid phase strategy for the **211** opened the opportunity to investigate more cyclization conditions. Besides the different coupling reagents, the effect of templation agent (KPF_6) was also studied in order to optimize macrolactamization conditions. PyBrop/HOAt coupling reagents afforded the macrocyclic **119** in the presence of inorganic basses Cs_2CO_3 or K_2CO_3/KPF_6 with reasonable yields (30-35 %). From the three cyclization precursors, the linear precursors **215**, **216** was shown to be the best choice for amide bond formation between the carboxylic acid of L-Tyr^6 and amine D-Ala^{1,} resulting in the cyclic precursor of RA-VII (**119**). The final conditions for macrolactamization used

HATU/HOAt in the presence of DIPEA in DMF to get the product in 40 % yield. Furthermore, epimer 234 was also subjected to macrolactamization to afford macrocycles **235** and **236**.

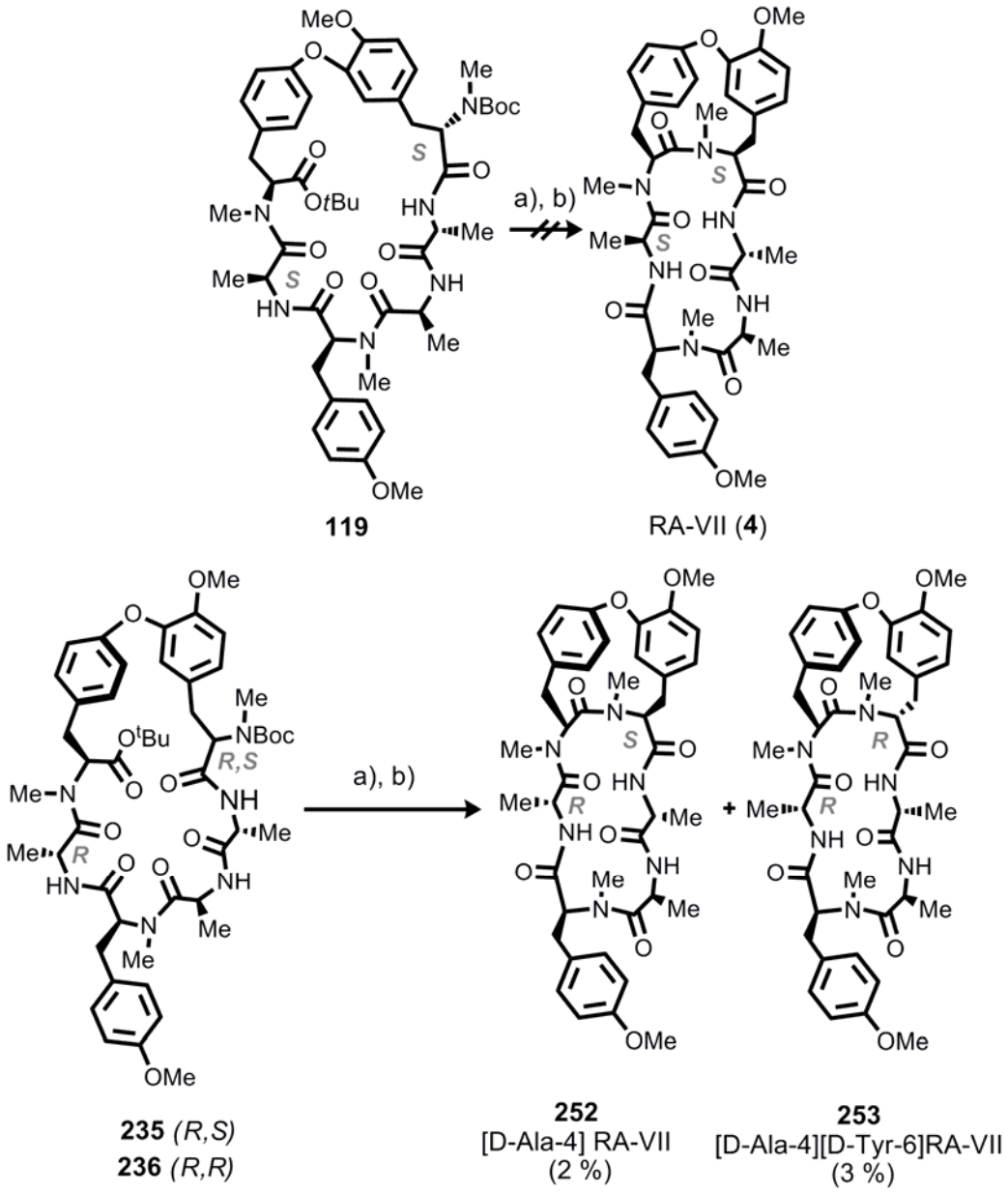

Scheme 70 Transannular macrolactamizations products. a) 50 % TFA, b) HATU/HOAt, DIPEA, DMF, 16h, slow addition.

Therefore, the natural cyclic epimer **119**, two epimeric macrocycles (**235** and **236**) were studied under the transannular macrolactamization conditions in comparison. Under typical coupling conditions with HATU/HOAt, **235** and **236** successfully gave the transannular macrolactamization product, whilst the natural did not afford the

natural product (**4**). Molecular mechanics calculations suggested a different population of transannular amide bond configuration. For the epimer **252** and **253** major population of conformers was found to adopt *trans* configuration whereas **4** was exclusively *cis*-configured. Future work should therefore focus on developing a suitable reagent for the transannular macrolactamization of RA-VII (**4**) and RA-VII like products in the future, perhaps by relay architecture which allows for a larger distance between the reactive centers. If successful, this will result in a highly versatile method to obtain these specialized bicyclic compounds, and will enable library formation synthesis for biological studies.

7. Summary

7.1 O-Arylations of tyrosine derivatives

The first chapter[73] of this work contains an extensive study about the application of *Chan-Evans-Lam* cross coupling conditions in order to obtain the biaryl ether containing scaffolds. The scope and limitations of the coupling substrates (boronic acids and phenols) was studied and the method was optimized for phenol containing α–amino acids, tri- and hexa- peptides, and finally for the biaryl ether subunit of natural product RA-VII (**4**).

Briefly, the optimized reaction conditions require catalytic amounts of $Cu(OAc)_2$ (10 - 20 mol%), 5 equiv. of pyridine and powdered MS 4Å in 1,2-dichloroethane. Regarding the boronic acids, it was found that no excess of boronic acid was required and reactions could be performed in stoechiometric fashion. A slow addition of boronic acids to the reaction mixture greatly enhanced the yields and reaction efficiency. Electron rich boronic acids were able to give the cross coupling products in reasonable to good yields. However, sterically hindered boronic acids tolerated the optimized reaction conditions only if they were electron poor.

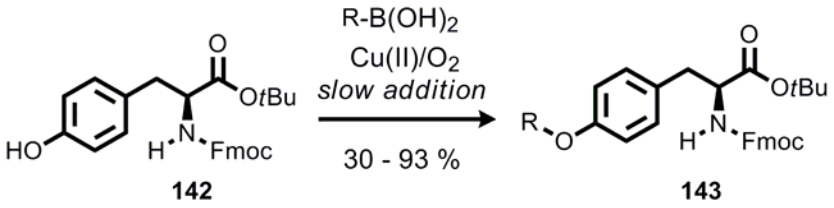

Figure 25 Aryl boronic acids for *Chan-Evans-Lam* cross couplings. Yields are based on recovered starting material.

Tyrosines with a carboxylic acid protected as a *t*Bu ester presented different reactivities depending on the substitution pattern on the amine (tertiary carbamates > secondary carbamates > secondary amines). In the case of primary amines, the nucleophilicity of the amine was found to favor arylation of the amine rather than the phenol in an oxidative copper(II) environment (**3**). Overall, nucleophilicity and steric factors need to be carefully adjusted to achieve optimal results in each case.

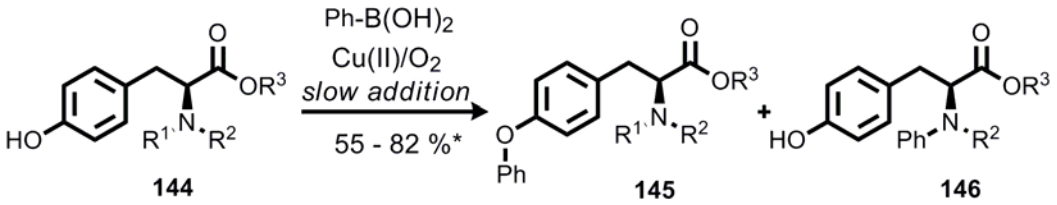

Figure 26 Tyosine derivatives for the *Chan-Evans-Lam* cross couplings.

Furthermore, the reactivities of tyrosine containing tripeptide derivatives were also investigated. The reactivity of tripeptides was dependent on the functionality present at the *C* terminus. The acid or ester derivatives were succefully arylated. However in the *C* terminus amide-containing tripeptide showed reactivity towards the amide residue. This later may be caused by the tendency of amides to strongly bind to copper ions. The reactivity of the arylations of longer peptides was also studied. In general, reactivites were similar to the tripeptides. All these results indicated that the *Chan-Evans-Lam* coupling can be used to site-specifically modify complex peptide substrates, but side chain *N*-terminal functionality prone to strongly interact with the copper catalyst should be avoided, even in a strongly competitive solvent (DMF).

The optimized coupling conditions were then successfully applied for the synthesis of biaryl ether linkage containing isodityrosine (**125**). It is an essential building block for the total synthesis of the natural compound RA-VII (**4**).

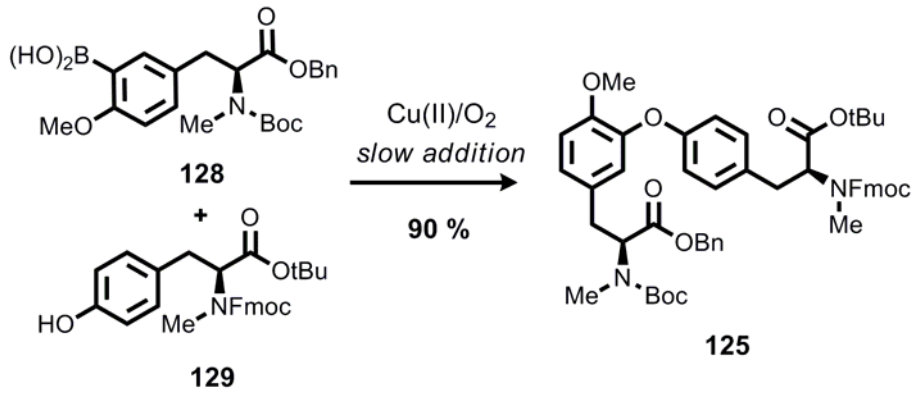

Figure 27 *Cham-Evans-Lam* coupling for the isodityrosine subunit (**125**) of RA-VII (**4**)

The corresponding boronic acid and phenol were coupled using the optimized reaction conditions: in the presence of catalytic amount of $Cu(OAc)_2$ (10 mol%) and pyridine as base/ligand in dichloroethane. The slow addition of boronic acid increased the reaction yields to 90 %.

7.2 Towards the total synthesis of RA-VII by transannular ring closure

The total synthesis plan for RA-VII (**4**) based on a transannular ring closure to form the bicyclic unit. The synthesis was based on the construction of the macrocyclic precursor **119** which may give direct access to study the transannular ring closure. For macrolactamization different sites were considered (A, B, C, Figure 28) non-substituted amide bonds.

Firstly, the synthesis of necessary tyrosine building blocks (**126**, **128**, **129**) were established on multi gram scale in high yields and with high enatiomeric purity (94% to 98% ee). Furthermore, successfully applied modified *Chan-Evans-Lam* coupling yield orthogonally protected isodityrosine building block **125**.

Isodityrosine **125** was selectively deprotected to obtain isodityrosine amine and acid building blocks. These were used for the two types of linear precursor synthesis of three different macrolactamization sites. One is a [4+2] fragment coupling strategy (disconnection A) and the other one linear solid phase synthesis strategy (disconnection B and C). By this approach we achieved the synthesis of **119** by different linear precursors which proved the exact structure.

The solid phase peptide strategy afforded two linear peptides (disconnection B and C) with good yields (18% - 35%). The **215** was the most effective hexapeptide in terms of purity and yields after the solid phase synthesis. However cyclization yields by typical macrolactamization conditions afforded **119** with very low yield. Therefore alternative templating reagents were investigated in order the improve cyclization efficency. The influence of different templating agents (KPF_6 or Cs_2CO_3) was investigated. Macrocyclization in the presence of inorganic bases such as Cs_2CO_3 or K_2CO_3/KPF_6 with PyBrop/HOAt as coupling reagents improved the desired macrocycle **119** yield up to 35 %.

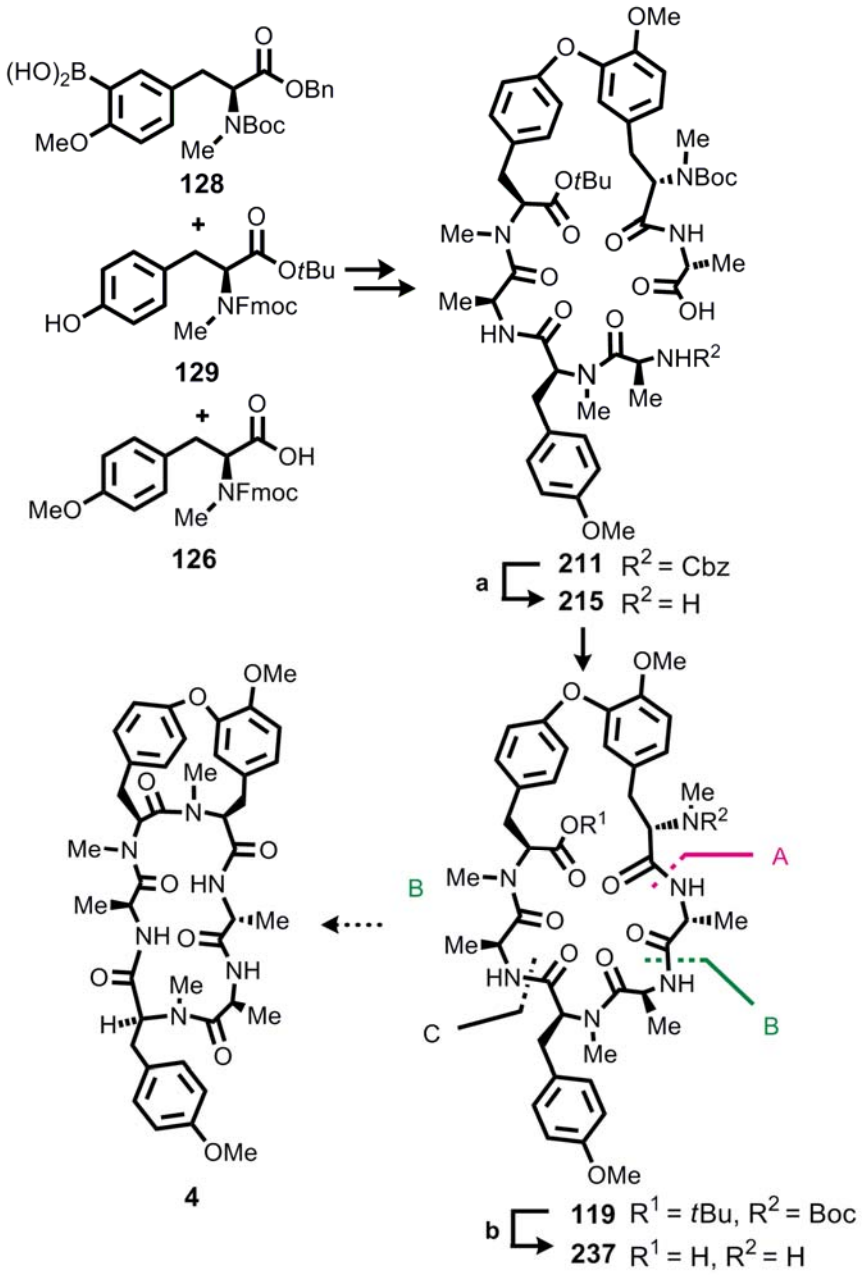

Figure 28 Synthetic strategy for RA-VII (**4**) *via* transannular ring closure of **119**. Possible disconnection sites fro the synthesis of **119**.

The second approach as [4+2] fragment coupling between biaryl residue and tetrapeptide yield the linear precursor **205** (40% yield) and the isomer **206** (30 %). By using microwave irradiation this fragment coupling this was improved to have a single natural isomer **205** with 35 % yields. The unnatural epimer **206** was also subjected to macrolactamization conditions which gave two cylic epimers (**235** and **236**). In the final step, transannular macrolactamization was studied for cyclic epimers **235** and **236**, and also for natural epimer **119**. Under typical coupling conditions with

HATU/HOAt, **235** and **236** successfully gave the transannular macrolactamization products (**252** and **253**), while unfortunately, under the same conditions the natural precursor **119** did not afford the natural product RA-VII (**4**).

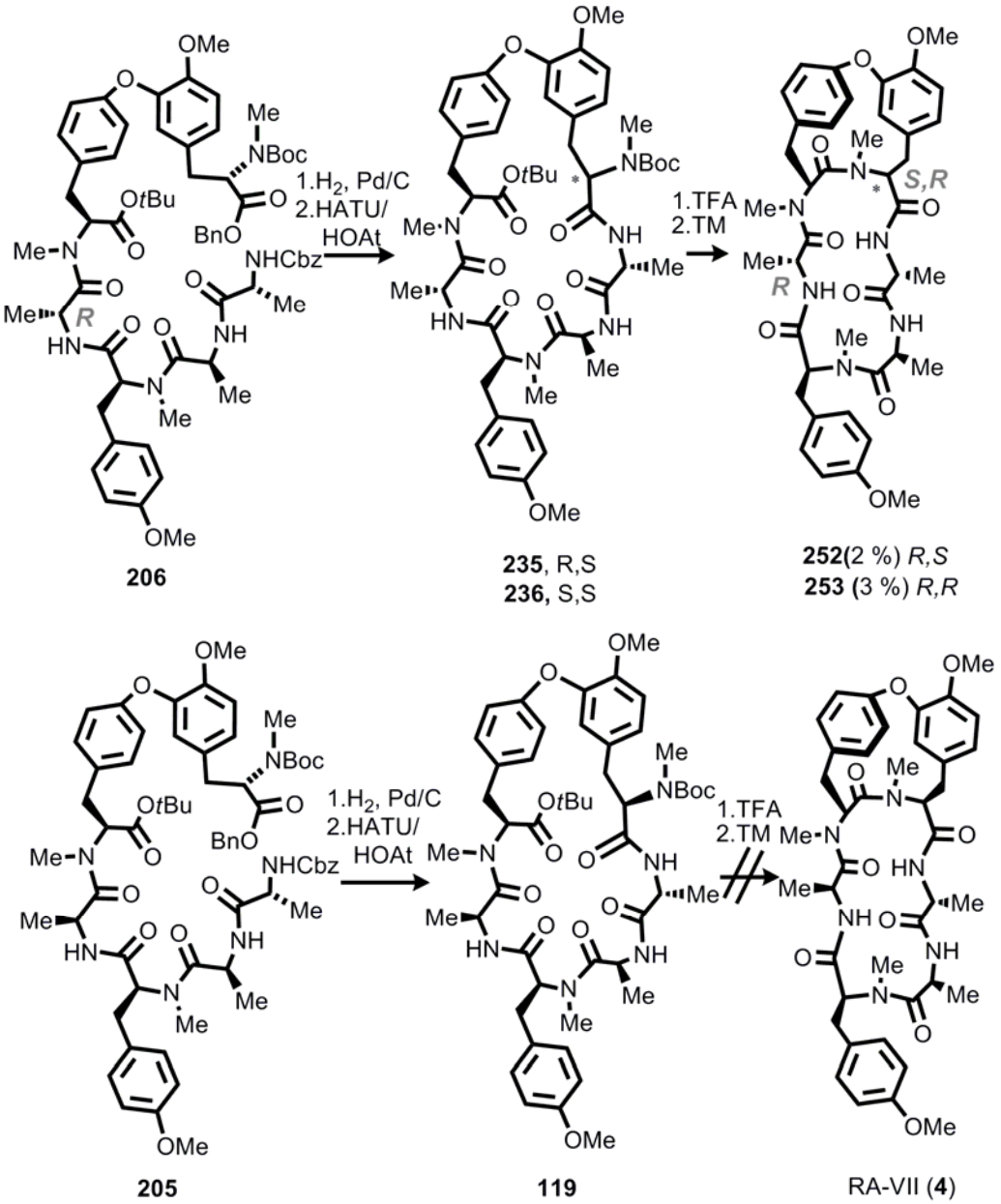

Figure 29 The synthesis of RA-VII (**4**) analogs *via* transannular ring closure. Transannular macrolactamization.

The results obtained in the above for the transannular ring closure can be explained by molecular mechanics calculations which suggested a different population of transannular amide bond configuration. In the case of cyclic epimers **252** and **253,** a major population of conformers was found to adopt *trans* configuration whereas RA-

VII (**4)** was exclusively *cis*-configured, which would difficult the final cyclization step, hence supporting the results obtained in this work.

In the course of the biological evaluations[i] the cytotoxicities and inhibitory effects on bacterial protein synthesis were investigated for fully characterized cyclic natural precursor **119** and the two macrocyclic epimers **235**, **236**. Unfortunately, they did not show any inhibitory effect on bacterial translation initiation assay until 40 μM concentration. In addition, they did not induce any cytotoxicity in L1210 tumor and MCF-7 breast cancer cells lines in concentrations up to 10 μM.

Future work should focus on developing a suitable reagent for the transannular macrolactamization of RA-VII (**4**) and RA-VII-like products, to enable in a highly versatile method to obtain a library of compounds based on RA-VII (**4**) structure.

[i] Bacterial coupled transduction/translation initiation assy was performed by Diplom. Biol. Sascha Baumann. Cytotoxicity assay was performed Diplom. Biol. Bernhard Ellinger.

8. Experimental Section

8.1 Analytical Instruments and Methods

Nuclear magnetic resonance spectroscopy (NMR): Spectra were recorded by Varian Mercury-VX 400, Bruker Avance DRX 500 and Varian Unity Inova 600 NMR spectrometers. Chemical shifts are expressed in parts per million (ppm) from internal deuterated solvent standard. All measurements were taken in deuterated solvents such as chloroform-d_1 (7.24 ppm (^{1}H) and 77.2 ppm (^{13}C)), acetonitrile-d_3 (1.94 ppm (^{1}H) and 118.69 ppm (^{13}C), methanol-d_4 (3.31 ppm (^{1}H) and 49.15 ppm (^{13}C)), dimethyl sulfoxide-d_6 (2.5 ppm (^{1}H) and 39.5 ppm (^{13}C)). (Coupling constants (*J*) are given in Hertz (Hz) and multiple signals were classified as s= singlet, d= doublet, t= triplet, q= quartet, tq = triple quartet, m= multiplet).

Liquid chromatography coupled mass spectrometry (LC-MS): Measurements were made with an Agilent Series 1100-System from Hewlett Packard with CC 250/4 Nucleosil 120-5 C4 and gravity C18 chromatography columns by Macherey-Nagel. The ESI mass spectrometer was an LCQ Advantage MAX from Finnigan. Flow rates were 1 ml/min, Eluent A: 0.1 % HCOOH in H_2O; Eluent B: 0.1 % HCOOH in Acetonitrile.
Method-LCMS-1 (C18-10): 0-1 min 10 % B, 1-10 min linear increase from 10 to 100 % B, 10-12 min 100 % B.
Method-LCMS-2 (C4-10): 0-1 min 10 % B, 1-10 min linear increase from 10 to 100 % B, 10-12 min 100 % B.
Method-LCMS-3 (C4-50): 0-1 min 50 % B, 1-10 min linear increase from 50 to 100 % B, 10-12 min 100 % B.

High resolution Mass Spectra were taken with a JEOL SX102A spectrometer. Fast Atom Bombardment (FAB) with matrix (*m*-nitrobenzyl alcohol) was used as an ionization method. Alternatively, high resolution mass spectra were obtained by ESI (electron spray ionization) on an Accela/LTQ Orbitrap (LC/ESI) system. (Thermo Scientific).

Optical rotations were measured by using the Schmidt + Hänsch Polatronic HH8 polarimeter (wave length sodium- D- line (589 nm). Concentrations (*c)* of substances in MeOH or Chloroform are given in g/100 mL.

Melting Points were measured by using a 540 Büchi melting point apparatus with no correction.

Infrared (IR) Spectra were measured on KBr using a Vector 22-Spectrometer (Bruker). Samples were prepared on KBr. The OPUS software package was used to acquire and manipulate the spectra. Description of the band intensities were abbreviated by: s = strong, m = middle, w = low, br = broad signals.

MALDI-TOF (matrix-Assisted laser desorption/ionization)- (time of flight) mass spectra were taken using a Voyager DE_{TM} Pro Biospectrometry Workstation Spectrometer (Perceptive Biosystems). DHB (2,5-dihydroxybenzoic acid) and CHCA (α-cyano-4-hydroxycinnamic acid) were used as matrix.

Analytical reversed-phase high performance liquid chromatography:
Chromatograms were recorded on a Varian ProStar; CC250/4 Nucleosil 100-5 C_6H_5, EC125/4 Nucleodur C18 Isis 3 mm and CC250/4 Nucleosil 100-5 C18 Nautilus (Macherey & Nagel); Detection mode was UV (270 nm); Flow rate 1 mL/min. Eluent A: H_2O[a] + 0.1% TFA; B: Acetonitrile + 0.1% TFA.
Method-A: 5→ 100 % B in 17 min.
Method-B: 50→ 100 % B in 17 min.
Method-C: 10→ 100 % B in 25 min.

Analytical reversed-phase chiral HPLC:
Chromatograms were recorded on Agilent/HP 1100 Series fitted with a ChiralCEL OD-R-AD column (Daicel Chemical Industries). UV absorptions were used for detection (270 nm); Flow rate 0.5 mL/min Eluent A: H_2O[a] + 0.1% TFA; B: Acetonitrile + 0.1% TFA
Method-RP-Ch-1: 50 % B (0–10 min), 50-100% B (1–25 min), 100–50% B (25–35 min). Method-RP-Ch-2: 50–100 % B (0–5 min), 100% B (5–25 min), 100–50% B (25–30 min).

[a] Water was obtained from a Milli-Q-System with Q-grade 2-cartidges (Milipore) and used for all chromatographic purposes.

Analytical normal phase chiral HPLC was recorded using an Agilent Series 1100-System fitted with Chiralpak® IC columns (Daicel Chemical Industries). IC-(250 x 4.6 mm): 10% CH_2Cl_2 + 2% EtOH, 90% *i*-Hexane.

Preparative reverse-phase high performance liquid chromatography (prep HPLC) was performed on Agilent system coupled with a MS detector from the 1100/LC/MSD VL (ESI) series and the chromatography columns used were VP50/21 Nucleodur C18 Gravity 5 μm (pre column), VP125/10 Nucleodur C18 Gravity 5 μm (column) (from Macherey and Nagel). Detection: 215 and 254 nm (UV detector) and ESI (the same system as LC-MS), Eluent A: H_2O + 0.1% TFA, Eluent B: Acetonitrile + 0.1% TFA.

Method-RP-prep-1: (10 mm), 1-5 min 50% B, 5-10 min linear increase up to 85% B, 10-20 min 85% B, 20-25 min 100% B, 26-28 min 50 %B, flow rate: 10 mL/min.

Method-RP-prep-2: (21 mm) 1-5 min 30% B, 5-10 min linear increase up to 80% B, 10-20 min 80% B, 20-25 min 100% B, 26-28 min 30% B, flow rate: 20 mL/min.

After preparative HPLC, the fractions containing pure product were combined and lyophilized to give the pure products.

For **TLC** (Thin Layer Chromatography) aluminum plates coated with Silica 60 F_{254} were used. Eluent and R_f values are given for each compound in section 8.5. UV-light (254 nm) and the following staining solutions were used for the detection.
Staining solution A: 2.5 g molybdatophosphoric acid, 1 g $Ce(SO_4)_2$ and 6 mL concentrated sulfuric acid in 94 mL H_2O.
Staining solution B: 5 g molybdatophosphoric acid in 10 mL EtOH.

UV/Vis Spectra were measured on a Cary 100 Bio UV/Vis-Spectrometer from Varian. Quartz glass cuvettes (with a path length of d= 1 mm) were used.

Microwave synthesizer:

Microwave-assisted reactions were performed in a Discover (CEM Corporation) single-mode microwave instrument producing controlled irradiation, using standard sealed microwave glass vials. Reaction temperatures were monitored with an IR

sensor on the outside wall of the reaction vials. Reaction times refer to hold times at the indicated temperatures, not to total irradiation times.

For **automated peptide synthesis** a microwave assisted peptide synthesizer (CEM) technology was used.

For **Column Chromatography** silica gel from Acros (35-70 μm) was used.

Dry solvents such as diethyl ether, *N,N*-dimethy formamide, methanol, tetrahydrofuran, *1,2*- dichloroethane were obtained from Acros and Fluka. Dichloromethane and Acetonitrile were distilled over Calcium hydride. Acetone was distilled over 3 Å molecular sieves. Chemicals were supplied by SIGMA-ALDRICH, ACROS, FLUKA, ABCR, Novabiochem, GL-Biochem, Bachem, Combi-blocks and used as received unless stated otherwise.

8.2 Molecular modelling calculation methods

Macromodel 9.1 (Schrödinger, Portland US) and Maestro 7.5 were used for the conformational search and conformational space was sampled via a low-mode search (LMOD) using low-frequency eigenvectors. The initial ensemble of 25,000 structures was condensed to unique structures based on root mean square deviation (RMSD) differences of more than 0.25 Å. All conformations with in 50 kcal/mol of the global energy minimum were kept for subsequent energy minimization. The energy of the conformers was minimized using a maximum of 10,000 steps of the truncated Newton conjugate gradient (TNCG) algorithm with the OPLS 2005 force field. The GB/SA salvation model for water as implemented in MacroModel was used. For line searching, i.e. the way how the direction towards the minimum of the energy gradient is calculated, MacroModel offers two methods: the common methods and a special implementation for TNCG. However, a problem with the line search implemented in TNCG was observed and reported and, hence, we switched to the common line search algorithm by setting the line search parameter to 0 instead of 1. All other parameters were left at the standard settings. Convergence was reached when the gradient was smaller or equal to 0.05 kJ/mol. Comprehensive sampling of conformational space is indicated by the fact that the lowest energy conformation was found significantly more than once in all cases. Images were created using PyMol 0.99 from Delano Scientific. Overlays were generated based on all heavy atoms in the macro cycle using Schrödinger Maestro 7.5.

8.3 Coupled in vitro transcription/translation Initiation assay

Coupled *in vitro* transcription/translation inhibition assays developed by Sascha Baumann by using an optimized protocol for the RTS 100 *E.coli* HY Kit from Roche Diagnostics which is performed in 384 well plates (OptiPlate 384F, Perkin Elmer). The assay set up allows determination of inhibitors for the prokaryotic protein biosynthesis. Inhibitors can target the RNA polymerase or the ribosome. Therefore active compounds have to be tested by a separate assay to differentiate between the T7 RNA polymerase inhibition and the ribosome inhibition. In the assay a plasmid containing a green fluoresent protein (GFP) driven by a T7 promoter is used. By the addition of T7 RNA polymerase the GFP gene is transcribed and is later on translated by the bacterial ribosome into a functional GFP protein. Chromophore is formed approx. in 24 h at 4°°C. This followed by the addition of the compound to the media which correlates the intensity of fluorescent which can further be quantified.

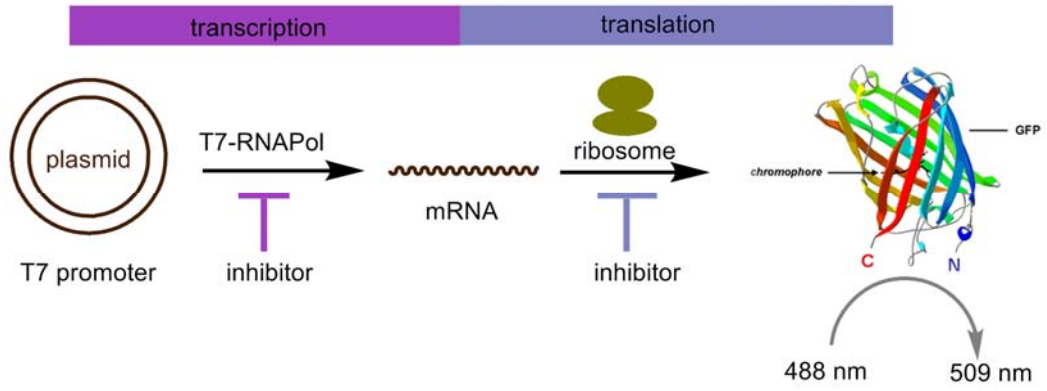

Scheme 71 Schematic presentation of coupled *in vitro* transcription and translation assay set up.

The *in vitro* transcription and translation was run 1-1.5h at 30°C and the system was stored over night at 4°°C for the development of GFP fluorophore. The fluorensent intensity was analyzed by TECAN infinite M200 plate reader at 395 nm excitation and 504 nm emission wavelength (25 reads/well, optimal gain) The assay results were normalized and plotted against the compound concentration. Sigmoidal shaped curves were fitted using Hill's equation[j] to yield IC_{50} values.

Fitted curves for control compounds and simplified structures were presented in Graphic 2. Chloramphenicol (euthentic sample) and Kirromycin (synthetic sample) are

[j] Hill's equation: $\frac{d^2y}{dx^2} + \left(\theta_0 + 2\sum_{n=1}^{\infty}\theta_n \cos(2nx)\right)y = 0$

known bacterial translation initiation inhibitors by targeting the ribosome.They both have inhibition of 8.4 +/- 1.5 μM and IC50: 0.53 +/- 0.08 μM, respectively. However non of the simplified RA-VII analogs showed any inhibitory effect on bacterial protein synthesis.

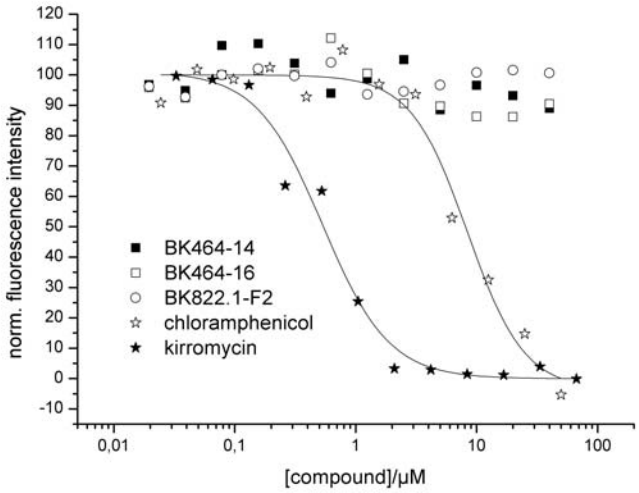

Graphic 2 Fluorescent titration curves for simplified analogs of RA-VII **119** (BK822.1-f2)**, 235** (BK464-14)**, 236** (BK464-16) and known inhibitors as controls (chloramphenicol and kirromycin) for IC_{50} values determination. Chloramphenicol IC50: 8.4 +/- 1.5 μM, Kirromycin IC50: 0.53 +/- 0.08 μM.

8.4 Cytotoxicity assay (WST mesurement)

The WST assay used to measure the toxicity of the tested compounds which was performed by Bernhard Ellinger. The inhibition of cytokinesis induces apoptosis and thereby leads to cell death. The mouse lymphocytic leukemia cell line L-1210 was obtained from DSMZ (No. ACC 123). Cells were seeded in a concentration of 4,000 cells per well in clear flat bottom 96 well plates. Cells were grown for 3 days in DMEM with 10 % horse serum in a total volume of 100 µl already containing the appropriate concentration of small molecules or DMSO as control. Measurement was done after applying 10 µl of wst reagent (Roche, Germany) by using a spectrophotometer at 440 nm. Between the measurements the cells were incubated at 37 °C under linear shaking. Every value is measured as quadruplicate. Viability is measured by the wst assay and is normalised by setting a positive control to 100 % and a blank to 0 %. RA-

VII precursor has an IC_{50} of 20 nM under these conditions in L-1210 cells (Boger *et al*.) [41]

Table 1:

	Concentration in nM	Relative viability in %
236	10,000	101.4
235	10,000	128.7
119	10,000	101.5
Jaspamide	40	24.7

Cytotoxicity measurements of RA-VII pecursors (**119**, **235**, **236**) in comparison with Jaspamide in L-1210 cells.

8.5 General Procedures

8.5.1 Loading of 2-Cl-trityl resin (GP1)

In a solid phase reactor 2-Cl-trityl resin (100-200 mesh, 1.4 mmol/g, 1 g, 1.4 mmol) was swollen for 10 min with dry CH_2Cl_2 (2 x 10 mL). The resin was drained and a solution of Fmoc-protected amino acid (7 mmol) was dissolved in dry CH_2Cl_2 and DIPEA was added (2.2 g, 14 mmol). The reaction was agitated under argon for 16 h. The resin was then washed with CH_2Cl_2 (3 x 5 min) and suspended in CH_2Cl_2/MeOH/DIPEA (17:2:1, 10 mL) for 30 min. It was subsequently washed with CH_2Cl_2 (3 x 10 ml), DMF (3 x 10 mL), CH_2Cl_2 (4 x 10 mL), Et_2O (4 x 10 mL) and dried under high vacuum overnight. Loading was determined by a Fmoc test (0.40 - 0.46 mmol/g).

8.5.2 Loading on benzyl alcohol resin (Sasrin, Wang) (GP2)

In a solid phase reactor the resin (100-200 mesh, 0.68 mmol/g, 1 g, 0.68 mmol) was swollen with dry CH_2Cl_2 (10 mL) and dry DMF (10 mL) for 10 min each time. In the meantime, 3 equiv. Fmoc-protected aminoacid (2.04 mmol) was dissolved in dry DMF (2 mL). Pyridine (274 μL, 3.4 mmol) and 2,6-dichlorobenzoyl chloride (293 μL, 2.04 mmol) were added to the solution of *N*-protected amino acid in DMF. After continuous agitation for 15 min., the resin (drained but not overdried) was added and the mixture was shaken gently for 16h under argon. The resin was washed with DMF (2 x 5 min), CH_2Cl_2 (2 x 5 min) and suspended in CH_2Cl_2/Ac_2O/pyridine (4:1:1, 10 mL) for 30 min. It was then drained and washed with CH_2Cl_2 (3 x 10 mL), DMF (3 x 10 mL), CH_2Cl_2 (4 x 10 mL), Et_2O (4 x 10 mL) and dried under high vacuum overnight. Loading was determined by the Fmoc test (0.40 - 0.44 mmol/g).

8.5.3 Loading on rink amide resin (GP3)

In a syringe reactor Rink amide resin (100-200 mesh, 500 mg, 0,64 mmol/g, 0.32 mmol) was swollen with dry CH_2Cl_2 (5 mL) and dry DMF (5 mL) each time for 30 min. The resin was sequentially treated with a de-blocking cocktail (5 mL, piperidine/DMF 1:4) for 5 s, 10 min, 15 min then washed with DMF (2 x 10 mL). In the meantime, 5 equiv. of the corresponding *N*-protected amino acid (1.60 mmol) was

dissolved in activator solution (HBTU (0.64 mmol), HOBt (0.64 mmol) in DMF (*c* = 0.4 M) DIPEA was added (3.2 mmol)) and the mixture was shaken for 10 min before it was added to the resin. The suspension was gently mixed for 3h at rt, then washed with DMF (3 x 10 mL) and CH_2Cl_2 (3 x 10 mL) and was then treated with capping solution (CH_2Cl_2/Ac_2O/pyridine 4:1:1, 10 mL) for 30 min. The resin was washed with CH_2Cl_2 (3 x 10 mL), DMF (3 x 10 mL), CH_2Cl_2 (2 x 10 ml) and Et_2O (4 x 10 mL), then dried under high vacuum overnight. Loading was determined by a Fmoc test. (0.40 - 0.45 mmol/g).

8.5.4 Loading on hydrazine resin (GP4)

Synthesis on the Fmoc-4-hydrazino-benzoyl AM NovaGel resin (100-200 mesh, 0.56 mmol/g, 893 mg, 0.5 mM) was performed using microwave peptide synthesizer (Liberty, CEM® etc.). Single couplings were executed with 5 equiv. of corresponding amino acid and activator solution (HBTU (1.5 mmol), HOBT (1.5 mmol) in DMF, *c* = 0.5 M) and 3 equiv. *N*-methyl-morpholine (NMM) in *N*-methyl-pyrolidinone (NMP) (c = 0.5 M). (MW conditions: power = 18 watt, T = 75 °C for 300 sc).
The peptide was released from the solid support by an oxidative cleavage with $Cu(OAc)_2$ (0.5 equiv. with respect to initial loading), pyridine (30 equiv.), acetic acid (50 equiv.) and methanol (215 equiv.) in dichloromethane (5 mL/0.1 g of resin). Cleavage solution was reacted with the resin for 3h under oxygen atmosphere. The resin was drained and washed with MeOH (3 x 20 mL), dichloromethane (2 x 10 mL) and collected residues were evaporated under reduced pressure.

8.5.5 Loading determination of first amino acid on solid support

10 mg of dried resin containing Fmoc-protected residues was suspended in piperidine/DMF (4:1, 10 mL) and shaken for 30 min. The suspension (3 mL) was placed in a UV cuvette. For the background correction, piperidine/DMF (4:1, 3 mL) was used. Concentration of released fulvene was evaluated by determining the UV absorption *Abs.* at 301 nM from the background-corrected spectrum for the fulvene adduct.

$$C_B = \frac{Abs \times V \times 1000}{\varepsilon \times d \times m} = \frac{Abs}{m} \times 1.923 \mu mol$$

Equation 2: c_B = loading in mmol/g; Abs = Absorption at 301 nm; V = Volume in ml; ε= extinction coefficient (7800 l/mol.cm for fulvene adduct); d = path length in cm; m = resin weight.

8.5.6 HOBt/HBTU mediated solid phase peptide couplings (GP5)

The *N*-Fmoc protected amino acid (2 equiv. with respect to the resin loading unless stated otherwise) was dissolved in activator solution (HBTU (2 equiv.), HOBT (2 equiv.) in DMF (0.4 M)) and DIPEA was added (2 equiv.). The mixture was agitated for 5 min and added to the deblocked resin. The couplings were proceeded for 3h at rt, then the resin was drained, washed with DMF (3 x 10 mL), CH_2Cl_2 (3 x 10 mL), and treated with capping solution (CH_2Cl_2/Ac_2O/pyridine 4:1:1, 10 mL) for 30 min. It was finally washed with CH_2Cl_2 (3 x10 mL) and DMF (3 x 10 mL). For the consecutive couplings removal of the Fmoc residue was executed in a syringe reactor, and the resin was treated in duplicate (10 s, 1 min, 15 min) with Fmoc deprotection solution (piperidine/DMF 1:3, 10 mL/g). The deprotected resin was washed with DMF (2 x 10 ml), CH_2Cl_2 (2 x 10 ml) and DMF (2 x 10 ml).

8.5.7 HATU/HOAt mediated solid phase peptide couplings (GP6)

The *N*-Fmoc protected amino acid (2 equiv. with respect to the resin loading) was dissolved in activator solution (HATU(2 equiv.), HOAt (2 equiv.), in DMF (0.4 M)) and EtN(*i*Pr)$_2$ (2 equiv.) was added. The mixture was agitated for 5 min. and added to the de-blocked resin. The reaction was shaken for 3h. (for double couplings the procedure was repeated). The resin was drained and washed with DMF (3 x 10 mL) and CH_2Cl_2 (3 x 10 mL) and was treated with capping solution (CH_2Cl_2/Ac_2O/pyridine 4:1:1, 10 mL) for 30 min., and then drained again and washed with CH_2Cl_2 (3 x10 mL) and DMF (3 x 10 mL). For the consecutive couplings removal of the Fmoc residue was executed in a syringe reactor, resin was was treated in duplicate (10 s, 1 min, 15 min) with Fmoc deprotection solution (piperidine/DMF 1:3, 10 mL/g). The deprotected resin was washed with DMF (2 x 10 ml), CH_2Cl_2 (2 x 10 ml) and DMF (2 x 10 ml).

8.5.8 BTC/2,4,6-collidine mediated solid phase peptide couplings (GP7)

Dried resin was swollen with THF (10 mL/g) for 10 min. (2 x). Triphosgene (BTC) (1.2 equiv. with respect to the resin loading) and *N*-Fmoc protected amino acid (4 equiv. respect to the resin loading) were separately dissolved in THF (5 mL/g). The two solutions were mixed and gently agitated until a clear solution was obtained (10 min.). *2,4,6*-collidine (2 equiv.) was added (fumes were observed during the formation of hydorchloric salts) and the white suspension was shaken for 3 min. The mixture was added to the resin suspended in THF/EtN(*i*Pr)$_2$ (1:0.2, 2 mL/g) and the reaction was shaken for 90 min. The resin was washed with THF (3 x 10 mL/g), CH_2Cl_2 (3 x 10 mL/g) and DMF (3 x 10 mL/g) and was treated with capping solution (CH_2Cl_2/Ac_2O/pyridine 4:1:1, 10 mL/g) for 30 min. then washed with CH_2Cl_2 (3 x10 mL/g) and DMF (3 x 10 mL/g).

8.5.9 Preparation of hydrated silver oxide

$AgNO_3$ (15 g, 88.3 mmol) was dissolved in degassed Millipore® water (177 mL) and was slowly added (within 1 h) to a solution of NaOH (8.7 g, 0.2 mol) in degassed Millipore® water (3.6 mL). The reaction was stirred in the dark under argon for 1h after the addition was complete. The brown precipitate was filtered by applying argon pressure and washed with degassed Millipore® water until flow-through water had pH 7. The residual solid was washed with dry acetone (3 x 30 mL) and diethyl ether (3 x 30 mL) and dried over night under high vacuum to give Ag_2O x H_2O as brown needles (22 g, quant.) which were dried overnight under high vacuum and stored at room temperature in dark.

8.5.10 General procedure for the arylation of phenols (GP8)

$Cu(OAc)_2$ (20 mol %) was suspended in 1,2-dichloroethane (*c* = 0.05 M). Pyridine (5 equiv.) was added and the suspension was stirred for 10 min under O_2 (1 atm). Phenol (1 equiv.) and 4 Å powdered molecular sieves (1.6 g/mmol of boronic acid) were added. Boronic acid (1.4 equiv.) was dissolved in 1,2-dichloroethane (*c* = 0.05 M) and was slowly added to the mixture by syringe pump (300 µL/h). The reaction mixture was then stirred under O_2 (1 atm) for 48 h, diluted with EtOAc, and

filtered over a pad of silica. Purification of the crude mixture by flash column chromatography gave the arylated phenol product.

8.5.11 General procedure for the hydrogenalysis (GP9)

MeOH/HCOOH (100:5, 7 mL) was stirred with active charcoal (4 g) for 30 min. and filtered through a silica/celite pad (3:2, 3 cm) under argon. Compound (0.03 mmol) was dissolved in that solvent mixture (7 mL) and added in to the Pd/C (10 wt. %) charged flask under argon. The reaction was flushed with H_2 and was stirred for 3 h under H_2. The reaction mixture was flushed with argon and the slurry was filtered through a short silica/celite pad (3:2, 3 cm) with MeOH (20 mL), EtOAc (20 mL) and concentrated.

8.6 O-Arylations of tyrosines

8.6.1 Phenol substrate synthesis

(*S*)-2-(9*H*-Fluoren-9-ylmethoxycarbonylamino)-3-(4'-hydroxy-phenyl)-propionic acid *tert*-butyl ester (142)

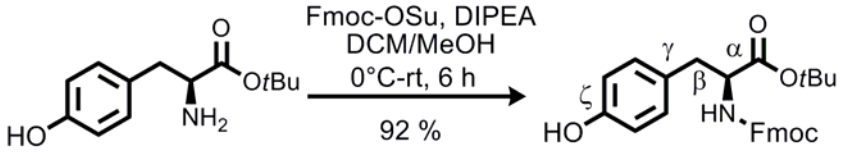

131 142

Phenol **131** (5 g, 21.1 mmol) was dissolved in CH_2Cl_2/MeOH (7:3, 100 mL) and cooled to 0°C. EtN(*i*Pr)$_2$ (3.4 mL, 21.1 mmol) was added. Fmoc-OSu (7.1 mg, 21.1 mmol) was dissolved in CH_2Cl_2/MeOH (30:2, 32 mL) and slowly added to the solution over 1h at 0°C. The suspension was stirred for 6h at rt. After the addition of EtOAc/H_2O (1:1, 100 mL), pH was adjusted to pH 2 with HCl (0.1 N). The layers were separated and the EtOAc layer was washed with saturated $NaHCO_{3(aq.)}$ solution (100 mL). The aqueous phase was re-extracted with EtOAc (2 x 200 mL) and organic layers were washed with saturated $NaCl_{(aq.)}$ solution (100 mL) dried with $MgSO_4$and concentrated. Recrystalization of the residual solid from EtOAc (cyclohexane (20 mL/ 150 mL, 40 °C)) afforded compound **142** as a colorless solid (8.5 g, 18.5 mmol, 92 %).

TLC: R_f = 0.54 ($CHCl_3$/CH_3OH/HCOOH 10:1:0.1).

HPLC: t_R = 11.25 min (Method A).

Optical Rotation: $[\alpha]_D^{20}$ = - 43 (*c* = 0.29, CH_3OH).

^{1}H-NMR: (400 MHz, CD_3OD): δ = 1.31, 1.32 (s, 9H, *t*Bu), 2.75 (dd, 1H, J_{AX} = 9.5 Hz, J_{AB} =13.7 Hz, Tyr-H$_\beta$), 2.86 (dd, 1H, J_{BX} = 5.7 Hz, J_{AB} =13.8 Hz, Tyr-H$_\beta$), 4.02 and 4.20 (two m, 4H, H$_\alpha$ and Fmoc-CH_2 and Fmoc-CH), 6.64 (d, 2H, *J* = 8.0 Hz, Tyr-Ar), 7.02 (d, 2H, *J* = 8.0 Hz, Tyr-Ar), 7.26 – 7.34 (m, 2H, Fmoc-Ar), 7.39 (t, 2H, *J* = 7.5 Hz, Fmoc-Ar), 7.57 – 7.72 (m, 2H, Fmoc-Ar), 7.86 (d, 2H, *J* = 7.5 Hz, Fmoc-Ar), 9.17 (s, 1H, PhOH).

^{13}C-NMR: (100 MHz, CD_3OD) δ = 28.3 (*t*Bu-C(**C**H$_3$)$_3$), 38.0 (C$_\beta$), 48.3 (Fmoc-

CH), 55.4 (Tyr-O**C**H_3), 57.7 (C_α), 61.5, 67.9, 67.94 (Fmoc-CH_2), 82.8 (*t*Bu-**C**$(CH_3)_3$), 116.3 (Tyr-Ar), 120.9, 126.1, 126.2, 128.1, (Fmoc-Ar), 131.5 (Tyr-Ar), 142.4, 145.1 (Fmoc-Ar), 157.3, 158.1 (C_q), 172.9 (Tyr-CO).

IR: KBr plate, $\tilde{\nu} = 3374$ (bs), 2978 (bs), 1711 (s), 1513 (m), 1226 (m), 1057 (m), 843 (m), 741 (m), 567 (w), 542 (m) cm^{-1}.

LC-MS (ESI): Method-LCMS-3: t_R = 10.57 min, for $C_{28}H_{29}NO_5$ [$(M+H^+)$] calcd. 460.5 found 460.6.

L,L,L-N-(4'*H*-Fluoren-9-ylmethoxycarbonyl)alaninyl-tyrosinyl-alanine (147a)

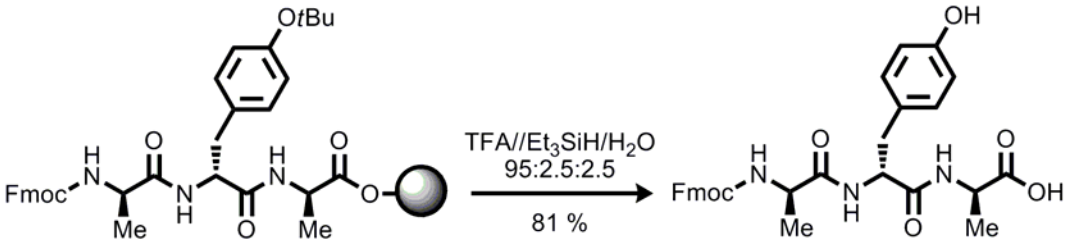

254 **147a**

The tetrapeptide **254** was assembled on Wang resin loaded with Fmoc-Ala-OH (GP2, 0.6 mmol/g, 1 g) using Fmoc-Tyr(OtBu)-OH and Fmoc-Ala-OH (GP5). The tripeptide was released from the solid support by the treatment with cleavage solution TFA/Et_3SiH/H_2O (95:2.5:2.5, 10 mL/g) in triplicate (5 sec, 5 min, 15 min). The resin was washed with CH_2Cl_2 (2 x 10 mL) and co-evaporated with toluene (50 mL) and concentrated under high vacuum. Purification of the residue by silica gel column chromatography (100 g, CH_2Cl_2/MeOH/HCOOH (100:0.1:0.1→100:10:0.1)) afforded tripeptide **147a** as a white foam (265 mg, 0.26 mmol, 81 %).

TLC: R_f = 0.24 (CH_2Cl_2/CH_3OH, 4:0.8).

HPLC: t_R = 8.4min (Method B).

Optical Rotation: $[\alpha]_D^{20}$ = - 91, *c* = (0.45, CH_3OH).

^{1}H-NMR: (400 MHz, DMSO-d_6): δ = 1.02 (d, 3H, *J* = 7.1 Hz, Ala^3-CH_3), 1.22 (d, 3H, *J* = 7.2 Hz, Ala^1-CH_3), 2.64 (dd, 1H, J_{AX} = 8.0 Hz, J_{AB} = 12.0 Hz, Tyr-H_β), 2.92 (dd, 1H, J_{BX} = 4.0 Hz, J_{AB} = 12.0 Hz, Tyr-H_β), 4.03 (qt, 1H, *J* = 7.1 Hz, Ala^3-H_α), 4.15 – 4.29 (m, 5H,

Ala[1]-H_α, Fmoc-CH_2 and Fmoc-CH), 4.44 (m, 1H, Tyr-H_α), 6.61 (d, 2H, *J* = 8.4 Hz, Tyr-Ar), 6.99 (d, 2H, *J* = 8.3 Hz, Tyr-Ar), 7.32 (t, 2H, *J* = 7.2 Hz, Fmoc-Ar), 7.41 (t, 2H, *J* = 7.3 Hz, Fmoc-Ar), 7.49 (d, 1H, *J* = 7.1 Hz, NH), 7.71 (t, 2H, *J* = 7.3 Hz, Fmoc-Ar), 7.88 (d, 2H, *J* = 7.5 Hz, Fmoc-Ar), 8.10 (d, 2H, *J* = 6.2 Hz, 2 x NH), 8.15 (s, 1H, Ph-OH).

^{13}C-NMR: (100 MHz, DMSO-*d_6*): δ= 17.3, 18.1 (2 x Ala-CH_3), 46.7 (C_β), 47.5 (Fmoc-CH), 50.3 (C_α), 50.4 (C_α), 53.9 (C_α), 65.6 (Fmoc-CH_2), 114.7, 120.1, 125.3, 127.1, 127.6, 130.1 (Tyr-Ar and Fmoc-Ar), 140.7, 144.0, 155.7, 163.1 (C_q), 170.6, 172.3, 173.9 (CO-C_q).

IR: KBr plate, $\tilde{\nu}$ = 3462 (bs), 1638 (w), 1537 (s), 1449 (m), 1259 (w), 1070 (m), 825 (w), 738 (w) cm^{-1}.

LC-MS (ESI): Method-LCMS-3: t_R = 8.67 min, for $C_{30}H_{31}O_7N_3$ $[M+H]^+$ calcd. 546.22, found 546.95.

L,L,L-N-(4'*H*-Fluoren-9'-ylmethoxycarbonyl)alaninyl-tyrosinyl-alanine amide (147b)

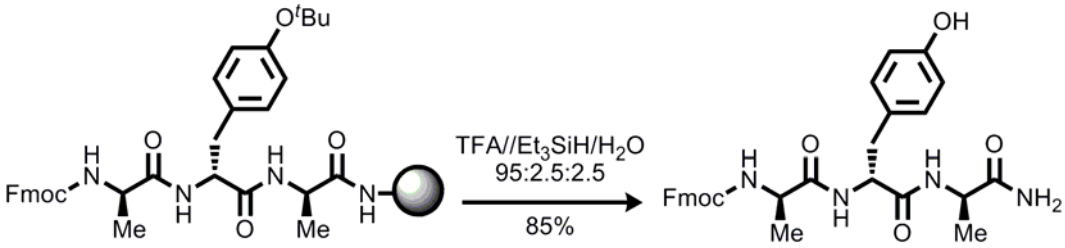

254 **147b**

The tetrapeptide **254** was assembled on rink amide resin loaded with Fmoc-Ala-OH (GP3, 0.6 mmol/g, 1 g) using Fmoc-Tyr(OtBu)-OH and Fmoc-Ala-OH (GP5). The tripeptide was released from the solid support by the treatment with cleavage solution TFA/Et_3SiH/H_2O (95:2.5:2.5, 10 mL/g) in triplicate (5 sec, 5 min, 15 min). The resin was washed with CH_2Cl_2 (2 x 10 mL) and co-evaporated with toluene (50 mL) and concentrated under high vacuum. The residue was redissolved in TFA (3 mL) and cold Et_2O (5 mL) was added dropwise. After the removal of TFA by co-evaporation with toluene (5 mL), the precipitate was collected and subjected to purification by silica gel column chromatography (50 g, CH_2Cl_2/MeOH/HCOOH

100:0:0.1→100:10:0.1) and afforded tripeptide (**147b**) as a white foam (147 mg, 0.27 mmol, 85 %).

TLC: R_f = 0.14 (EtOAc/cyclohexane, 1:1).
R_f = 0.51 ($CHCl_3$/CH_3OH/HCOOH 10:1:0.1).

HPLC: t_R = 7.97 min, (Method B).

Optical Rotation: $[\alpha]_D^{20}$ = -150, *c* = (0.6, CH_3OH).

^{1}H-NMR: (400 MHz, DMSO-*d*$_6$): δ = 1.17 (d, 3H, *J* = 7.1 Hz, Ala^3-CH_3), 1.21 (d, 3H, *J* = 7.0 Hz, Ala^1-CH_3), 2.73 (dd, 1H, J_{AX} = 8.7 Hz, J_{AB} = 13.9 Hz, Tyr-H$_\beta$), 2.92 (dd, 1H, J_{BX} = 4.7 Hz, J_{AB} = 14.0 Hz, Tyr-H$_\beta$), 4.01 (m, 1H, Ala^3-H$_\alpha$), 4.13 – 4.32 (m, 5H, Ala^1-H$_\alpha$, Fmoc-CH_2 and Fmoc-CH), 4.41 (m, 1H, Tyr-H$_\alpha$), 6.63 (d, 1H, *J* = 8.2 Hz, Tyr-Ar), 7.01 (d, 1H, *J* = 8.0 Hz, Tyr-Ar), 7.17 (s, 1H, NH), 7.33 (t, 2H, *J* = 7.4 Hz, Fmoc-Ar), 7.41 (t, 2H, *J* = 7.3 Hz, Fmoc-Ar), 7.52 (d, 1H, *J* = 7.2 Hz, NH), 7.72 (t, 2H, *J* = 7.3 Hz, Fmoc-Ar), 7.88 (d, 4H, *J* = 7.4 Hz, Fmoc-Ar, PhOH and NH).

^{13}C-NMR: (100 MHz, DMSO-*d*$_6$): δ = 18.7, 19.0 (2 x Ala-CH_3), 37.0 (C_β), 47.3 (Fmoc-CH), 48.7 (C_α), 50.9 (C_α), 54.8 (C_α), 66.4 (Fmoc-CH_2), 115.5 (Tyr-Ar), 120.8, 125.9, 127.8, 128.3 (Tyr-Ar and Fmoc-Ar), 130.8 (Tyr-Ar), 140.7, 143.9, 155.7, 155.8 (C_q), 170.7, 171.3, 173.2 (CO-C_q).

IR: KBr plate, $\tilde{\nu}$ = 3438 (bs), 2097 (bs), 1676 (s), 1471 (s), 1203 (s), 1136 (m), 826 (w), 802 (m), 721 (w) cm^{-1}.

LC-MS (ESI): Method-LCMS-3: t_R = 8.67 min, for $C_{30}H_{31}O_7N_3$ $[M+H]^+$ calcd. 545.2, found 545.9.

***L*,*L*,*L*-*N*-(4'*H*-Fluoren-9'-ylmethoxycarbonyl)alaninyl-tyrosinyl-alanine allyl ester (147c)**

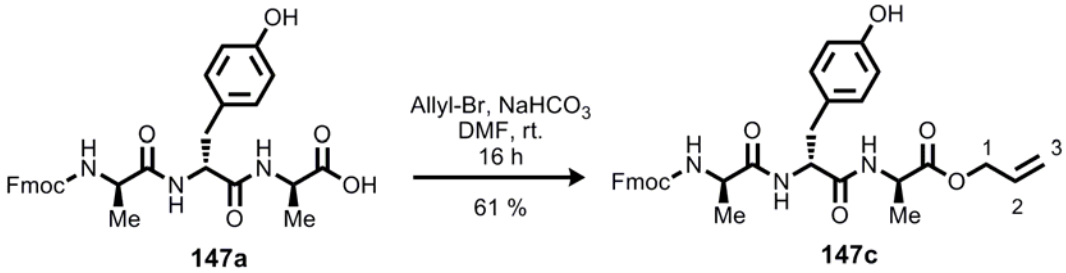

147a **147c**

Tetra peptide **147a** (103 mg, 0.19 mmol) was dissolved in DMF (2.5 mL) under argon. $NaHCO_3$ (31.8 mg, 0.38 mmol) and allyl bromide (24 μL, 0.28 mmol) were added to the solution and the mixture was stirred for 16h under argon. After 50 % of conversion (16h), volatiles were removed under reduced pressure. The residue was dissolved in EtOAc (3 x 5 mL) and was washed with saturated $NaCl_{(aq)}$ solution (1 x 4 mL), dried with $MgSO_4$, filtered and concentrated. Purification by silica gel column chromatography (30 g, MeOH/EtOAc/cyclohexane 0.2:1:1) afforded tetrapeptide allyl ester (**147c**) as a white foam (47.6 mg, 0.08 mmol, 43 %). Unreacted starting metarial (30 mg, 0.06 mmol, 30 %) was recovered by eluting with (HCOOH/MeOH/EtOAc/cyclohexane 0.01:0.2:1.3:1) as white foam.

TLC: R_f = 0.33 (CH_2Cl_2/CH_3OH/HCOOH, 95:5:0.01).

HPLC: t_R = 7.8 min, (Method A).

Optical Rotation: $[\alpha]_D^{20}$ = - 151.4, *c* = (0.45, CH_3OH).

^{1}H-NMR: (400 MHz, DMSO-d_6): δ = 1.02 (d, 3H, *J* = 7.1 Hz, Ala-CH_3), 1.25 (d, 3H, *J* = 7.2 Hz, Ala-CH_3), 2.54 – 2.69 (m, 1H, Tyr-H_β), 2.76 – 2.85 (m, 1H, Tyr-H_β), 4.03 (qt, 1H, *J* = 8.1 Hz, Ala-H_α), 4.16 – 4.32 (m, 5H, Ala^1-H_α, Fmoc-CH_2 and Fmoc-CH), 4.45 (m, 1H, Tyr-H_α), 4.56 (m, 2H, allyl-H^3), 5.18 (d, 1H, *J* = 10.50 Hz, allyl-H^1), 5.29 (d, 1H, *J* = 10.44 Hz, allyl-H^1), 5.81 – 5.96 (m, 1H, allyl-H^2), 6.61 (d, 2H, *J* = 8.4 Hz, Tyr-Ar), 6.99 (d, 2H, *J* = 8.3 Hz, Tyr-Ar), 7.32 (t, 2H, *J* = 7.3 Hz, Fmoc-Ar), 7.41 (t, 2H, *J* = 7.3 Hz, Fmoc-Ar), 7.50 (d, 1H, *J* = 7.5 Hz, NH), 7.71 (t, 2H, *J* = 7.3 Hz, Fmoc-Ar), 7.88 (d, 2H, *J* = 7.5 Hz, Fmoc-Ar), 7.95 (s, 2H, PhOH), 8.13 (d, 2H, *J* = 8.7 Hz, NH), 8.23 (d, 2H, *J* = 6.9 Hz, NH).

^{13}C-NMR: (100 MHz, DMSO-d_6): δ = 17.3, 18.1 (2 x Ala-CH_3), 46.7 (C_β), 47.5 (Fmoc-CH), 50.3 (C_α), 50.4 (C_α), 53.9 (C_α), 65.6 (Fmoc-CH_2), 65.8 (allyl-C_1) 114.7, 118.2, 120.1, 125.3, 127.1, 127.6, 130.1, 133.1, 136.3 (Tyr-Ar, Fmoc-Ar, allyl-C_2 and allyl-C_3), 140.7, 144.0, 155.7, 163.1 (C_q), 170.6, 172.3, 173.9 (CO-C_q).

IR: KBr plate, $\tilde{\nu}$ = 3256 (bs), 2986 (w), 1980 (w), 1714 (s), 1720 (s), 1655 (m), 1548 (m), 1023 (m), 827 (w), 7 (38m), 610 (w) cm^{-1}.

LC-MS (ESI): Method-LCMS-3: t_R = 8.3 min, for $C_{35}H_{36}O_7N_3$ $[M+H]^+$ calcd. 586.3, found 586.6.

L,L,L-N-(4'*H*-Fluoren-9'-ylmethoxycarbonyl)tyrosinyl-tyrosinyl-tyrosine (256)

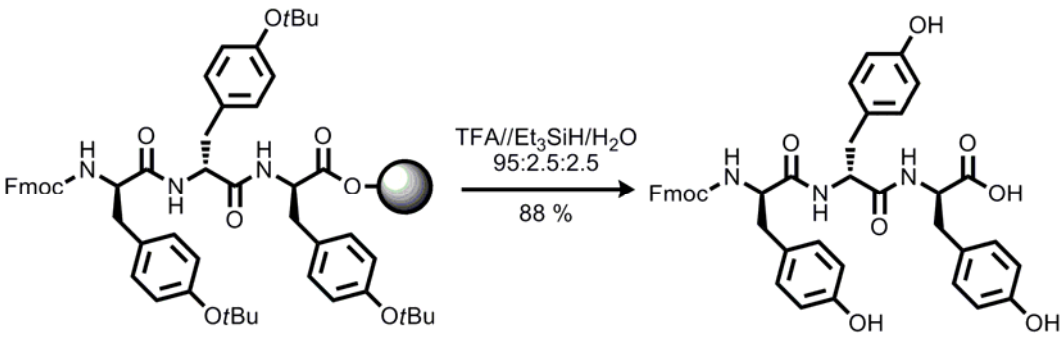

The tetrapeptide **255** was assembled on Wang resin loaded with Fmoc-Ala-OH (GP2, 0.54 mmol/g, 1 g) using Fmoc-Tyr(OtBu)-OH (GP5). The tripeptide was released from the solid support by the treatment with cleavage solution TFA/Et_3SiH/H_2O (95:2.5:2.5, 10 mL/g) in triplicate (5 sec, 5 min, 15 min). The resin was washed with CH_2Cl_2 (2 x 10 mL) and co-evaporated with toluene (50 mL) and concentrated under high vacuum. The residue was redissolved in TFA (1.5 mL) and cold Et_2O (4 mL) was added dropwise. Purification of the collected precipitate by silica gel (100 g) column chromatography CH_2Cl_2/MeOH/HCOOH (100:0.1:0.1→100:10:0.1) afforded tripeptide (**256**) as a white foam (350 mg, 0.48 mmol, 88 %).

TLC: R_f = 0.24 (CH_2Cl_2/CH_3OH, 4:0.8).

HPLC: t_R = 7.8 min (Method A).

Optical Rotation: $[\alpha]_D^{20}$ = - 142, *c* = (0.11, CH_3OH).

^{1}H-NMR: (400 MHz, DMSO-d_6): δ = 2.53 – 2.63 (m, 1H, Tyr-H_β), 2.64 – 2.75 (m, 1H, Tyr-H_β), 2.75 – 2.87 (m, 2H, Tyr-H_β), 2.87 – 2.98 (m, 2H, Tyr-H_β), 4.04 – 4.21 (m, 3H, Fmoc-CH_2, Fmoc-CH, Tyr-H_α), 4.32 – 4.41 (m, 1H, Tyr-H_α), 4.44 – 4.54 (m, 1H, Tyr-H_α), 6.62 (d, 3H, *J* = 8.2 Hz, Tyr-Ar), 6.66 (d, 3H, *J* = 8.3 Hz, Tyr-Ar), 7.02 (m, 2H, Tyr-Ar), 7.24 – 7.34 (m, 2H, Tyr-Ar), 7.36 – 7.43 (m, 2H, Fmoc-Ar), 7.47 (d, 1H, *J* = 8.7 Hz, NH), 7.57 –7.65 (t, 2H, *J* = 6.9 Hz, Fmoc-Ar), 7.87 (d, 2H, *J* = 7.5 Hz, Fmoc-Ar), 8.10 (d, 2H, *J* = 8.1 Hz, NH), 8.18 (d, 1H, *J* = 7.6 Hz, Ph-OH).

^{13}C-NMR: (100 MHz, DMSO-d_6): δ = 46.7 (C_β), 47.5 (Fmoc-CH), 50.3 (C_α),

50.4 (C_α), 54.5 (C_α), 57.2 (C_α), 66.4 (Fmoc-CH_2), 115.5, 115.7, 120.7, 125.9, 127.7, 128.3, 128.9, 130.7, 130.8, 130.9 (Tyr-Ar and Fmoc-Ar), 141.3, 144.3, 144.5, 156.3, 156.5, 156.6, 163.1 (C_q), 171.7, 171.9, 173.5 (CO-C_q).

IR: KBr plate, $\tilde{\nu}$ = 3399 (bs), 1641 (s), 1537 (s), 1447 (m), 1261 (m), 1043 (w), 547 (w) cm^{-1}.

LC-MS (ESI): Method-LCMS-3: t_R = 8.54 min, for $C_{42}H_{40}O_9N_3$ $[M+H]^+$ calcd. 730.28, found 730.61.

L,L,L-N-(4'*H*-Fluoren-9'-ylmethoxycarbonyl)tyrosinyl-tyrosinyl-tyrosine allyl ester (152)

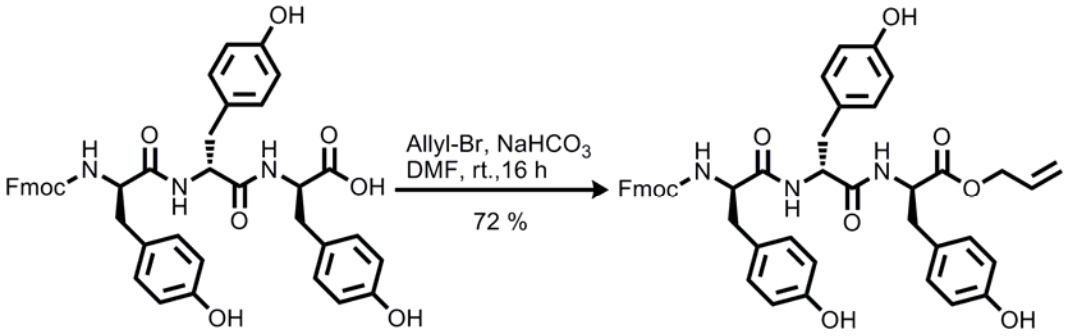

256 **152**

Tetra peptide **256** (103 mg, 0.12 mmol) was dissolved in DMF (2.5 mL) under argon. $NaHCO_3$ (20.2 mg, 0.24 mmol) and allyl bromide (11.4 μL, 0.13 mmol) were added and the reaction mixture was stirred with HPLC control. The transformation was stopped after 50 % of conversion (16h) and the volatiles were removed under reduced pressure. The residue was dissolved in EtOAc (3 x 5 mL) and washed with saturated $NaCl_{(aq)}$ solution (1 x 4 mL), dried with Na_2SO_4, filtered and concentrated. Purification by silica gel (30 g) column chromatography (MeOH/EtOAc/cyclohexane 0.2:1:1) afforded tetrapeptide allyl ester (**152**) as a white foam (47.6 mg, 0.08 mmol, 43 %). Unreacted starting metarial (30 mg, 0.06 mmol, 30 %) was recovered by eluting with (HCOOH/MeOH/EtOAc/cyclohexane 0.01:0.2:1.3:1) as white foam (42.6 mg, 0.06 mmol, 40 %).

TLC: R_f = 0.20 (EtOAc/cyclohexane/HCOOH, 1:1:0.01).

HPLC: t_R = 9.5 min (Method A).

Optical Rotation: $[\alpha]_D^{20}$ = - 124, *c* = (0.66, CH_3OH).

^{1}H-NMR: (400 MHz, DMSO-d_6): δ = 2.57 – 2.72 (m, 3H, Tyr-H$_\beta$), 2.75 – 2.85 (m, 3H, Tyr-H$_\beta$), 4.06 – 4.22 (Fmoc-CH$_2$ and Fmoc-CH), 4.39 – 4.48 (m, 1H, Tyr-H$_\alpha$), 4.50 (m, 2H, allyl-H^3), 5.17 (d, 1H, *J* = 10.5 Hz, allyl-H^1), 5.26 (m, 1H, *J* = 10.5 Hz, allyl-H^1), 5.74 – 5.89 (m, 1H, allyl-H^2), 6.62 (d, 3H, *J* = 8.4 Hz, Tyr-Ar), 6.67 (d, 2H, *J* = 8.5 Hz, Tyr-Ar), 7.01 (m, 6H, Tyr-Ar), 7.30 (m, 2H, Fmoc-Ar), 7.40 (t, 2H, *J* = 7.4 Hz, Fmoc-Ar), 7.46 (d, 1H, *J* = 8.9 Hz, NH), 7.62 (t, 2H, *J* = 7.1 Hz, Fmoc-Ar), 7.87 (d, 2H, *J* = 7.5 Hz, Fmoc-Ar), 7.92 (s, 1H, NH), 8.43 (d, 2H, *J* = 7.4 Hz, NH), 9.12 (s, 2H, PhOH), 9.21 (s, 1H, PhOH).

^{13}C-NMR: (100 MHz, DMSO-d_6): δ = 46.5, 48.6 (C$_\beta$), 53.7 (C$_\alpha$), 54.6 (C$_\alpha$), 56.5 (C$_\alpha$), 64.8 (Fmoc-CH), 65.6 (Fmoc-CH$_2$), 65.9 (allyl-C$_1$) 114.7, 115.6, 117.8, 125.2, 126.8, 127.4, 128.2, 130.1 (Tyr-Ar, Fmoc-Ar, allyl-C$_2$ and allyl-C$_3$), 140.6, 143.6, 143.8, 155.6, 155.7, 155.8, 156.0, 163.1 (C$_q$), 170.9, 171.3, 171.3 (CO-C$_q$). 65.8.

IR: KBr plate, $\tilde{\nu}$ = 3439 (bs), 2926 (s), 2856 (bs), 1729 (m), 1676 (s), 1465 (m), 1283 (m), 1200 (w), 1074 (m), 574 (w) cm^{-1}.

LC-MS (ESI): Method-LCMS-3: t_R = 8.67 min, for $C_{45}H_{44}O_9N_3$ $[M+H]^+$ calcd. 770.3, found 770.9.

***L,L,L,L,L,L,L-N*-(4'*H*-Fluoren-9'-ylmethoxycarbonyl)phenylalaninyl-glysinyl-tyrosinyl-alaninyl-serinyl-alanine methyl ester (153)**

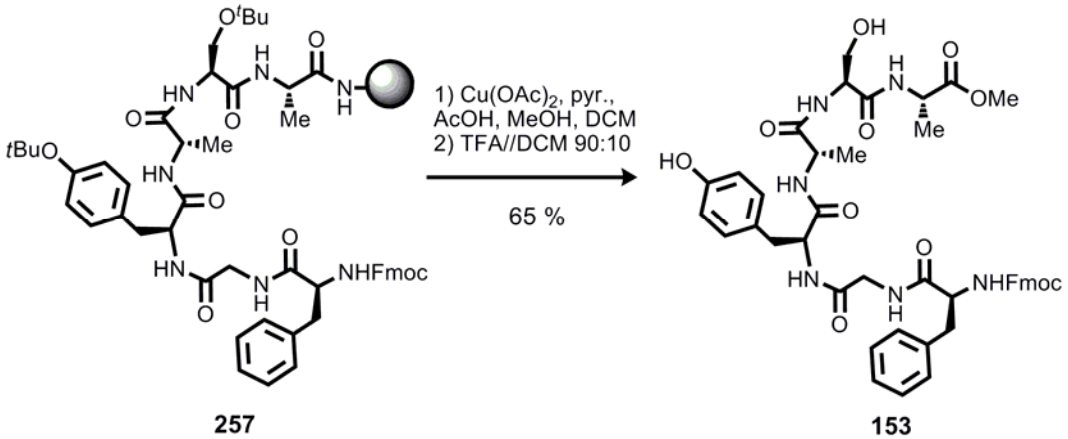

The hexapeptide **257** was assembled on hydrazine resin by using microwave assited peptide synthesizer (GP4). Loading the resin with Fmoc-Alanine-OH (0.3 mmol/g, 1 g) followed the coupling of amino acids, respectively, Fmoc-Ser-OH, Fmoc-Ala-OH, Fmoc-Tyr-OH, Fmoc-Gly-OH, Fmoc-Phe-OH. The hexa peptide was released from the solid support by oxidative cleavage (GP4). After the cleavage residue was treated with TFA/Et_3SiH/H_2O (95:2.5:2.5, 10 mL/g) for 10 min to remove the side change protection. After the removal of TFA by co-evaporation with toluene (5 mL), the precipitate was collected and subjected to purification by silica gel column chromatography (50 g, CH_2Cl_2/MeOH/HCOOH 100:0:0.1→100:10:0.1) and afforded tripeptide (**153**) as a white foam (166 mg, 0.2 mmol, 65 %).

TLC: R_f = 0.24 (CH_2Cl_2/CH_3OH, 4:0.8).

HPLC: t_R = 7.8 min (Method A).

Optical Rotation: $[\alpha]_D^{20}$ = - 130, *c* = (0.25, CH_3OH).

^{1}H-NMR: (400 MHz, DMSO-d_6): δ = 1.02 (d, 3H, *J* = 7.1 Hz, Ala^3-CH_3), 1.22 (d, 3H, *J* = 7.2 Hz, Ala^1-CH_3), 2.64 (dd, 1H, J_{AX} = 8.0 Hz, J_{AB} = 12.0 Hz, Tyr-H_β), 2.92 (dd, 1H, J_{BX} = 4.0 Hz, J_{AB} = 12.0 Hz, Tyr-H_β), 4.03 (qt, 1H, *J* = 7.1 Hz, Ala^3-H_α), 4.15 – 4.29 (m, 5H, Ala^1-H_α, Fmoc-CH_2 and Fmoc-CH), 4.44 (m, 1H, Tyr-H_α), 6.61 (d, 2H, *J* = 8.4 Hz, Tyr-Ar), 6.99 (d, 2H, *J* = 8.3 Hz, Tyr-Ar), 7.32 (t, 2H, *J* = 7.2 Hz, Fmoc-Ar), 7.41 (t, 2H, *J* = 7.3 Hz, Fmoc-Ar), 7.49 (d, 1H, *J* = 7.1 Hz, NH), 7.71 (t, 2H, *J* = 7.3 Hz, Fmoc-Ar), 7.88 (d, 2H, *J* = 7.5 Hz, Fmoc-Ar), 8.10 (d, 2H, *J* = 6.2 Hz, 2 x NH), 8.15 (s, 1H, Ph-OH).

^{13}C-NMR: (100 MHz, DMSO-d_6): δ = 17.3, 18.1 (2 x Ala-CH_3), 46.7 (C_β), 47.5 (Fmoc-CH), 50.3 (C_α), 50.4 (C_α), 53.9 (C_α), 65.6 (Fmoc-CH_2), 114.7, 120.1, 125.3, 127.1, 127.6, 130.1 (Tyr-Ar and Fmoc-Ar), 140.7, 144.0, 155.7, 163.1 (C_q), 170.6, 172.3, 173.9 (CO-C_q).

IR: KBr plate, $\tilde{\nu}$ = 3284 (bs), 2973 (bs), 1660 (s), 1512 (s), 1507 (w), 1455 (s), 1255 (m), 1125 (m), 1075 (m), 834 (w), 697 (m), 564 (w) cm^{-1}.

LC-MS (ESI): Method-LCMS-3: t_R = 8.67 min, for $C_{30}H_{31}O_7N_3$ $[M+H]^+$ calcd. 546.22, found 546.95.

***L,L,L,L,L,L,L-N*-(4'*H*-Fluoren-9'-ylmethoxycarbonyl)prolinyl-tyrosinyl-glysinyl-alaninyl-isoleucinyl-alanine methyl ester (155)**

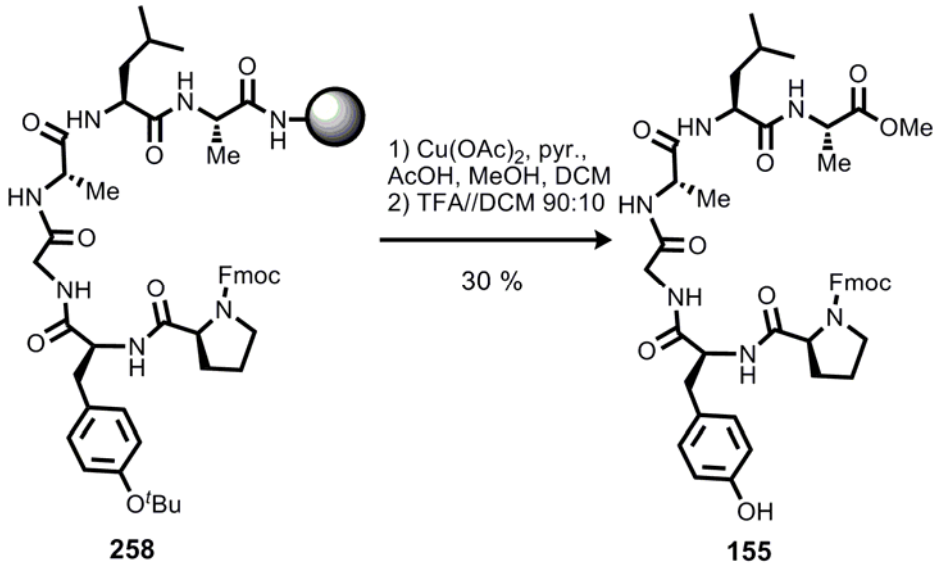

258 **155**

The hexapeptide **258** was assembled on hydrazine resin by using microwave assited peptide synthesizer (GP4). Loading the resin with Fmoc-Ala-OH (0.3 mmol/g, 1 g) followed the coupling of amino acids, respectively, Fmoc-Ile-OH, Fmoc-Ala-OH, Fmoc-Gly-OH, Fmoc-Tyr-OH, Fmoc-Pro-OH. The hexa peptide was released from the solid support by oxidative cleavage (GP4). After the cleavage residue was treated with TFA/Et_3SiH/H_2O (95:2.5:2.5, 10 mL/g) for 10 min to remove the side change protection. After the removal of TFA by co-evaporation with toluene (5 mL), the precipitate was collected and subjected to purification by silica gel column chromatography (50 g, CH_2Cl_2/MeOH/HCOOH 100:0:0.1→100:10:0.1) and afforded tripeptide (**155**) as a white foam (74 mg, 0.1 mmol, 30 %).

TLC: R_f = 0.24 (CH_2Cl_2/CH_3OH, 4:0.8).

HPLC: t_R = 7.8 min (Method A).

Optical Rotation: $[\alpha]_D^{20}$ = - 198, *c* = (0.45, CH_3OH).

^{1}H-NMR: (400 MHz, DMSO-d_6): δ = 0.85 (dd, 6H, *J* = 6.5 Hz, *J* = *1*6.3 Hz Leu-CH_3), 1.07 (s, 3H, Ala-CH_3), 1.31 – 1.25 (m, 7H, pro-H, Ala-CH_3), 1.27 (d, 2H, *J* = 7.3 Hz, Leu-CH_2), 1.47 (m, 1H, Leu-CH), 2.82 (m, 1H, Tyr-H_β), 2.98 (m, 1H, Tyr-H_β), 3.42 (m, 1H, pro-H), 3.59 (m, 3H, $COOCH_3$), 3.69 (m, 1H, Gly-H), 4.04 – 412 (m, 1H,

Fmoc-CH_2 and Fmoc-CH), 4.32 (m, 4H, CH_α), 4.43 – 4.60 (m, 1H, CH_α), 6.59 (d, 2H, *J* = 8.1 Hz, Tyr-Ar), 6.81 (d, 2H, *J* = 8.1 Hz, Tyr-Ar), 7.11 (q, 2H, *J* = 8 Hz, Tyr-Ar), 7.32 (m, 2H, Fmoc-Ar), 7.42 (s, 1H, Ph-OH), 7.59 (m, 2H, Fmoc-Ar), 7.66 (d, 1H, *J* = 7.7 Hz, Fmoc-Ar), 7.71 (m, 2H, Fmoc-Ar), 7.91 (m, 4H, *J* = 7.5 Hz, Fmoc-Ar, NH), 8.04 (d, 1H, *J* = 7.9 Hz, NH), 8.04 (d, 1H, *J* = 7.9 Hz, 2 x NH).

^{13}C-NMR: (100 MHz, DMSO-d_6): δ = 17.9, 18.1 (2 x Ala-CH_3), 22.3 (2 x Leu-CH_3), 24.8 (Leu-CH), 24.9, 29.5 (2 x Pro-CH_2), 37.7 (C_β), 41.2 (Leu-CH_2), 43.2 (Gly-CH_2), 47.5 (Fmoc-CH), 48.1 (Pro-CH_2), 50.3, 50.4, 53.9, 58.5, 66.3 (C_α), 65.6 (Fmoc-CH_2), 114.8, 115.5, 118.5, 120.1, 125.3, 127.1, 127.6, 128.1 (Tyr-Ar and Fmoc-Ar), 140.7, 141.3 144.0, 155.7, 163.1 (C_q), 171.6, 171.7, 172.9, 173.2 (CO-C_q).

IR: KBr plate, $\tilde{\nu}$ = 3486 (s), 2976 (w), 2845 (w), 1660 (s), 1673 (s), 1513 (m), 1514 (s), 1455 (s), 1249 (m), 1170 (m), 925 (w), 799 (m), 586 (w) cm^{-1}.

LC-MS (ESI): Method-LCMS-3: t_R = 8.67 min, for $C_{30}H_{31}O_7N_3$ $[M+H]^+$ calcd. 546.22, found 546.95.

8.6.2 Arylations of Phenols

(S)-2-(8*H*-Fluoren-9-ylmethoxycarbonylamino)-3-(4-phenoxy-phenyl)-propionic acid *tert*-butyl ester (142a)

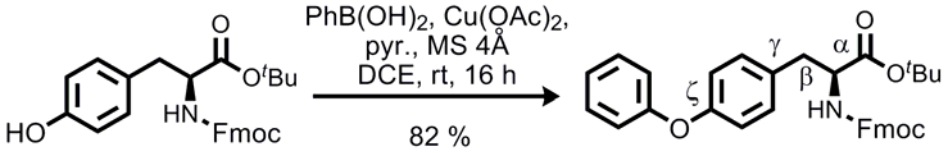

By following **GP8** Phenol **142** (50 mg, 0.11 mmol) and phenyl boronic acid (19 mg, 0.15 mmol, 1.4 eq.) were coupled in the presence of $Cu(OAc)_2$ (2 mg, 20 mmol %), pyridine (24 µL, 0.55 mmol) and 4 Å powdered molecular sieves (100 mg) in 1,2-dichloroethane (1 ml). Flash column chromatography on silica gel (10 g, EtOAc/cyclohexane 30:70) gave the biarylether **142a** (48 mg, 0.1 mmol, 82 %) as a sticky colorless oil.

TLC: R_f = 0.36 (EtOAc/cyclohexane 1:1).

HPLC: t_R = 11.25 min, (Method B).

Optical Rotation: $[\alpha]_D^{20}$ = -52.5 (*c* = 0.39, CH_3OH).

^{1}H-NMR: (500 MHz, DMSO-d_6): δ = 1.34 (s, 9H, *t*Bu), 2.89 (m, 1H, Tyr-H_β), 2.99 (dd, 1H, J_{BX} = 5.7 Hz, J_{AB} =13.8 Hz, Tyr-H_β), 4.12 – 4.19 (m, 2H, H_α and Fmoc-CH_2), 4.25 (2H, Fmoc-CH_2 and Fmoc-CH), 6.91 and 6.93 (two d, *J* = 8.1 Hz, 4H, Tyr-Ar), 7.30 (m, 5H, Ph-Ar), 7.40 (m, 2H, Fmoc-Ar), 7.67 (d, 2H, *J* = 7.5 Hz, Fmoc-Ar), 7.78 (d, 1H, *J* = 8.2 Hz, Fmoc-Ar), 7.88 (d, 2H, *J* = 7.5 Hz, Fmoc-Ar), 9.17 (s, 1H, NH).

^{13}C-NMR: (125 MHz, DMSO-d_6) δ = 27.5 (*t*Bu-C(**C**H_3)$_3$), 30.7 (C_β), 46.6 (Fmoc-CH), 56.0 (Tyr-OCH_3), 65.6 (Fmoc-CH_2), 80.6 (*t*Bu-**C**$(CH_3)_3$), 118.3, 118.40, 120.0, 123.2, 125.2, 126.9, 127.6, 129.9, 130.7, 140.7, 143.7, 143.8 (Ar), 155.1, 155.8, 156.8 (C_q), 162.2, 170.9 (Tyr-CO).

IR: KBr plate, $\tilde{\nu}$ = 3375 (bs), 2926 (w), 2553 (w), 1710 (s), 1712 (m), 1386 (m), 1257 (m), 843 (m), 741 (m), 567 (w), 542 (m) cm^{-1}.

LC-MS (ESI): t_R = 11.11 min, (method-RP-LCMS-2) for $C_{34}H_{33}O_5NNa$ [(M+Na^+)] calcd. 558.2, found 558.6.

HRMS (ESI): for $C_{34}H_{34}O_5N$ [(M+H^+)] calcd. 536.2437, found 536.2425.

(S)-2-[(8*H*-Fluoren-9-ylmethoxycarbonyl)-methyl-amino]-3-(4-phenoxy-phenyl)-propionic acid *tert*-butyl ester (145a)

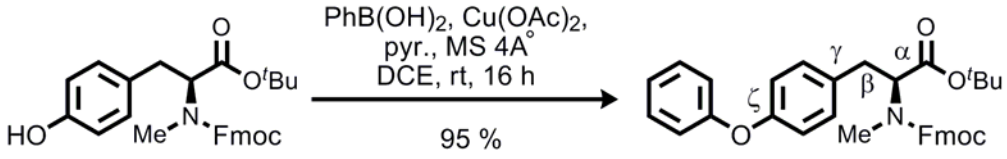

144a **145a**

By following **GP8** Phenol **144a** (50 mg, 0.11 mmol) and phenyl boronic acid (19 mg, 0.15 mmol, 1.4 eq.) were coupled in the presence of $Cu(OAc)_2$ (2 mg, 20 mmol %), pyridine (24 µL, 0.55 mmol) and 4 Å powdered molecular sieves (100 mg) in 1,2-dichloroethane (1 ml). Flash column chromatography on silica gel (10 g, EtOAc/cyclohexane 30:70) gave the biarylether **145a** (56 mg, 0.1 mmol, 95 %) as a sticky oil.

TLC: R_f = 0.28 (EtOAc/cyclohexane 4:10).

HPLC: t_R = 11.55 min (Method B).

Optical Rotation: $[\alpha]_D^{20°C}$ = -33 (*c* = 0.29, CH_3OH).

^{1}H-NMR: (400 MHz, DMSO-d_6): δ = 1.34 (s, 9H, *t*Bu), 2.60 and 2.66 (two s, 3H, NCH_3), 2.86 (m, 1H, Tyr-H_β), 3.02 (dd, 1H, J_{BX} = 4.7 Hz, J_{AB} = 14.9 Hz, Tyr-H_β), 4.14 – 4.31 (m, 2H, Fmoc-CH_2), 4.41 (m, 1H, Fmoc-CH), 4.61 (m, 1H, H_α), 6.71 (d, 2H, *J* = 8.4 Hz, Tyr-Ar), 6.96 (d, 2H, *J* = 8.4 Hz, Tyr-Ar), 7.02 (m, 5H, Ph-Ar), 7.29 (m, 2H, Fmoc-Ar), 7.39 (m, 2H, Fmoc-Ar), 7.52 (m, 2H, Fmoc-Ar), 7.87 (d, 2H, *J* = 7.4 Hz, Fmoc-Ar).

^{13}C-NMR: (100 MHz, DMSO-d_6) δ = 27.3 (*t*Bu-C(**C**H_3)$_3$), 32.3 (NCH_3), 33.1 (C_β) 47.9 (Fmoc-CH), 59.9 (Tyr-OCH_3), 56.7 (C_α), 65.6 (Fmoc-CH_2), 81.3 (*t*Bu-**C**$(CH_3)_3$), 114.7, 115.7, 118.5, 118.7, 119.0, 121.2, 126.7, 130.3, 131.2, 138.4, 140.5, 141.3 (Ar), 158.1 (C_q), 159.3, 160.7 (C_q), 175.0 (Tyr-CO).

IR: KBr plate, $\tilde{\nu}$ = 3388 (m), 2924 (m), 2355 (w), 1696 (m), 1613 (w), 1449 (m), 1238 (m), 1028 (w), 739 (m) cm^{-1}.

LC-MS (ESI): t_R = 12.51 min, (method-RP-LCMS-2) for $C_{35}H_{36}O_5N$ [$(M+H^+)$] calcd. 550.3, found 550.7.

HRMS (ESI): for $C_{35}H_{36}O_5N$ [$(M+H^+)$] calcd. 550.2593, found 550.2542.

(S)-3-(4'-Hydroxy-phenyl)-2-phenylamino-propionic acid *tert*-butyl ester (146)

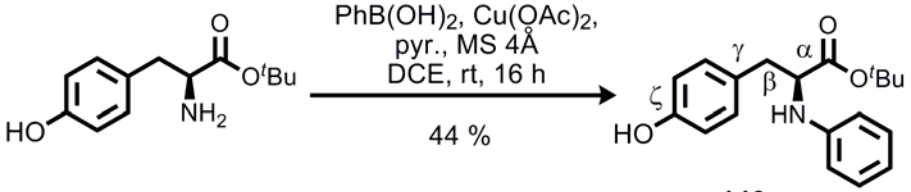

144c **146**

By following **GP8** Phenol **144c** (50 mg, 0.21 mmol) and phenyl boronic acid (36 mg, 0.3 mmol, 1.4 eq.) were coupled in the presence of $Cu(OAc)_2$ (4 mg, 20 mmol %), pyridine (24 µL, 1.05 mmol) and 4 Å powdered molecular sieves (100 mg) in 1,2-dichloroethane/DMF (1:1, 1 mL). Flash column chromatography on silica gel (10 g, EtOAc/cyclohexane 30:70) gave the arylamine **146** (29 mg, 0.09 mmol, 44 %) as a sticky oil.

TLC: R_f = 0.21 (EtOAc/cyclohexane 4:10).

HPLC: t_R = 10.25 min (Method B).

Optical Rotation: $[\alpha]_D^{20°C}$ = -25.0 (*c* = 0.78, CH_3OH).

^{1}H-NMR: (500 MHz, DMSO-d_6): δ = 1.26 (s, 9H, *t*Bu), 2.75 (m, 2H, Tyr-H_β), 3.97 (q, 1H, H_α), 5.84 (d, 1H, NH), 6.56 (d, 2H, *J* = 8.2 Hz, Tyr-Ar), 6.66 (m, 2H, *J* = 8.2 Hz, Tyr-Ar), 7.02 – 7.10 (m, 5H, Tyr-Ar), 9.18 (s, 1H, PhOH).

^{13}C-NMR: (125 MHz, DMSO-d_6) δ = 27.5 (*t*Bu-C(**C**H_3)$_3$), 39.0 (C_β), 58.4 (C_α), 80.2 (*t*Bu-**C**$(CH_3)_3$), 112.5, 114.8, 116.3 (Tyr-Ar), 127.7, 128.7, 130.2 (Ph-Ar), 147.8 (Ph-C_q), 155.7 (PhOH-C_q), 172.0 (Tyr-CO and Tyr-Cγ).

IR: KBr plate, $\tilde{\nu}$ = 3421 (m), 2960 (m), 1790 (s), 1714 (s), 1514 (m), 1248 (m), 1060 (m), 833 (m), 760 (m), 741 (m), 621 (w), 564 (w), 540 (m) cm^{-1}.

LC-MS (ESI): t_R = 9.97 min, (method-RP-LCMS-2) for $C_{19}H_{24}O_3N$ [$(M+H^+)$] calcd. 314.2 found 314.9.

HRMS (ESI): for $C_{19}H_{24}O_3N$ [$(M+H^+)$] calcd. 314.1756, found 314.1740.

(S)-2-(8*H*-Fluoren-9-ylmethoxycarbonylamino)-3-[4'-(2''-methoxy-phenoxy)-phenyl]-propionic acid *tert*-butyl ester (143c)

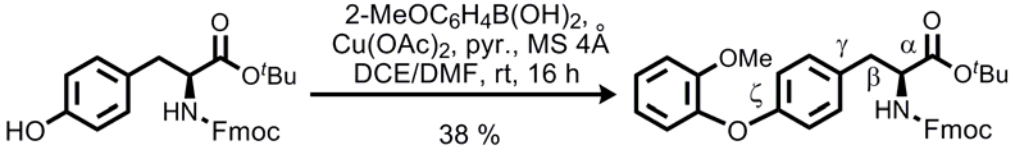

142 **143c**

By following **GP8** Phenol **142** (50 mg, 0.11 mmol) and boronic acid **ZZ** (23 mg, 0.15 mmol, 1.4 eq.) were coupled in the presence of $Cu(OAc)_2$ (2 mg, 20 mmol %), pyridine (24 µL, 0.55 mmol) and 4 Å powdered molecular sieves (100 mg) in 1,2-dichloroethane/DMF (1 ml:0.2 mL). Flash column chromatography on silica gel (10 g, EtOAc/cyclohexane 30:70) gave the product **143c** (24 mg, 0.42 mmol, 38 %) as sticky oil.

TLC: R_f = 0.36 (EtOAc/cyclohexane 4:10).

HPLC: t_R = 11.75 min, (Method B).

Optical Rotation: $[\alpha]_D^{20}$ = - 77.7 (*c* = 0.3, CH_3OH).

^{1}H-NMR: (400 MHz, DMSO-d_6): δ = 1.32 (s, 9H, *t*Bu), 2.85 (dd, 1H, J_{AX} = 9.96 Hz, J_{AB} = 13.6 Hz, Tyr-H$_\beta$), 2.91 (dd, 1H, J_{BX} = 5.92 Hz, J_{AB} = 13.9 Hz, Tyr-H$_\beta$), 3.70 (s, 3H, Ar-OCH_3), 4.09 (m, 1H, H$_\alpha$), 4.17 (m, 1H, Fmoc-CH), 4.24 (m, 2H, Fmoc-CH_2), 6.72 (d, 2H, *J* = 8.6 Hz, Tyr-Ar), 6.93 (m, 2H, Tyr-Ar), 7.11 – 7.34 (m, 5H, Ph-Ar), 7.40 (t, 2H, *J* = 7.5 Hz, Fmoc-Ar), 7.66 (d, 2H, *J* = 7.5 Hz, Fmoc-Ar), 7.74 (d, 2H, *J* = 8.2 Hz, Fmoc-Ar), 7.88 (d, 2H, Fmoc-Ar).

^{13}C-NMR: (100 MHz, DMSO-d_6): δ = 27.4 (*t*Bu-C(**C**H$_3$)$_3$), 34.8 (C$_\beta$), 55.6 (C$_\alpha$), 56.1 (Ar-OCH_3), 80.9 (*t*Bu-**C**$(CH_3)_3$), 113.2, 115.9, 120.3 (Tyr-Ar), 125.1, 125.2 (Ph-Ar), 126.8, 127.6, 130.3 (Fmoc-Ar), 140.7, 143.9 151.6, 156.7 (C$_q$), 168.9, 171.9 (Tyr-CO).

IR: KBr plate, $\tilde{\nu}$ = 3428 (m), 2356 (w), 1644 (m), 1499 (w), 1225 (w), 615 (w) cm^{-1}.

HRMS (ESI): For $C_{35}H_{36}O_6N$ [(M+H$^+$)] calcd. 566.2537, found 566.2533.

(S)-2-(8*H*-Fluoren-9-ylmethoxycarbonylamino)-3-[4'-(2'',4'',6''-tris-trifluoromethyl-phenoxy)-phenyl]-propionic acid *tert*-butyl ester (143c)

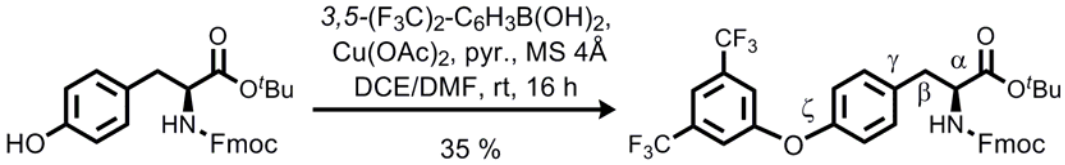

142 **143c**

By following **GP8** Phenol **142** (50 mg, 0.11 mmol) and boronic acid (49 mg, 0.15 mmol, 1.4 eq.) were coupled in the presence of $Cu(OAc)_2$ (2 mg, 20 mmol %), pyridine (24 µL, 0.55 mmol) and 4 Å powdered molecular sieves (100 mg) in 1,2-dichloroethane/DMF (1 ml:0.2 mL). Flash column chromatography on silica gel (10 g, EtOAc/cyclohexane 30:70) gave the product **143c** (24 mg, 0.42 mmol, 38 %) as sticky oil.

TLC: R_f = 0.54 (EtOAc/cyclohexane 1:1).

HPLC: t_R = 13.7 min (Method B).

Optical Rotation: $[\alpha]_D^{20}$ = -100 (*c* = 0.20, CH_3OH).

^{1}H-NMR: (400 MHz, DMSO-d_6): δ = 1.34 (s, 9H, *t*Bu), 2.97 (m, 2H, Tyr-H_β), 4.22 (m, 4H, H_α and Fmoc-CH_2 and Fmoc-CH), 6.90 (d, 1H, NH), 7.11 (d, 2H, *J* = 8.5 Hz, Tyr-Ar), 7.32 (d, 2H, *J* = 8.0 Hz, Tyr-Ar), 7.35 – 7.48 (m, 3H, Ph-Ar), 7.54 (m, 2H, Fmoc-Ar), 7.67 (m, 2H, Fmoc-Ar), 7.81 (m, 2H, Fmoc-Ar), 7.88 (d, 2H, *J* = 7.8 Hz, Fmoc-Ar).

^{13}C-NMR: (100 MHz, DMSO-d_6) δ = 27.5 (*t*Bu-C(**C**H_3)$_3$), 35.9 (C_β), 45.8 (Tyr-OCH_3), 56.4 (C_α), 68.4 (C_β), 80.9 (*t*Bu-**C**$(CH_3)_3$), 117.8, 118.1 (Tyr-Ar), 119.7, 120.0, 124.9, 126.5, 127.6, 131.1, 135.2, 131.8 , 140.9, 143.6 (Ar), 154.3, 157.1, 158.6, 158.7 171.0, 185.7, 188.5, 199.2 (C_q).

IR: KBr plate, $\tilde{\nu}$ = 3440 (m), 2926 (m), 1603 (m), 1644 (m), 1450 (s), 833 (w), 570 (w) cm^{-1}.

LC-MS (ESI): t_R = 10.57 min, (method-RP-LCMS-2) for $C_{36}H_{31}O_5NF_6$ [$(M+H^+)$] calcd. 740.2 found 740.9.

HRMS (ESI): for $C_{36}H_{31}O_5NF_6$ [$(M+H^+)$] calcd. 740.2059, found 740.2054.

(S)-2-(8*H*-Fluoren-9-ylmethoxycarbonylamino)-3-[4'-(naphth-1''-yloxy)-phenyl]-propionic acid *tert*-butyl ester (143e)

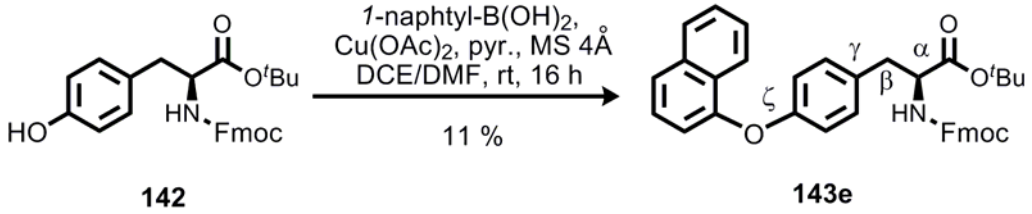

142 **143e**

By following **GP8** Phenol **142** (50 mg, 0.11 mmol) and boronic acid **LL** (26 mg, 0.15 mmol, 1.4 eq.) were coupled in the presence of $Cu(OAc)_2$ (2 mg, 20 mmol %), pyridine (24 µL, 0.55 mmol) and 4 Å powdered molecular sieves (100 mg) in 1,2-dichloroethane/DMF (1 ml:0.2 mL). Flash column chromatography on silica gel (10 g, EtOAc/cyclohexane 30:70) gave the product **143e** (7 mg, 0.01 mmol, 11 %) as sticky oil.

TLC: R_f = 0.28 (EtOAc/cyclohexane 4:10).

HPLC: t_R = 15.0 min (Method B).

Optical Rotation: $[\alpha]_D^{20}$ = -32.4 (*c* = 0.68, CH_3OH).

^{1}H-NMR: (400 MHz, DMSO-d_6): δ = 1.38 (s, 9H, *t*Bu), 2.91 (dd, 1H, J_{AX} = 9.6 Hz, J_{AB} = 13.7 Hz, Tyr-H$_\beta$), 2.99 (dd, 1H, J_{BX} = 5.9 Hz, J_{AB} = 13.9 Hz, Tyr-H$_\beta$), 4.18 and 4.25 (two m, 4H, H$_\alpha$ and Fmoc-CH_2 and Fmoc-CH), 6.85 and 6.98 (two m, 4H, Tyr-Ar), 7.31 and 7.44 (two m, 7H, Naph-Ar), 7.54 – 7,64 (m, 4H, Fmoc-Ar), 7.67 (d, 2H, *J* = 7.5 Hz, Fmoc-Ar), 7.80 (d, 2H, *J* = 8.3 Hz, NH), 7.88 (d, 2H, *J* = 7.5 Hz, Fmoc-Ar).

^{13}C-NMR: (100 MHz, DMSO-d_6) δ = 27.3 (*t*Bu-C(**C**H_3)$_3$), 36.4 (C$_\beta$), 47.3 (Tyr-OCH_3), 56.7 (C$_\alpha$), 66.3 (C$_\beta$), 81.4 (*t*Bu-**C**$(CH_3)_3$), 116.4, 119.2, 119.2, 119,5, 120.4, 125.9, 126.5, 127.6, 128.3, 128.8, 129.5, 129.6 (Tyr-Ar, Fmoc-Ar, Naph-Ar), 131.1, 133.6, 135.8, 140.1, 141.4, 144.3 (Tyr-Ar, Fmoc-Ar, Naph-Ar), 155.6, 157.3, 171.6, 185.7, 188.5, 199.2 (C$_q$).

IR: KBr plate, $\tilde{\nu}$ = 3412 (w), 2974 (w), 2359 (s), 1729 (m), 1607 (w), 1503 (m), 1450 (w), 1239 (m), 1046 (w), 839 (w), 761 (w), 697 (w), 514 (m) cm^{-1}.

HRMS (ESI): for $C_{38}H_{36}O_5N$ [(M+H$^+$)] calcd. 586.2588, found 586.2585.

(S)-2-(8*H*-Fluoren-9-ylmethoxycarbonylamino)-3-[4'-(biphenyl-1''-yloxy)-phenyl]-propionic acid *tert*-butyl ester (143d)

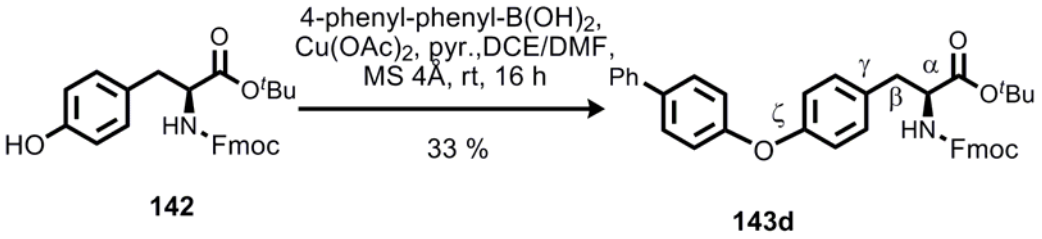

142 **143d**

By following **GP8** phenol **142** (50 mg, 0.11 mmol) and boronic acid **LL** (26 mg, 0.15 mmol, 1.4 eq.) were coupled in the presence of $Cu(OAc)_2$ (2 mg, 20 mmol %), pyridine (24 µL, 0.55 mmol) and 4 Å powdered molecular sieves (100 mg) in 1,2-dichloroethane/DMF (1 ml:0.2 mL). Flash column chromatography on silica gel (10 g, EtOAc/cyclohexane 30:70) gave the product **143d** (7 mg, 0.01 mmol, 11 %) as sticky oil.

TLC: R_f = 0.28 (EtOAc/cyclohexane 4:10).

HPLC: t_R = 15.5 min (Method B).

Optical Rotation: $[\alpha]_D^{20}$ = -29.6 (*c* = 0.54, CH_3OH).

^{1}H-NMR: (400 MHz, DMSO-d_6): δ = 1.33 (s, 9H, *t*Bu), 2.87 (dd, 1H, J_{AX} = 9.9 Hz, J_{AB} = 13.4 Hz, Tyr-H$_\beta$), 2.96 (dd, 1H, J_{BX} = 5.8 Hz, J_{AB} = 14.5 Hz, Tyr-H$_\beta$), 4.15 and 4.23 (two m, 4H, H$_\alpha$ and Fmoc-CH_2 and Fmoc-CH), 6.90 (m, 4H, *J* = 8.0 Hz, Tyr-Ar), 7.26 (m, 5H, Ph-Ar), 7.38 (m, 4H, Ph-Ar), 7.64 (m, 2H, Fmoc-Ar), 7.80 (d, 2H, *J* = 8.3 Hz, NH), 7.86 (m, 2H, Fmoc-Ar), 7.99 (m, 2H, Fmoc-Ar).

^{13}C-NMR: (100 MHz, DMSO-d_6) δ = 28.3 (*t*Bu-C(**C**H$_3$)$_3$), 36.4 (C$_\beta$), 47.3 (Tyr-O**C**H$_3$), 56.7 (C$_\alpha$), 66.3 (C$_\beta$), 81.4 (*t*Bu-**C**(CH$_3$)$_3$), 114.4, 118.4, 120.8, 127.7, 128.3, 128.8, 131.3, 135.8, 141.4 (Tyr-Ar, Fmoc-Ar, biphenyl).

IR: KBr plate, $\tilde{\nu}$ = 3414 (m), 2976 (w), 2356 (w), 1730 (m), 1600 (w), 1503 (m), 1449 (w), 1241 (s), 1156 (w), 762 (w), 698 (w) cm^{-1}.

HRMS (ESI): for $C_{40}H_{38}O_5N$ [(M+H$^+$)] calcd. 612.2745, found 612.2741.

L,L,L-N-(4'*H*-Fluoren-9-ylmethoxycarbonyl)alaninyl-(*O*-Phenyl)tyrosinyl-alanine (148a)

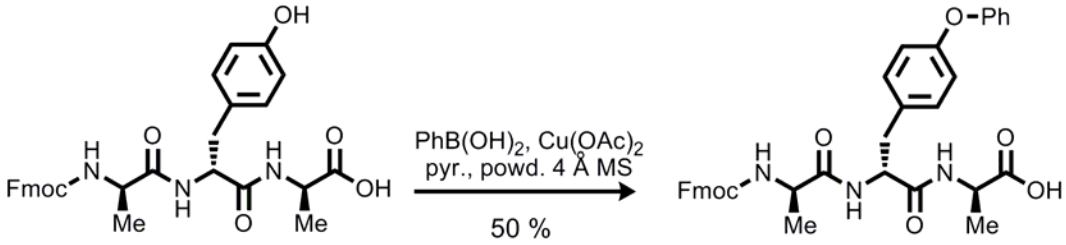

By following **GP8** peptide **147a** (50 mg, 0.09 mmol) and phenyl boronic acid (15 mg, 0.13 mmol, 1.4 eq.) were coupled in the presence of $Cu(OAc)_2$ (2 mg, 20 mmol %), pyridine (24 µL, 0.45 mmol) and 4 Å powdered molecular sieves (100 mg) in 1,2-dichloroethane/DMF (10:1, 4 ml). Flash column chromatography on silica gel (10 g, ($CHCl_3$/MeOH/ HCOOH 90:10:1)) gave the *O*-arylated **148a** (28 mg, 0.1 mmol, 50 %) as a sticky oil.

TLC: R_f = 0.12 ($CHCl_3$/MeOH/ HCOOH 9.2:0.8:0.01).

HPLC: t_R = 8.9 min (Method B).

Optical Rotation: $[\alpha]_D^{20}$ = - 98, *c* = (0.55, CH_3OH).

^{1}H-NMR: (400 MHz, DMSO-d_6): δ = 1.03 (d, 3H, *J* = 7.1 Hz, Ala^3-CH_3), 1.23 (d, 3H, *J* = 7.1 Hz, Ala^1-CH_3), 2.65 (m, 1H, Tyr-H_β), 2.86 (m, 1H, Tyr-H_β), 4.03 (m, 1H, Ala^3-H_α), 4.21 and 4.25 (two m, 4H, Ala^1-H_α, Fmoc-CH_2 and Fmoc-CH), 4.45 (m, 1H, Tyr-H_α), 6.62 (d, 2H, *J* = 8.5 Hz, Tyr-Ar), 7.01 (d, 2H, *J* = 8.4 Hz, Tyr-Ar), 7.31 (t, 5H, Ph-Ar), 7.41 (m, 2H, Fmoc-Ar), 7.42 (m, 2H, Fmoc-Ar), 7.50 (d, 1H, *J* = 7.1 Hz, NH), 7.71 (m, 2H, Fmoc-Ar), 7.87 (m, 2H, Fmoc-Ar), 8.12 (d, 2H, *J* = 6.2 Hz, 2 x NH).

^{13}C-NMR: (100 MHz, DMSO-d_6): δ = 17.3, 18.1 (2 x Ala-CH_3), 46.7 (C_β), 47.5 (Fmoc-CH), 50.3 (C_α), 50.4 (C_α), 53.9 (C_α), 65.6 (Fmoc-CH_2), 114.7, 120.1, 125.3, 126.8, 127.1, 127.6, 130.1, 131.2, 132.2 (Ph-Ar, Tyr-Ar and Fmoc-Ar), 140.7, 144.0, 155.7, 163.1 (C_q), 170.6, 171.4, 172.3, 173.9 (CO-C_q).

IR: KBr plate, $\tilde{\nu}$ = 3288 (bs), 2974 (bs), 1660 (s), 1514 (s), 1507 (s), 1455 (s), 1250 (m), 1070 (m), 825 (w), 699 (m), 576 (w) cm^{-1}.

LC-MS (ESI): Method-LCMS-3: t_R = 9.8 min, for $C_{36}H_{36}O_7N_3$ $[M+H]^+$ calcd. 622.2, found 622.7.

HRMS (ESI): for $C_{36}H_{36}O_7N_3$ $[(M+H^+)]$ calcd. 622.2466, found 622.2464.

L,L,L-N-(4'*H*-Fluoren-9-ylmethoxycarbonyl)alaninyl-tyrosinyl-alanine phenyl amide (149)

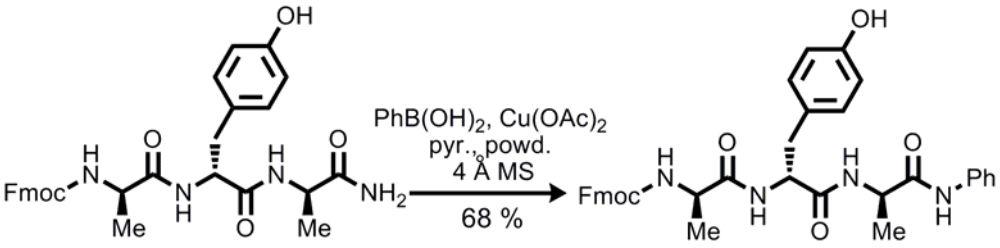

147b **149**

By following **GP8** peptide **147b** (50 mg, 0.09 mmol) and phenyl boronic acid (15 mg, 0.13 mmol, 1.4 eq.) were coupled in the presence of $Cu(OAc)_2$ (2 mg, 20 mmol %), pyridine (24 µL, 0.45 mmol) and 4 Å powdered molecular sieves (100 mg) in 1,2-

dichloroethane/DMF (10:1, 4 ml). Preparative reversed phase HPLC-(method-3) afforded the *N*-arylated peptide **149** (38 mg, 0.06 mmol, 68 %) as a sticky oil.

TLC: R_f = 0.14 (EtOAc/cyclohexane, 1:1).
R_f = 0.25 ($CHCl_3$/CH_3OH/HCOOH 10:1:0.1).

HPLC: t_R = 9.4 min (Method B).

Optical Rotation: $[\alpha]_D^{20}$ = - 96.6, *c* = (0.65, CH_3OH).

^{1}H-NMR: (400 MHz, DMSO-*d*$_6$): δ = 1.16 (m, 3H, Ala-CH_3), 1.22 (d, 3H, Ala-CH_3), 2.73 (dd, 1H, J_{AX} = 9.7 Hz, J_{AB} = 14.9 Hz, Tyr-H$_\beta$), 2.92 (dd, 1H, J_{BX} = 4.8 Hz, J_{AB} = 13.0 Hz, Tyr-H$_\beta$), 4.02 (m, 1H, H$_\alpha$), 4.21 – 4.42 (m, 5H, H$_\alpha$, Fmoc-CH_2 and Fmoc-CH), 4.41 (m, 1H, Tyr-H$_\alpha$), 6.83 (d, 1H, *J* = 9.9 Hz, Tyr-Ar), 6.89 (d, 1H, *J* = 9.8 Hz, Tyr-Ar), 7.17 (s, 1H, NH), 7.25 (m, 5H, Ph-Ar), 7.39 (m, 2H, Fmoc-Ar), 7.52 (d, 1H, *J* = 8.2 Hz, NH), 7.68 (m, 2H, Fmoc-Ar), 7.92 (d, 2H, *J* = 7.3 Hz, Fmoc-Ar), 9.93 (d, 1H, Ph-OH).

^{13}C-NMR: (100 MHz, DMSO-*d*$_6$): δ = 18.7, 19.1 (2 x Ala-CH_3), 46.6 (C_β), 47.8 (Fmoc-CH), 50.4 (C_α), 50.5 (C_α), 53.5 (C_α), 66.6 (Fmoc-CH_2), 114.6, 114.7, 120.1, 125.3, 124.4, 126.8, 127.1, 127.6, 130.1, 131.2, 132.2 (Ph-Ar, Tyr-Ar and Fmoc-Ar), 140.7, 144.0, 155.7, 163.1 (C_q), 170.6, 171.4, 172.3, 173.9 (CO-C_q).

IR: KBr plate, $\tilde{\nu}$ = 3455 (s), 2976 (w), 1650 (m), 1350 (m), 1450 (w), 1025 (m), 751 (w), 701 (m), 574 (w) cm^{-1}.

LC-MS (ESI): Method-LCMS-3: t_R = 8.67 min, for $C_{36}H_{37}O_6N_4$ $[M+H]^+$ calcd. 621.3 found 621.9.

HRMS (ESI): for $C_{36}H_{37}O_6N_4$ [(M+H$^+$)] calcd. 621.2703, found 621.2706.

L,L,L-N-(4'*H*-Fluoren-9-ylmethoxycarbonyl)alaninyl-(*O*-Phenyl)tyrosinyl-alanine allyl ester (148c)

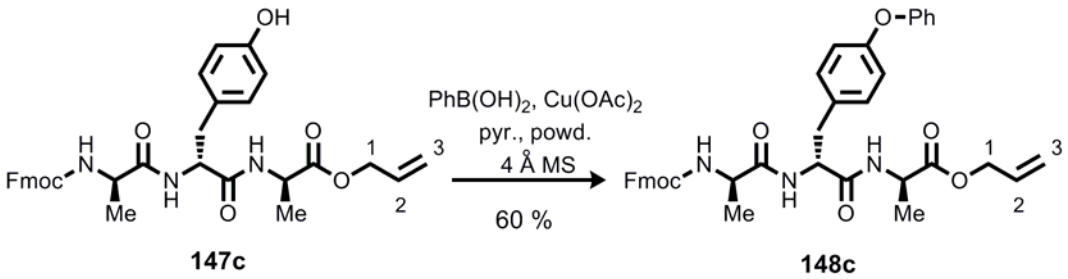

147c **148c**

By following **GP8** peptide **147c** (10 mg, 0.02 mmol) and phenyl boronic acid (3 mg, 0.03 mmol, 1.4 eq.) were coupled in the presence of $Cu(OAc)_2$ (3.6 mg, 0.02 mmol), pyridine (4.5 µL, 0.1 mmol) and 4 Å powdered molecular sieves (10 mg) in 1,2-dichloroethane/DMF (10:1, 1 ml). Flash column chromatography on silica gel (5 g, EtOAc/cyclohexane/MeOH 5:2:0.5) gave *O*-arylated peptide **148c** (7.9 mg, 0.01 mmol, 60 %) as a sticky oil.

TLC: R_f = 0.33 (EtOAc/cyclohexane/MeOH 1:1:0.5).

HPLC: t_R = 7.8 min (Method B)

Optical Rotation: $[\alpha]_D^{20}$ = - 53.4, *c* = (0.65, CH_3OH).

^{1}H-NMR: (400 MHz, DMSO-*d*$_6$): δ = 1.02 (d, 3H, *J* = 7.1 Hz, Ala-CH_3), 1.25 (d, 3H, *J* = 7.2 Hz, Ala-CH_3), 2.54 – 2.69 (m, 1H, Tyr-H$_\beta$), 2.76 – 2.85 (m, 1H, Tyr-H$_\beta$), 4.03 (qt, 1H, *J* = 8.1 Hz, Ala-H$_\alpha$), 4.16 – 4.32 (m, 5H, Ala^1-H$_\alpha$, Fmoc-CH_2 and Fmoc-CH), 4.45 (m, 1H, Tyr-H$_\alpha$), 4.56 (m, 2H, Allyl-H^3), 5.18 (d, 1H, Allyl-H^1), 5.29 (d, 1H, Allyl-H^1), 5.81 – 5.96 (m, 1H, Allyl-H^2), 6.61 (d, 2H, *J* = 8.4 Hz, Tyr-Ar), 6.99 (d, 2H, *J* = 8.3 Hz, Tyr-Ar), 7.11 (m, 5H, Ph-Ar), 7.32 (m, 2H, Fmoc-Ar), 7.41 (m, 2H, Fmoc-Ar), 7.50 (d, 1H, *J* = 7.5 Hz, NH), 7.71 (m, 2H, Fmoc-Ar), 7.88 (d, 2H, *J* = 7.5 Hz, Fmoc-Ar), 7.95 (s, 2H, PhOH), 8.13 (d, 2H, *J* = 8.7 Hz, NH), 8.23 (d, 2H, *J* = 6.9 Hz, NH).

^{13}C-NMR: (100 MHz, DMSO-*d*$_6$): δ = 17.3, 18.1 (2 x Ala-CH_3), 46.7 (C_β), 47.5 (Fmoc-CH), 50.3 (C_α), 50.4 (C_α), 53.9 (C_α), 65.6 (Fmoc-CH_2), 65.7 (Allyl-C_1) 113.7, 118.3, 120.1, 125.3, 127.1, 127.6, 130.1, 133.1, 136.5 (Tyr-Ar, Fmoc-Ar, Allyl-C_2 and Allyl-C_3), 140.8, 144.0, 155.7, 163.1 (C_q), 170.6, 172.3, 173.9 (CO-C_q).

IR: KBr plate, $\tilde{\nu}$ = 3346 (bs), 2260 (w), 1740 (s), 1666 (s), 1513 (s), 1220 (m), 1025 (m), 827 (m), 757 (m) cm^{-1}.

LC-MS (ESI): Method-LCMS-3: t_R = 9.8 min, for $C_{39}H_{40}O_7N_3$ $[M+H]^+$ calcd. 662.3, found 662.9.

HRMS (ESI): for $C_{39}H_{40}O_7N_3$ [(M+H$^+$)] calcd. 662.2859, found 662.2855.

L,L,L-N-(4'*H*-Fluoren-9'-ylmethoxycarbonyl)tyrosinyl-(*O*-phenyl)-tyrosinyl-tyrosine allyl ester (152a)

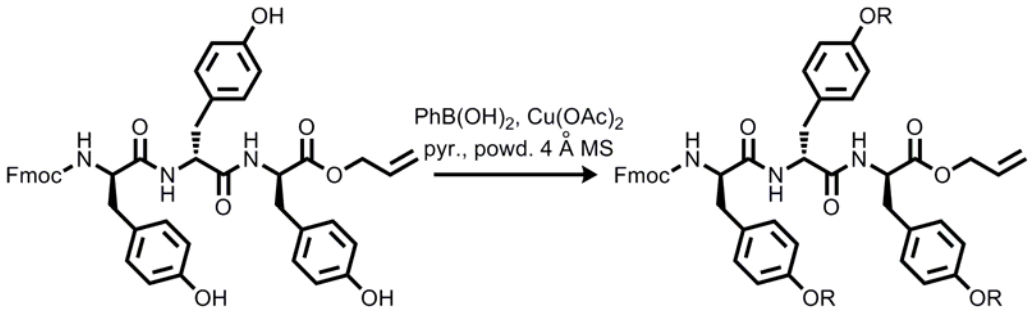

By following **GP8** peptide **151** (10 mg, 0.01 mmol) and phenyl boronic acid (4 mg, 0.03 mmol, 3 eq.) were coupled in the presence of $Cu(OAc)_2$ (2 mg, 0.01 mmol), pyridine (2.6 µL, 0.06 mmol) and 4 Å powdered molecular sieves (80 mg) in 1,2-dichloroethane/DMF (10:1, 4 ml). Flash column chromatography on silica gel (10 g, cyclohexane/EtOAc/MeOH/HCOOH 1:1:0.1:0.1) gave the product **152a** as a mixture of regio isomers (7 mg, 0.01 mmol, 31 %). Compounds **152b** (4.1 mg, 0.005 mmol, 44 %) and **152c** were also isolated (2.8 mg, 0.003 mmol, 28 %).

TLC: R_f = 0.25 (CH_2Cl_2/MeOH/HCOOH, 8:0.9:0.1).

HPLC: t_R = 8.2 min (Method B).

Optical Rotation: $[\alpha]_D^{20}$ = - 111, *c* = (0.17, CH_3OH).

^{1}H-NMR: (400 MHz, DMSO-*d*$_6$): 2.55 and 2.98 (two m, 6H, Tyr-H$_\beta$), , 4.09 and 4.24 (two x m, 4H, Tyr-H$_\alpha$, Fmoc-CH_2 and Fmoc-CH), 4.53 (m, 2H, Tyr-H$_\alpha$), 5.71 – 5.81 (m, 1H, Allyl-C$_2$), 5.9 (m, 3H, Allyl-C$_1$, Allyl-C$_3$, Allyl-C$_4$), 6.63 and 6.92 (m, 4H, Tyr-Ar), 7.34 (m, 10H, Ph-Ar and Tyr-Ar), 7.58 (m, 2H, Fmoc-Ar), 7.88 (m, 2H, Fmoc-Ar), 7.98 (d, 2H, *J* = 7.5 Hz, Fmoc-Ar), 8.07 (d, 1H, *J* = 8.4 Hz, NH), 8.23 (d, 1H, *J* = 8.7 Hz, NH).

^{13}C-NMR: (100 MHz, DMSO-*d*$_6$): δ = 37.3 (C_β), 46.4 (Fmoc-CH), 54.6 (C_α), 54.5 (C_α), 56.7 (C_α), 65.3 (Fmoc-CH_2), 114.7 (Tyr-Ar), 120.1, 125.3, 127.1, 127.6, 128.2, 129.1 (Tyr-Ar, Fmoc-Ar, Ph-Ar), 130.3 (Tyr-Ar), 141.4, 144.4, 156.4, 158.8 (C_q), 171.2, 173.1, 174.6 (CO-C_q).

IR: KBr plate, $\tilde{\nu}$ = 3350 (s), 2257 (w), 1666 (m), 1512 (w), 1241 (s),

1026 (w), 736 (w) cm^{-1}.

HRMS (ESI): for $C_{51}H_{48}O_9N_3$ $[M+H]^+$ calcd. 846.3385, found 846.3391.

L,L,L-N-(4'*H*-Fluoren-9'-ylmethoxycarbonyl)tyrosinyl-(*O*-phenyl)-tyrosinyl-(*O*-phenyl)tyrosine allyl ester (152b)

TLC: R_f = 0.40 (CH_2Cl_2/MeOH/HCOOH, 8:0.9:0.1).

HPLC: t_R = 8.2 min (Method B).

Optical Rotation: $[\alpha]_D^{20}$ = - 186, *c* = (0.50, CH_3OH).

^{1}H-NMR: (400 MHz, DMSO-d_6): 2.55 and 2.98 (two m, 6H, Tyr-H_β), 4.09 and 4.24 (two m, 4H, Tyr-H_α, Fmoc-CH_2 and Fmoc-CH), 4.53 (m, 2H, Tyr-H_α), 5.11 – 5.8 (m, 1H, Allyl-C_2), 5.11 – 5,8 (m, 3H, Allyl-C_1 , Allyl-C_3, Allyl-C_4), 6.63 and 6.92 (m, 4H, Tyr-Ar), 7.34 (m, 10H, Ph-Ar and Tyr-Ar), 7.58 (m, 2H, Fmoc-Ar), 7.88 (m, 2H, Fmoc-Ar), 7.98 (d, 2H, *J* = 7.5 Hz, Fmoc-Ar), 8.07 (d, 1H, *J* = 8.4 Hz, NH), 8.23 (d, 1H, *J* = 8.7 Hz, NH).

IR: KBr plate, $\tilde{\nu}$ = 3344 (s), 2257 (w), 1744 (s), 1665 (m), 1574 (s), 1449 (m), 13376 (m), 1240 (m), 1025 (m), 826 (w), 737 (m), 625 (w) cm^{-1}.

HRMS (ESI): for $C_{57}H_{52}O_9N_3$ $[M+H]^+$ calcd. 922.3698, found 922.3699.

L,L,L-N-(4'*H*-Fluoren-9'-ylmethoxycarbonyl)-(*O*-phenyl)-tyrosinyl-(*O*-phenyl)-tyrosinyl-(*O*-phenyl)tyrosine allyl ester (152c)

TLC: R_f = 0.62 (CH_2Cl_2/MeOH/HCOOH, 8:0.9:0.1)

HPLC: t_R = 12 min (Method B).

Optical Rotation: $[\alpha]_D^{20}$ = - 124, *c* = (0.15, CH_3OH).

^{1}H-NMR: (400 MHz, DMSO-d_6): 2.55 and 2.98 (two m, 6H, Tyr-H_β), 4.09 and 4.24 (two m, 4H, Tyr-H_α, Fmoc-CH_2 and Fmoc-CH), 4.53 (m, 2H, Tyr-H_α), 5.11 – 5.8 (m, 1H, Allyl-C_2), 5.11 – 5,,8 (m, 3H, Allyl-C_1 , Allyl-C_3, Allyl-C_4), 6.63 and 6.92 (m, 4H, Tyr-Ar), 7.34 (m, 12H, Ph-Ar and Tyr-Ar), 7.58 (m, 2H, Fmoc-Ar), 7.88 (m, 2H, Fmoc-Ar), 7.98 (d, 2H, *J* = 7.5 Hz, Fmoc-Ar), 8.07 (d, 1H, *J* = 8.4 Hz, NH), 8.23 (d, 1H, *J* = 8.7 Hz, NH).

IR: KBr plate, $\tilde{\nu}$ = 3345 (bs), 2134 (m), 1644 (s), 1565 (m), 1574 (m), 1345 (m), 1376 (m), 1238 (m), 1025 (m), 822 (w), 734 (m),

628 (w) cm^{-1}.

LC-MS (ESI): Method-LCMS-3: t_R = 12.57 min, for $C_{63}H_{56}O_9N_3$ $[M+H]^+$ calcd. 730.28, found 730.61.

HRMS (ESI): for $C_{63}H_{56}O_9N_3$ $[M+H]^+$ calcd. 998.4009, found 998.4011.

L,L,L,L,L,L,L-N-(4'*H*-Fluoren-9'-ylmethoxycarbonyl)prolinyl-tyrosinyl-glycinyl-alaninyl-isoleucinyl-alanine methyl ester (154)

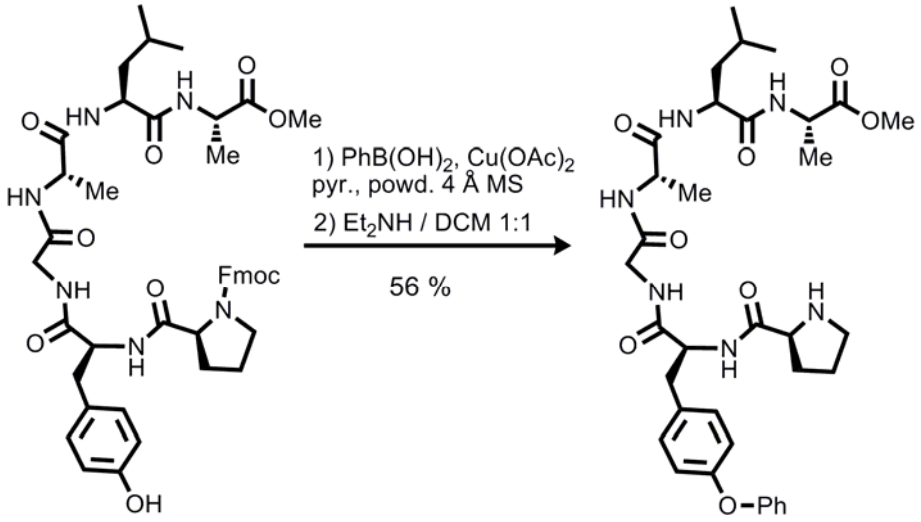

259 **154**

By following **GP8** peptide **259** (10 mg, 0.01 mmol) and phenyl boronic acid (4 mg, 0.03 mmol, 3 eq.) were coupled in the presence of $Cu(OAc)_2$ (2 mg, 0.01 mmol), pyridine (2.6 µL, 0.06 mmol) and 4 Å powdered molecular sieves (80 mg) in 1,2-dichloroethane/DMF (10:1, 4 ml). Residual oil was treated with Et_2NH/dichloromethane 1:1 to complete the Fmoc deprotection. Flash column chromatography on silica gel (10 g, dichloromethane/CH_3OH 100:10) gave product **154** as a sticky oil (4.6 mg, 0.007 mmol, 56 %).

TLC: R_f = 0.36 (CH_2Cl_2/CH_3OH, 4:0.8).

HPLC: t_R = 9.2 min (Method B).

Optical Rotation: $[\alpha]_D^{20}$ = - 77.4, *c* = (0.65, CH_3OH).

^{1}H-NMR: (400 MHz, DMSO-d_6): δ = 0.86 (dd, 6H, *J* = 6.5 Hz, *J* = 16.3 Hz Leu-CH_3), 1.06 (s, 3H, Ala-CH_3), 1.32 – 1.26 (m, 7H, Pro-H, Ala-CH_3), 1.28 (d, 2H, *J* = 7.3 Hz, Leu-CH_2), 1.48 (m, 1H, Leu-CH),

2.83 (m, 1H, Tyr-H_{β}), 2.98 (m, 1H, Tyr-H_{β}), 3.41 (m, 1H, Pro-H), 3.59 (m, 3H, $COOCH_3$), 3.69 (m, 1H, Gly-H), 4.31 (m, 4H, CH_{α}), 4.44 – 4.64 (m, 1H, CH_{α}), 6.59 (d, 2H, *J* = 8.1 Hz, Tyr-Ar), 6.82 (d, 2H, *J* = 8.1 Hz, Tyr-Ar), 7.12 (q, 2H, *J* = 8.1 Hz, Tyr-Ar), 7.24 (m, 5H, Ph-Ar), 7.92 (m, 2H, *J* = 7.5 Hz, NH), 8.05 (d, 1H, *J* = 7.9 Hz, NH), 8.07 (d, 1H, *J* = 7.9 Hz, 2 x NH).

^{13}C-NMR: (100 MHz, DMSO-*d*$_6$): δ= 17.3, 18.2 (2 x Ala-CH_3), 46.7 (C_{β}), 47.5 (Fmoc-CH), 50.4 (C_{α}), 50.5 (C_{α}), 53.9 (C_{α}), 65.7 (Fmoc-CH_2), 114.6, 120.1, 125.3, 125.6, 127.1, 127.6, 130.1, 131.2 (Tyr-Ar, Fmoc-Ar, Ph-Ar), 140.7, 144.0, 155.7, 163.1 (C_q), 170.6, 171.3, 172.9 (CO-C_q).

IR: KBr plate, $\tilde{\nu}$ = 3288 (s), 2976 (s), 1660 (s), 1670 (s), 1514 (s), 1455 (s), 1250 (m), 1070 (m), 825 (w), 699 (m), 576 (w) cm^{-1}.

HRMS (ESI): for $C_{35}H_{49}O_8N_6$ $[M+H]^+$ calcd. 681.3609, found 681.3611.

8.7 Work towards the total synthesis of RA-VII

8.7.1 Boronic acid building block

(S)-2-*tert*-butoxycarbonylamino-3-(4-hydroxy-phenyl)-propionic acid (166)

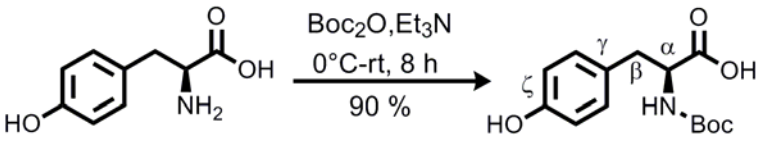

132 **166**

L-Tyrosine (50 g, 0.28 mol) was dissolved in dioxane/H_2O (1:1, 4 L). Et_3N (57 mL, 0.4 mol) and Boc_2O (76.17 mL, 0.3 mol) were added at 0°C and the reaction was stirred for 8 h at this temperature. Dioxane was removed under reduced pressure and the aqueous phase was adjusted to pH 3 by the addition of $HCl_{(aq)}$ (1 N) solution. This mixture was extracted with EtOAc (3 x 500 mL), the combined organic layers were washed with saturated $NaCl_{(aq)}$ solution (1 x 400 mL), dried with Na_2SO_4, filtered and concentrated. The solid residue was recrystallized from EtOAc/cyclohexane (1:9) by dissolving in EtOAc and adding cyclohexane to give carbamate (**166**) as colorless solid (69 g, 0.25 mol, 90 %).

TLC:	R_f = 0.60 ($CHCl_3$/MeOH/HCOOH 9:1:0.1).
HPLC:	t_R = 6.96 min (Method C).
M.p.:	140.2 - 142.2 °C.
Optical Rotation:	$[\alpha]_D^{20}$ = +10.8 (*c* = 2.0, CH_3OH).
^{1}H-NMR:	(400 MHz, DMSO-*d*$_6$): δ = 1.33 (s, 9H, *t*Bu), 2.69 (dd, 1H, J_{AX} = 9.8 Hz, J_{AB} = 13.8 Hz, H_β), 2.90 (dd, 1H, J_{BX} = 4.6 Hz, J_{AB}= 13.8 Hz, H_β), 4.00 (td, 1H, J_{BX} = 4.7 Hz, J_{AX}= 9.8 Hz, H_α), 6.66 (d, 2H, *J* = 8.4 Hz, H_{Ar}), 6.98 (d, 1H, *J* = 8.3, NH), 7.03 (d, 2H, *J* = 1.9 Hz, H_{Ar}), 9.17 (s, 1H, PhOH), 12.50 (s, 1H, COOH).
^{13}C-NMR:	(100 MHz, DMSO-*d*$_6$) δ= 28.1 (Boc, C(**C**H$_3$)$_3$), 35.6 (C_β), 55.4 (C_α), 77.9 (Boc-**C**(CH$_3$)$_3$), 114.8 (Tyr-Ar), 127.9 (Tyr-Ar), 129.8 (C_γ), 155.3 (Boc, **C**O), 155.7 (C_ζ), 173.6 (**C**OOH).

IR: KBr plate, $\tilde{\nu}$ = 3389 (s), 3260 (m), 1686 (s), 1515 (s), 1236 (m), 829 (w), 581 w.

HRMS (ESI): For $C_{14}H_{20}NO_5$ $[M+H]^+$ calcd. 281.1263, found 281.1264.

(S)-2-*tert*-*b*utoxycarbonylamino-3-(4'-hydroxy-3'-iodo-phenyl)-propionic acid (130)

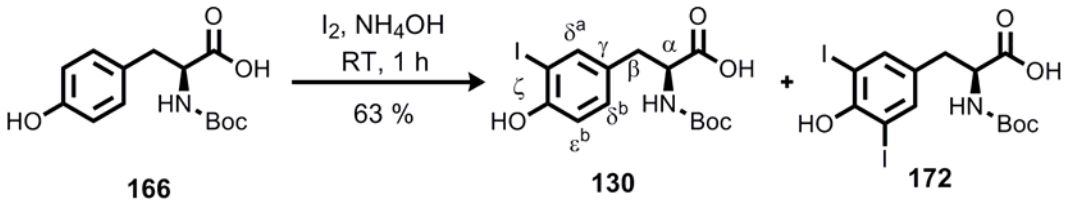

Tyrosine derivative **166** (69 g, 0.25 mol) was dissolved in NH_4OH (2.8 L, 88 mM) and the resulting solution was cooled to 0°C. A solution of I_2 (62.4 g, 0.25 mol) in EtOH (668 mL) was added dropwise with stirring over 1.5 h and then the mixture was stirred in the dark for 1 h. Excess iodine was quenched by the addition of solid $Na_2S_2O_3$ (39 g, 0.25 mol, 1 equiv.). The pH was adjusted to pH = 3 by HCl solution (1 N) and the mixture was extracted with EtOAc (3 x 500 mL). The combined organic layers were washed with 10 % $Na_2S_2O_{3(aq.)}$ (3 x 400 mL) and saturated $NaCl_{(aq)}$ (2 x 400 mL), dried with Na_2SO_4 and concentrated. The residue was purified by flash column chromatography (500 g silica gel, $MeOH/CH_2Cl_2$, 1:15→2:8) to give aryl iodide **130** as a colorless powder (63 g, 0.15 mol, 63 %). Bis iodinated compound **172** (20 g, 40 mmol, 20 %) was also isolated.

TLC: R_f = 0.53 (CH_2Cl_2/MeOH/HCOOH 20:1:0.1).

HPLC: t_R = 8.04 min (Method A).

M.p.: 63.6 – 64.6°C

Optical Rotation: $[\alpha]_D^{20}$ = +18 (*c* = 2, CH_3OH).

^{1}H-NMR: (400 MHz, DMSO-*d*$_6$): δ = 1.33 (s, 9H, *t*Bu), 2.68 (dd, 1H, J_{AX} = 10.3 Hz, J_{AB} = 13.8 Hz, H_β), 2.89 (dd, 1H, J_{BX} = 4.4 Hz, J_{AB} = 13.9 Hz, H_β), 4.00 (td, J_{BX} = 4.5 Hz, J_{AX} =10.3 Hz, 1H, H_α), 6.79 (d, *J* = 8.2 Hz, 1H, *Ar-H*$_{\varepsilon b}$), 7.04 (m, 2H, NH and *Ar-H*$_{\delta b}$), 7.53 (d, 1H, *J* = 1.9 Hz, *Ar-H*$_{\delta a}$), 10.08 (s, 1H, PhOH), 12.56 (s, 1H, COOH).

^{13}C-NMR: (100 MHz, DMSO-*d*$_6$): δ= 28.1 (Boc, C(**C**H$_3$)$_3$), 34.9 (C_β), 55.5 (C_α), 79.1 (Boc-**C**$(CH_3)_3$), 84.1 (Tyr-Ar), 114.5 (Tyr-Ar), 130.4

(Tyr-Ar), 139.1 (C_γ), 154.4 (C_ζ), 155.3 (Boc, CO), 173.3 (COOH).

IR: KBr plate, $\tilde{\nu}$ = 3380 bm, 2975 m, 1741 s, 1695 s, 1235 w, 1172 w, 1041 w, 813 w, 754 w, 698 w. cm^{-1}

HRMS (EI): For $C_{14}H_{19}O_5NI$ ($M+H^+$) calcd. 408.0302, found 408.0302.

(S)-2-*tert-b*utoxycarbonylamino -3-(4'-hydroxy-3',5'-diiodo-phenyl)-propionic acid (172)

TLC: R_f = 0.61 (CH_2Cl_2/MeOH/HCOOH 20:1:0.1).

HPLC: t_R = 8.93 min (method A).

^{1}H-NMR: (400 MHz, CD_3CN-d_6): δ = 1.39 (s, 9H, *t*Bu), 2.77 (m, 1H, H_β), 2.89 (m, 1H, H_β), 4.30 (m, 1H, H_α), 5.54 (d, 2H *J* = 7.2 Hz, *Ar-H*$^{\delta ab}$), 7.63 (s, 1H, NH).

^{13}C-NMR: (100 MHz, DMSO-d_6): δ = 28.1 (Boc, C(**C**H_3)$_3$), 34.9 (C_β), 55.5 (C_α), 79.1 (Boc, C_q), 84.1 ($C_{\varepsilon b}$), 86 ($C_{\varepsilon b}$), 130.4 (Tyr-Ar), 139.1 ($C\gamma$), 154.4 (C_ζ), 155.3 (Boc, CO), 173.3 (**C**OOH).

LC-MS (ESI): Method-LCMS-1: t_R = 8.93 min, for $C_9H_{10}O_3NI_2$ $[M+H\text{-Boc}]^+$ calcd. 433. 41, found 433.81.

(S)-2-*tert-b*utoxycarbonylamino -3-(4'-hydroxy-3'-iodo-phenyl)-propionic acid benzyl ester (167)

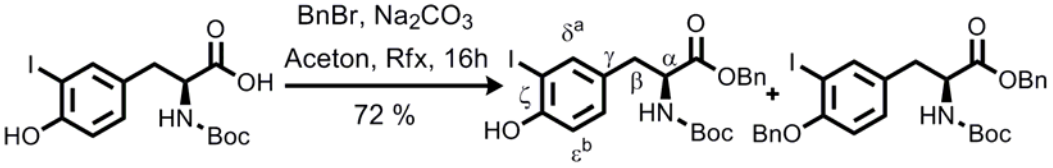

Na_2CO_3 (7.3 g, 68.7 mmol) was added to a stirred solution of acid **130** (28 g, 69 mmol) in freshly distilled acetone (800 mL). Benzyl bromide (9 mL, 75.6 mmol) was slowly added at room temperature and the reaction mixture was heated to reflux for 16 h. After cooling, the solids were filtered off, the solvent was removed *in vacuo* and the residue was redissolved in EtOAc (300 mL). The organic layer was washed with H_2O (1 x 100 mL), saturated Na_2CO_3 solution (1 x 100), saturated $NaCl_{(aq.)}$ solution (1 x 100 mL) and dried with Na_2SO_4. Purification by column chromatography (EtOAc/cyclohexane 1:15→1:9) afforded the benzyl ester **167** as a colorless solid

(25 g, 49.3 mmol, 72 %). Bis benzylated derivative **260** was isolated as a minor byproduct (2.1 g, 3.5 mmol, 5 %).

TLC: R_f = 0.69 (CH_2Cl_2/MeOH/HCOOH 30:1:0.1).

HPLC: t_R = 10.59 min (Method A).

M.p.: 99.6 – 101.6 °C.

Optical Rotation: $[\alpha]_D^{20}$ = - 10.0 (*c* = 0.81, CH_3OH).

^{1}H-NMR: (400 MHz, DMSO-d_6): δ = 1.33 (s, 9H, *t*Bu), 2.77 (dd, 1H, J_{AX} = 8.1 Hz, J_{AB} =13.8, H_β), 2.87 (dd, 1H, J_{BX} = 5.5 Hz, J_{AB} = 13.9 Hz, H_β), 4.14 (td, 1H, J_{BX} = 5.5 Hz, J_{AX} = 8.1 Hz, H_α), 5.06 (s, 2H, Bn-CH_2), 6.78 (d, *J* = 8.3 Hz, 1H, *Ar-H*$^{\varepsilon b}$), 7.05 (dd, 1H, *J* = 2.1 Hz, *J* = 8.3 Hz, *Ar-H*$^{\delta b}$), 7.34 (m, 6H, Bn-Ar and NH), 7.54 (d, *J* = 1.8 Hz, 1H, Ar-*H*$^{\delta a}$), 10.11 (s, 1H, PhOH).

^{13}C-NMR: (100 MHz, DMSO-d_6): δ = 28.1 (Boc, C(**C**H_3)$_3$), 34.8 (C_β), 55.3 (C_α), 65.7 (Bn-CH_2), 78.2 (Boc-**C**$(CH_3)_3$), 84.1 ($C_{\varepsilon a}$), 114.6 (Tyr-Ar), 127.6 (Bn-Ar), 127.8 (Bn-Ar), 128.2 (Tyr-Ar), 130.1 ($C\gamma$), 135.7 (Bn-C_q), 139.1 (Tyr-Ar), 155.1 (C_ζ), 155.3 (Boc-**C**O), 171.8 (Bn-C_q).

IR: KBr plate, $\tilde{\nu}$ = 3374 (m), 2978 (m), 1689 (s), 1501 (w), 1450 (m), 1365 (m), 1059 (w), 822 (w), 748 (w), 698 (w) cm^{-1}.

HRMS (EI): For $C_{21}H_{25}O_5NI$ ($M+H^+$) calcd. 498.0772, found 498.0774.

(S)-2-*tert-b*utoxycarbonylamino-3-(4'-benzyloxy -3'-iodo-phenyl)-propionic acid (260)

TLC: R_f = 0.82 (CH_2Cl_2/MeOH/HCOOH 30:1:0.1).

HPLC: t_R = 10.5 min (Method A).

^{1}H-NMR: (400 MHz, DMSO-d_6): δ = 1.34 (s, 9H, *t*Bu), 2.84 (dd, 1H, J_{AX} = 10.5 Hz, J_{AB} = 13.6, H_β), 3.00 (dd, 1H, J_{BX} = 5.5 Hz, J_{AB} = 13.8 Hz, H_β), 3.31 (s, 1H, NH) 4.25 (m, 1H, H_α), 4.88 (s, 2H, Bn-CH_2), 5.13 (d, 2H, *J* = 4.3 Hz, Bn-CH_2), 6.78 (d, 1H, *J* = 8.3 Hz, *Ar-H*$^{\varepsilon b}$), 7.05 (dd, 1H, *J* = 2.1, 8.3 Hz, *Ar-H*$_{\delta b}$), 7.36 (m, 10H, 2 x Bn-Ar), 7.61 (d, *J* = 6.9 Hz , 2H, Ar-*H*$_{\delta a}$).

^{13}C-NMR: (100 MHz, DMSO-d_6): δ = 28.1 (*t*Bu, C(**C**H_3)$_3$), 34.8 (C_β), 55.3 (C_α), 65.7 (Bn-CH_2), 78.2 (Boc-**C**$(CH_3)_3$), 84.1 ($C_{\varepsilon a}$), 114.6 (Tyr-

Ar), 127.6 (Bn-Ar), 127.8 (Bn-Ar), 128.2 (Tyr-Ar), 129.9 (Bn), 130.1 (Cγ), 135.7 (Bn-C_q), 136.2 (Bn-C_q), 139.1 (Tyr-Ar), 155.1 (C_ζ), 155.3 (Boc-**C**O), 171.8 (Bn-C_q).

LC-MS (ESI): Method-LCMS-1: t_R = 10.92 min, for $C_{23}H_{23}O_3NI$ [(M+H^+)-Boc] calcd. 488.1 found 488.8.

(S)-2-*tert-butoxycarbonyl*amino -3-(4'-methoxy-3'-iodo-phenyl)-propionic acid benzyl ester (168)

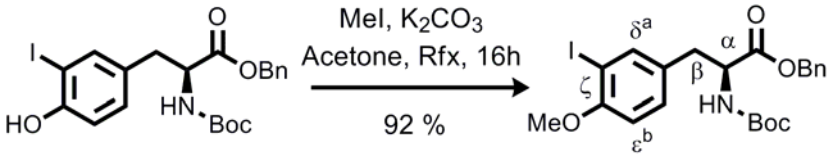

167 168

K_2CO_3 (7.3 g 68.7 mmol) was added to a stirred solution of phenol **167** (24.5 g, 49.2 mmol) in freshly distilled acetone (70 mL). MeI (31 mL, 492 mmol) was slowly added at 0°C, the reaction mixture was heated to reflux for 16 h under argon. The crude mixture was filtered and concentrated *in vacuo,* then redissolved in EtOAc (200 mL) and washed with H_2O (100 mL), saturated $Na_2CO_{3(aq.)}$ solution (100 mL), saturated $NaCl_{(aq.)}$ solution (100 mL), dried with Na_2SO_4, filtered and concentrated. Purification of the residue by column chromatography (400 g silica gel, EtOAc/cyclohexane, 1:15→2:8) afforded methyl ether **168** as a pale yellow oil (23 g, 45 mmol, 92 %).

TLC: R_f = 0.59 (EtOAc/cyclohexane 2:5).

HPLC: t_R = 11.99 min (Method A).

Optical Rotation: $[\alpha]_D^{20}$ = +11 (*c* = 3, CH_3OH).

^{1}H-NMR: (400 MHz, DMSO-d_6): δ = 1.33 (s, 9H, *t*Bu), 2.85 (dd, 1H, J_{AX} = 10.1 Hz, J_{AB} = 13.7, H_β), 2.93 (dd, 1H, J_{BX} = 5.3 Hz, J_{AB} = 13.8 Hz, H_β), 3.78 (s, 3H, OMe), 4.17 (td, 1H, J_{BX} = 5.5 Hz, J_{AX} = 9.7 Hz, H_α), 5.09 (s, 2H, Bn-CH_2), 6.89 (d, 1H, *J* = 8.5 Hz, *Ar-H*$^{\varepsilon b}$), 7.21 (dd, 1H, *J* = 2.1, 8.4 Hz, *Ar-H*$^{\delta b}$), 7.34 (m, 6H, Bn-Ar and NH), 7.66 (d, 1H, *J* = 1.9 Hz, Ar-*H*$^{\delta a}$).

^{13}C-NMR: (100 MHz, DMSO-d_6): δ = 28.0 (Boc-C(**C**H_3)$_3$), 34.7 (C_β), 55.3 (C_α), 65.7 (Bn-CH_2), 78.2 (Boc-**C**$(CH_3)_3$), 84.1 ($C_{\varepsilon a}$), 114.6 (Tyr-

Ar), 127.6, 127.8 (Bn-Ar), 128.2 (Tyr-Ar), 130.3 (Bn-Ar), 131.6 (C_γ), 135.7 (Bn-C_q), 139.3 (Tyr-Ar), 155.2 (C_ζ), 156.3 (Boc-CO), 171.7 (Bn-C_q).

IR: KBr plate, $\tilde{\nu}$ = 3436 (m), 2974 (m), 2934 (m), 2359 (m), 1713 (s), 1492 (s), 1166 (s), 1051 (w), 813 (w), 751 (w), 699 (w), 663 (w) cm^{-1}.

HRMS (ESI): For $C_{22}H_{27}O_5NI$ ($M+H^+$) calcd. 512.0928, found 512.0923.

(S)-2-(*tert-b*utoxycarbonyl-methyl-amino)-3-(3'-iodo-4'-methoxy-phenyl)-propionic acid benzyl ester (169)

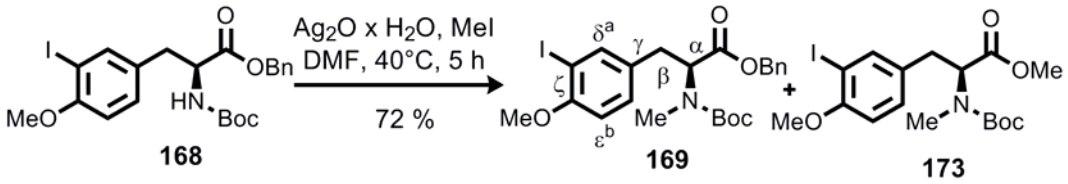

Carbamate (**168**) (23 g, 45 mmol) was dissolved in dry DMF (900 mL, *c* = 0.05 M). MeI (8.4 mL, 135 mmol) was added at 0°C, the solution was allowed to warm to room temperature and was stirred for 10 min. At this point, freshly prepared $Ag_2O \times H_2O$ (25 g, 0.11 mol) was added and reaction mixture was heated to exactly 40°C (external temperature) for 5h under argon. The formation of product **XX** was monitored by reversed phase HPLC. When conversion was complete, the mixture was cooled to room temperature and Et_2O (200 mL) was added. The resulting slurry was filtered over a short pad of celite (2 cm). The filtrate was washed with 0.05 N $KCN_{(aq.)}$ solution (100 mL), H_2O (3 ×100 mL), saturated $NaCl_{(aq)}$ solution (100 mL), then dried with $MgSO_4$, and concentrated *in vacuo*. The residue was purified by column chromatography (150 g, EtOAc/cyclohexane 1:15→2:8) to afford N-methyl carbamate as a product (**169**) (17.4 g, 33.1 mmol, 72 % yield) and methyl ester (**173**) as side product (3 g, 6.7 mmol, 15 % yield).

TLC: R_f = 0.59 (EtOAc/cyclohexane 2:5).

HPLC: t_R = 12.61 min, (Method A).

Optical Rotation: $[\alpha]_D^{20}$ = +19 (*c* = 2, CH_3OH).

^{1}H-NMR: (400 MHz, DMSO-d_6): δ = 1.24, 1.35 (s, 9H, *t*Bu)*, 2.58, 2.59 (s, 3H, N-CH_3)*, 2.95 (m, 1H, H_β), 3.11 (dd, 1H, *J* = 4.5 Hz,

14.4 Hz, H_β), 3.78 (s, 3H, O-CH_3), 4.76 (m, 1H, H_α), 5.14, 5.17 (s, 2H, Bn-CH_2)*, 6.93 (d, 1H, *J* = 8.4 Hz, *Ar-*$H_{\varepsilon b}$), 7.21 (d, 1H, *J* = 7.9, 8.4 Hz, *Ar-*$H_{\delta b}$), 7.37 (m, 5H, Bn-Ar), 7.58, 7.68 (s, 1H, Ar-$H_{\delta a}$)*. *Rotamers are present.

^{13}C-NMR: (100 MHz, DMSO-d_6): δ = 28.0 (Boc-C(**C**H_3)$_3$), 32.4 (N-**C**H_3), 33.0 (C_β), 56.2 (O**C**H_3), 60.5 (C_α), 65.9 (Bn-CH_2), 79.1 (Boc-C_q), 109.2 (Tyr-Ar), 111.1 (Tyr-Ar), 127.7, 128.3 (Bn-Ar), 130.1 (Tyr-Ar), 131.6 ($C\gamma$), 135.7 (Bn-C_q), 139.3 (Tyr-Ar), 154.0 (C_ζ), 156.3 (Boc-**C**O), 170.3 (Bn-C_q).

IR: KBr plate, $\tilde{\nu}$ = 2974 (m), 1741 (s), 1695 (s), 1490 (m), 1392 (m), 1326 (m), 738 (w), 699 (w), 663 (w) cm^{-1}.

HRMS (ESI): For $C_{23}H_{29}O_5NI$ ($M+H^+$) calcd. 526.1089, found 526.1100.

(S)-2-(*tert-b*utoxycarbonyl-methyl-amino)-3-(3'-iodo-4'-methoxy-phenyl)-propionic acid methyl ester (173)

TLC: R_f = 0.45 (EtOAc/cyclohexane 2:5).

HPLC: t_R = 10.64 min (Nucleosil C18 A: H_2O B: Acetonitrile C: 0.1 Vol% TFA/H_2O, 5→100 % B in 25 min, 1 ml/min).

1H-NMR: (400 MHz, DMSO-d_6): δ = 1.24, 1.33 (s, 9H, *t*Bu)*, 2.57, 2.58 (s, 3H, *N*-CH_3)*, 2.88 (m, 1H, H_β), 3.07 (dd, 1H, J_{BX} = 4.7 Hz, J_{AB} = 14.2 Hz, H_β), 3.68 (s, 3H, O-CH_3), 3.78 (s, 3H, COOMe), 4.48 (m, 1H, H_α), 6.92 (m, 1H, *Ar-*$H_{\varepsilon b}$), 7.22 (m, 1H, *Ar-*$H_{\delta b}$), 7.65, 7.68 (d, 1H, Ar-$H_{\delta a}$)*. *Rotamers are present

LC-MS (ESI): Method-LCMS-1: t_R = 9.93 min, for $C_{12}H_{17}O_3NI$ $[M+H-Boc]^+$ calcd. 350.0, found 350.5.

(*S*)-2-(*tert*-butoxycarbonyl-methyl-amino)-3-[4'-methoxy-3'-(4'',4'',5'',5''-tetramethyl-1'',3'',2''-dioxaborolan-2''-yl)-phenyl]-propionic acid benzyl ester (170)

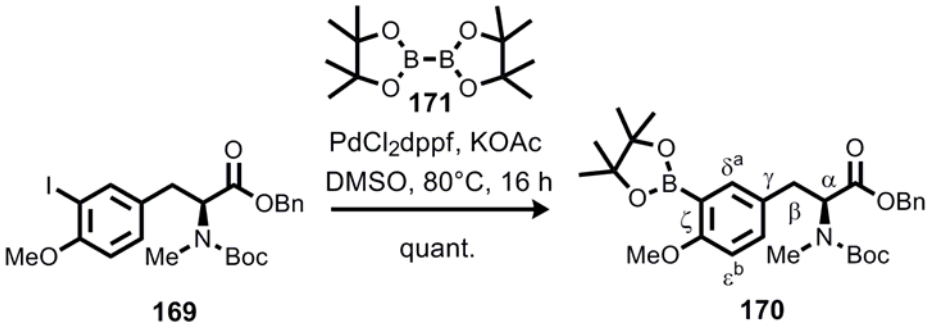

Bis(pinacol)diboron **171** (8.2 g, 32 mmol), KOAc (8.6 g, 88 mmol) and $PdCl_2$dppf (641 mg, 8.7 mmol) were charged in a two necked flask, fitted with a condensator under argon and a solution of iodide **169** (15 g, 29.2 mmol) in dry DMSO (147 mL, *c* = 200 mM) was added. The resulting suspension was heated to 80°C for 16 h with stirring. The mixture was cooled to room temperature and 50 % $NaCl_{(aq.)}$ solution was added (100 mL). The resulting slurry was filtered through a sinter filter and the filtrate was extracted with EtOAc (3 x 300 mL). The organic layer was washed with saturated $NaCl_{(aq.)}$ solution (200 mL), dried with $MgSO_4$, filtered and concentrated *in vacuo*. The residue was filtered through a short pad of silica gel (100 g, EtOAc/cyclohexane, 2:8→8:2) to afford **(169)** as a brown oil (16 g, 29.2 mmol, quant.) which was suitable for use in the next step without further purification.

TLC: R_f = 0.44 (EtOAc/cyclohexane 2:5).

HPLC: t_R = 12.6 min (Method A).

^{1}H-NMR: (400 MHz, DMSO-d_6): δ = 1.25, 1.32 (s, 21H, *t*Bu and pinacol - 4 x CH_3)*, 2.58, 2.59 (s, 3H, N-CH_3)*, 2.95 (m, 1H, H_β), 3.12 (m, 1H, H_β), 3.70 (s, 3H, O-CH_3), 4.73 (m, 1H, H_α), 5.13, 5.17 (s, 2H, Bn-CH_2)*, 6.88 (d, 1H, *J* = 8.5 Hz, *Ar-*$H_{\varepsilon b}$), 7.27 (m, 1H, *Ar-*$H_{\delta b}$), 7.37 (m, 5H, Bn-Ar), 7.43 (d, 1H, *J* = 1.6 Hz, Ar-$H_{\delta a}$). *Rotamers are present.

^{13}C-NMR: (100 MHz, DMSO-d_6): δ = 24.7 (pinacol-CH_3), 27.6 (Boc-$C(CH_3)_3$), 32.9 (N-CH_3), 33.5 (C_β), 55.3 (O-CH_3), 60.5 ($C_{\varepsilon a}$), 65.9 (C_α), 65.8 (Bn-CH_2), 79.0 (Boc-$C(CH_3)_3$), 82.8 (pinacol-C_q), 110.5 (Tyr-Ar), 127.5, 127.7 (Bn-Ar), 128.3 ($C_{\delta b}$), 133.2 ($C\gamma$), 135.8 ($C_{\delta a}$), 136.7 (Bn-C_q), 162.4 (C_ζ), 170.5 (Boc-CO),

172.2 (COOBn).

IR: KBr plate, $\tilde{\nu}$ = 2977 (s), 2334 (w), 1743 (s), 1697 (s), 1496 (m), 1146 (m), 857 (w), 814 (w), 753 (w) cm^{-1}.

HRMS (ESI): For $C_{29}H_{41}O_7NB$ $(M+H^+)$ calcd. 526.2971, found 526.2969.

***(S)*-2-(*tert*-butoxycarbonyl-methyl-amino)-3-[4'-methoxy-3'-borono-phenyl]-propionic acid benzyl ester (128)**

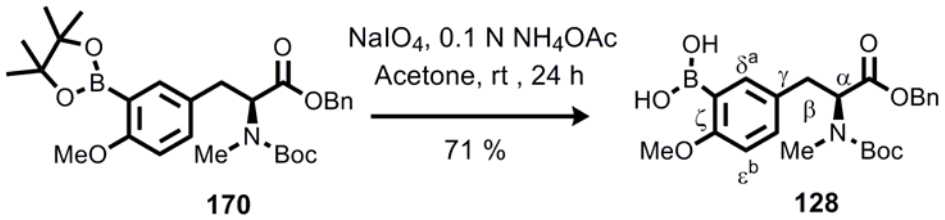

An NH_4OAc aqueous solution (450 mL, 0.1 N) and $NaIO_4$ (8.4 mL, 135 mmol) were added to a solution of boronic acid ester **(170)** (16 g, 29.2 mmol) in acetone (450 mL) and the reaction mixture was stirred for 24 h at 20°C. The mixture was filtered and concentrated *in vacuo*. The residue was taken up in EtOAc/MeOH (99:1, 300 mL), washed with a saturated $NaCl_{(aq)}$ solution (20 mL), dried with $MgSO_4$. The solvent was removed *in vacuo* and the residue was purified by column chromatography (50 g, EtOAc/cyclohexane, 2:8→1:1) to afford boronic acid (**128**) as a light yellow resin (9.2 g, 21.2 mmol, 71% yield).

TLC: R_f = 0.24 (EtOAc/Cyclohexane 2:5).

HPLC: t_R = 10.29 min (Method A).

Optical Rotation: $[\alpha]_D^{20}$ = -16.5 (*c* = 0.66, CH_3OH).

^{1}H-NMR: (400 MHz, DMSO-d_6): δ = 1.24, 1.31 (s, 9H, Boc-*t*Bu)*, 2.58, 2.61 (s, 3H, N-CH_3)*, 3.00 (m, 1H, H_β), 3.12 (dd, 1H, *J* = 4.6 Hz, 14.3 Hz, H_β), 3.78 (s, 3H, O-CH_3), 4.71 (m, 1H, H_α), 5.13*, 5.17 (s, 2H, Bn-CH_2), 6.89 (m, 1H, *J* = 8.5 Hz, *Ar-H*$^{\varepsilon b}$), 7.21 (m, 1H, *Ar-H*$^{\delta b}$), 7.37 (m, 5H, Bn-Ar), 7.44, 7.49 (s, 1H, Ar-*H*$^{\delta a}$)*, 7.62 (s, 2H, 2 x B-OH). *Rotamers are present.

^{13}C-NMR: (100 MHz, DMSO-d_6): δ = 27.6 (*Boc*-C(**C**H_3)$_3$), 32.9 (N-CH_3), 33.8 (C_β), 55.2 (O-CH_3), 60.0 ($C_{\varepsilon a}$), 60.7 (C_α), 65.9 (Bn-CH_2), 79.1 (Boc-C_q), 110.1 (Tyr-Ar), 127.6, 127.7 (Bn-Ar), 128.9 (Tyr-Ar), 132.0 ($C\gamma$), 135.7 (Tyr-Ar), 136.7 (Bn-C_q), 162.2 (C_ζ), 162.2 (Boc-CO), 170.5 (COOBn).

IR: KBr plate, $\tilde{\nu}$ = 3379 bm, 2978 m, 2362 s, 1687 m, 1603 w, 1504 m, 1165 m, 822 w, 749 w, 697 w cm^{-1}.

HRMS (ESI): For $C_{23}H_{31}O_7NB$ ($M+H^+$) calcd. 444.2188, found 444.2192.

8.7.2 Phenol building block

(S)-2-Benzyloxycarbonylamino-3-(4'-hydroxy-phenyl)-propionic acid *tert*-butyl ester (187)

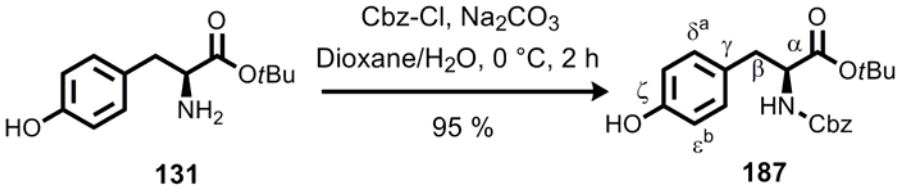

L-Tyrosine-*tert*-butylester **(131)** (20 g, 84.2 mmol) was dissolved in dioxane/H_2O, (2:1, 120 mL) and Na_2CO_3 (2 M, 42 mL, 84 mmol) and Cbz-Cl (13 mL, 92.7 mmol) were added at 0°C. The reaction mixture was stirred for 2 h at 20°C (TLC control). The dioxane was removed *in vacuo* and the remaining aqueous solution was adjusted to pH 3 with 1 N HCl solution. The mixture was extracted with EtOAc (3 x 300 mL) and the combined organic layers were washed with saturated NaCl solution (300 mL), dried with Na_2SO_4, filtered and concentrated under reduced pressure Recrystallization (EtOAc/cyclohexane 1:9) gave **187** (29.5 g, 79 mmol, 95 %) as a colorless solid.

TLC: R_f = 0.39 (CH_3OH/ $CHCl_3$ 1:15).

HPLC: t_R = 9.81 min (Method A).

Optical Rotation: $[\alpha]_D^{20}$ = -77.1 (*c* = 0.74, CH_3OH).

M.p.: 83.1 - 83.6 °C.

^{1}H-NMR: (400 MHz, DMSO-d_6): δ = 1.34 (s, 9H, *t*Bu), 2.74 (dd, 1H, J_{AX} = 9.4 Hz, J_{AB} = 13.8 Hz, H_β), 2.85 (dd, 1H, J_{BX} = 5.8 Hz, J_{BA} = 13.9 Hz, H_β), 3.99-4.09 (m, 1H, H_α), 4.99 (s, 2H, Bn-CH_2), 6.66 (d, 2H, *J* = 8.5 Hz, Tyr-Ar), 7.03 (d, 2H, Tyr-Ar), 7.35 (m, 5H, Bn-Ar), 7.59 (d, 1H, OH), 9.21 (s, 1H, COOH).

^{13}C-NMR: (100 MHz, DMSO-d_6): δ = 27.5 (*t*Bu-C(**C**H_3)$_3$), 35.9 (C_β), 56.3 (C_α), 65.2 (Bn-CH_2), 80.4 (*t*Bu-C_q), 114.8 (Tyr-Ar), 127.6 ($C\gamma$),

127.6 (C_ζ), 128.17 (Bn-Ar), 129.9 (Tyr-Ar); 136.9 (C_q), 155.8 (C_q), 171.0 (C_q).

IR: KBr plate, $\tilde{\nu}$ = 3379 (m), 2978 (m), 2362 (s), 1687 (m), 1603 (w), 1504 (m), 1165 (m), 822 (w), 749 (w), 697 cm^{-1}(w) cm^{-1}.

HRMS (ESI): For $C_{21}H_{26}O_5N$ ($M+H^+$) calcd. 372.1806, found 372.1805.

(S)-2-Benzyloxycarbonylamino-3-(4'-benzyloxy-phenyl)-propionic acid *tert*-butyl ester (188)

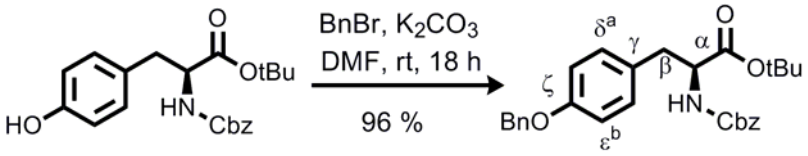

187 188

K_2CO_3 (13 g, 68.7 mmol) was added to a stirred solution of phenol (**187**) (30 g, 80 mmol) in freshly distilled DMF (250 mL). After the slow addition of benzyl bromide (14.1 mL, 0.12 mol) at room temperature, the slurry was refluxed for 18 h. The crude mixture was cooled to room temperature, filtered, concentrated *in vacuo,* and redissolved in EtOAc (300 mL). The organic layer was washed with H_2O (100 mL), saturated $NaHCO_3$ solution (100 mL), saturated NaCl solution (100 mL) and dried with $MgSO_4$ and concentrated. Purification by column chromatography (EtOAc/cyclohexane 1:30→3:20) afforded benzyl ether **188** as a colorless solid (24 g, 51.1 mmol, 64 %).

TLC: R_f = 0.65 (EtOAc/cyclohexane 2:5).

HPLC: t_R = 12.49 min (Method A).

M.p.: 77.7 – 78.1°C.

Optical Rotation: $[\alpha]_D^{20}$ = -10 (*c* = 0.45, CH_3OH).

^{1}H-NMR: (400 MHz, DMSO-*d*$_6$): δ = 1.33 (s, 9H, *t*Bu), 2.79 (dd, 1H, J_{AX} = 9.6 Hz, J_{AB} = 13.8 Hz, H_β), 2.82 (dd, 1H, J_{BX} = 5.8 Hz, J_{AB} = 13.8 Hz, H_β), 4.04 (m, 1H, H_α), 4.97 (d, 2H, *J* = 4.0 Hz, Bn-CH_2), 5.07 (s, 2H, Bn-CH_2), 6.91 (m, 2H, Tyr-Ar), 7.15 (d, 2H, *J* = 8.6 Hz, Tyr-Ar), 7.35 (m, 10H, Bn-Ar), 7.62 (d, 1H, *J* = 8.1 Hz, NH), 9.21 (s, 1H, COOH).

^{13}C-NMR: (100 MHz, DMSO-*d*$_6$): δ = 27.5 (*t*Bu-C(**C**H_3)$_3$), 35.8 (C_β), 56.2

(C_α), 65.2 (Bn-CH_2), 69.0 (Bn-CH_2), 80.5 (*t*Bu-C_q), 114.4 (Tyr-Ar), 127.5, 127.6 (Bn-Ar), 128.2, 128.3 (Bn-Ar), 129.5 (C_γ), 130.1 (Tyr-Ar), 136.9, 137.1 (Bn-Ar), 155.8 (C_ζ), 156.9 (C_q), 170.9 (C_q).

IR: KBr plate, $\tilde{\nu}$ = 3392 (m), 2931 (m), 1740 (s), 1707 (s), 1584 (m), 1241 (m), 741 (w), 700 (w), 544 (w) cm^{-1}.

HRMS (ESI): For $C_{28}H_{32}O_5N$ ($M+H^+$) calcd. 462.2275, found 462.2272.

(S)-2-(Benzyloxycarbonyl-methyl-amino)-3-(4'-benzyloxy-phenyl)-propionic acid *tert*-butyl ester (189)

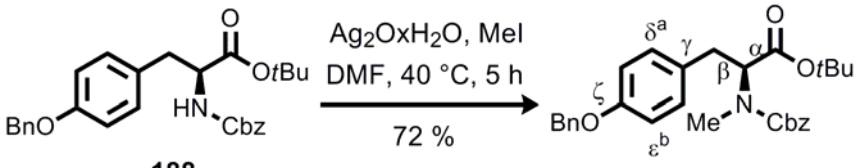

Carbamate (**188**) (11.7 g, 25.4 mmol) was dissolved in dry DMF (510 mL, *c* = 50 mM) and cooled to 0°C. MeI (4.8 mL, 76.3 mmol) was added the solution was allowed to warm to room temperature and stirred for 10 min. Freshly prepared $Ag_2O \times H_2O$ (14 g, 61 mmol) was added and the reaction mixture was heated to 40°C for 5h with stirring (HPLC control). After completion of conversion, the reaction mixture was cooled to room temperature and Et_2O (200 mL) was added. The resulting suspension was filtered over a short pad of celite (2 cm), the filtrate was washed with KCN (100 mL, 0.05 N), H_2O (3 × 100 mL). The organic layer was washed with saturated NaCl solution (100 mL), dried with $MgSO_4$ and concentrated *in vacuo.* The residue was purified by column chromatography (EtOAc/cyclohexane, 1:15→2:8) to afford *N*-methyl carbamate **(189)** (11.6 g, 24.4 mmol, 94% yield) as an colorless oil.

TLC: R_f = 0.65 (EtOAc/Cyclohexane, 2:5).

HPLC: t_R = 13.08 min (Method A).

Optical Rotation: $[\alpha]_D^{20}$ = -31.5 (*c* = 0.81, CH_3OH).

^{1}H-NMR: (400 MHz, DMSO-d_6): δ = 1.36, 1.38* (s, 9H, *t*Bu), 2.70, 2.73 (s, 3H, N-CH_3)*, 2.95 (m, 1H, H_β), 3.08 (m, 1H, H_β), 4.70 (dd, 1H, J_{BX} = 4.9 Hz, J_{AX} = 9.9 Hz, H_α), 5.05 (d, 4H, *J* = 3.8 Hz, Bn-CH_2), 6.93 (m, 2H, Ar-$H_{\delta a,\delta b}$), 7.23 (m, 2H, Ar-$H_{\varepsilon a,\varepsilon b}$), 7.38 (s, 10H, 2 x Bn). *Rotamers are present.

^{13}C-NMR: (100 MHz, DMSO-d_6): δ = 27.5 (*t*Bu-C(**C**H$_3$)$_3$), 31.6 (N-CH$_3$), 33.5 (C$_\beta$), 60.8 (C$_\alpha$), 65.2, 66.1 (Bn-CH$_2$), 69.0 (Bn-CH$_2$), 80.9 (*t*Bu-C$_q$), 114.4 (Tyr-Ar), 126.9, 127.5, 127.6 (Bn-Ar), 128.2, 128.3 (Bn-Ar), 129.6 (Cγ), 129.7 (Bn-Ar), 136.9 (C$_q$), 137.1 (C$_q$), 155.8 (C$_\zeta$), 156.9 (C$_q$), 170.9 (COO*t*Bu).

IR: KBr plate, $\tilde{\nu}$ = 3036 (m), 2985 (m), 1732 (s), 1512 (w), 1334 (m), 1240 (w), 824 (w), 735 (w), 610 cm^{-1} (w) cm^{-1}.

HRMS (EI): For $C_{29}H_{34}NO_5$ (M+H$^+$) calcd. 476.2432, found 476.2428.

(S)-3-(4'-Hydroxy-phenyl)-2-methylamino-propionic acid *tert*-butyl ester (190)

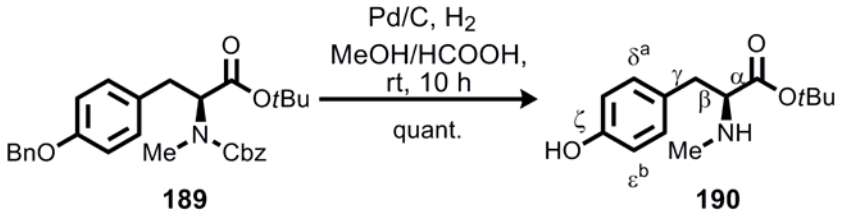

3 % Formic acid in MeOH (250 mL) was treated with active charcoal for 30 min. The charcoal was removed by filtration over a short pad of silica/celite (3:2, 3 cm) under argon compound (**189**) (11.6 g, 24.4 mmol) was dissolved in the activated solvent mixture (244 mL) Pd/C (156 mg, 1.5 mmol, 6 mmol %) was added under argon. The flask was purged with H_2 (1 bar, balloon, 3 x) and suspension was stirred for 10 h under H_2 (1 atm). The slurry was filtered off using a short silica/celite pad (3:2, 3 cm) and the pad was washed with MeOH (50 mL) and EtOAc (50 mL). The solvents were removed *in vacuo* affording compound (**190**) (6 g, 24.4 mmol, quant.) as a foam that could be used in the next step without further purification.

TLC: R_f = 0.27 (CH_3OH/CH_2Cl_2 1:9).

HPLC: t_R = 5.68 min (Method A).

Optical Rotation: $[\alpha]_D^{20}$ = -35.7 (*c* = 0.81, CH_3OH).

^{1}H-NMR: (400 MHz, DMSO-d_6): δ = 1.30 (s, 9H, *t*Bu), 2.27 (s, 3H, N-CH$_3$), 2.68 (1H, J_{AX} = 8.3 Hz, J_{AB} =13.6 Hz, H$_\beta$), 2.78 (dd, 1H, J_{BX} = 6.0 Hz, J_{BA} 13.6 Hz, H$_\beta$), 3.26 (dd, 1H, J_{XB} = 6.0 Hz, J_{XA} = 8.4 Hz, H$_\alpha$), 6.66 (m, 2H, Ar-$H_{\delta a,\delta b}$), 6.96 (m, 2H, Ar-H$_{\varepsilon a,\varepsilon b}$), 8.23 (s, 1H, Ph-OH).

^{13}C-NMR: (100 MHz, DMSO) δ = 27.5 (*t*Bu-C(**C**H$_3$)$_3$), 33.3 (N-CH$_3$), 37.3 (C$_\beta$), 64.4 (C$_\alpha$), 80.3 (*t*Bu-C$_q$), 114.8 (Tyr-Ar), 127.1 (C$_q$), 130.1 (Tyr-Ar), 155.8 (C$_q$), 172.3 (C$_q$).

IR: KBr plate, $\tilde{\nu}$ = 2986 (m), 2358 (w), 1729 (s), 1570 (s), 1250 (s), 879 (m), 842 (m), 544 cm^{-1} (w) cm^{-1}.

HRMS (ESI): For $C_{14}H_{22}O_3N$ (M+H$^+$) calcd. 252.1594, found 252.1594.

(S)-2-[(9*H*-Fluoren-9''-ylmethoxycarbonyl)-methyl-amino]-3-(4'-hydroxy-phenyl)-propionic acid *tert*-butyl ester (129)

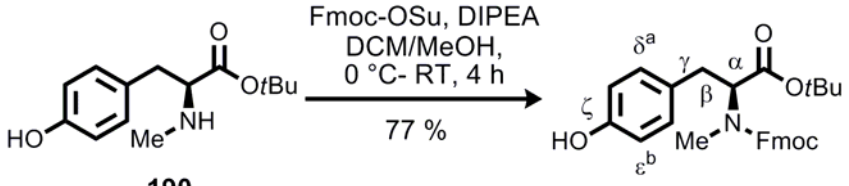

EtN(*i*Pr)$_2$ (4 mL, 24 mmol) was added to a stirred solution of **190** (6.1 g, 24 mmol) in dry CH_2Cl_2/MeOH (123 mL, 7:3) at 0 °C. Fmoc-OSu was dissolved in CH_2Cl_2/MeOH (94:6, 44 mL) and slowly added to the mixture over 90 min. The reaction mixture was stirred for 150 min and during this time slowly warmed to room temperature. H_2O (50 mL) and 1 N HCl (8 mL) were added and the organic solvents were removed *in vacuo*. The residue was extracted with EtOAc/Et_2O (9:1, 200 mL), washed with H_2O (100 mL), saturated $NaHCO_{3(aq.)}$ solution (1 x 100 mL) and saturated $NaCl_{(aq.)}$ solution (100 mL), dried with $MgSO_4$ and concentrated. Purification by column chromatography (80 g, EtOAc/cyclohexane 2:20→2:8) followed by crystalization from EtOAc/cyclohexane (50 mL / 150 mL, 5°C) afforded compound **129** as colorless crystals (8.9 g, 18.8 mmol, 77 %).

TLC: R_f = 0.51 (EtOAc/cyclohexane 5:2).

HPLC: t_R = 11.81 min (method A).

M.p.: 50.8 - 51.3°C.

Optical Rotation: $[\alpha]_D^{20}$ = -23.5, (*c* = 0.79, CH_3OH).

^{1}H-NMR: (400 MHz, DMSO-*d*$_6$): δ = 1.38 (s, 9H, *t*Bu), 2.68 (s, 3H, N-CH$_3$)*, 2.88 (m, 1H, H$_\beta$), 3.03 (dd, 1H, *J* = 5.3 Hz, 14.4 Hz, H$_\beta$), 4.22 (m, 2H, Fmoc-CH$_2$), 4.43 (m, 1H; Fmoc-CH), 4.65 (dd, *J* = 5.3 Hz, 10.8 Hz, H$_\alpha$), 6.62, (m, 2H, Tyr-Ar), 6.75 (d, 2H, J= 8.3, Tyr-Ar), 6.98 (d, 2H, *J* = 8.4 Hz, Tyr-Ar), 7.31 (m, 2H, Fmoc-Ar)

7.41 (m, 2H, Fmoc-Ar), 7.57 (m, 2H, Fmoc-Ar), 7.87 (m, 2H, Fmoc-Ar), 9.81 (s, 1H, Ph-OH). *Rotamers are present.

^{13}C-NMR: (100 MHz, DMSO) δ = 27.5 (*t*Bu-C(**C**H$_3$)$_3$), 31.4 (N-CH$_3$), 46.4 (C$_\beta$), 46.4 (Fmoc-CH), 59.6 (C$_\alpha$), 66.6 (Fmoc-CH$_2$), 80.8 (*t*Bu-C(CH$_3$)$_3$), 114.8, 119.9, 124.6, 126.9, 127.5, 129.4, 129.5 (Ar) (Cγ), 130.1 (Tyr-Ar), 155.8 155.3, 155.6, 170.2 (C$_q$)

IR: KBr plate, $\tilde{\nu}$ = 3380 (m), 2976 (m), 1680 (s), 1516 (s), 1541 (s), 1228 (m), 1153 (m), 1104 (m), 811 (m), 759 (w), 740 (w), 559 cm^{-1} (w) cm^{-1}.

HRMS (ESI): For C$_{29}$H$_{32}$NO$_5$ (M+H$^+$) calcd. 474.2275, found 474.2270.

8.7.3 Tyrosine building block

L-Tyrosine-benzyl ester toluene-4''-sulfonate (157)

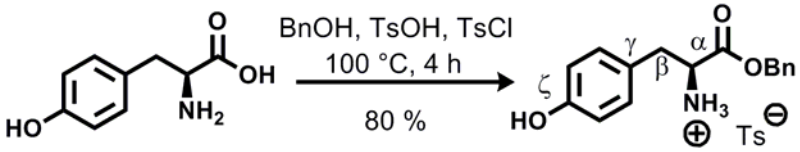

132 157

L-Tyrosine-OH (10 g, 55.2 mmol) was suspended in benzyl alcohol (100 mL). *p*-toluenesulfonic acid (9.4 g, 55.2 mmol) and *p*-toluenesulfonyl chloride (12.7 g, 66.2 mmol) were added and the resulting suspension was stirred at 100 °C for 4 h. The reaction was cooled down to room temperature and volatiles were removed under reduced pressure. The crude product was dissolved in EtOAc (30 mL) and precipitated with diethylether (500 mL). After 16 h, the precipiate was filtered and resuspended in diethylether (200 mL) for 30 min. This suspension was filtered off again, the precipitate was collected and dried under high vacuum to yield benzyl ester salt **157** (19.6 g, 44.4 mmol, 80 %) as a colorless solid.

TLC: R_f = 0.86 ($CHCl_3$/CH_3OH/HCOOH 10:1:0.1).

HPLC: t_R = 5.92 min (Method A).

M.p.: 163.5 °C.

Optical Rotation: $[\alpha]_D^{20}$ = -17.4 (*c* = 0.78, CH_3OH).

^{1}H-NMR: (400 MHz, CD_3OD): δ = 2.36 (s, 3H, Ts-CH_3), 3.09 (dd, 2H, *J* = 2.1, 6.7 Hz, H$_\beta$), 4.26 (m, 1H, H$_\alpha$), 5.22 (q, 2H, *J* = 12.0 Hz, Bn-CH_2), 6.67 – 6.78 (m, 2H, Tyr-Ar), 6.94 – 7.00 (m, 2H, Tyr-Ar),

7.22 (dd, 2H, *J* = 0.7, 8.5 Hz, Ts-Ar), 7.26 – 7.50 (m, 5H, Bn-Ar), 7.66 – 7.79 (m, 2H, Ts-Ar).

^{13}C-NMR: (100 MHz, CD_3OD) δ = 21.5 (Ts-CH_3), 36.8 (Bn-CH_2), 55.5 (C_β) 69.2 (C_α), 80.2 (Bn-CO), 117.0 (Tyr-Ar), 125.6, 127.1 (Ts-Ar), 130.0, 131.7 (Ts-Ar), 136.3 (C_q), 141.9, 143.6 (C_q, Ts-Ar), 158.4 (C_q), 170.1 (Tyr-CO).

IR: KBr plate, $\tilde{\nu}$ = 3110 (s), 1740 (s), 1680 (m), 1500 (s), 1350 (m), 1200 (s), 1120 (m), 820 (m), 761 (m), 550 (m) cm^{-1}.

HRMS (FAB): For $C_{23}H_{24}NSO_5$ ($M+H^+$) calcd. 444.1475, found 474.1480.

(S)-2-Benzyloxycarbonylamino-3-(4'-hydroxy-phenyl)-propionic acid benzyl ester (158)

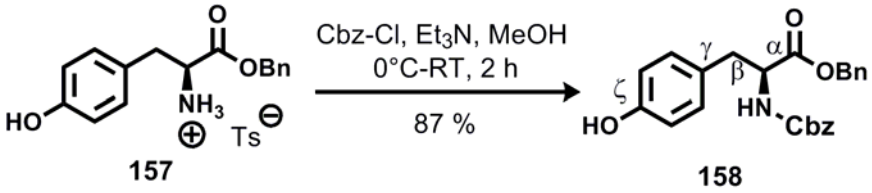

157 158

Ammonium salt **157** (19.6 g, 44.4 mmol) was dissolved in MeOH (150 mL) and cooled to 0 °C. Et_3N (12.4 mL, 88.8 mmol) and benzyl chloroformate (6.34 mL, 44.4 mmol) were respectively added dropwise at 0 °C. The resulting suspension was stirred for 2 h at 0 °C. H_2O was added (50 mL) and MeOH was removed *in vacuo*. The mixture was extracted with diethylether (2 x 150 mL). The combined organic extracts were washed with H_2O (100 mL), saturated $NaHCO_3$ solution (100 mL) and saturated NaCl solution (100 mL), dried with $MgSO_4$ and concentrated. Recrystallization from EtOAc/cyclohexane (50 mL / 150 mL, 2 x o/n) afforded the carbamate **158** as a colorless solid (15.7 g, 38.8 mmol, 87 %).

TLC: R_f = 0.86 (EtOAc/cyclohexane 1:2).

HPLC: t_R = 9.69 min (Method A).

M.p.: 114 °C.

Optical Rotation: $[\alpha]_D^{20}$ = -12.13 (*c* = 0.61, CH_3OH).

^{1}H-NMR: (400 MHz, CD_3OD): δ = 2.91 (dd, 1H, J_{AX} = 8.5 Hz, J_{AB} = 13.9 Hz, H_β), 3.01 (dd, 1H, J_{BX} = 6.0 Hz, J_{AB} = 13.9 Hz, H_β), 4.42 (dd, 1H, J_{XB} = 6.1 Hz, J_{XA} = 8.5 Hz, H_α), 5.01 - 5.11 (m, 4H, Bn-CH_2), 6.71, 7.01 (m, 4H, Tyr-Ar), 7.31 – 7.42 (m, 10H, Bn-Ar).

^{13}C-NMR: (100 MHz, CD_3OD) δ = 37.7 (Bn-CH_2), 57.2 (C_β), 67.8 (C_α), 116.1 (Tyr-Ar), 129.4, 131.1 (Bn-Ar), 136.7 (Cbz-Ar), 157.2 (C_q), 158.4 (C_q), 173.3 (Tyr-CO).

IR: KBr plate, $\tilde{\nu}$ = 3376 (s), 3033 (m), 2955 (m), 1695 (s), 1516 (s), 1454 (m), 1216 (s), 1058 (m), 827 (m), 739 (m), 698 (m) cm^{-1}.

HRMS (FAB): For $C_{24}H_{24}NO_5$ ($M+H^+$) calcd. 406.1639, found 406.1636.

(S)-2-Benzyloxycarbonylamino-3-(4'-methoxy-phenyl)-propionic acid benzyl ester (159)

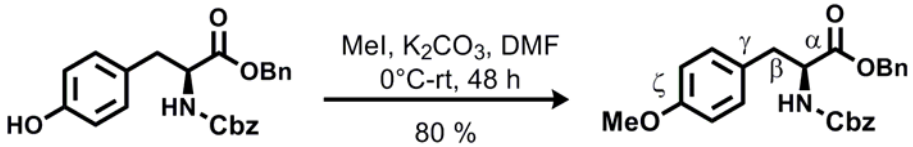

158 159

Phenol (**158**) (9.4 g, 23.2 mmol) was dissolved in DMF (90 mL) and cooled to 0 °C. K_2CO_3 (8.1 g, 58.0 mmol) and MeI (14.4 mL, 232 mmol) were added at 0 °C. The mixture was stirred at room temperature for 48 h. Et_2O (200 mL) was added and the mixture was washed with saturated $NaHCO_3$ solution (3 x 100 mL). The combined aqueous phases were re-extracted with EtOAc (2 x 200 mL). The organic layers were combined, washed with saturated NaCl solution (100 mL), dried with $MgSO_4$, filtered and concentrated. The crude product was purified by flash column chromatography (90 g, EtOAc/cyclohexane 1:3) to provide **159** (7.8 g, 18.6 mmol, 80 %) as a colorless solid.

TLC: R_f = 0.86 ($CHCl_3$/CH_3OH/HCOOH 10:1:0.1).

HPLC: t_R = 10.95 min. (Method A).

M.p.: 56.1 °C.

Optical Rotation: $[\alpha]_D^{20}$ = -15.0 (*c* = 1.0, CH_3OH).

^{1}H-NMR: (400 MHz, CD_3OD): δ = 2.93 (dd, 1H, J_{AX} = 8.6 Hz, J_{AB} = 13.9 Hz, H_β), 3.01 (dd, 1H, J_{BX} = 6.1 Hz, J_{AB} =13.9 Hz, H_β), 3.71 (s, 3H, Tyr-O**C**H_3) 4.42 (m, 1H, H_α), 5.1 (m, 4H, Bn-CH_2), 7.01 (m, 2H, Tyr-Ar), 7.33 (m, 10H, Bn-Ar).

^{13}C-NMR: (100 MHz, CD_3OD) δ = 38.3 (Bn-CH_2), 56.2 (Tyr-O**C**H_3), 57.8 (C_α), 68.4 (C_β), 115.4 (Tyr-Ar), 129.4, 131.1 (Bn-Ar), 136.7

(Cbz-Ar), 157.2 (C_q), 158.4 (C_q), 173.3 (Tyr-CO).

IR: KBr plate, $\tilde{\nu}$ = 3340 (bm), 3033 (bm), 2956 (bm), 1729 (s), 1513 (s), 1249 (m), 1036 (m), 1120 (m), 824 (m), 746 (m), 697 (m), 550 (m) cm^{-1}.

HRMS (FAB): For $C_{25}H_{26}NO_5$ ($M+H^+$) calcd. 420.1805 found 420.1832.

(S)-2-Amino-3-(4'-methoxy-phenyl)-propionic acid (160)

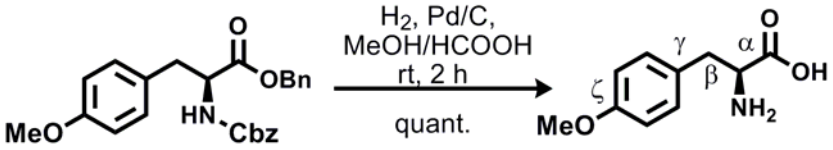

3 % Formic acid in MeOH (244 mL) was stirred with active charcoal for 30 min and the charcoal was filtered over a pad of silica/celite (3:2, 3 cm) under argon. Compound (**159**) (7.8 g, 18.6 mmol) was dissolved in the activated solvent mixture (244 mL) and added to a flask charged with Pd/C (156 mg, 1.5 mmol, 6 mmol %) under argon. A H_2 balloon was added and the reaction was stirred for 2 h under H_2 (1 atm). The slurry was filtered off using a short pad of silica/celite (3:2, 3 cm) eluting with MeOH (50 mL) and EtOAc (50 mL). The organic layer was concentrated *in vacuo* to afford compound **(160)** (3.6 g, 18.6 mmol, quant.) as a foam that could be used without further purification.

TLC: R_f = 0.26 ($CHCl_3$/CH_3OH/HCOOH 10:2:0.1).

HPLC: t_R = 10.95 min. (method A).

Optical Rotation: $[\alpha]_D^{20}$ = -18.0 (*c* = 1, CH_3OH).

^{1}H-NMR: (400 MHz, CD_3OD): δ = 2.92 (dd, 1H, J_{AX} = 8.6 Hz, J_{AB} =13.9 Hz, H_β), 3.01 (dd, 1H, J_{BX} = 6.1, J_{AB} =13.9, H_β), 3.71 (s, 3H, Tyr-O**C**H_3) 4.42 (m, 1H, H_α), 7.03 (m, 2H, Tyr-Ar), 7.62 (m, 2H, Tyr-Ar).

^{13}C-NMR: (100 MHz, CD_3OD): δ = 38.3 (Bn-CH_2), 56.2 (Tyr-O**C**H_3), 57.8 (C_α), 68.4 (C_β), 116.1 (Tyr-Ar), 157.2 (C_q), 158.4 (C_q), 173.3 (Tyr-CO).

IR: KBr plate, $\tilde{\nu}$ = 2956 (bm), 2352 (bw), 1714 (s), 1513 (s), 1249 (m), 1036 (m), 832 (m), 759 (m), 740 (m), 540 (m) cm^{-1}.

HRMS (FAB): For $C_{10}H_{14}NO_3$ ($M+H^+$) calcd. 196.0895, found 196.0899.

(S)-2-(9''*H*-Fluoren-9''-ylmethoxycarbonylamino)-3-(4'-methoxy-phenyl)-propionic acid (161)

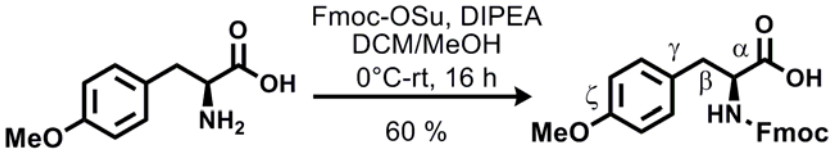

160 **161**

Amino acid (**160**) (3 g, 15.4 mmol) was dissolved in CH_2Cl_2/MeOH (1:1, 45 mL) and cooled to 0°C. EtN(*i*Pr)$_2$ (5.1 mL, 31 mmol) was added. Fmoc-OSu (6.1 mg, 18 mmol) was dissolved in CH_2Cl_2/MeOH (1:1, 45 mL) and slowly added to the reaction mixture over 1h at 0°C. The suspension was stirred for 16 h at 20°C. EtOAc/H_2O (1:1, 200 mL) was added, pH was adjusted to pH 2 with HCl (0.1 N) and the mixture was extracted with EtOAc (100 mL) and washed with saturated $NaHCO_{3(aq.)}$ solution (1 x 100 mL). The aqueous layer was re-extracted with EtOAc (2 x 200 mL), the combined organic extracts were washed with saturated NaCl solution (100 mL) and dried with $MgSO_4$. Recrystalization from EtOAc/cyclohexane (20 mL/150 mL, 40 °C, 2 x 16h) was afforded carbamate **161** as a colorless solid (5.2 g, 11.4 mmol, 60 %).

TLC:	R_f = 0.86 ($CHCl_3$/CH_3OH/HCOOH 10:1:0.1).
HPLC:	t_R = 9.81 min (method A).
M.p.:	142.4 °C.
Optical Rotation:	$[\alpha]_D^{20°C}$ = -26.0 (*c* = 0.78, CH_3OH).
^{1}H-NMR:	(400 MHz, CD_3OD): δ = 2.81 (m, 1H, H_β), 3.01 (dd, 1H, J_{BX} = 4.4 Hz, J_{AB} = 13.8 Hz, H_β), 3.71 (s, 3H, Tyr-OCH_3) 4.43 (m, 4H, H_α and Fmoc-CH_2 and Fmoc-CH), 6.82 (d, 2H, *J* = 8.61 Hz, Tyr-Ar), 7.22 (d, 2H, *J* = 8.6 Hz, Tyr-Ar), 7.25 - 7.37 (m, 2H, Fmoc-Ar), 7.37 - 7.47 (m, 2H, Fmoc-Ar), 7.62 - 7.72 (m, 2H, Fmoc-Ar), 7.80 - 7.93 (d, 2H, Fmoc-Ar), 12.67 (s, 1H, COOH).
^{13}C-NMR:	(100 MHz, CD_3OD) δ = 37.6 (C_β), 55.4 (Tyr-OCH_3), 56.7 (C_α), 68.4 (C_β), 114.7 (Tyr-Ar), 120.7, 126.0, 127.9, 128.5 (Fmoc-Ar), 131.1 (Tyr-Ar), 142.3, 131.1 (Fmoc-Ar), 158.1 (C_q), 159.3, 160.7 (C_q), 175.0 (Tyr-CO).
IR:	KBr plate, $\tilde{\nu}$ = 3421 (m), 2960 (m), 1790 (s), 1714 (s), 1514 (m), 1248 (m), 1060 (m), 833 (m), 760 (m), 741 (m), 621 (w), 564 (w), 540 (m) cm^{-1}.
HRMS (FAB):	For $C_{25}H_{24}NO_5$ ($M+H^+$) calcd. 418.1649 found 418.1655.

_(S)_-4-(4'-Methoxy-benzyl)-oxazolidine-5-one-3-carboxylic acid 9_H_-fluoren-9''-ylmethyl ester (162)

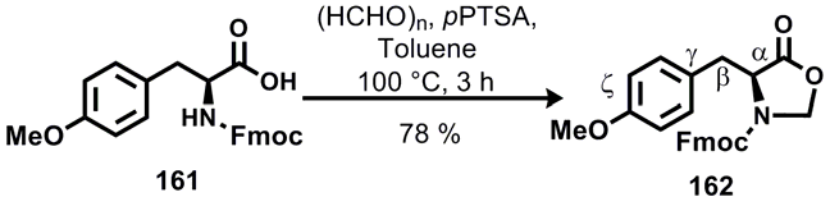

Acid **161** (1.6 g, 3.8 mmol) and *p*PTSA (0.27 g, 1.04 mmol) were suspended in toluene (240 mL). The mixture was dissolved by heating to 120 °C and *para*-formaldehyde (1 g) was added in two portions in 1 hour. The suspension was heated to reflux in a flask coupled to a *Dean-Stark* apparatus for 3 h at 100 °C (TLC control). The solvent was removed *in vacuo,* the residue dissolved in EtOAc (150 mL), washed with saturated $NaHCO_3$ solution (100 mL) and saturated NaCl solution (100 mL). Flash column chromatography (EtOAc/cyclohexane 1:3) gave **162** (1.4 g, 3.2 mmol, 78 %) as a colorless solid.

TLC: R_f = 0.45 (EtOAc/cyclohexane 3:1).

HPLC: t_R = 11.28 min (Method A).

M.p.: 163.5 °C.

Optical Rotation: $[\alpha]_D^{20}$ = +53.3 (*c* = 0.54, CH_3OH).

^{1}H-NMR: (400 MHz, DMSO-d_6): δ = 3.70 (s, 3H, Tyr-OCH_3), 2.16 (s, 1H, H_α), 4.31-4.33 (m, 3H, H_β and oxa-CH_2), 4.53 - 4.73 (m, 2H, Fmoc-CH_2), 5.11 (d, 1H, Fmoc-CH), 6.78 (m, 4H, Tyr-Ar), 7.34 – 7.45 (m, 4H, Fmoc-Ar).

^{13}C-NMR: (100 MHz, CD_3CN): δ = 34.6 (C_β), 47.4 (C_α), 55.1 (Tyr-OCH_3), 56.6 (O-CH_2-N), 78.1 (Fmoc-CH_2), 114.1 (Tyr-Ar), 117.6 (Fmoc-Ar), 120.3 (Fmoc-CH), 125.2 (C_q), 127.5, 127.5, 128.1 (Tyr-Ar), 130.9 (Tyr-Ar), 141.61 (C_q), 141.3 (C_q), 159.2 (C_q), 172.3 (Tyr-CO).

IR: KBr plate, $\tilde{\nu}$ = 2353 (w), 1798 (s), 1715 (s), 1613 (w), 1513 (m), 1418 (m), 1360 (m), 1250 (m), 1129 (m), 830 (w), 760 (w), 742 (m), 570 (w) cm^{-1}.

HRMS (FAB): For $C_{26}H_{24}NO_5$ ($M+H^+$) calcd. 430.1649 found 430.1650.

(S)-2-[(9*H*-Fluoren-9''-ylmethoxycarbonyl)-methyl-amino]-3-(4'-methoxy-phenyl)-propionic acid (162)

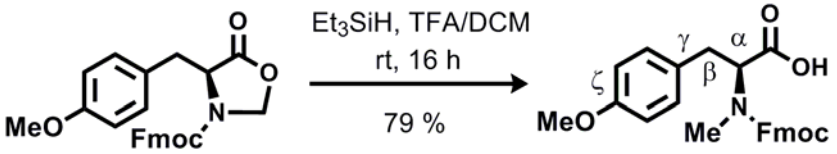

161 126

The oxazolidinone **161** (1.4 g, 3.2 mmol) was dissolved in CH_2Cl_2/TFA (1:1, 100 mL) and Et_3SiH (4.4 g, 27.7 mmol) was added. The suspension was stirred for 16 h at 20°C. After the conversion was complete, the mixture was co-evaporated with toluene (3 x 100 mL). The residue was purified by flash column chromatography (EtOAc/cyclohexane/HCOOH 1:1:0.03) to give acid **126** (1.1 g, 2.5 mmol, 79 %) as a colorless solid.

TLC: R_f = 0.38 ($CHCl_3$/CH_3OH/HCOOH 10:1:0.1).

HPLC: t_R = 10.20 min (Method A).

M.p.: 59.7 °C.

Optical Rotation: $[\alpha]_D^{20}$ = -17.4 (*c* = 0.78, CH_3OH).

^{1}H-NMR: (400 MHz, DMSO): δ = 2.69 (s, 3H, N-CH_3)*, 2.92 - 3.1 (m, 1H, H_β), 3.15 (dd, 1H, J_{BX} = 4.7 Hz, J_{AB} = 14.6 Hz, H_β), 3.67 (s, 3H, Tyr-OCH_3)*, 4.13 – 4.37 (m, 1H, Fmoc-CH_2)*, 4.62 - 4.43 (m, 2H, Fmoc-CH)*, 4.81 (d, 1H, J_{XB} = 4.7 Hz, J_{XA} = 11.3 Hz, H_α), 6.84 - 6.94 (m, 2H, Tyr-Ar), 7.11 (d, 2H, Tyr-Ar), 7.42 (m, 6H, Fmoc-Ar), 7.80 (d, 2H, *J* = 7.5 Hz, Fmoc-Ar). *Rotamers are present.

^{13}C-NMR: (100 MHz, CD_3CN) δ = 34.6 (C_β), 47.4 (C_α), 55.1 (Tyr-OCH_3), 78.1 (Fmoc-CH_2), 114.1 (Tyr-Ar), 117.6 (Fmoc-Ar), 120.3 (Fmoc-CH), 125.2 (C_q), 127.52, 127.53, 128.1 (Tyr-Ar), 130.9 (Tyr-Ar), 141.27 (C_q), 141.61 (C_q), 159.2 (C_q), 172.3 (Tyr-CO).

IR: KBr plate, $\tilde{\nu}$ = 2933 (s), 1755 (s), 1715 (s), 1690 (s), 1115 (s), 1110 (m), 828 (w), 760 (w), 570 (w), 510 (w) cm^{-1}.

HRMS (FAB): For $C_{26}H_{26}NO_5$ ($M+H^+$) calcd. 432.1805 found 432.1822.

8.7.4 Isodityrosine building blocks

(S,S)-3-(3-{4-[2-*tert*-butoxycarbonyl-2-(9*H*-fluoren-9''ylmethoxycarbonylamino)-ethyl]-phenoxy}-4-methoxy-phenyl)-2-(*tert*-butoxycarbonyl-methyl-amino)-propionic acid benzyl ester (125)

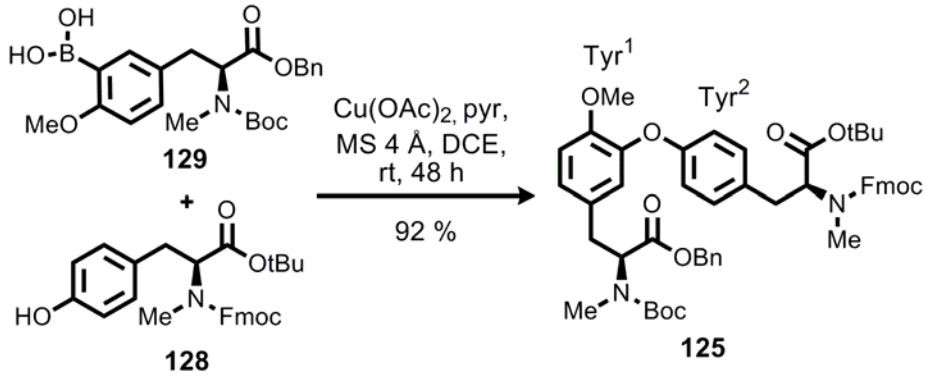

$Cu(OAc)_2$ (11.7 mg, 0.064 mmol, 20 mol %) was suspended in 1,2-dichloroethane (2 mL). Pyridine (130 µL, 1.6 mmol, 5 eq.) was added and the suspension was stirred for 10 min under O_2 (1 atm). Phenol **128** (152 mg, 0.32 mmol) and 4 Å powdered molecular sieves (800 mg) were added. Boronic acid **129** (200 mg, 0.45 mmol, 1.4 eq.) was dissolved in 1,2-dichloroethane (5 ml) and was slowly added to the mixture by syringe pump (300 µL/h). The reaction mixture was then stirred under O_2 (1 atm) for 48 h, diluted with EtOAc, and filtered over a pad of silica. Flash column chromatography (EtOAc/cyclohexane 30:70) gave the *iso*-dityrosine **125** (256 mg, 0.30 mmol, 92 %) as a colorless solid.

TLC: R_f = 0.39 (EtOAc/cyclohexane 5:2).

HPLC: t_R = 15.21 min (Method A).

M.p.: 56-57 °C.

Optical Rotation: $[\alpha]_D^{20}$ = -52.72 (*c* = 0.98, CH_3OH).

^{1}H-NMR: (500 MHz, DMSO-d_6): δ = 1.21 (s, 9H, *t*Bu)*, 1.34 (s, 9H, *t*Bu)*, 2.68 (s, 3H, N-CH_3)*, 2.57 (s, 3H, N-CH_3)*, 2.62 (s, 3H, N-CH_3)*, 2.92 (m, 3H, H_β), 3.12 (m, 2H, H_β), 3.68 (s, 3H, Ph-OMe)*, 4.26 (m, 2H, Fmoc-CH_2), 4.44 (m, 1H; Fmoc-CH), 4.65 (m, 1H, Tyr^1-H_α), 4.74 (m, 1H, Tyr^2-H_α), 5.12 (s, 2H, Bn-CH_2)*,

6.67 (d, 1H, *J* = 8.2 Hz, Tyr[1]-Ar)*, 6.81 (m, 1H, Tyr[1]-Ar), 6.85 (m, 1H, Tyr[2]-Ar), 7.03 (m, 2H, Tyr[2]-Ar), 7.10 (m, 1H, Tyr[1]-Ar), 7.29-7.38 (m, 2H, Fmoc-Ar), 7.56 (d, 2H, *J* = 7.5 Hz, Fmoc-Ar)*, 7.87 (d, 2H, *J* = 7.4 Hz, Fmoc-Ar). *Rotamers are present

^{13}C-NMR: (125 MHz, DMSO-d_6): δ = 27.3, 27.5 (2 x *t*Bu-C(**C**H$_3$)$_3$), 30.1, 31.4 (2 x N-CH$_3$), 33.1 (C$_\beta$), 46.3 (Fmoc-**C**H), 55.5 (Ph-O**C**H$_3$), 59.6 (C$_\alpha$), 60.42 (C$_\alpha$), 65.6 (Fmoc-CH$_2$), 66.5 (Fmoc-CH$_2$), 109.1 (*t*Bu-**C**(CH$_3$)$_3$), 112.2, 113.0 (Tyr-Bn), 115.9 (Tyr-Bn), 119.9 (Fmoc-Ar), 122.1 (Tyr-Ar), 124.2, 125.4, 126.9 (Fmoc-Ar), 127.3 (Tyr-C$_q$), 127.3 (Bn-Ar), 127.9 (Fmoc-**C**H), 128.5 (Bn-Ar), 130.0 (Tyr[1]-C$_\zeta$), 131.1 (Tyr[2]-C$_\zeta$), 141.0 (Bn-**C**H), 143.6 (Fmoc-CH), 143.7 (Tyr[1]-Cγ), 149.8 (Tyr[1]-C$_\zeta$), 155.5 (Fmoc-**C**O), 156.6 (Tyr[2]-Cγ), 156.6 (Boc-**C**O), 156.36 (Tyr[2]-CO), 170.4 (Tyr[1]-C$_q$).

IR: KBr plate, $\tilde{\nu}$ = 2979 (m), 1738 (s), 1697 (s), 1508 (s), 1453 (m), 1267 (m), 1139 (m), 810 (w), 741 (w), 698 (w) cm^{-1}.

HRMS (EI): For $C_{52}H_{58}N_2O_{10}$ (M+H$^+$) calcd. 871.4164, found 871.41672.

(S,S)-3-[3-(4-{2-*tert*-butoxycarbonyl-2-[(9*H*-fluoren-9-ylmethoxycarbonyl)-methyl-amino]-ethyl}-phenoxy)-4-methoxy-phenyl]- *(S)*-2-(*tert*-butoxycarbonyl-methyl-amino)-propionic acid (127)

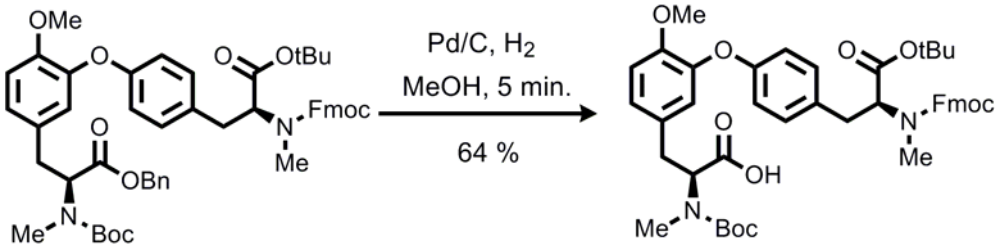

125 **127**

MeOH (20 mL) was stirred with active charcoal (8 g) for 30 min. and subsequently filtered over a pad of silica/celite (3:2, 3 cm) under argon. Ester (**125**) (600 mg, 0.7 mmol) was dissolved in the pretreated MeOH (18 mL) and added under argon to a flask charged with Pd/C (65 mg, 0.07 mmol, 5 wt. %) The flask was purged with H_2 (balloon) and the reaction was stirred for 5 min. under H_2 (1 atm). The slurry was filtered through a short silica/celite pad (3:2, 3 cm) with MeOH (20 mL) and EtOAc (20 mL). The organic layer was concentrated *in vacuo* to afford acid **127** (350 mg, 0.45 mmol, 64 %) as a foam that could be used without further purification.

TLC: R_f = 0.22 ($CHCl_3$/*i*-PrOH/HCOOH 9:1:0.1).

HPLC: t_R = 12.6 min (Method A).

Optical Rotation: $[\alpha]_D^{20}$ = -42.5 (*c* = 0.16, CH_3OH).

^{1}H-NMR: (500 MHz, DMSO-*d*$_6$): δ = 1.19, 1.25 (s, 18 H, 2 x *t*Bu)*, 2.68 (s, 3H, N-CH_3)*, 2.59, 2.62, 2.65 (s, 6H, 2 x N-CH_3)*, 2.92 – 3.30 (m, 4H, 2 x H_β), 3.12 (m, 2H, H_β), 3.62 (s, 3H, Ph-OMe)*, 4.2 (m, 2H, Fmoc-CH_2), 4.3 (m, 1H, Fmoc-CH), 4.41 – 4.52 (m, 1H, Tyr^1-H_α), 4.61 – 4.70 (m, 1H, Tyr^2-H_α), 6.72 (d, 2H, *J* = 10 Hz, Tyr^2-$H_{\varepsilon a,b}$)*, 6.83 – 6.90 (m, 2H, Tyr^1-$H_{\delta a,b}$), 6.93 – 7.15 (m, 3H, Tyr^2- H^δa,b and Tyr^1-H^εa), 7.20 – 7.38 (m, 2H, Fmoc-Ar), 7.34 – 7.44 (m, 2H, Fmoc-Ar), 7.48 – 7.61 (m, 2H, Fmoc-Ar), 6.97 – 7.15 (m, 2H, Fmoc-Ar), 12.73 (COOH). *Rotamers are present.

^{13}C-NMR: (125 MHz, DMSO-*d*$_6$) δ = 27.7, 29.7 (2 x *t*Bu-C(**C**H_3)$_3$), 30.7 (N-CH_3), 31.5 (N-CH_3), 34.1, 33.3, 34.3 (2 x C_β), 46.6 (Fmoc-**C**H_2), 56.5 (Ph-O**C**H_3), 60.7 (Tyr^1-C_α), 60.9 (Tyr^2-C_α), 65.6 (Fmoc-CH), 79.2 (*t*Bu-**C**$(CH_3)_3$), 82.6 (Boc-**C**$(CH_3)_3$), 115.8, 115.9, 116.0 (Tyr^1-$C_{\varepsilon b}$ and Tyr^2-$C_{\varepsilon a,b}$), 120.9 (Fmoc-Ar), 125.6 (Fmoc-Ar), 127.4 (Fmoc-C_q), 127.6 (Tyr^2-C_γ), 125.6, 125.7, 125.85 (Fmoc-Ar), 130.3 (Tyr^1-$C_{\delta a,b}$), 130.5 (Tyr^2-$C_{\delta a,b}$), 131.5 (Tyr^1-C_γ), 141.1, 141.2 (Fmoc-CH), 143.9 (COO-C_q), 155.4 (COO-C_q), 156.1, 156.2 (Tyr^1-$C_{\varepsilon a}$ and Tyr^2-C_ζ), 158.3 (Tyr^1-C_ζ), 171.1, 171.2 (COO-C_q).

IR: KBr plate, $\tilde{\nu}$ = 3430 (w), 2978 (m), 1696 (s), 1511 (s), 1393 (w), 1267 (m), 1143 (m), 973 (w), 859 (w), 807 (w), 662 (w) cm^{-1}.

HRMS (ESI): For $C_{45}H_{53}O_{10}N_2$ ($M+H^+$) calcd. 781.3695, found 781.3696.

_(S,S)_-3-[3-(4-{2-_tert_-butoxycarbonyl-2-[(9_H_-fluoren-9-ylmethoxycarbonyl)-methyl-amino]-ethyl}-phenoxy)-4-methoxy-phenyl]- _(S)_-2-(_tert_-butoxycarbonyl-methyl-amino)-propionic acid benzyl ester (121)

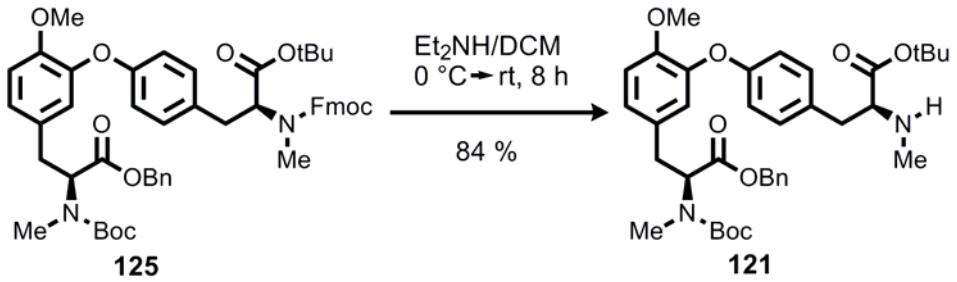

Carbamate (**125**) (800 mg, 0.918 mmol) was dissolved in CH_2Cl_2/Et_2NH (5:3, 160 mL) at 0°C and stirred for 8 h at rt. After the conversion was complete, the mixture was washed with H_2O (60 mL) and NaCl (sat) aqueous solution (20 mL), and was concentrated *in vacuo* at 25 °C. Purification by column chromatography (25 g, PE/EtOAc/Et_2NH, 10:1:0.1→1:1:0.1) afforded amine **121** as a yellow viscous oil, (498 mg, 0.76 mmol, 84 %).

TLC: R_f = 0.15 (PE/EtOAc/Et_2NH 5:1:0.1).

HPLC: t_R = 9.8 min (Method A).

Optical Rotation: $[\alpha]_D^{20}$ = -49.5, *c* = (0.98, CH_3OH).

^{1}H-NMR: (500 MHz, CD_3CN): δ = 1.27, 1.36 (s, 18H, 2 x *t*Bu)*, 2.68 (s, 3H, N-CH_3)*, 2.60, 2.64, 2.66 (s, 6H, 2 x N-CH_3)*, 2.93 – 3.02 (m, 1H, Tyr^1-H_β), 3.10 (dd, 1H, J_{AX} = 8.3 Hz, J_{AB} = 14.1 Hz, Tyr^2-H_β), 3.18 (dd, 1H, J_{BX} = 4.8 Hz, J_{AB} = 14.3 Hz, Tyr^1-H_β), 3.31 (dd, 1H, J_{BX} = 4.9 Hz, J_{AB} = 14.2 Hz, Tyr^2-H_β), 3.72 (s, 3H, Ph-OMe)*, 3.96 (m, 1H, Tyr^2-H_α), 4.59 (m, 0.47H, Tyr^2-H_α) and 4.78 (dd, 0.41H, J_{XB} = 4.8 Hz, J_{XB} = 11.0 Hz Tyr^2-H_α)*, 5.14 (m, 2H, Bn-CH_2), 6.72 (d, 2H, *J* = 10 Hz, Tyr^2-$H_{\varepsilon a,\varepsilon b}$)*, 6.90 (d, 2H, Tyr^2-$H_{\varepsilon a,\varepsilon b}$), 6.87 (s, 3H, Tyr^1-$H_{\varepsilon b}$), 7.01 - 7.04 (m, 2H, Tyr^1- $H_{\delta a,b}$), 7.17 (d, 2H, Tyr^2- $H_{\delta a,b}$), 7.36 (Bn-Ar). *Rotamers are present

^{13}C-NMR: (125 MHz, CD_3CN): δ = 27.3, 27.7 (2 x *t*Bu-C(**C**H_3)$_3$), 32.2 (N-CH_3), 32.6 (N-CH_3), 33.8 (Tyr^1-C_β), 33.84 (Tyr^2-C_β), 34.46 (Tyr^1-C_β), 34.52 (Tyr^2-C_β), 55.8 (Ph-O**C**H_3), 59.9

(*t*Bu-C_q), 60.4 (Tyr^1-C_α), 61.8 (Tyr^1-C_α)*, 62.7 (Tyr^2-C_α), 64.4 (*t*Bu-C_q), 66.76 (Bn-CH_2), 96.6 (Tyr^2-$C_{\varepsilon a,b}$), 107.9 (Tyr^2-$C_{\delta ab}$), 111.2 (Tyr^2-C_γ), 111.7 (Tyr^1-C_γ), 113.5 (Tyr^1-$C_{\delta a\ or\ b}$), 116.7 (Tyr^2-$C_{\varepsilon a,b}$), 122.3 (Tyr^1-$C_{\varepsilon b}$), 126.6 (Tyr^1-$C_{\delta a\ or\ b}$), 130.3 (Tyr^1-$C_{\delta ab}$), 131.4 (Tyr^1-C_ζ), 138.2 (Tyr^2-C_ζ), 147.2 (Bn-CO), 147.4 (*t*Bu-CO), 168.1, 172.1 (COO-C_q).

IR: KBr plate, $\tilde{\nu}$ = 3301 (w), 2976 (m), 1727 (s), 1614 (m), 1516 (m), 1455 (m), 1251 (m), 1153 (s), 981 (w), 845 (m), 550 (w) cm^{-1}.

HRMS (ESI): For $C_{37}H_{49}O_8N_2$ ($M+H^+$) calcd. 649.3483, found 649.3482.

8.7.5 Tetrapeptide preparation on solid support

Cbz-D-alanyl-L-alanyl-*N,O*-dimethyl-L-tyrosinyl-L-alanine (197)

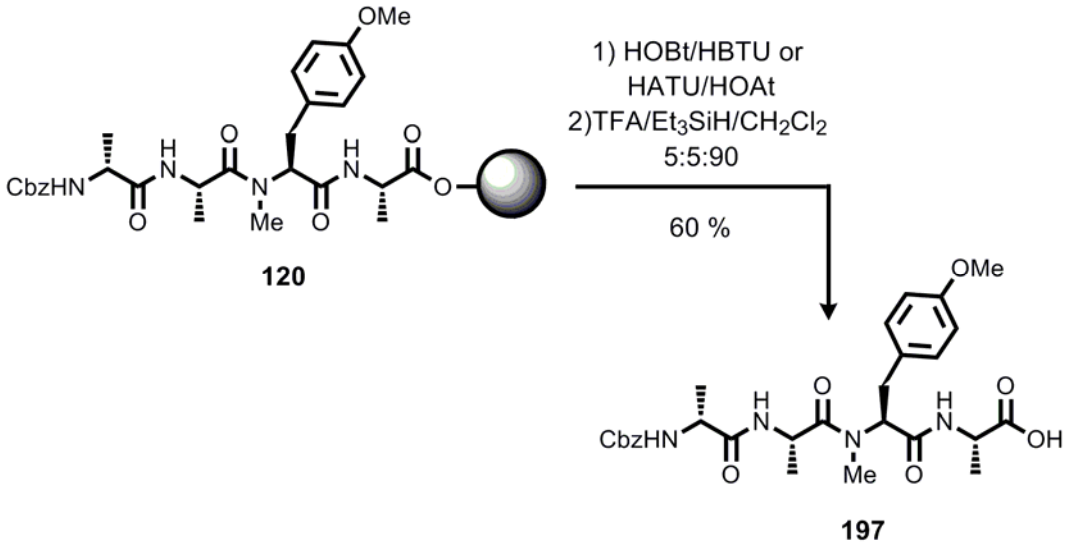

The tetrapeptide was assembled on 2-Cl-Trityl resin loaded with Fmoc-Ala-OH (GP1, 0.426 mmol/g, 1 g, 0.426 mmol). The amino acids were coupled by using Fmoc-NMe-Tyr(OMe)-OH (GP5, 431.17 g/mol, 202 mg, 0.47 mmol), Fmoc-Ala-OH (GP6, 311.33 g/mol, 1.3 g, 1.28 mmol, double coupling), D-Cbz-Ala-OH (GP5, 223.23 g/mol, 285 mg, 1.28 mmol). The tetrapeptide was released from the solid support by the treatment with cleavage solution TFA/Et_3SiH/CH_2Cl_2 (5:5:90, 10 mL/g) in triplicate (5 sec, 5 min, 15 min). The resin was washed with CH_2Cl_2 (2 x 10 mL) and co-evaporated with toluene (50 mL) and concentrated under high vacuum. Purification of

the residue by silica gel column chromatography (100 g, CH_2Cl_2/MeOH/HCOOH (100:0.1:0.1→100:10:0.1)) afforded tetrapeptide **197** as a colorless foam (142 mg, 0.26 mmol, 60 %).

TLC: R_f = 0.24 (CH_2Cl_2/CH_3OH, 5:1).

HPLC: t_R = 7.8 min (Method A).

Optical Rotation: $[\alpha]_D^{20}$ = - 53.4, *c* = (0.65, CH_3OH).

^{1}H-NMR: (500 MHz, CD_3CN): δ = 0.43 (s, 1.42H, Ala^3-CH_3)*, 1.17 (d, 1.46H, *J* = 10.77 Hz, Ala^3-CH_3)*, 1.19 – 1.24 (m, 3H, Ala-CH_3)*, 1.34 (d, 3H, *J* = 7.2 Hz, Ala-CH_3)*, 2.77 and 2.83 (s, 3H, N-CH_3), 2.86 – 3.03 (m, 1H, Tyr-H^{β}), 3.10 (ddd, 1H, *J* = 4.7 Hz, *J* = 14.7 Hz, *J* = 17.9 Hz, Tyr-H^{β}), 3.73 (s, 3H, Ph-OMe)*, 3.98 – 4.16 (m, 1H, Ala-H_{α}), 4.23 – 4.40 (m, 1H, Ala^3-H_{α}), 4.55 – 4.72 (m, 1H, Ala-H_{α}), 4.79 – 4.96 (m, 1H, Tyr-H_{α}), 5.05 (m, 2H, Bn-CH_2)*, 5.96 (s, 1H, NH), 6.83 (d, 2H, *J* = 8.7 Hz, Tyr-Ar)*, 6.97 (s, 1H, NH), 7.05 (s, 1H, NH), 7.12 (d, 2H, *J* = 9.1, Tyr-Ar)*, 7.34 (m, 5H, Bn-Ar). *Rotamers are present.

^{13}C-NMR: (125 MHz, CD_3CN): δ = 16.1 (Ala-CH_3)*, 16.9 (Ala-CH_3)*, 17.3, 17.9 (Ala-CH_3), 28.7 (N-CH_3), 33.4 (Tyr-C_{β}), 33.4 (Tyr-C_{β}), 44.3 (Ala-C_{α}), 45.6 (Ala-C_{α}), 51.5 (Ala-C_{α}), 55.8 (Ph-OCH_3), 61.6 (Tyr-C_{α}), 67.4 (Bn-CH_2), 113.4 (Tyr-Ar), (Tyr-Ar), 128.2 (Cbz-Ar), 125.9 (Tyr-Ar), 129.9 (Tyr-C_q), 130.4 (Tyr-C_q), 137.5 (Bn-C_q), 156.1 (Bn-CO), 172.7, 173.1, 174.0 (CO).

IR: KBr plate, $\tilde{\nu}$ = 3283 (s), 2976 (s), 1660 (s), 1514 (s), 1455 (s), 1250 (m), 1070 (m), 825 (w), 699 (m), 576 (w) cm^{-1}.

HRMS (ESI): For $C_{28}H_{37}O_4N_8$ ($M+H^+$) calcd. 557.2602, found 557.2606.

8.7.6 Hexapeptide assembly

8.7.6.1 [2 + 4] segment coupling

Cbz-D-alanyl-L-alanyl-*N,O*-dimethyl-L-tyrosinyl-L-alanyl-N-methyl-L-tyrosinyl-tert-butoxycarbonyl-Boc-*N,O*-dimethyl-L-tyrosine-5^4→6^3 ether, benzyl ester (205)

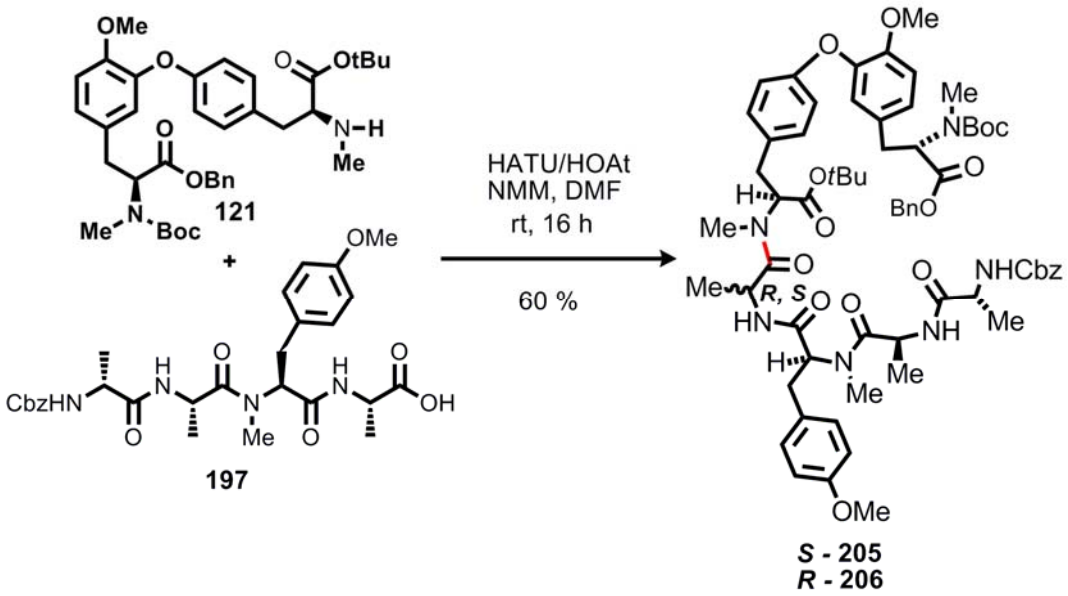

Tetrapaptide (**197**) (237 mg, 0.425 mmol) was dissolved in dry DMF (30 mL) and added to a solution of HATU (266 mg, 0.7 mmol), HOAt (110 mg, 0.81 mmol) and *N*-methylmorpholine (NMM) (154 μL, 1.4 mmol) mixture in DMF (10 mL) at 0°C. The mixture was stirred for 15 min. and biaryl ether (**121**) (230 mg, 0.35 mmol) was slowly added. The solution was stirred at 20°C for 24 h and then concentrated *in vacuo*. The residue was dissolved in EtOAc (50 mL), washed with H_2O (30 mL), saturated $NaHCO_{3(aq)}$ solution (30 mL), saturated $NaCl_{(aq)}$ solution (20 mL), dried with $MgSO_4$, filtered and concentrated. Purification by column chromatography (EtOAc/PE/Et_2NH, 1:15:0.1→2:8:0.1) afforded two diastreomeric peptides **205** (*S*) (164 mg, 0.14 mmol, 40 %) and **206** (*R*) (82 mg, 0.07 mmol, 20 %) and unreacted biaryl ether (80 mg, 0.123 mmol) as colorless foam.

TLC: R_f = 0.18 (EtOAc/Cyclohexane/HCOOH 1:1:0.01).
R_f = 0.62 ($CHCl_3$/MeOH 5.1/0.4).

HPLC: t_R = 12.90 min (Method A).

Optical Rotation: $[\alpha]_D^{20}$ = -118, (*c* = 0.2, CH_3OH).

^{1}H-NMR: (600 MHz, CD_3CN): δ = 0.42 (s, 1H, Ala-CH_3)*, 0.92 (s, 1H, Ala-CH_3)*, 1.09 – 1.26 (m, 7H, Ala-CH_3)*, 1.26 and 1.31 (two s, 9H, *t*Bu)*, 1.39 and 1.41 (two s, 9H, *t*Bu)*, 2.61 and 2.62 (s, 3H, N-CH_3)*, 2.75 and 2.76 (s, 3H, N-CH_3)*, 2.82 and 2.83 (s, 3H, N-CH_3)*, 2.87 – 3.07 (m, 4H, 3 x Tyr-H_β), 3.07 – 3.23 (m, 2H, 3 x Tyr-H_β), 3.69 and 3.70 (s, 3H, Ph-OMe)*, 3.72 and 3.73 (s, 3H, Ph-OMe)*, 4.05 (m, 1H, Ala-H_α), 4.56 (m, 1H, Ala-H_α)*, 4.61 (m, 1H, Tyr-H_α), 4.66 (m, 1H, Ala-H_α), 4.73 (m, 1H, Tyr-H_α), 4.85 (m, 1H, Tyr-H_α), 4.98 – 5.25 (m, 4H, 2 x Bn-CH_2)*, 6.71 (d, 2H, *J* = 8.16 Hz, Tyr-Ar)*, 6.75 – 6.88 (m, 3H, Tyr-Ar)*, 6.95 – 7.05 (m, 3H, Tyr-Ar)*, 7.03 – 7.05 (m, 3H, Tyr-Ar)*, 7.21 – 7.46 (m, 10H, Bn-Ar). *Rotamers are present.

^{13}C-NMR: (150 MHz, CD_3CN): δ = 16.1 (Ala-CH_3)*, 16.9 (Ala-CH_3)*, 17.3, 17.9 (Ala-CH_3), 27.3, 27.6 (2 x *t*Bu-C(**C**H_3)$_3$), 28.7 (N-CH_3)*, 29.4 (N-CH_3)*, 31.9 (N-CH_3)*, 32.3 (N-CH_3)*, 33.1 (Tyr-C_β), 33.3 (Tyr-C_β), 33.4 (Tyr-C_β), 34.1 (Tyr-C_β), 44.3 (Ala-C_α), 45.6 (Ala-C_α), 51.5 (Ala-C_α), 55.0 (Ph-OCH_3), 55.6 (Ph-OCH_3), 61.6 (Tyr-C_α), 60.4 (Tyr-C_α), 61.6 (Tyr-C_α), 66.2, 66.6 (Bn-CH_2), 79.8, 81.4 (*t*Bu-C_q), 113.4 (Tyr-Ar), 113.9 (Tyr-Ar), 114.2 (Tyr-Ar), 116.3 (Tyr-Ar), 122.6 (Tyr-Ar), 125.9 (Tyr-Ar), 128.2, 128.3 (Cbz-Ar and Bn-Ar), 125.9 (Tyr-Ar), 129.9 (Tyr-C_q), 130.4 (Tyr-C_q), 157.1, 158.8 (Tyr-C_q), 137.5 (Bn-C_q), 150.6 (Tyr-C_q), 156.1 (Bn-CO), 157.1 (Tyr-C_q), 158.8 (Tyr-C_q), 172.7, 173.1 (CO), 173.4 (*t*Bu-CO).

IR: KBr plate, $\tilde{\nu}$ = 3293 (m), 2935 (m), 1695 (s), 1633 (s), 1511 (s), 1251 (m), 1155 (m), 964 (w), 810 (m), 698 (w), 539 (w) cm^{-1}.

LC-MS(ESI) Method-LCMS-1: t_R = 12.11 min for $C_{65}H_{83}O_{15}N_6$ ($M+H^+$) calcd. 1187.59, found 1187.41.

HRMS (ESI): For $C_{65}H_{83}O_{15}N_6$ ($M+H^+$) calcd. 1187.5910, found 1187.5963.

Cbz-D-alanyl-L-alanyl-*N,O*-dimethyl-L-tyrosinyl-D-alanyl-*N*-methyl-L-tyrosinyl-tert-butoxycarbonyl-Boc-*N,O*-dimethyl-L-tyrosine-5^4→6^3 ether, benzyl ester (206)

TLC: R_f = 0.26 (EtOAc/cyclohexane/HCOOH 1:1:0.01).

HPLC: t_R = 12.75 min (Method A).

Optical Rotation: $[\alpha]_D^{20}$ = -110, (*c* = 0.2, CH_3OH).

^{1}H-NMR: (600 MHz, CD_3CN): δ = 0.41 (s, 2H, Ala-CH_3)*, 0.90 (d, 2H, *J* = 8.2 Hz, Ala-CH_3)*, 1.13 – 1.25 (m, 5H, Ala-CH_3)*, 1.26 and 131 (two s, 9H, *t*Bu)*, 1.41 and 1.42 (two s, 9H, *t*Bu)*, 2.61 and 2.62 (s, 3H, N-CH_3)*, 2.75 and 2.76 (s, 3H, N-CH_3)*, 2.82 and 2.83 (s, 3H, N-CH_3)*, 2.85 – 3.08 (m, 4H, 3 x Tyr-H^β), 3.12 – 3.28 (m, 2H, 3 x Tyr-H^β), 3.69 and 3.70 (s, 3H, Ph-OMe)*, 3.72 and 3.73 (s, 3H, Ph-OMe)*, 4.1 (m, 1H, Ala-H_α), 4.29 (m, 1H, Ala-H_α)*, 4.57 (m, 1H, Tyr-H_α), 4.67 (m, 1H, Ala-H_α), 4.75 (m, 1H, Tyr-H_α), 4.84 (m, 1H, Tyr-H_α), 4.92 – 5.07 (m, 4H, Bn-CH_2)*, 6.13 (s, 1H, NH), 6.36 (s, 1H, NH), 6.71 (d, 2H, *J* = 8.04 Hz, Tyr-Ar)*, 6.74 – 6.88 (m, 3H, Tyr-Ar)*, 6.96 – 7.06 (m, 3H, Tyr-Ar)*, 7.03 – 7.15 (m, 4H, Tyr-Ar)*, 7.24 – 7.41 (m, 10H, Bn-Ar). *Rotamers are present.

^{13}C-NMR: (150 MHz, CD_3CN): δ = 15.9 (Ala-CH_3)*, 16.82 (Ala-CH_3)*, 17.6, 17.2, 18.0 (Ala-CH_3), 27.4, 27.7 (2 x *t*Bu C(**C**H_3)$_3$), 28.7 (N-CH_3)*, 29.1 (N-CH_3)*, 29.4 (N-CH_3)*, 32.6 (N-CH_3)*, 33.4 (N-CH_3)*, 33.1 (Tyr-C_β), 33.3 (Tyr-C_β), 33.4 (Tyr-C_β), 34.1 (Tyr-C_β), 44.2 (Tyr^3-C_α), 45.4 (Ala-C_α), 50.6 (Ala-C_α), 55.0 (Ph-OCH_3), 55.7 (Ph-OCH_3), 60.3 (Tyr-C_α), 60.4 (Tyr-C_α), 61.5 (Ala-C_α), 66.3, 66.5 (Bn-CH_2), 79.9, 81.4 (*t*Bu-C_q), 113.4 (Tyr-Ar), 114.2 (Tyr-Ar), 116.2 (Tyr-Ar), 122.5 (Tyr-Ar), 128.1 (Tyr-Ar), 128.1, 128.2 (Cbz-Ar and Bn-Ar), 130.2 (Tyr-C_q), 131.6 (Tyr-C_q), 137.2 (Bn-C_q), 156.1 (Bn-CO), 157.2 (Tyr-C_q), 159.5 (Tyr-C_q), 172.7, 173.1 (CO), 174.8 (*t*Bu-CO).

IR: KBr plate, $\tilde{\nu}$ = 3283 (s), 2976 (s), 1660 (s), 1514 (s), 1455 (s), 1250 (m), 1070 (m), 825 (w), 699 (m), 576 (w) cm^{-1}.

LC-MS(ESI) Method-LCMS-1: t_R = 11.9 min, for $C_{65}H_{83}O_{15}N_6$ ($M+H^+$) calcd. 1187.59, found 1187.45.

HRMS (ESI): For $C_{65}H_{83}O_{15}N_6$ ($M+H^+$) calcd. 1187.5910, found 1187.5840.

8.7.6.2 Hexapeptide on solid support

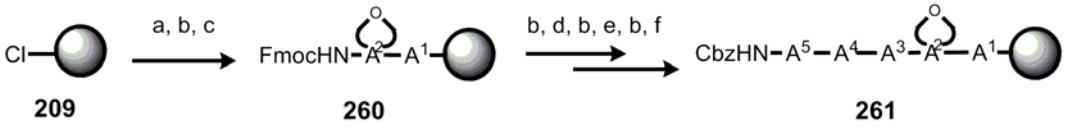

209 260 261

a) Following **GP1**, Fmoc-D-Ala-OH (**A**^{1}) (2,2 g, 7 mmol) was dissolved in dry CH_2Cl_2 and EtN(*i*Pr)$_2$ (2,8 mL, 14 mmol) was added. The reaction was shaken under argon for 16 h. Loading was determined by the Fmoc test. (0.43 mmol/g)

b) In a syringe reactor, resin was swollen in DMF (2 x 10 mL) for 10 min and treated in duplicate (10 sec, 1 min, 15 min) with Fmoc deprotection solution (piperidine/DMF 1:3, 10 mL/g). Deblocked resin was washed with DMF (2 x 10 mL), CH_2Cl_2 (2 x 10 ml) and DMF (2 x 10 ml).

c) Following **GP5**, Biaryl (**A**^{2}) (71 mg, 0.09 mmol) was dissolved in activator solution ((HBTU (85 mg, 0,23 mmol), HOBT (31 mg, 0,23 mmol) in DMF (1 mL)) and subsequently EtN(*i*Pr)$_2$ was added (58 µL, 0.4 mmol).

d) Following **GP6**, Fmoc-L-Ala-OH (**A**^{3}) (84 mg, 0.27 mmol) was dissolved in activator solution (HATU (102 mg, 0.27 mmol), HOAt (37 mg, 0.27 mmol) in DMF (1 mL)) and subsequently EtN(*i*Pr)$_2$ was added (81 µL, 0.5 mmol). This coupling mixture was then added to the resin. (double coupling)

e) Following **GP5**, Fmoc-NMe-Tyr(OMe)-OH (**A**^{4}) (39 mg, 0.09 mmol) was dissolved in activator solution (HBTU (85 mg, 0,23 mmol), HOBT (31 mg, 0,23 mmol) in DMF (1 mL)) and subsequently EtN(*i*Pr)$_2$ was added (58 µL, 0.4 mmol).

f) Following **GP6**, Cbz-Ala-OH (**A**^{5}) (60 mg, 0.27 mmol) was dissolved in activator solution [(HATU (102 mg, 0.27 mmol), HOAt (37 mg, 0.27 mmol) in DMF (1 mL)] and subsequently EtN(*i*Pr)$_2$ was added (81 µL, 0.5 mmol). This coupling mixture was then added to the resin. (double coupling)

Cbz-L-alanyl-*N,O*-dimethyl-L-tyrosinyl-L-alanyl-N-methyl-L-tyrosinyl-*tert*-butoxycarbonyl-Boc-*N,O*-dimethyl-L-tyrosine-4^4→5^3 ether-D-alanine (211)

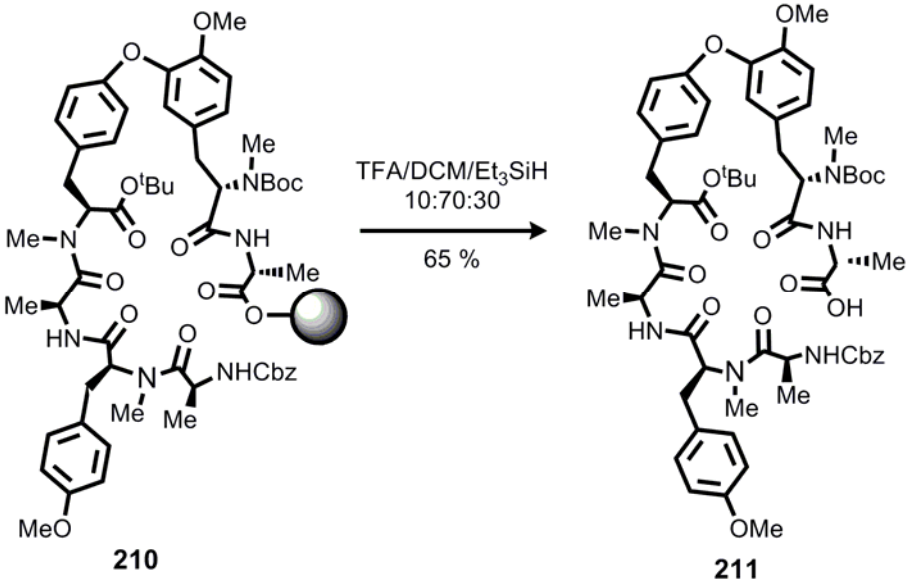

210 **211**

Hexapeptide (0.43 mmol/g) immobilized on solid support **210** was dried under high vacuum overnight and re-swollen with CH_2Cl_2 (3 x 5 min). It was then treated with cleavage solution TFA/Et_3SiH/CH_2Cl_2 (10:20:70, 10 mL/g) three consecutive times (5 s, 5 min, 15 min), and washed with CH_2Cl_2 (2 x 10 mL). The resulting solution was co-evaporated with toluene (50 mL) and dried under high vacuum. The residue was purified by silica gel (25 g) column chromatography using CH_2Cl_2/MeOH/HCOOH as eluent (100:0.1:0.1→100:10:0.1) to afford the desired product **211** as a colorless foam (150 mg, 0.14 mmol, 68 %).

TLC: R_f = 0.23 (CH_2Cl_2/MeOH/HCOOH 9:1:0.1).

HPLC: t_R = 11 min (Method A).

^{1}H-NMR: (500 MHz, DMSO-d_6): δ = 0.5 (s, 1.4H, Ala-CH_3)*, 0.5 (d, 1.4H, *J* = 6.0 Hz Ala-CH_3)*, 1.06 – 1.18 (m, 4H, Ala-CH_3)*, 1.18 and 1.31 (m, 13H, *t*Bu and Ala-CH_3)*, 1.32 and 1.46 (m, 9H, *t*Bu)*, 2.68 and 2.70 (s, 3H, N-CH_3)*, 2.77 and 2.79 (s, 3H, N-CH_3)*, 2.83 and 2.85 (s, 3H, N-CH_3)*, 2.95 – 3.11 (m, 6H, Tyr-H^{β}), 3.59 and 3.76 (s, 6H, 2 x Ph-OMe)*, 4.22 (m, 1H, Ala-H_{α}), 4.41 (m, 1H, Ala-H_{α})*, 4.52 – 4.76 (m, 2H, Ala-H_{α}), 4.76 – 4.81 (m, 1H, Ala-H_{α}), 4.81 – 4.94 (m, 1H, Tyr-H_{α}), 4.93 – 5.08 (m, 4H, Bn-CH_2)*, 6.62 – 6.81 (m, 1H, Tyr-Ar)*, 6.84 (d, 1H, *J* = 8.4 Hz, Tyr-Ar)*, 6.92 (m, 3H, Tyr-Ar)*, 7.01 – 7.15 (m, 5H, Tyr-Ar)*, 7.11 –

7.25 (m, 1H, Tyr-Ar)*, 7.25 – 7.38 (m, 5H, Bn-Ar), 8.53 (d, 1H, *J* = 7.2 Hz, NH), 8.53 (d, 1H, *J* = 7.2 Hz, NH), 12.6 (m, 5H, COOH). *Rotamers are present.

^{13}C-NMR: (125 MHz, DMSO-d_6): δ= 17.1, 20.4 (2 x *t*Bu-C(**C**H$_3$)$_3$), 27.5, 27.6 (2 x *t*Bu-**C**(CH$_3$)$_3$), 29.0 (N-CH$_3$), 30.4 (N-CH$_3$), 31.5 (N-CH$_3$), 32.8, 32.9, 33.6, 33.7, 33.8 (Tyr-C$^{\beta}$), 45.6, 47.147.5 (C$_{\alpha}$), 54.8, 55.8 (Ph-O**C**H$_3$), 45.4, 47.1, 47.5 (C$_{\alpha}$), 60.6, 61.3 (C$_{\alpha}$), 65.7 (Bn-CH$_2$), 78.7, 80.7 (*t*Bu-C$_q$), 113.6, 113.9 (Tyr-Ar), 127.6, 127.8, 128.3 (Tyr-Ar), 128.6 (Cbz-Ar), 129.6, 129.9, 130.3 (Tyr-C$^{\gamma}$), 137.1 (Cbz-CO), 150.9 (Tyr^3-C$_{\zeta}$), 155.2 (Cbz-C$_q$), 157.5 (Tyr^6-C$_{\zeta}$), 157.5 (Cbz-C$_q$), 158.5 (Tyr-C$_{\zeta}$), 172.9 (*t*Bu-CO), 173.9 (Amide-CO).

IR: KBr plate, $\tilde{\nu}$ = 3391 (bs), 2983 (m), 2363 (s), 1681 (s), 1514 (s), 1452 (m), 1267 (m), 1151 (w), 807 (w), 741 (w), 516 (w) cm^{-1}.

MS (MALDI-TOF): For $C_{58}H_{76}O_{15}N_6Na$ (M+Na$^+$) calcd. 1119.53, found 1119.20.

LC-MS(ESI): Method-LCMS-1: t_R= 9.2 min, for $C_{58}H_{77}O_{15}N_6$ (M+H$^+$) calcd. 1097.54, found 1097.05.

HRMS (ESI): For $C_{58}H_{77}O_{15}N_6$ (M+H$^+$) calcd. 1097.5441, found 1097.5454.

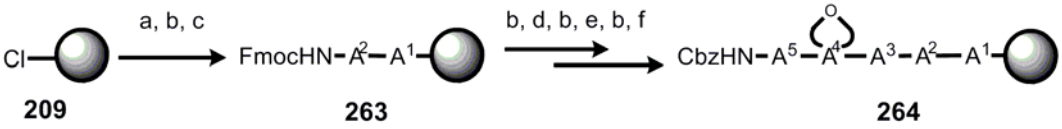

a) Following **GP1**, Fmoc-NMe-Tyr(OMe)-OH (**A^1**) (333 mg, 0.77 mmol, 1.1 eq) was dissolved in dry CH_2Cl_2 and EtN(*i*Pr)$_2$ (2,8 mL, 14 mmol). Loading was determined by the Fmoc test. (0.38 mmol/g).

b) In a syringe reactor, resin was swollen in DMF (2 x 10 mL) for 10 min and treated in duplicate (10 s, 1 min, 15 min) with Fmoc deprotection solution (piperidine/DMF 1:3, 10 mL/g). Deblocked resin was washed with DMF (2 x 10 mL), CH_2Cl_2 (2 x 10 ml) and DMF (2 x 10 ml).

c) Following **GP6**, Fmoc-L-Ala-OH (**A^2**) (75 mg, 0.24 mmol) was dissolved in activator solution (HATU (91 mg, 0.24 mmol), HOAt (33 mg, 0.24 mmol) in DMF (1 mL)) and subsequently EtN(*i*Pr)$_2$ was added (81 µL, 0.5 mmol).

d) Following **GP5**, Fmoc-D-Ala-OH (**A**^{3}) (75 mg, 0.24 mmol) was dissolved in activator solution (HBTU (91 mg, 0.24 mmol), HOBT (33 mg, 0.24 mmol) in DMF (1 mL)) and subsequently EtN(*i*Pr)$_2$ was added (81 µL, 0.5 mmol). This coupling mixture was then added to the resin.

e) Following **GP5**, Biaryl (**A**^{4}) (71 mg, 0.08 mmol) was dissolved in activator solution (HBTU (91 mg, 0.24 mmol), HOBT (33 mg, 0.24 mmol) in DMF (1 mL)) and subsequently EtN(*i*Pr)$_2$ was added (81 µL, 0.5 mmol).

g) Following **GP6**, Cbz-Ala-OH (**A**^{5}) (54 mg, 0.24 mmol) was dissolved in activator solution (HATU (91 mg, 0.24 mmol), HOAt (33 mg, 0.24 mmol) in DMF (1 mL) and subsequently EtN(*i*Pr)$_2$ was added (81 µL, 0.5 mmol).

Cbz-L-alanyl-*N*-methyl-L-tyrosinyl-*tert*-butoxycarbonyl-Boc-*N,O*-dimethyl-L-tyrosine-D-alanyl-L-alanyl-*N,O*-dimethyl-L-tyrosine-2^{4}→3^{3} ether (213)

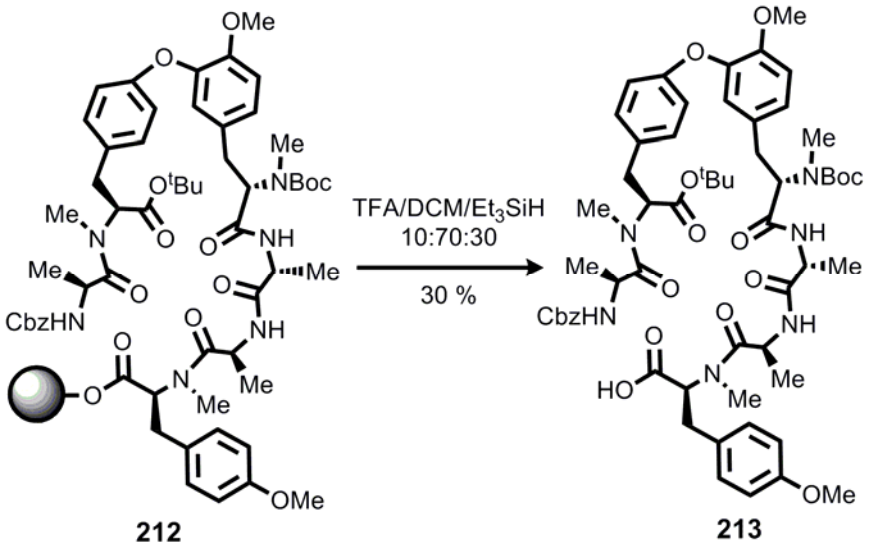

Immobilized hexapeptide (0.38 mml/g) on solid support **212** was dried under high vacuum overnight and re-swollen with CH_2Cl_2 (3 x 5 min.). It was then treated with cleavage solution TFA/Et_3SiH/CH_2Cl_2 (10:20:70, 10 mL/g) three consecutive times (5 s, 5 min, 15 min), and washed with CH_2Cl_2 (2 x 10 mL). The resulted cleavage solution was co-evaporated with toluene (50 mL) and dried under high vacuum. The residue obtained was purified by silica gel (25 g) column chromatography using a

CH_2Cl_2/MeOH/HCOOH eluent (100:0.1:0.1→100:10:0.1) to afford the desired product **213** as a colorless foam (150 mg, 0.14 mmol, 30 %).

TLC:	R_f = 0.25 (CH_2Cl_2/MeOH/HCOOH 9:1:0.1).
HPLC:	t_R = 10.6 min (Method A).
Optical Rotation:	$[\alpha]_D^{20}$ = -118, (*c* = 0.2, CH_3OH).
^{1}H-NMR:	(500 MHz, DMSO-*d*$_6$): δ = 0.44 (s, 0.4H, Ala-CH_3)*, 0.87 (d, 2H, *J* = 6.0 Hz Ala-CH_3)*, 1.06 – 1.18 (m, 4H, Ala-CH_3)*, 1.18 and 1.31 (m, 12H, *t*Bu and Ala-CH_3)*, 1.32 and 1.46 (m, 9H, *t*Bu)*, 2.68 and 2.71 (s, 3H, N-CH_3)*, 2.74 and 2.78 (s, 3H, N-CH_3)*, 2.83 and 2.85 (s, 3H, N-CH_3)*, 2.95 – 3.11 (m, 6H, Tyr-H^{β}), 3.59 and 3.76 (s, 6H, 2 x Ph-OMe)*, 4.22 (m, 1H, Ala-H_{α}), 4.41 (m, 1H, Ala-H_{α})*, 4.52 – 4.76 (m, 2H, Ala-H_{α}), 4.70 (m, 1H, Ala-H_{α}), 4.84 (m, 1H, Tyr-H_{α}), 4.93 – 5.08 (m, 4H, 2 x Bn-CH_2)*, 6.62 – 6.81 (m, 1H, Tyr-Ar)*, 6.84 (d, 1H, *J* = 8.4 Hz, Tyr-Ar)*, 6.92 (m, 3H, Tyr-Ar)*, 7.01 – 7.15 (m, 5H, Tyr-Ar)*, 7.11 – 7.25 (m, 1H, Tyr-Ar)*, 7.25 – 7.38 (m, 5H, Bn-Ar), 8.53 (d, 1H, *J* = 7.2 Hz, NH), 8.53 (d, 1H, *J* = 7.2 Hz, NH), 12.6 (m, 1H, COOH). *Rotamers are present.
^{13}C-NMR:	(125 MHz, $CDCl_3$): δ = 20.2, 22.1 (2 x *t*Bu-C(**C**H_3)$_3$), 28.1, 28.6 (2 x *t*Bu-**C**(CH_3)$_3$), 28.4 (N-CH_3), 31.4 (N-CH_3), 33.5 (N-CH_3), 32.9, 33:1, 33.5, 33.7, 33.9 (Tyr-C^{β}), 47.3 (C_{α}), 56.8 (Ph-O**C**H_3), 47.2, 47.4 (C_{α}), 60.6, 61.3 (C_{α}), 67.7 (Bn-CH_2), 77.7, 77.8 (*t*Bu-C_q), 113.6, 113.9 (Tyr-Ar), 117.6, 121.8, 128.3 (Tyr-Ar), 128.6 (Cbz-Ar), 129.6, 129.9, 130.3 (Tyr-C^{γ}), 137.1 (Cbz-CO), 150.9 (Tyr^3-C^{ζ}), 156.2 (Cbz-C_q), 157.5 (Tyr^6-C^{ζ}), 157.5 (Cbz-C_q), 158.5 (Tyr-C^{ζ}), 172.9 (*t*Bu-CO), 174.9 (Amide-CO).
MS (MALDI-TOF):	For $C_{58}H_{76}O_{15}N_6Na$ ($M+Na^+$) calcd. 1119.5, found 1119.5.
LC-MS(ESI):	Method-LCMS-1: t_R= 10.2, for $C_{58}H_{77}O_{15}N_6$ ($M+H^+$) calcd. 1097.5, found 1097.4.
HRMS (ESI):	For $C_{58}H_{77}O_{15}N_6$ ($M+H^+$) calcd. 1097.5441, found 1097.5448.

8.7.7 Macrolactam formation

Cyclo(Boc-*N,O*-dimethyl-L-tyrosinyl-D-alanyl-L-alanyl-*N,O*-dimethyl-L-tyrosinyl-L-alanyl-*N*-methyl-L-tyrosinyl-*tert*-butyl ester) $5^4 \rightarrow 6^3$ ether (119)

8.7.7.1 Method 1:

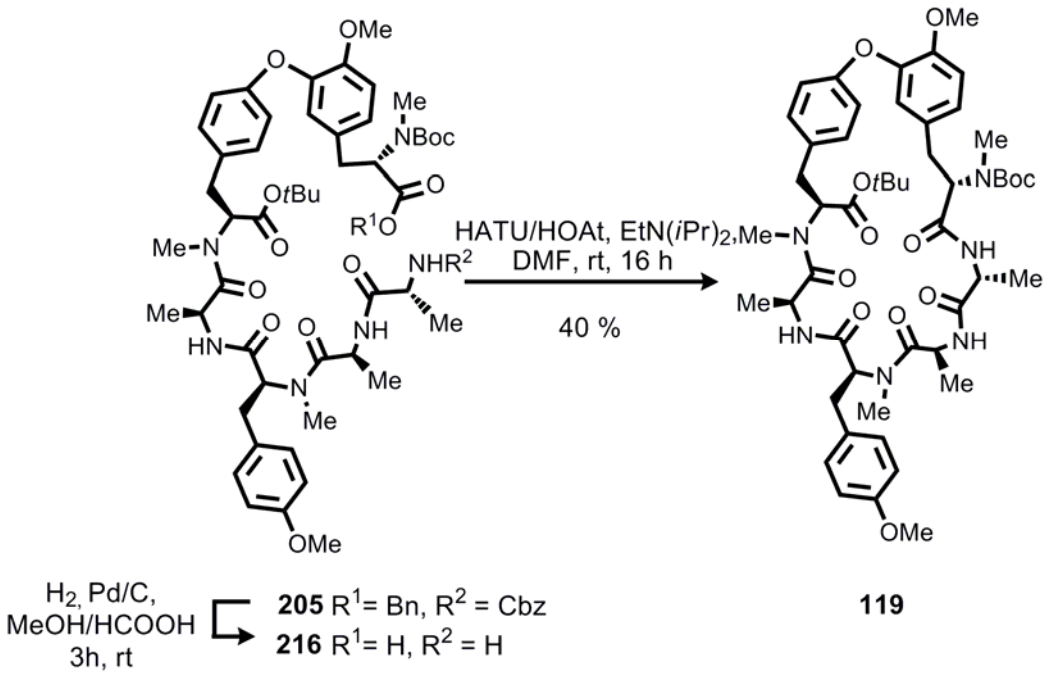

Hexapeptide **205** (33 mg, 0.03 mmol) was hydrogenated folowing **GP9.** The residue was used without further purification to afford **(216)** as white crystals (29 mg, 0.03 mmol, quant.).

TLC: R_f = 0.31 ($CHCl_3$/MeOH 5.1/0.1).

HPLC: t_R = 8.6 min (Method A).

LC-MS(ESI): Method-LCMS-1: t_R= 6.1, For $C_{50}H_{69}O_{13}N_6$ ($M\text{-}H^+$) calcd. 961.5, found 961.3.

MS (MALDI-TOF): For $C_{50}H_{70}O_{13}N_6Na$ ($M+Na^+$) calcd. 985.5, found 985.4.

The crude aminoacid **216** (29 mg, 0.03 mmol) was dissolved in dry DMF (59 mL) added slowly by syringe pump (2.4 mL/h) to a stirred solution of HATU (22.1 mg, 0.06 mmol), HOAt (7.9 mg, 0.06 mmol), EtN(*i*Pr)$_2$ (14 μL, 0.09 mmol) in DMF (39 mL). The mixture was stirred for 48 h and concentrated *in vacuo.* The residue was

dissolved in EtOAc (10 mL), washed with H_2O (5 mL), $NaHCO_3$ (5 mL), and the combined organic layers were washed with saturated $NaCl_{(aq)}$ solution (20 mL) and dried with Na_2SO_4. Purification by flash column chromatography (5 g, MeOH/CH_2Cl_2, 100:1→100:5) afforded the cyclopeptide **119** as a white foam (13.3 mg, 0.01 mmol, 40 %).

TLC:	R_f = 0.42 ($CHCl_3$/MeOH/HCOOH 10:0.8:0.01).
HPLC:	t_R = 10.75 min (Method A), t_R = 14.3 min (Method C).
Optical Rotation:	$[\alpha]_D^{20}$ = -112 (*c* = 0.2, CH_3OH).
^{1}H-NMR:	(600 MHz, $CDCl_3$): δ = 0.34 (s, 1H, Ala-CH_3)*, 0.53 (s, 3H, Ala-CH_3)*, 0.81 (s, 1H, Ala-CH_3)*, 1.15 – 1.24 (m, 4H, Ala-CH_3)*, 1.28 and 1.45 (m, 18H, 2 x *t*Bu)*, 2.62 (s, 3H, Tyr-NCH_3)*, 2.78 – 2.82 (two s, 6H, Tyr-NCH_3)*, 2.85 – 2.96 (m, 3H, Tyr-H_β), 3.08 – 3.34 (m, 3H, Tyr-H_β), 3.68 and 3.71 (two s, 6H, Tyr-OMe)*, 4.27 (m, 1H, Ala-H_α), 4.48 (m, 1H, Ala-H_α), 4.59 (m, 3H, Ala-H_α and Tyr-H_α), 4.89 (m, 1H, Tyr-H_α), 5.23 (m, 1H, Tyr^3-H_α), 6.67 – 6.81 (m, 5H, Tyr-Ar), 6.82 – 6.90 (m, 2H, Tyr^3-Ar)*, 6.93 – 7.06 (m, 4H, Tyr-Ar)*, 8.61 (m, 1H, NH). *Rotamers are present.
^{13}C-NMR:	(150 MHz, $CDCl_3$): δ = 14.6, 16.9, 17.1, 17.9 (3 x Ala-CH_3), 27.4, 28.5 (2 x *t*Bu-C(**C**H_3)$_3$), 29.0 (Tyr-NCH_3), 29.7 (Tyr-NCH_3), 31.4 (Tyr-NCH_3), 33.8 (Tyr-C_β), 34.0 (Tyr-C_β), 33.9 (Tyr-C_β), 45.1 (Tyr-C_α), 45.2 (Ala-C_α), 48.7 (Ala-C_α), 48.9 (Ala-C_α), 55.9 (Ph-OCH_3), 56.5 (Ph-OCH_3), 58.3 (Tyr-C_α), 61.5 (Tyr-C_α), 61.8 (Ala-C_α), 79.6, 81.3 (*t*Bu-C_q), 113.6, 114.0, 114.3, 116.1, 120.2, 123.6 (Tyr-Ar), 129.8, 129.9 130.1, 131.4, 131.8, 156.7, 158.1, 158.4, 159.6 (Tyr-C_q), 172.2, 173.5, 174.4 (Amide-CO).
MS (MALDI-TOF):	For $C_{50}H_{68}O_{12}N_6Na$ ($M+Na^+$) calcd. 967.5, found 967.4.
LC-MS (ESI)	Method-LCMS-1: t_R= 9.3, for $C_{50}H_{68}O_{12}N_6Na$ ($M+Na^+$) calcd. 967.5, found 967.3.
HRMS (ESI):	For $C_{50}H_{69}O_{12}N_6$ ($M+H^+$) calcd. 945.4968, found 945.4979.

8.7.7.2 Method 2:

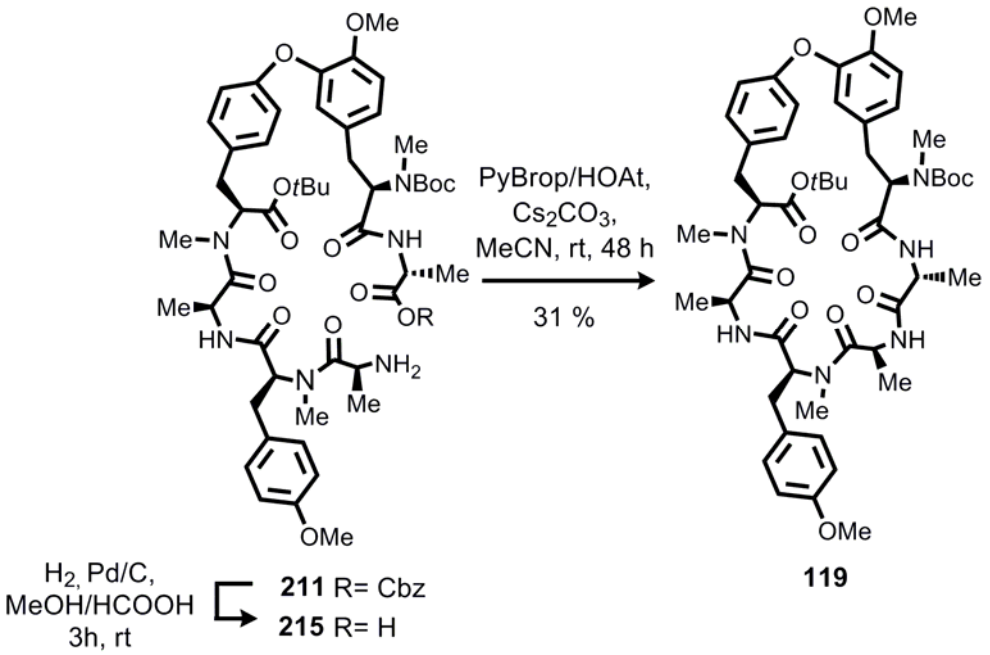

Hexapeptide **211** (20 mg, 0.02 mmol) was hydrogenated following **GP9.** The residue was used without further purification to afford **215** as white crystals (17 mg, 0.02 mmol, quant.).

TLC: R_f = 0.31 ($CHCl_3$/MeOH 5:0.1).

HPLC: t_R = 8.4 min (Method C)

MS (MALDI-TOF): For $C_{50}H_{70}O_{13}N_6Na$ ($M+Na^+$) calcd. 985.49, found 985.01.

LC-MS(ESI): Method-LCMS-1: t_R= 6.1, for $C_{50}H_{71}O_{13}N_6$ ($M+H^+$) calcd. 963.50, found 963.16.

The crude aminoacid **215** (17 mg, 0.02 mmol) was dissolved in dry MeCN (8 mL) and added slowly by syringe pump (200 μL/h) to a stirred suspension of PyBrop (25 mg, 0.05 mmol), HOAt (13 mg, 0.09 mmol) and Cs_2CO_3 (20 mg, 0.11 mmol) in MeCN (14 mL). The mixture was stirred for 48 h then the slurry was filtered through a sinter filter with MeCN (20 mL) and concentrated *in vacuo.* The residue was dissolved in EtOAc (15 mL), washed with H_2O (5 mL), a saturated solution of $NaHCO_3$ (5 mL) and $NaCl_{(aq)}$ (20 mL), dried with Na_2SO_4 and concentrated. Purification with a C4 reversed phase catridge (5 g, H_2O/MeCN/HCOOH, 95:5:0.01→45:55:0.01) afforded the cyclopeptide **119** as a white foam (6 mg, 0.01 mmol, 31 %).

8.7.7.3 Method 3:

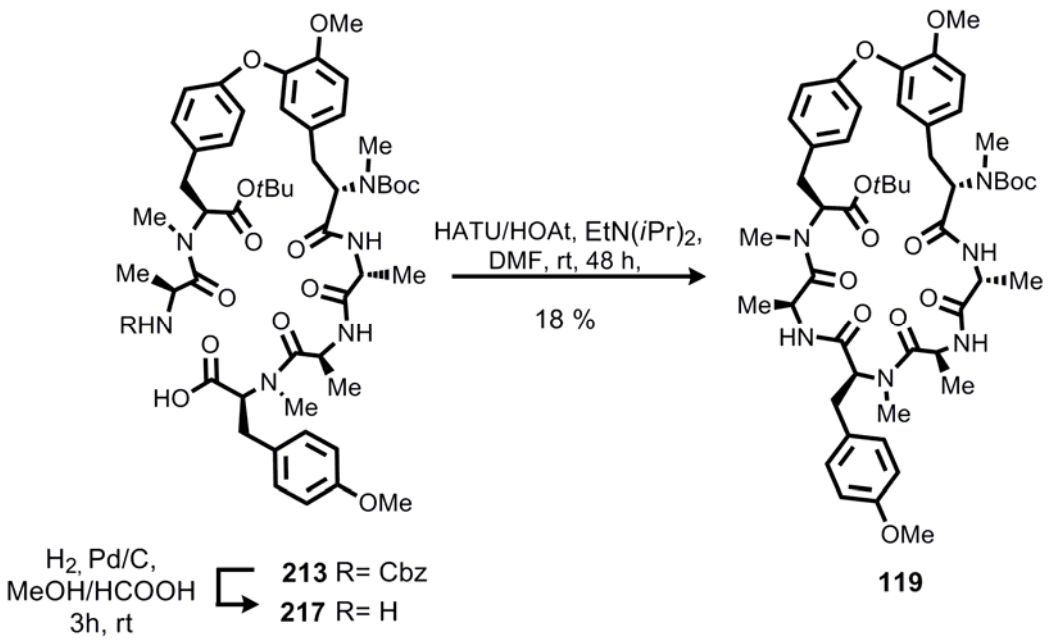

Hexapeptide **213** (20 mg, 0.02 mmol) was hydrogenated folowing **GP9.** The residue was used without further purification to afford **(217)** as white crystals (17 mg, 0.02 mmol, quant.).

TLC:	R_f = 0.31 ($CHCl_3$/MeOH 5.1/0.1).
HPLC:	t_R = 8.6 min (Method C).
LC-MS(ESI):	Method-LCMS-1: t_R= 6.1, for $C_{50}H_{69}O_{13}N_6$ ($M\text{-}H^+$) calcd. 961.5, found 961.4.
MS (MALDI-TOF):	For $C_{50}H_{70}O_{13}N_6Na$ ($M+Na^+$) calcd. 985.5, found 985.2.

217 (hexapeptide) (17 mg, 0.03 mmol) in dry DMF (59 mL) was added slowly by syringe pump (2.4 mL/h) over a solution of HATU/HOAt/EtN(*i*Pr)$_2$ (22.1 mg, 0.06 mmol/ 7.9 mg, 0.06 mmol/ 14 μL, 0.09 mmol) in DMF (14 mL). The mixture was stirred for 48 h and concentrated *in vacuo*. The product was dissolved in EtOAc (10 mL), washed with H_2O (5 mL), $NaHCO_3$ (5 mL), and the combined organic layers were washed with saturated $NaCl_{(aq)}$ solution (20 mL) and dried with Na_2SO_4. Flash column chromatography (5 g, MeOH/CH_2Cl_2, 100:1→100:5) afforded the cyclopeptide **119** as a white foam (5 mg, 0.01 mmol, 18 %).

Cyclo(Boc-*N,O*-dimethyl-L,D-tyrosinyl-D-alanyl-L-alanyl-*N,O*-dimethyl-L-tyrosinyl-D-alanyl-*N*-methyl-L-tyrosinyl-*tert*-butyl ester) $5^4 \rightarrow 6^3$ ether (235)

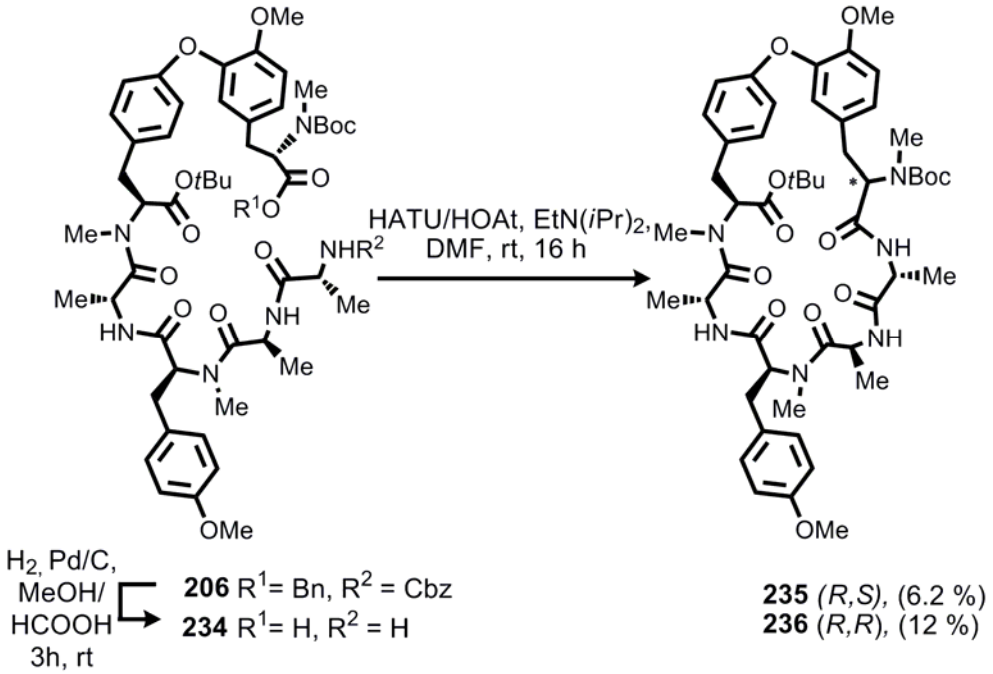

Hexapeptide **206** (34 mg, 0.03 mmol) was hydrogenated folowing **GP9.** The residue was used without further purification to afford **(234)** as white crystals (27 mg, 0.03 mmol, quant.).

TLC: R_f = 0.31 ($CHCl_3$/MeOH 5/0.1).

HPLC: t_R = 8.67 (Method C).

LC-MS (ESI): Method-LCMS-1: t_R= 6.1, for $C_{50}H_{69}O_{13}N_6$ ($M\text{-}H^+$) calcd. 961.5, found 961.4.

MS (MALDI-TOF): For $C_{50}H_{70}O_{13}N_6Na$ ($M+Na^+$) calcd. 985.5, found 985.3.

234 (hexapeptide) (28.1 mg, 0.03 mmol) in dry DMF (29 mL) was added slowly by syringe pump (2.4 mL/h) over a solution of HATU (22.1 mg, 0.06 mmol), HOAt (7.9 mg, 0.06 mmol), EtN(*i*Pr)$_2$ (29 μL, 0.09 mmol) in DMF (29 mL). The mixture was stirred for 5 h and concentrated *in vacuo.* The product was dissolved in EtOAc (10 mL), washed with H_2O (5 mL), $NaHCO_3$ (5 mL), and the combined organic layers were washed with saturated $NaCl_{(aq)}$ solution (20 mL) and dried with Na_2SO_4. Flash column chromatography (5 g, MeOH/CH_2Cl_2, 100:1→100:5) afforded a white foam (10.3 mg, 0.14 mmol, 40 %) as 2 diastreomeric mixture. After purification by reversed phase

preparative HPLC the diastereomers were resolved to give the cyclopeptide **235** (*R,S)* (1.3 mg, mmol, 6.2 %) and cyclopeptide **236** (*R,R)* (2.4 mg, mmol, 12 %) products.

Cyclo(Boc-*N,O*-dimethyl-D-tyrosinyl-D-alanyl-L-alanyl-*N,O*-dimethyl-L-tyrosinyl-D-alanyl-*N*-methyl-L-tyrosinyl-*tert*-butyl ester) $5^4 \rightarrow 6^3$ ether (235)

TLC: R_f = 0.4 ($CHCl_3$/MeOH/HCOOH 10:0.8:0.01).

HPLC: t_R = 11.4 (Method A). t_R = 15.2 min (Method C).

Optical rotation: $[\alpha]_D^{20}$ = -150, (*c* = 1.0, CH_3OH).

^{1}H-NMR: (600 MHz, $CDCl_3$): δ = 0.66 (s, 1.4H, Ala-CH_3)*, 1.17 (d, 2.6H, *J* = 6.7 Hz, Ala-CH_3)*, 1.19 – 1.33 (m, 5H, Ala-CH_3)*, 1.38 and 1.50 (two s, 18H, 2 x *t*Bu)*, 2.44 and 2.45 (s, 3H, Tyr^3-NCH_3)*, 2.64 and 2.71 (s, 3H, Tyr^6-NCH_3)*, 2.76 – 2.87 (m, 2H, Tyr^6-H_β), 2.94 (s, 3H, Tyr^5-NCH_3)*, 3.03 – 3.14 (m, 2H, Tyr-H_β), 3.19 - 3.28 (m, 1H, Tyr^6-H_β), 3.31 (m, 1H, Tyr^3-H_β), 3.45 (m, 1H, Ala^3-H_β), 3.73 and 3.76 (m, 3H, Tyr^3-OMe)*, 3.83 (s, 3H, Tyr^6-OMe)*, 4.25 (m, 1H, Ala^1-H_α), 4.50 (m, 1H, Tyr^5-H_α), 4.65 (m, 1H, Ala^4-H_α), 4.78 (m, 1H, Ala^2-H_α), 4.95 (m, 1H, Tyr^3-H_α), 5.71 (dd, 1H, *J* = 3.5 Hz, *J* = 13.8 Hz, Tyr^6-H_α), 6.42 – 6.62 (m, 1H, Tyr^6-Ar), 6.71 (m, 1H, Tyr^6-Ar), 6.78 (d, 2H, *J* = 8.2 Hz, Tyr^3-Ar)*, 6.87 (m, 1H, Tyr^6-Ar), 6.92 – 6.99 (m, 1H, Tyr^6-Ar)*, 7.01 – 7.11 (m, 4H, Tyr^5-Ar and Tyr^3-Ar)*, 6.78 (d, 2H, *J* = 8.24 Hz, Tyr^3-Ar)*, 8.70 (s, 1H, NH). *Rotamers are present.

^{13}C-NMR: (150 MHz, $CDCl_3$): δ = 16.6, 16.9, 17.8 (3 x Ala-CH_3), 28.1, 28.9 (2 x *t*Bu-C(**C**H_3)$_3$), 29.4 (Tyr^6-C_β), 29.9 (Tyr^3-NCH_3), 30.1 (Tyr^5-NCH_3), 30.7 (Tyr^3-C_β), 33.4 (Tyr^6-C_β), 34.2 (Tyr^5-C_β), 38.4 (Tyr^3-NCH_3), 43.9 (Tyr^3-C_α), 44.6 (Ala^2-C_α), 44.7 (Ala^2-C_α), 48.6 (Ala^1-C_α), 54.9 (Ph-OCH_3), 55.9 (Ph-OCH_3), 56.3 (Tyr^6-C_α), 60.2 (Tyr^5-C_α), 67.9 (Ala^3-C_α), 81.0, 82.5 (*t*Bu-C_q), 114.0 (Tyr^2-C^εa,b), 112.7 (Tyr^6-Ar), 113.7 (Tyr^3-Ar), 116.4 (Tyr^6-Ar), 129.9 (Tyr^5-Ar), 131.5 (Tyr^5-C_q), 132.0 (Tyr^3-C_q), 171.1, 171.6 (Amide-CO).

IR: KBr plate, $\tilde{\nu}$ = 3289 (m), 2835 (m), 1705 (s), 1643 (w), 1633 (s), 1513 (w), 1251 (m), 1155 (m), 964 (w), 810 (m), 696 (w), 539 (w), 522 (w) cm^{-1}.

MS (MALDI-TOF): For $C_{50}H_{68}O_{12}N_6Na$ ($M+Na^+$) calcd. 967.5, found 967.4.

LC-MS(ESI) Method-LCMS-1: t_R= 9.5, for $C_{50}H_{72}O_{12}N_7$ ($M+NH_4^+$) calcd. 962.5, found 962.7.

HRMS (ESI): For $C_{50}H_{70}O_{13}N_6$ ($M+H^+$) calcd. 945.4968, found 945.4978.

Cyclo(Boc-*N,O*-dimethyl-L-tyrosinyl-D-alanyl-L-alanyl-*N,O*-dimethyl-L-tyrosinyl-D-alanyl-*N*-methyl-L-tyrosinyl-*tert*-butyl ester) $5^4 \rightarrow 6^3$ ether (236)

TLC: R_f = 0.4 ($CHCl_3$/MeOH/HCOOH 10:0.8:0.01).

HPLC: t_R = 10.96 (method A), t_R = 14.2 min (method C).

Optical Rotation: $[\alpha]_D^{20°C}$ = -118, (*c* = 1, CH_3OH).

^{1}H-NMR: (600 MHz, $CDCl_3$): δ = 0.40 (s, 1.4H, Ala-CH_3)*, 0.87 (s, 3H, Ala-CH_3)*, 1.29 (m, 5H, Ala-CH_3)*, 1.23 and 1.48 (two s, 18H, *t*Bu)*, 2.65 (s, 3H, Tyr-NCH_3)*, 2.77 (m, 2H, Tyr-H_β), 2.81 (s, 3H, Tyr-NCH_3)*, 3.09 (s, 3H, Tyr-NCH_3)*, 2.92 – 3.03 (m, 1H, Tyr-H_β), 3.16 - 3.33 (m, 1H, Tyr^6-H_β), 3.31 (m, 1H, Tyr^3-H_β), 3.45 (m, 1H, Ala^3-H_β), 3.71, 3.73, 3.75 (three s, 3H, Tyr^3-OMe)*, 3.81, 3.84, 3.87 (three s, 3H, Tyr^6-OMe)*, 4.23 (m, 1H, Ala^1-H_α), 4.48 (m, 1H, Tyr^5-H_α), 4.60 (m, 1H, Ala^4-H_α), 4.80 (m, 1H, Ala^2-H_α), 5.33 (m, 1H, Tyr^3-H_α), 5.47 (m, 1H, Tyr^6-H_α), 6.62 (m, 1H, Tyr-Ar), 6.80 (m, 3H, Tyr-Ar), 6.84 (m, 2H, Tyr-Ar)*, 6.92 – 6.94 (m, 1H, Tyr-Ar), 6.97 – 7.02 (m, 2H, Tyr-Ar)*, 7.03 – 7.16 (m, 2H, Tyr-Ar)*. *Rotamers are present.

^{13}C-NMR: (150 MHz, $CDCl_3$): δ = 14.0, 16.5, 19.6 (3 x Ala-CH_3), 28.3, 29.7, (2 x *t*Bu-C(**C**H_3)$_3$), 29.4 (Tyr-C_β), 29.5 (Tyr^3-NCH_3), 29.9 (Tyr^3-C_β), 30.1 (Tyr^5-NCH_3), 31.2 (Tyr^3-NCH_3), 33.1 (Tyr^6-C_β), 33.8 (Tyr^5-C_β), 43.9 (Tyr^3-C_α), 44.6 (Ala^2-C_α), 45.3 (Ala^2-C_α), 45.5 (Ala^2-C_α), 48.4 (Ala^1-C_α), 54.9 (Ph-OCH_3), 55.9 (Ph-OCH_3), 56.3 (Tyr^6-C_α), 60.2 (Tyr^5-C_α), 62.7 (Ala^3-C_α), 80.6, 82.8 (*t*Bu-C_q), 112.5 (Tyr^6-Ar), 114.5 (Tyr^2-C^εa,b), 115.8 (Tyr^3-Ar), 130.1 (Tyr^6-Ar), 130.3 (Tyr^5-Ar), 147.0, 158.7, 158.9 (Tyr-C_q).

IR: KBr plate, $\tilde{\nu}$ = 3293 (m), 2935 (m), 1695 (s), 1633 (s), 1511 (s), 1251 (m), 1155 (m), 964 (w), 810 (m), 698 (w), 539 (w) cm^{-1}.

MS (MALDI-TOF): For $C_{50}H_{68}O_{12}N_6Na$ ($M+Na^+$) calcd. 967.5, found 967.4.

LC-MS(ESI) Method-LCMS-1: t_R= 9.6, for $C_{50}H_{72}O_{12}N_7$ ($M+NH_4^+$) calcd. 962.5, found 962.7.

HRMS (ESI): For $C_{50}H_{70}O_{13}N_6$ ($M+H^+$) calcd. 945.4968, found 945.4978.

8.7.8 Transannular macrolactamization reactions

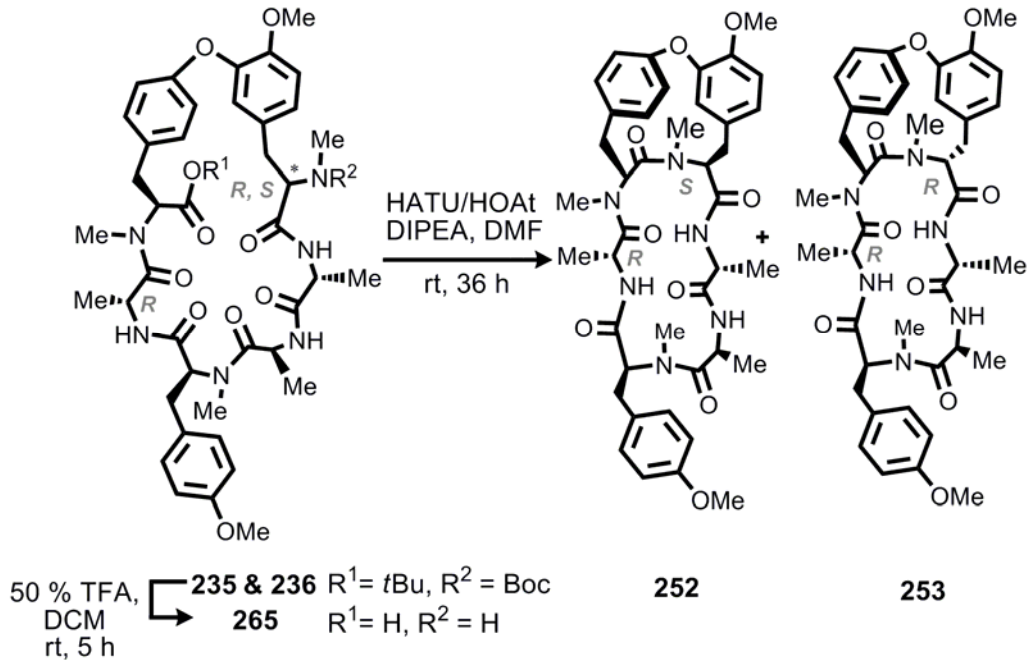

Mixture of diastereomers **235** and **236** (7.4 mg, 8 μmol) was dissolved in CH_2Cl_2/TFA (2:1, 3 mL) and was stirred for 2 h under argon. The reaction mixture was co-evaporated with toluene and the crude aminoacid product (**265**) was obtained as a colorless powder (7 mg, 8 μmol, quant.) and carried to the next step without purification.

TLC: R_f = 0.18 (*R,S*), R_f = 0.21 (*R,R*) (CH_2Cl_2/MeOH/HCOOH 10:1:0.1).

HPLC: t_R = 5.8 min (*R,R),* t_R = 6.1 min *(R,S)* (method A)

LC-MS(ESI): Method-LCMS-1: t_R= 6.5, 7.3, for $C_{41}H_{53}O_{10}N_6$ ($M+H^+$) calcd. 789.4, found 789.4.

MS (MALDI-TOF): For $C_{41}H_{53}O_{10}N_6$ ($M+H^+$) calcd. 789.4, found 789.3.

Aminoacid as diastereomeric mixtures **265** (7 mg, 0.009 mmol) in dry DMF (10 mL) was slowly added by syringe pump to a solution of HATU (5.5 mg, 0.013 mmol), HOAt (2.1 mg, 0.013 mmol), EtN(*i*Pr)$_2$ (6 μL, 0.03 mmol) in DMF (5 mL) at rt. The mixture

was stirred for 36 h and concentrated *in vacuo.* The residue was dissolved in EtOAc (10 mL), washed with H_2O (5 mL), saturated $NaHCO_3$ (5 mL), and NaCl solution (5 mL) and dried with Na_2SO_4. The pure diastereoisomeric products were isolated after purification by reversed phase preparative HPLC *R,S* **BB** (0.9 mg, mmol, 13 %) and *R,R* **JJ** (1.1 mg, mmol, 16 %).

Cyclo(Cbz-D-alanyl-L-alanyl-*N,O*-dimethyl-L-tyrosinyl-D-alanyl-*N*-methyl-L-tyrosinyl-*tert*-butoxycarbonyl-Boc-*N,O*-dimethyl-D-tyrosinyl) cyclo $5^4 \rightarrow 6^3$ ether (252)

TLC: R_f = 0.19 (*R,S*) (pentane/CH_2Cl_2/MeOH 6:6:0.1).

HPLC: t_R = 8.2 min *(R,S)* (Method A).

LC-MS(ESI): Method-LCMS-1: t_R= 9.3, For $C_{41}H_{51}O_9N_6$ ($M+H^+$) calcd. 771.4, found 771.2.

HRMS (ESI): For $C_{41}H_{51}O_9N_6$ ($M+H^+$) calcd. 771.3712, found 771.3702.

Cyclo(Cbz-D-alanyl-L-alanyl-*N,O*-dimethyl-L-tyrosinyl-D-alanyl-*N*-methyl-L-tyrosinyl-*tert*-butoxycarbonyl-Boc-*N,O*-dimethyl-D-tyrosinyl) cyclo $5^4 \rightarrow 6^3$ ether (252)

TLC: R_f = 0.19 (*R,R*) (pentane/CH_2Cl_2/MeOH 6:6:0.1).

HPLC: t_R = 7.7 min (*R,R),* (Method A).

LC-MS (ESI): Method-LCMS-1: t_R= 8.3, For $C_{41}H_{51}O_9N_6$ ($M+H^+$) calcd. 771.4, found 771.3.

HRMS (ESI): For $C_{41}H_{51}O_9N_6$ ($M+H^+$) calcd. 771.3712, found 771.3705.

8.7.9 Byproducts by transannular macrolactamization reactions

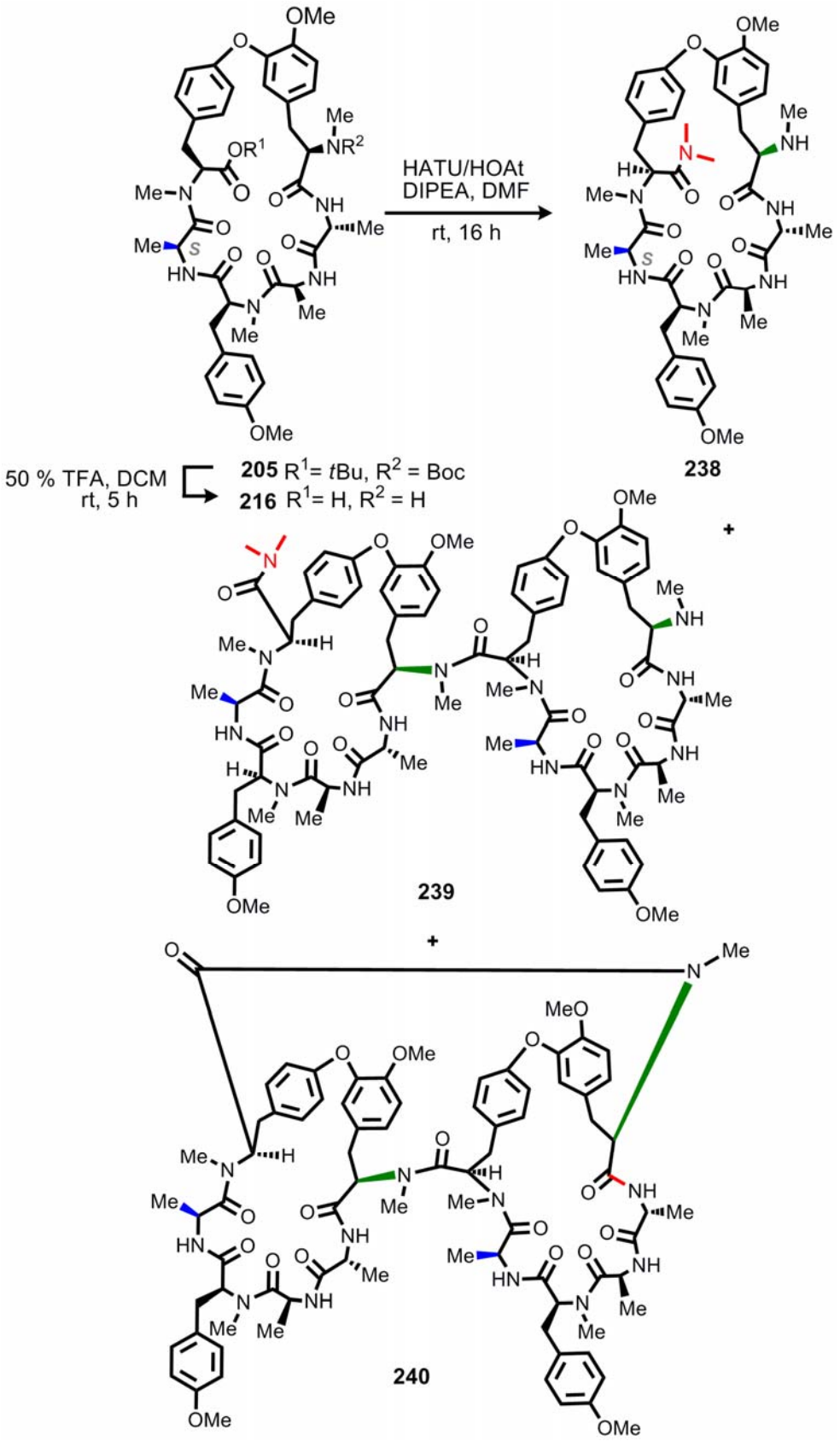

Cyclic hexapeptide **(205)** (5 mg, 5.3 μmol) was dissolved in CH_2Cl_2/TFA (2:1, 3 mL) and stirred for 2 h under argon. The reaction mixture was co-evaporated with toluene and the crude amino acid was obtained as a white foam **216** (4.3 mg, 5.3 μmol, quant.) without further purification.

1

TLC: R_f = 0.18 (*R,S*), R_f = 0.21 (*R,R*) (CH_2Cl_2/MeOH/HCOOH 10:1:0.1).

HPLC: t_R = 5.8 min (*R,R),* t_R = 6.1 min *(R,S)* (Method A).

LC-MS(ESI): For $C_{41}H_{53}O_{10}N_6$ ($M+H^+$) calcd. 789.4, found 789.4.

MS (MALDI-TOF): For $C_{41}H_{53}O_{10}N_6$ ($M+H^+$) calcd. 789.4, found 789.3.

216 (3 mg, 0.004 mmol) in dry DMF (5mL) was slowly added by syringe pump to a solution of HATU (2.3 mg, 0.013 mmol), HOAt (1.8 mg, 0.013 mmol), EtN(*i*Pr)$_2$ (4 μL, 0.03 mmol) in DMF (5 mL) at rt. The mixture was stirred for 36 h, concentrated *in vacuo* and the residue was dissolved in EtOAc (5 mL), washed with H_2O (3 mL), $NaHCO_3$ (3 mL). The combined organic layer was washed with saturated $NaCl_{(aq)}$ solution (3 mL), dried with Na_2SO_4 and concentrated. Purification by reversed phase preparative HPLC gave amide **238** (0.4 mg, 0.0049 mmol, 12 %) and a mixture of dimers **(239, 240)** (1.2 mg).

Cyclo(*N,O*-dimethyl-L,D-tyrosinyl-D-alanyl-L-alanyl-*N,O*-dimethyl-L-tyrosinyl-D-alanyl-*N*-methyl-L-tyrosine-dimethyl amide) $6^4 \rightarrow 1^3$ ether (238)

TLC: R_f = 0.19 (pentane/CH_2Cl_2/MeOH 6:6:0.1).

HPLC: t_R = 7.9 min, (method A).

LC-MS(ESI): Method-LCMS-1: t_R= 8.7, For $C_{43}H_{58}O_9N_7$ ($M+H^+$) calcd. 816.4, found 816.4.

HRMS (ESI): For $C_{43}H_{58}O_9N_7$ ($M+H^+$) calcd. 816.4296, found 816.4295.

Biscyclo(*N,O*-dimethyl-L,D-tyrosinyl-D-alanyl-L-alanyl-*N,O*-dimethyl-L-tyrosinyl-D-alanyl-*N*-methyl-L-tyrosine-dimethyl amide) $6^4 \rightarrow 1^3$ ether (239)

HPLC: t_R = 8.92 min, (Method C).

LC-MS(ESI): Method-LCMS-1: t_R= 9.3, For $C_{84}H_{108}O_{18}N_{13}$ ($M+H^+$) calcd. 1586.8, found 1586.8.

HRMS (ESI): For $C_{84}H_{108}O_{18}N_{13}$ ($M+H^+$) calcd. 1587.8008, found 1587.7983.

Biscyclo(*N,O*-dimethyl-L,D-tyrosinyl-D-alanyl-L-alanyl-*N,O*-dimethyl-L-tyrosinyl-D-alanyl-*N*-methyl-L-tyrosine-dimethyl amide) cyclo 6→1', 6^4→1^3 ether (240)

HPLC:	t_R = 8.95 min, (Method C).
LC-MS(ESI):	Method-LCMS-1: t_R= 9.3, for $C_{82}H_{101}O_{18}N_{12}$ ($M+H^+$) calcd. 1541.7, found 1541.3.
HRMS (ESI):	For $C_{82}H_{101}O_{18}N_{12}$ ($M+H^+$) calcd. 1541.7357, found 1541.7983.

9. References

(1) Li, J. W. H.; Vederas, J. C. *Science* **2009**, *325*, 161-165.

(2) Breinbauer, R.; R. Vetter, I.; Waldmann, H. *Angew. Chem. Int. Ed.* **2002**, *41*, 2878-2890; *Angew. Chem.* **2002**, *114*, 3002-3015.

(3) Koch, M. A.; Waldmann, H. *Drug Discov. Today* **2005**, *10*, 471-483.

(4) Pearson, A. J.; Chelliah, M. V. *J. Org. Chem.* **1998**, *63*, 3087-3098.

(5) Itokawa, H.; Takeya, K.; Hitotsuyanagi, Y.; Morita, H. *Mol. Biol. Biochem. Biophys.* **2000**, *4*, 213-222.

(6) Kohli, R. M.; Walsh, C. T.; Burkart, M. D. *Nature* **2002**, *418*, 658-661.

(7) Davies, H. M. L.; Sorensen, E. J. *Chem. Soc. Rev.* **2009**, *38*, 2981-2982.

(8) Fürstner, A.; Kirk, D.; Fenster, M. D. B.; Aissa, C.; De Souza, D.; Müller, O. *Proc. Natl. Acad. Sci. U. S. A.* **2005**, *102*, 8103-8108.

(9) Borel, J. F.; Feurer, C.; Gubler, H. U.; Stahelin, H. *Agents Actions* **1976**, *6*, 468-475.

(10) Oliva, R.; Falcigno, L.; Auria, G. D.; Saviano, M.; Paolillo, L.; Ansanelli, G.; Zanotti, G. *Biopolymers* **2000**, *53*, 581-595.

(11) Luckett, S.; Garcia, R. S.; Barker, J. J.; Konarev, A. V.; Shewry, P. R.; Clarke, A. R.; Brady, R. L. *J. Mol. Biol.* **1999**, *290*, 525-533.

(12) Catalioto, R. M.; Criscuoli, M.; Cucchi, P.; Giachetti, A.; Giannotti, D.; Giuliani, S.; Lecci, A.; Lippi, A.; Patacchini, R.; Quartara, L.; Renzetti, A. R.; Tramontana, M.; Arcamone, F.; Maggi, C. A. *Br. J. Pharmacol.* **1998**, *123*, 81-91.

(13) Juan , M. B.; Morten, M. *QSAR Comb. Sci.* **2004**, *23*, 117-129.

(14) Sieber, S. A.; Marahiel, M. A. *Chem. Rev.* **2005**, *105*, 715-738.

(15) Bradley , S. M. *Angew. Chem. Int. Ed.* **2008**, *47*, 9386-9388; *Angew. Chem.* **2002**, *120*, 9526-9528.

(16) McIntosh, J. A.; Donia, M. S.; Schmidt, E. W. *Nat. Prod. Rep.* **2009**, *26*, 537-559.

(17) Schmidt, E. W.; Nelson, J. T.; Rasko, D. A.; Sudek, S.; Eisen, J. A.; Haygood, M. G.; Ravel, J. *Proc. Natl. Acad. Sci. U. S. A.* **2005**, *102*, 7315-7320.

(18) Ahrendt, K. A.; Olsen, J. A.; Wakao, M.; Trias, J.; Ellman, J. A. *Bioorg. Med. Chem. Lett.* **2003**, *13*, 1683-1686.

(19) Shin-ya, K.; Wierzba, K.; Matsuo, K.-i.; Ohtani, T.; Yamada, Y.; Furihata, K.; Hayakawa, Y.; Seto, H. *J. Am. Chem. Soc.* **2001**, *123*, 1262-1263.

(20) van Kraaij, C.; de Vos, W. M.; Siezen, R. J.; Kuipers, O. P. *Nat. Prod. Rep.* **1999**, *16*, 12.

(21) Itokawa, H.; Takeya, K.; Mori, N.; Hamanaka, T.; Sonobe, T.; Mihara, K. *Chem. Pharm. Bull.* **1984**, *32*, 284-290.

(22) Itokawa, H.; Saitou, K.; Morita, H.; Takeya, K.; Yamada, K. *Chem. Pharm. Bull.* **1992**, *40*, 2984-2989.

(23) Sirdeshpande, B. V.; Toogood, P. L. *Bioorg. Chem.* **1995**, *23*, 460-470.

(24) Karskela, T.; Virta, P.; Lonnberg, H. *Curr. Org. Synth.* **2006**, *3*, 283-311.

(25) Wakamiya, T.; Ueki, Y.; Shiba, T.; Kido, Y.; Motoki, Y. *Bull. Chem. Soc. Jpn.* **1990**, *63*, 1032-1038.

(26) Eickhoff, H.; Jung, G.; Rieker, A. *Tetrahedron* **2001**, *57*, 353-364.

(27) Noda, H.; Niwa, M.; Yamamura, S. *Tetrahedron Lett.* **1981**, *22*, 3247-3248.

(28) Fry, S. C. *Biochem. J.* **1982**, *204*, 449-455.

(29) Fry, S. C. *Biochem. J.* **1982**, *203*, 493-504.

(30) Miao, S. C.; Andersen, R. J.; Allen, T. M. *J. Nat. Prod.* **1990**, *53*, 1441-1446.
(31) Pordesimo, E. O.; Schmitz, F. J. *J. Org. Chem.* **1990**, *55*, 4704-4709.
(32) Kazlauskas, R.; Lidgard, R. O.; Murphy, P. T.; Wells, R. J. *Tetrahedron Lett.* **1980**, *21*, 2277-2280.
(33) Sano, S.; Ikai, K.; Kuroda, H.; Nakamura, T.; Obayashi, A.; Ezure, Y.; Enomoto, H. *J. Antibiot.* **1986**, *39*, 1674-84.
(34) Kase, H.; Kaneko, M.; Yamada, K. *J. Antibiot.* **1987**, *40*, 450-454.
(35) Boger, D. L.; Yohannes, D. *Bioorg. Med. Chem. Lett.* **1993**, *3*, 245-250.
(36) Nagarajan, R. *J. Antibiot.* **1993**, *46*, 1181-1195.
(37) Ma, N.; Jia, Y.; Liu, Z.; Gonzalez-Zamora, E.; Bois-Choussy, M.; Malabarba, A.; Brunati, C.; Zhu, J. *Bioorg. Med. Chem. Lett.* **2005**, *15*, 743-746.
(38) Hubbard, B. K.; Walsh, C. T. *Angew. Chem. Int. Ed.* **2003**, *42*, 730-765; *Angew. Chem.* **2003**, *115*, 752-789.
(39) Zieminska, E.; Lazarewicz, J. W.; Couladouros, E. A.; Moutsos, V. I.; Pitsinos, E. N. *Bioorg. Med. Chem. Lett.* **2008**, *18*, 5734-5737.
(40) Masuno, M. N.; Pessah, I. N.; Olmstead, M. M.; Molinski, T. F. *J. Med. Chem.* **2006**, *49*, 4497-4511.
(41) Boger, D. L.; Myers, J. B.; Yohannes, D. *Bioorg. Med. Chem. Lett.* **1991**, *1*, 313-316.
(42) Clayden, J.; Worrall, C. P.; Moran, W. J.; Helliwell, M. *Angew. Chem., Int. Ed.* **2008**, *47*, 3234-3237; *Angew. Chem.* **2008**, *120*, 3278-3281.
(43) Betson, M. S.; Clayden, J.; Worrall, C. P.; Peace, S. *Angew. Chem. Int. Ed.* **2006**, *45*, 5803-5807; *Angew. Chem.* **2006**, *118*, 5935-5939.
(44) Nolan, E. M.; Walsh, C. T. *ChemBioChem* **2009**, *10*, 34-53.
(45) Saitoh, T.; Ichikawa, J. *J. Am. Chem. Soc.* **2005**, *127*, 9696-9697.
(46) Hedrick, J. L.; Labadie, J. W. *J. Polym. Sci. A.* **1992**, *30*, 105-110.
(47) Eicher, T.; Walter, M. *Synthesis* **1991**, 469-473.
(48) Bigot, A.; Elise, M.; Dau, T. H.; Zhu, J. P. *J. Org. Chem.* **1999**, *64*, 6283-6296.
(49) Nicolaou, K. C.; Boddy, C. N. C.; Natarajan, S.; Yue, T. Y.; Li, H.; Bräse, S.; Ramanjulu, J. M. *J. Am. Chem. Soc.* **1997**, *119*, 3421-3422.
(50) Crimmin, M. J.; Brown, A. G. *Tetrahedron Lett.* **1990**, *31*, 2017-2020.
(51) Rao, A. V. R.; Gurjar, M. K.; Reddy, K. L.; Rao, A. S. *Chem. Rev.* **1995**, *95*, 2135-2167.
(52) Pearson, A. J.; Park, J. G.; Zhu, P. Y. *J. Org. Chem.* **2002**, *57*, 3583-3589.
(53) Ulmann, F. *Ber. Dtsch. Chem. Ges.* **1904**, *37*, 853-857.
(54) Ullmann, F. *Ber. Dtsch. Chem. Ges.* **1903**, *36*, 2389-2391.
(55) Lindley, J. *Tetrahedron* **1984**, *40*, 1433-1456.
(56) Byeong-Seon, J.; Qian, W.; Jong-Keun, S.; Yurngdong, J. *Eur. J. Org. Chem.* **2007**, *2007*, 1338-1344.
(57) Mann, G.; Hartwig, J. F. *Tetrahedron Lett.* **1997**, *38*, 8005-8008.
(58) Marcoux, J. F.; Doye, S.; Buchwald, S. L. *J. Am. Chem. Soc.* **1997**, *119*, 10539-10540.
(59) Chan, D. M. T.; Monaco, K. L.; Wang, R.-P.; Winters, M. P. *Tetrahedron Lett.* **1998**, *39*, 2933-2936.
(60) Evans, D. A.; Katz, J. L.; West, T. R. *Tetrahedron Lett.* **1998**, *39*, 2937-2940.
(61) Lam, P. Y. S.; Clark, C. G.; Saubern, S.; Adams, J.; Winters, M. P.; Chan, D. M. T.; Combs, A. *Tetrahedron Lett.* **1998**, *39*, 2941-2944.
(62) Evans, D. A.; Katz, J. L.; Peterson, G. S.; Hintermann, T. *J. Am. Chem. Soc.* **2001**, *123*, 12411-12413.
(63) Wang, Y. C.; Georghiou, P. E. *Org. Lett.* **2002**, *4*, 2675-2678.
(64) Cousin, D.; Mann, J.; Nieuwenhuyzen, M.; Berg, H. v. d. *Org. Biomol. Chem.* **2006**, *4*, 54-62.

(65) Decicco, C. P.; Song, Y.; Evans, D. A. *Org. Lett.* **2001**, *3*, 1029-1032.
(66) Powers, D. C.; Ritter, T. *Nature Chemistry* **2009**, *1*, 302-309.
(67) Furuya, T.; Ritter, T. *J. Am. Chem. Soc.* **2008**, *130*, 10060-10061.
(68) Chan, V. S.; Bergman, R. G.; Toste, F. D. *J. Am. Chem. Soc.* **2007**, *129*, 15122-15123.
(69) Goossen, L. J.; Deng, G.; Levy, L. M. *Science* **2006**, *313*, 662-664.
(70) Lockhart, T. P. *J. Am. Chem. Soc.* **1983**, *105*, 1940-1946.
(71) Barton, D. H. R.; Finet, J. P.; Khamsi, J. *Tetrahedron Lett.* **1987**, *28*, 887-890.
(72) Lam, P. Y. S.; Clark, C. G.; Saubern, S.; Adams, J.; Averill, K. M.; Chan, D. M. T.; Combs, A. *Synlett* **2000**, *2000*, 0674-0676.
(73) Kilitoglu, B.; Arndt, H. D. *Synlett* **2009**, 720-723.
(74) Collman, J. P.; Zhong, M.; Zhang, C.; Costanzo, S. *J. Org. Chem.* **2001**, *66*, 7892-7897.
(75) Collman, J. P.; Zhong, M. *Org. Lett.* **2000**, *2*, 1233-1236.
(76) Solomon, E. I.; Sundaram, U. M.; Machonkin, T. E. *Chem. Rev.* **1996**, *96*, 2563-2606.
(77) Zalacain, M.; Zaera, E.; Vazquez, D.; Jimenez, A. *FEBS Lett.* **1982**, *148*, 95-97.
(78) Inoue, K.; Mukaiyama, T.; Kobayashi, T.; Ogawa, M. *Invest. New Drugs* **1986**, *4*, 231-236.
(79) Majima, H.; Tsukagoshi, S.; Furue, H.; Suminaga, M.; Sakamoto, K.; Wakabayashi, R.; Kishino, S.; Niitani, H.; Murata, A.; Genma, A.; et al. *Gan To Kagaku Ryoho* **1993**, *20*, 67-78.
(80) Yoshida, F.; Asai, R.; Majima, H.; Tsukagoshi, S.; Furue, H.; Suminaga, M.; Sakamoto, K.; Niitani, H.; Murata, A.; Kurihara, M.; et al. *Gan To Kagaku Ryoho* **1994**, *21*, 199-207.
(81) Kato, T.; Suzumura, Y.; Takamoto, S.; Ota, K. *Anticancer Res.* **1987**, *7*, 329-34.
(82) Kato, T.; Suzumura, Y.; Liu, F. Z.; Tateno, H.; Ogiu, T.; Ota, K. *Jpn. J. Cancer Res.* **1989**, *80*, 290-293.
(83) Wakita, K.-I.; Minami, M.; Venkateswarlu, A.; Sharma, V. M.; Ramesh, M.; Akahane, K. *Anti-Cancer Drugs* **2001**, *12*, 433-439.
(84) Fujiwara, H.; Saito, S.-y.; Hitotsuyanagi, Y.; Takeya, K.; Ohizumi, Y. *Cancer Lett.* **2004**, *209*, 223-229.
(85) Itokawa, H.; Morita, H.; Takeya, K. *Chem. Pharm. Bull.* **1992**, *40*, 1050-1052.
(86) Morita, H.; Kondo, K.; Hitotsuyanagi, Y.; Takeya, K.; Itokawa, H.; Tomioka, N.; Itai, A.; Iitaka, Y. *Tetrahedron* **1991**, *47*, 2757-2772.
(87) Itokawa, H.; Morita, H.; Takeya, K.; Tomioka, N.; Itai, A.; Iitaka, Y. *Tetrahedron* **1991**, *47*, 7007-7020.
(88) Inaba, T.; Umezawa, I.; Yuasa, M.; Inoue, T.; Mihashi, S.; Itokawa, H.; Ogura, K. *J. Org. Chem.* **1987**, *52*, 2957-2958.
(89) Nishiyama, S.; Nakamura, K.; Suzuki, Y.; Yamamura, S. *Tetrahedron Lett.* **1986**, *27*, 4481-4484.
(90) Inoue, T.; Inaba, T.; Umezawa, I.; Yuasa, M.; Itokawa, H.; Ogura, K.; Komatsu, K.; Hara, H.; Hoshino, O. *Chem. Pharm. Bull.* **1995**, *43*, 1325-35.
(91) Ninomiya, K.; Shioiri, T.; Yamada, S. *Tetrahedron* **1974**, *30*, 2151-2157.
(92) Boger, D. L.; Yohannes, D. *J. Am. Chem. Soc.* **1991**, *113*, 1427-1429.
(93) Boger, D. L.; Yohannes, D.; Zhou, J. C.; Patane, M. A. *J. Am. Chem. Soc.* **1993**, *115*, 3420-3430.
(94) Boger, D. L.; Zhou, J. C. *J. Am. Chem. Soc.* **1995**, *117*, 7364-7378.
(95) Boger, D. L.; Patane, M. A.; Zhou, J. C. *J. Am. Chem. Soc.* **1995**, *117*, 7357-7363.

(96) Inoue, T.; Sasaki, T.; Takayanagi, H.; Harigaya, Y.; Hoshino, O.; Hara, H.; Inaba, T. *J. Org. Chem.* **1996**, *61*, 3936-3937.

(97) Boger, D. L.; Zhou, J. C.; Borzilleri, R. M.; Nukui, S.; Castle, S. L. *J. Org. Chem.* **1997**, *62*, 2054-2069.

(98) Felix, A. M.; Heimer, E. P.; Lambros, T. J.; Tzougraki, C.; Meienhofer, J. *J. Org. Chem.* **1978**, *43*, 4194-4196.

(99) Miyaura, N.; Suzuki, A. *Chem. Rev.* **1995**, *95*, 2457-2483.

(100) Chiarello, J.; Joullie, M. M. *Synth. Commun.* **1988**, *18*, 2211-2223.

(101) Aurelio, L.; Brownlee, R. T. C.; Hughes, A. B. *Chem. Rev.* **2004**, *104*, 5823-5846.

(102) Knapp, D. M.; Gillis, E. P.; Burke, M. D. *J. Am. Chem. Soc.* **2009**, *131*, 6961-6963.

(103) Santucci, L.; Triboulet, C. *J. Chem. Soc. A* **1969**, 392-396.

(104) Hitotsuyanagi, Y.; Ishikawa, H.; Naito, S.; Takeya, K. *Tetrahedron Lett.* **2003**, *44*, 5901-5903.

(105) Lam, P. Y. S.; Vincent, G.; Clark, C. G.; Deudon, S.; Jadhav, P. K. *Tetrahedron Lett.* **2001**, *42*, 3415-3418.

(106) Walker, T. E.; Matheny, C.; Storm, C. B.; Hayden, H. *J. Org. Chem.* **2002**, *51*, 1175-1179.

(107) Freidinger, R. M.; Hinkle, J. S.; Perlow, D. S. *J. Org. Chem.* **1983**, *48*, 77-81.

(108) Aurelio, L.; Box, J. S.; Brownlee, R. T. C.; Hughes, A. B.; Sleebs, M. M. *J. Org. Chem.* **2003**, *68*, 2652-2667.

(109) Chatterjee, J.; Gilon, C.; Hoffman, A.; Kessler, H. *Acc. Chem. Res.* **2008**, *41*, 1331-1342.

(110) Ishiyama, T.; Murata, M.; Miyaura, N. *J. Org. Chem.* **1995**, *60*, 7508-7510.

(111) Skaff, O.; Jolliffe, K. A.; Hutton, C. A. *J. Org. Chem.* **2005**, *70*, 7353-7363.

(112) Coutts, S. J.; Adams, J.; Krolikowski, D.; Snow, R. J. *Tetrahedron Lett.* **1994**, *35*, 5109-5112.

(113) Carpino, L. A. *J. Am. Chem. Soc.* **1993**, *115*, 4397-4398.

(114) Carpino, L. A.; Imazumi, H.; El-Faham, A.; Ferrer, F. J.; Zhang, C. W.; Lee, Y. S.; Foxman, B. M.; Henklein, P.; Hanay, C.; Mügge, C.; Wenschuh, H.; Klose, K.; Beyermann, M.; Bienert, M. *Angew. Chem. Int. Ed.* **2002**, *41*, 442-445; *Angew. Chem.* **2002**, *114*, 457-461.

(115) Thern, B.; Rudolph, J.; Jung, G. *Angew. Chem. Int. Ed.* **2002**, *41*, 2307-2309; *Angew. Chem.* **2002**, *114*, 2401-2403.

(116) Falb, E.; Yechezkel, Y.; Salitra, Y.; Gilon, C. *J .Pept. Res.* **1999**, *53*, 507-517.

(117) Lambert, J. N.; Mitchell, J. P.; Roberts, K. D. *J. Chem. Soc., Perkin Trans. 1* **2001**, 471-484.

(118) Boger, D. L.; Zhou, J. C. *J. Org. Chem.* **1996**, *61*, 3938-3939.

(119) Li, H.; Jiang, X.; Ye, Y.-h.; Fan, C.; Romoff, T.; Goodman, M. *Org. Lett.* **1999**, *1*, 91-94.

(120) Yun-hua, Y.; Haitao, L.; Xiaohui, J. *Peptide Sci.* **2005**, *80*, 172-178.

(121) Han, S. Y.; Kim, Y. A. *Tetrahedron* **2004**, *60*, 2447-2467.

(122) Coste, J.; Dufour, M. N.; Pantaloni, A.; Castro, B. *Tetrahedron Lett.* **1990**, *31*, 669-672.

(123) Montalbetti, C. A. G. N.; Falque, V. *Tetrahedron* **2005**, *61*, 10827-10852.

(124) Chen, S.; Xu, J. *Tetrahedron Lett.* **1991**, *32*, 6711-6714.

(125) Valeur, E.; Bradley, M. *Chem. Soc. Rev.* **2009**, *38*, 606-631.

(126) Kamenecka, T. M.; Danishefsky, S. J. *Angew. Chem. Int. Ed.* **1998**, *37*, 2993-2995; *Angew. Chem.* **1998**, *110*, 3164-3166.

(127) Kamenecka, T. M.; Danishefsky, S. J. *Angew. Chem. Int. Ed.* **1998**, *37*, 2995-2998; *Angew. Chem.* **1998**, *110*, 3166-3168.

(128) Boger, D. L.; Zhou, J. *J. Org. Chem.* **1996**, *61*, 3938-3939.

(129) Gibson, H. W.; Wang, H.; Bonrad, K.; Jones, J. W.; Slebodnick, C.; Zackharov, L. N.; Rheingold, A. L.; Habenicht, B.; Lobue, P.; Ratliff, A. E. *Org. Biomol. Chem.* **2005**, *3*, 2114-2121.

(130) Consoli, G. M. L.; Cunsolo, F.; Geraci, C.; Neri, P. *Org. Lett.* **2001**, *3*, 1605-1608.

(131) Hoss, R.; Vögtle, F. *Angew. Chem. Int. Ed.* **1994**, *33*, 375-384; ; *Angew. Chem.* **1998**, *106,* 389-398.

(132) Galli, C. *Org. Prep. Proced. Int.* **1992**, *24*, 285 - 307.

(133) Lippert, J. W. *Arkivoc* **2005**, 87-95.

(134) Wenschuh, H.; Beyermann, M.; Elfaham, A.; Ghassemi, S.; Carpino, L. A.; Bienert, M. *J. Chem. Soc.* **1995**, 669-670.

(135) Vommina, S. B.; Kuppanna, A. *Lett. Pept. Sci.* **2000**, *7*, 41-46.

10. Abbreviations

[a]	Optical rotation
Ac	Acetyl
AcOH	Acetic acid
All	Allyl
Ala	alanine (A)
aq.	Aqueous
Ar	Aryl
Arg	arginine (R)
arom	Aromatic
Asn	asparagine (N)
ax	Axial
Bn	Benzyl
Boc	*tert*-butoxycarbonyl
br	Broad
Bu	Butyl
Bz	Benzoyl
ºC	Degrees Celcius (centigrade)
calcd	Calculated
Cbz	Benzyloxycarbonyl
CDI	Carbonyldiimidazole
COSY	Correlated Spectroscopy
CSA	Camphorsulfonic acid
compd	Compound
Cys	cysteine (C)
d	days
d (NMR)	doublet
dba	dibenzylidene acetone
DBU	1,8-diazabicyclo [5.4.0]undec-7-ene
dd (NMR)	doublet of doublets
d.e.	diastereomeric excess
DEPBT	3-(Diethoxy-phosphoryloxy)-3H-benzo[d][1,2,3] triazin-4-one
DCC	*N*,*N*-dicyclohexylcarbodiimide
DCM	Dichloromethane

DIBAL	Diisobutylaluminum hydride
DIPEA	Diisopropylethylamine
DMAP	4-dimethylaminopyridine
DMF	*N*,*N*-dimethylformamide
DMSO	dimethyl sulfoxide
DPPA	Diphenylphosphonic azide
dt (NMR)	Doublet of triplets
e.e.	enantiomeric excess
e.g.	*exempli gratia* (for example)
ESI	Electronspray ionization
equiv.	equivalents
ESI	Electrospray ionization
Et	Ethyl
et al.	*et alia* (and others)
Fmoc	9-fluorenylmethoxycarbonyl
FDPP	Pentafluorophenyl diphenylphosphinate
GC	Gas chromatography
Gly	glycine (G)
Glu	glutamate (E)
Gln	glutamine (Q)
h	hours
HATU	*O*-(7-Azabenzotriazole-1-yl)-1,1,3,3-tetramethyluronium hexafluorophosphate
HBTU	2-(1H-Benzotriazole-1-yl)-1,1,3,3-tetramethyluronium hexafluorophosphate
His	histidine (H)
HOAt	1-Hydroxy-7-Azabenzotriazole
HOBt	*N*-hydroxybenzotriazole
HMBC	Heteronuclear multiple bond coherence
HPLC	High performance liquid chromatography
HRMS	High resolution mass spectrometry
HSQC	Heteronuclear single quantum coherence
i.e.	*id est* (that is)
IR	infrared
IC_{50}	half maximal inhibitory concentration
Ile	isoleucine (I)
Lys	lysine (K)

m (NMR)	multiplet
M	molar
MALDI	matrix-assisted laser desorption ionization
Me	methyl
MeCN	acetonitrile
Met	methionine (M)
min	minutes
mp	melting point
MS	mass spectrometry
m/*z*	mass to charge ratio
N	normal (equivalents per liter)
NBS	*N*-bromosuccinimide
NMR	nuclear magnetic resonance
NMM	*N*-methyl morpholine
nOe	nuclear Overhauser effect
NRPS	Non ribosomal peptide synthesis
o	ortho
OSu	hydroxysuccinimide
p	para
PEG	polyethyleneglycol
Ph	phenyl
Phe	phenylalanine (F)
ppm	parts per million
Pro	proline (P)
q	quartet
quant.	quantitatively
R_f	retention factor
RPS	Ribosomal peptide synthesis
rt	room temperature
s	singlet (NMR)
sat.	saturated
Ser	serine (S)
t (NMR)	triplet
TBDMS	*tert*-butyldimethylsilyl
*t*Bu	*tert*-butyl
TEA	triethylamine
TFA	trifluoroacetic acid

THF	tetrahydrofuran
Thr	threonine (T)
TLC	thin layer chromatography
TMS	trimethylsilyl
Trt	trityl (triphenylmethyl)
Trp	tryptophane (W)
Ts	*p*-toluenesulfonyl
Tyr	tyrosine (Y)
UV	ultraviolet
Val	valine (V)
Vide infra	*see below*

11. Supporting information

11.1 O-Arylations of tyrosines

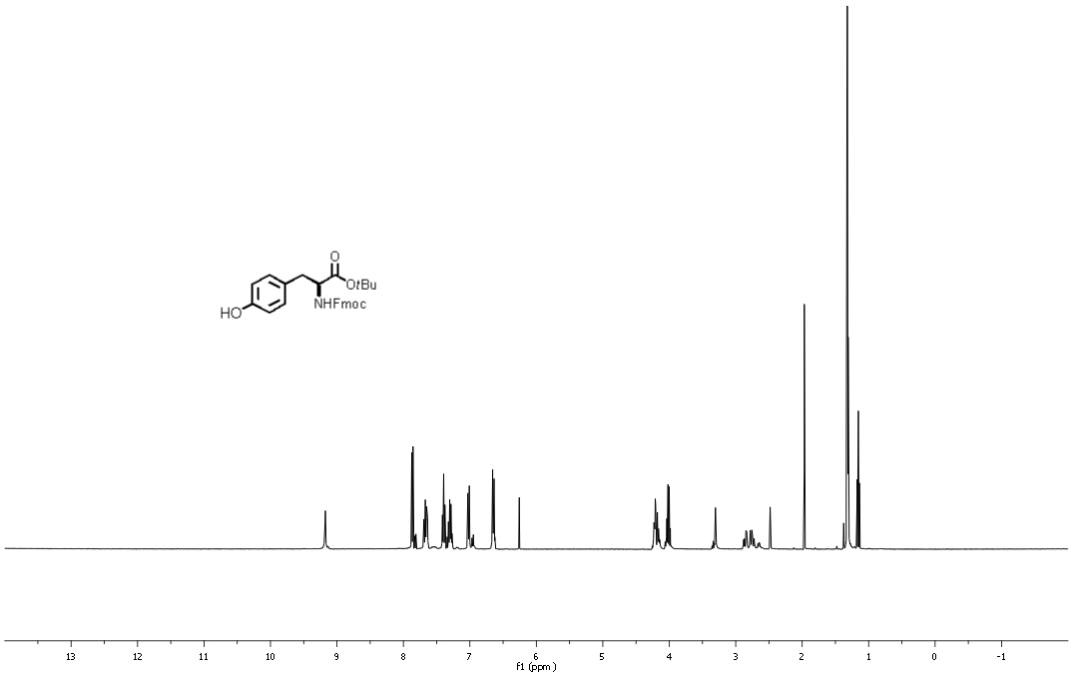

Spectrum 2 ^{1}H NMR of tyrosine **142** in DMSO-d_6.

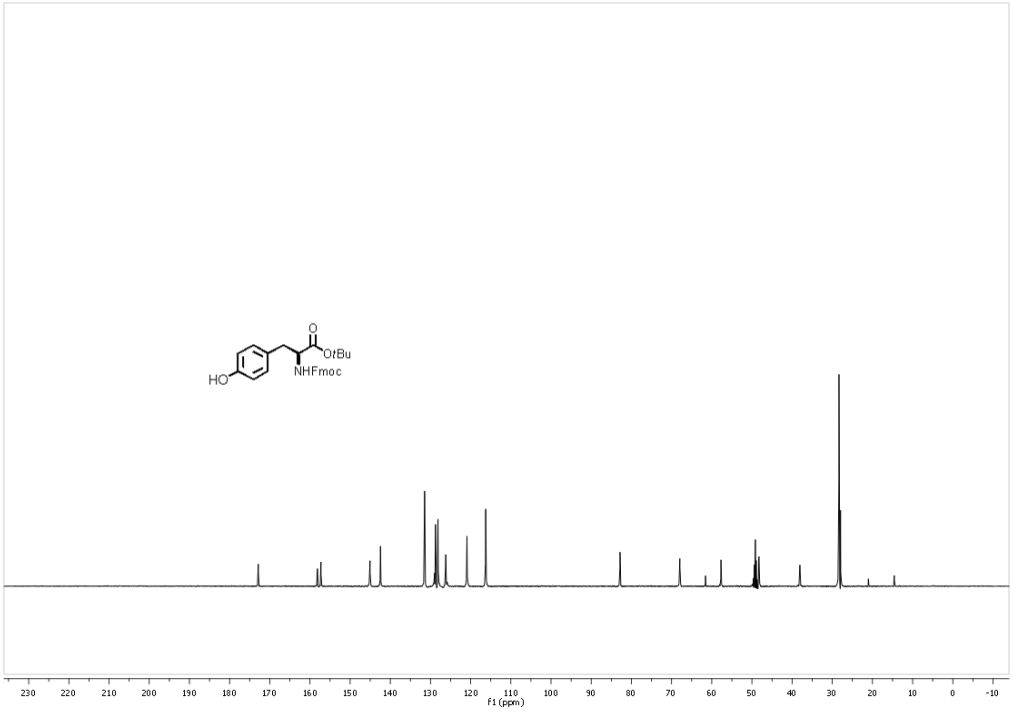

Spectrum 3 ^{13}C NMR of tyrosine **142** in DMSO-d_6.

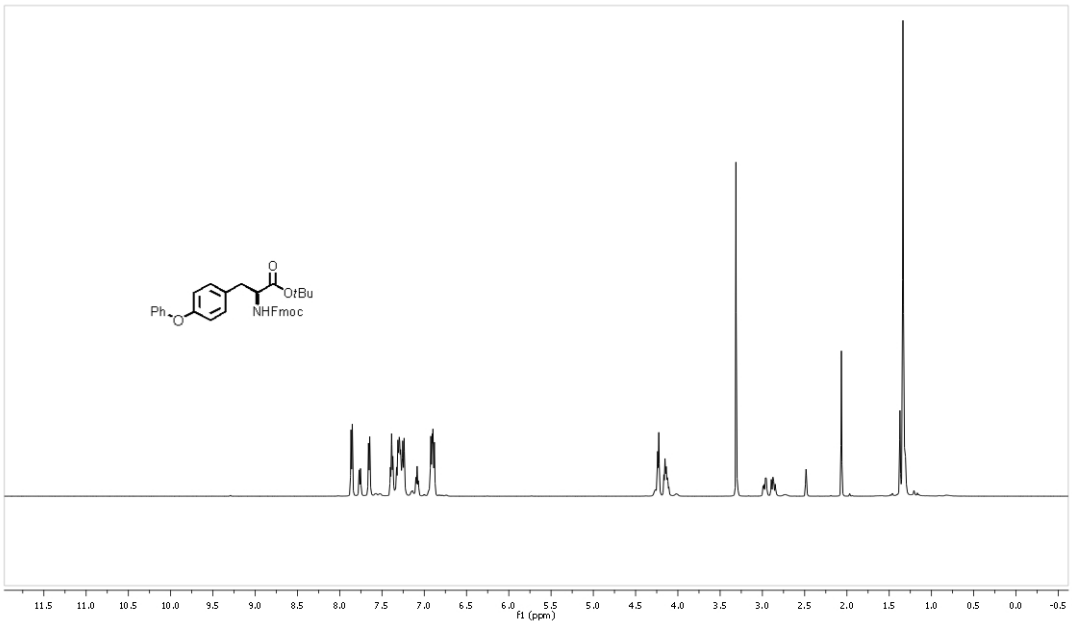

Spectrum 4 ^{1}H NMR of tyrosine **143a** in DMSO-d_6.

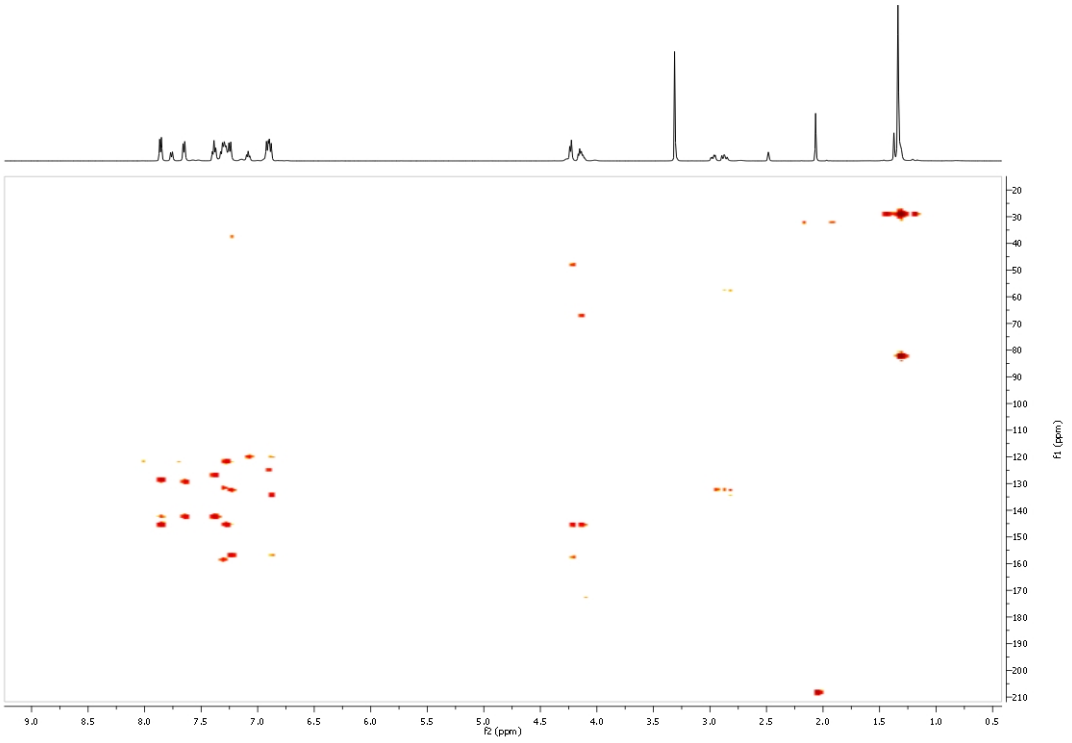

Spectrum 5 ^{13}C NMR of tyrosine **143a** in DMSO-d_6.

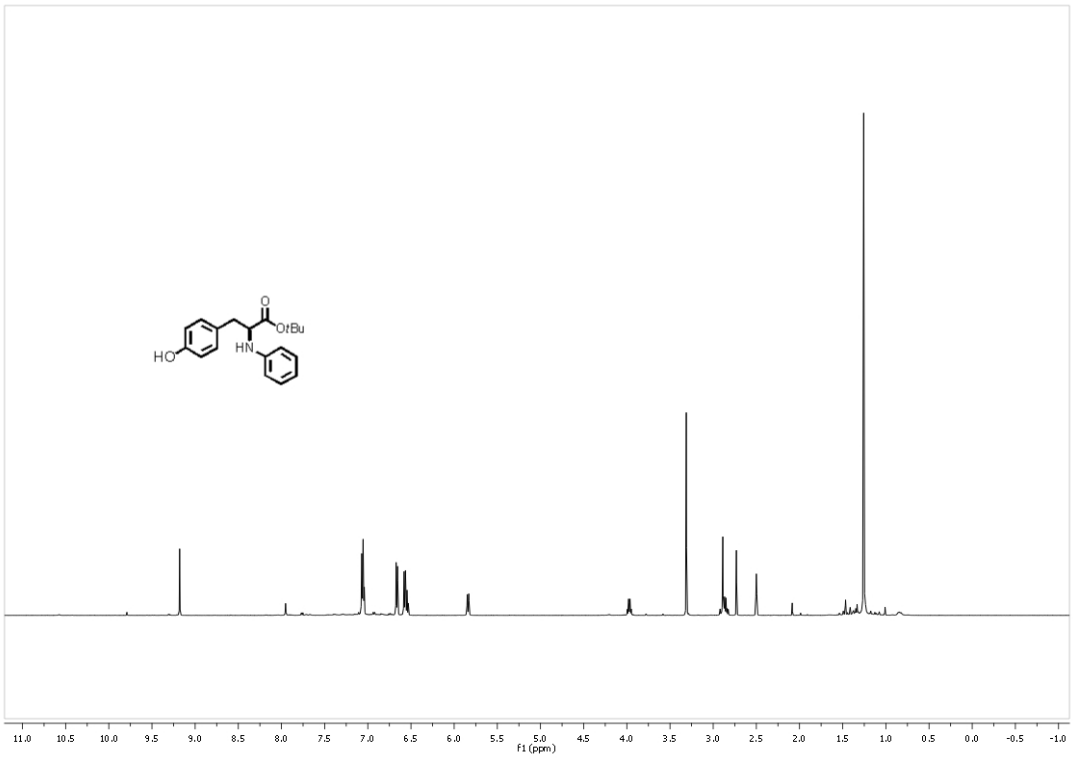

Spectrum 6 ^{1}H NMR of tyrosine **146** in DMSO-d_6.

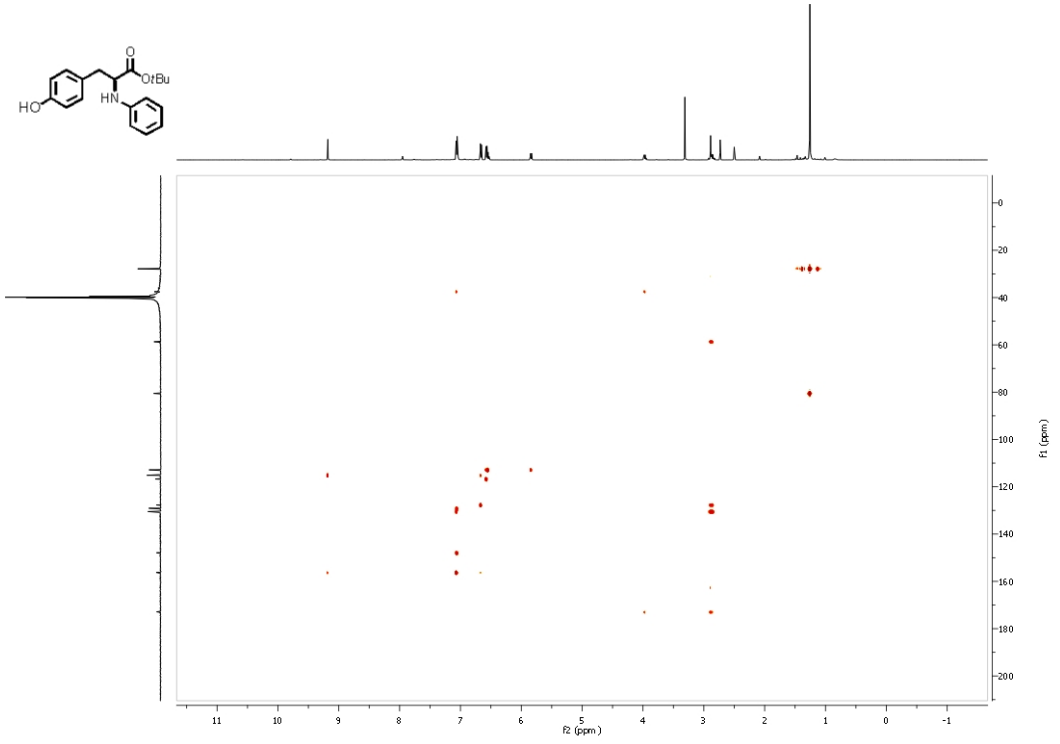

Spectrum 7 HMBC of tyrosine **146** in DMSO-d_6.

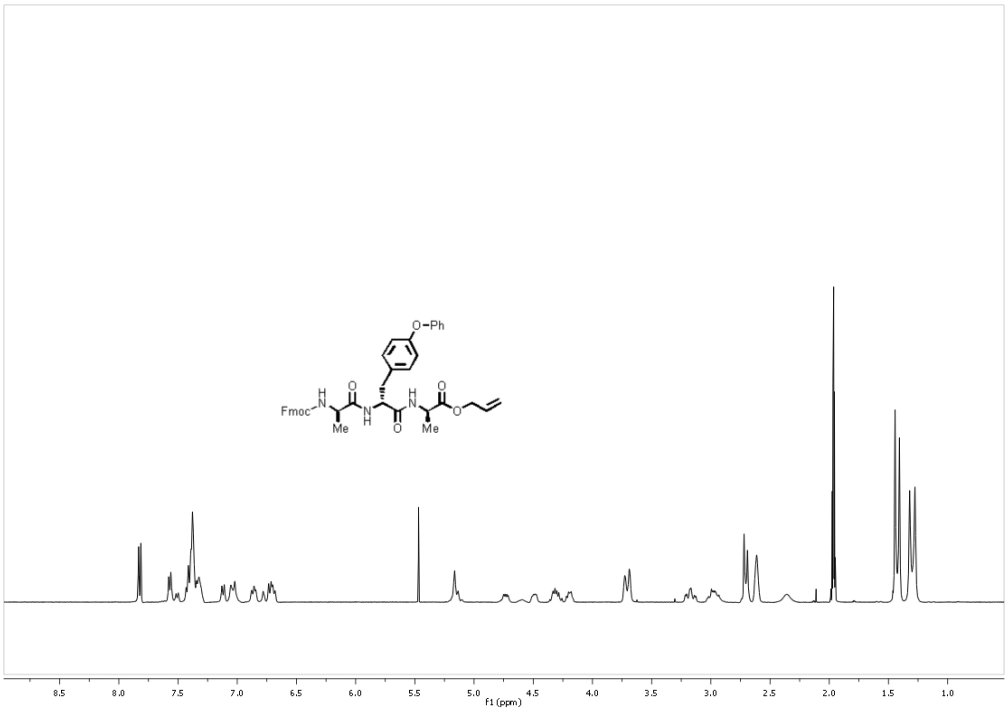

Spectrum 8 ^{1}H NMR of tyrosine **147a** in DMSO-d_6.

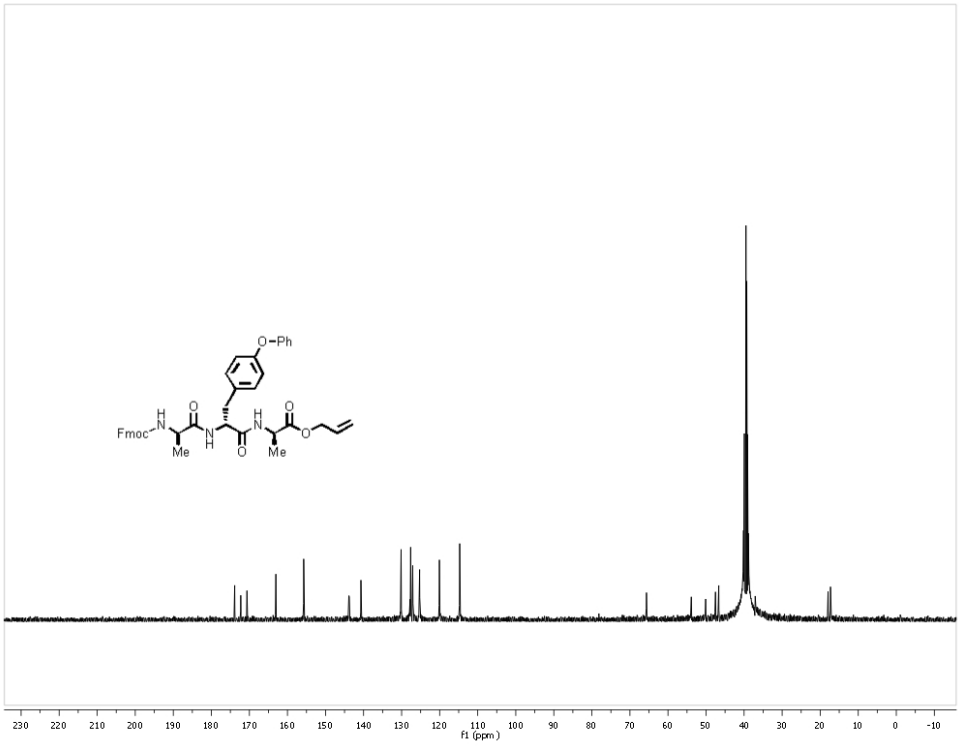

Spectrum 9 ^{13}C NMR of tyrosine **147c** in DMSO-d_6.

11.2 Towards the total synthesis of RA-VII (4)

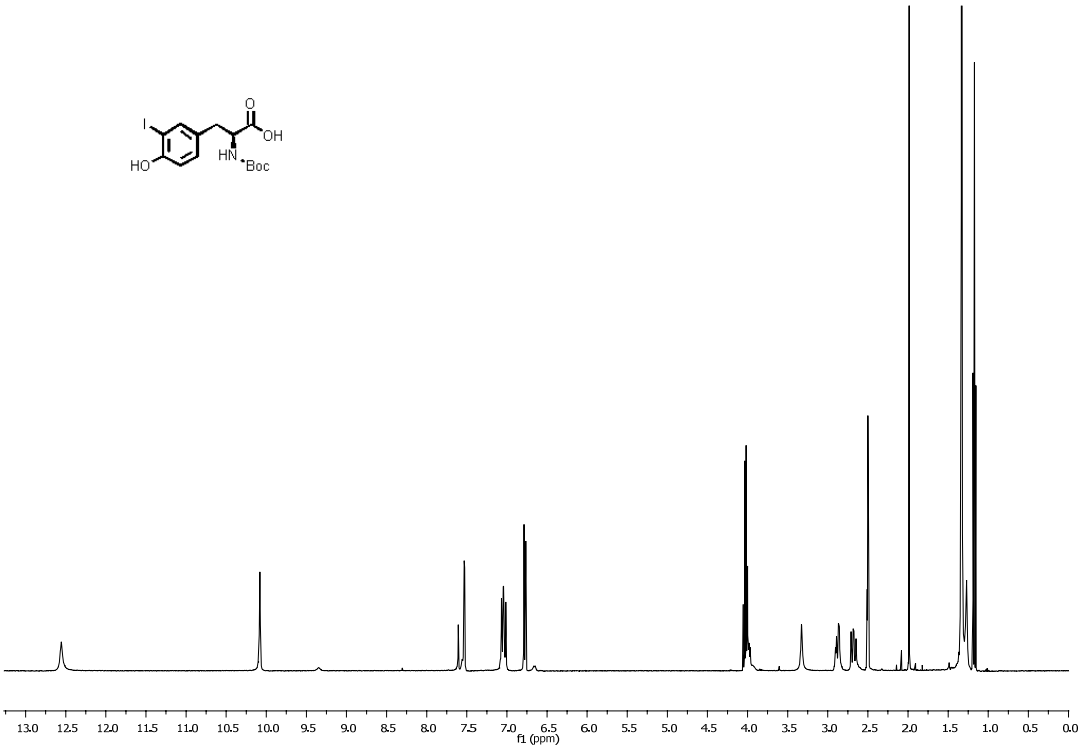

Spectrum 10 ^{13}C NMR tyrosine **130** in DMSO-$d_{6.}$

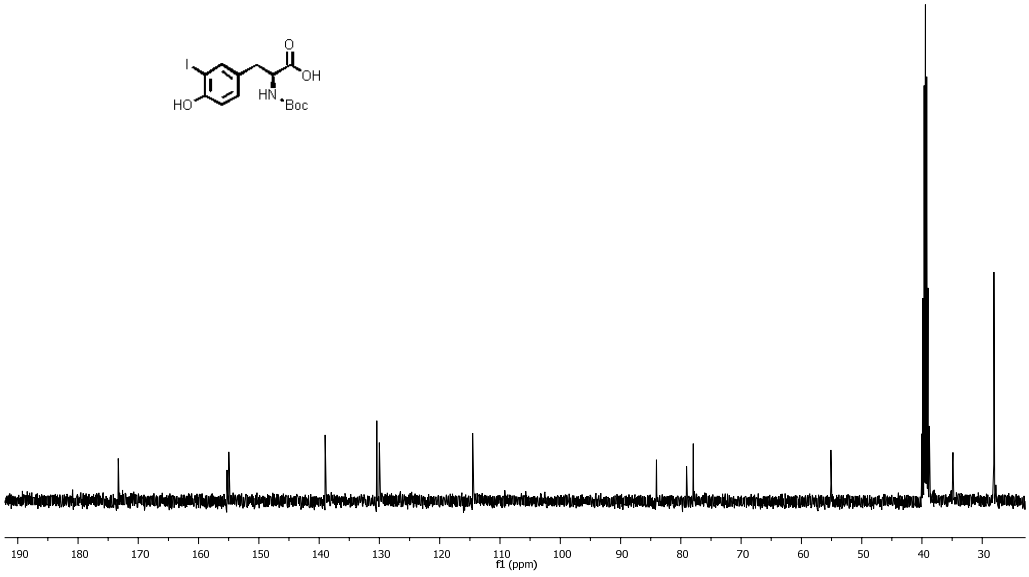

Spectrum 11 ^{13}C tyrosine **130** in DMSO-d_6

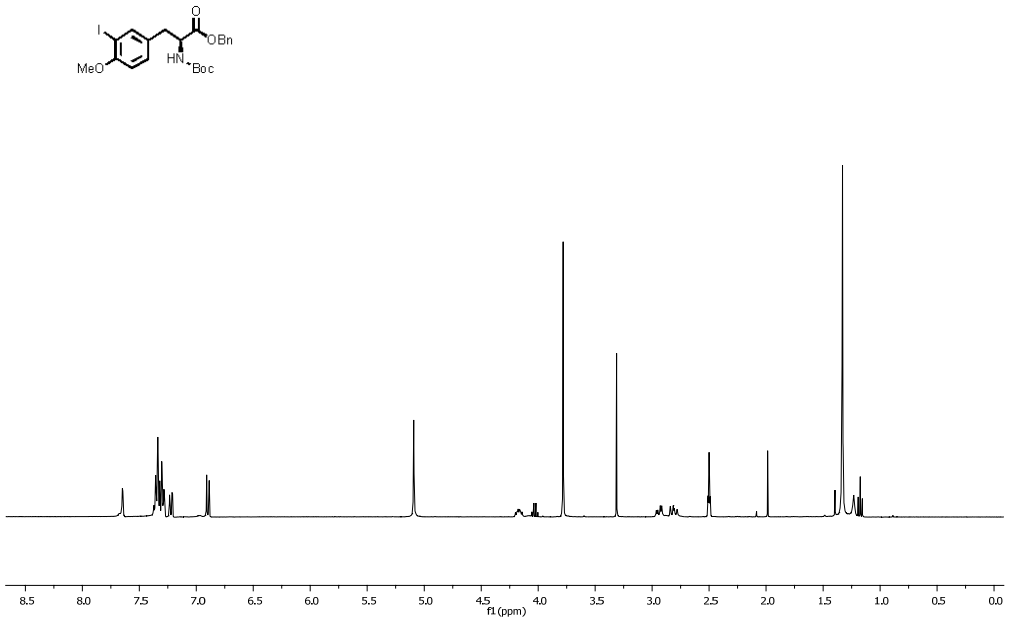

Spectrum 12 ^{13}C NMR tyrosine **168** in DMSO-d_6.

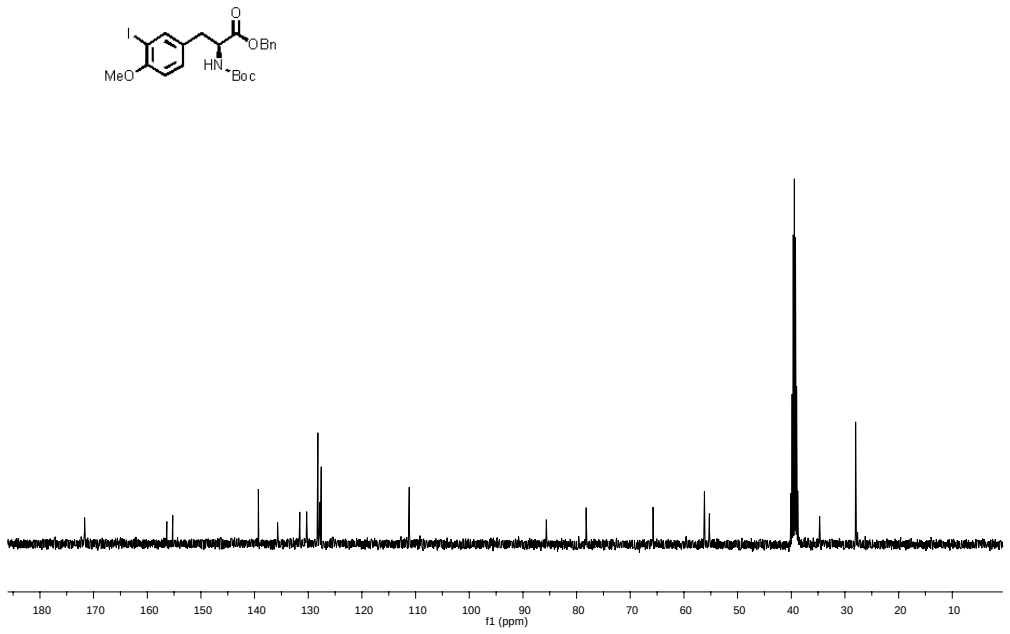

Spectrum 13 ^{13}C NMR tyrosine **168** in DMSO-d_6

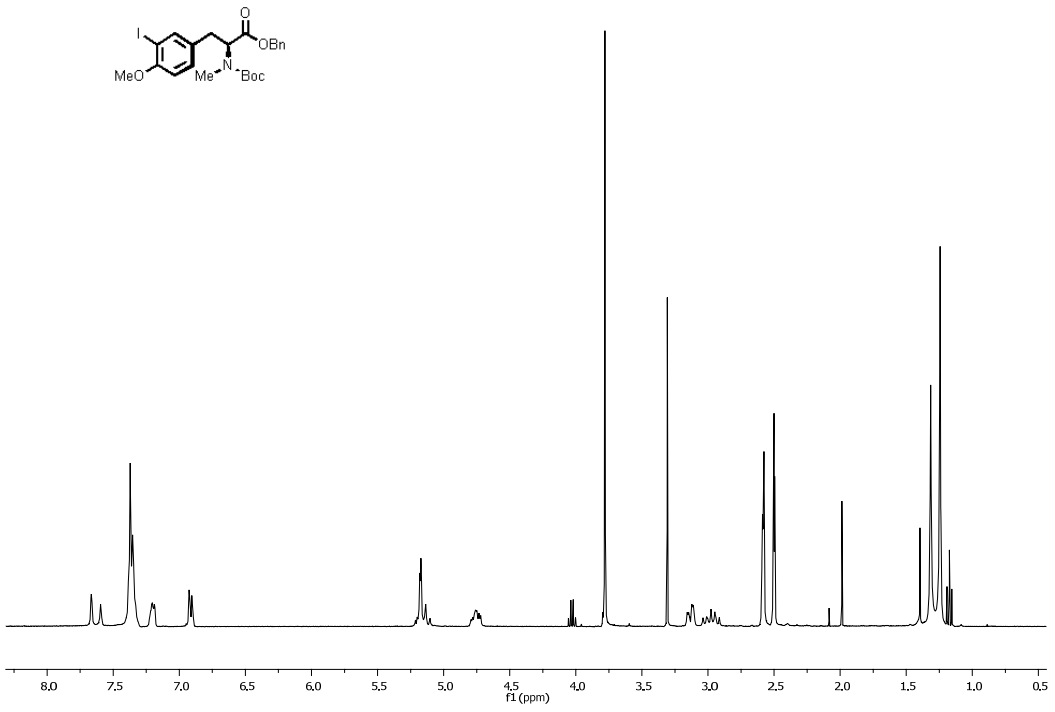

Spectrum 14 ^{13}C NMR tyrosine **169** in DMSO-d_6

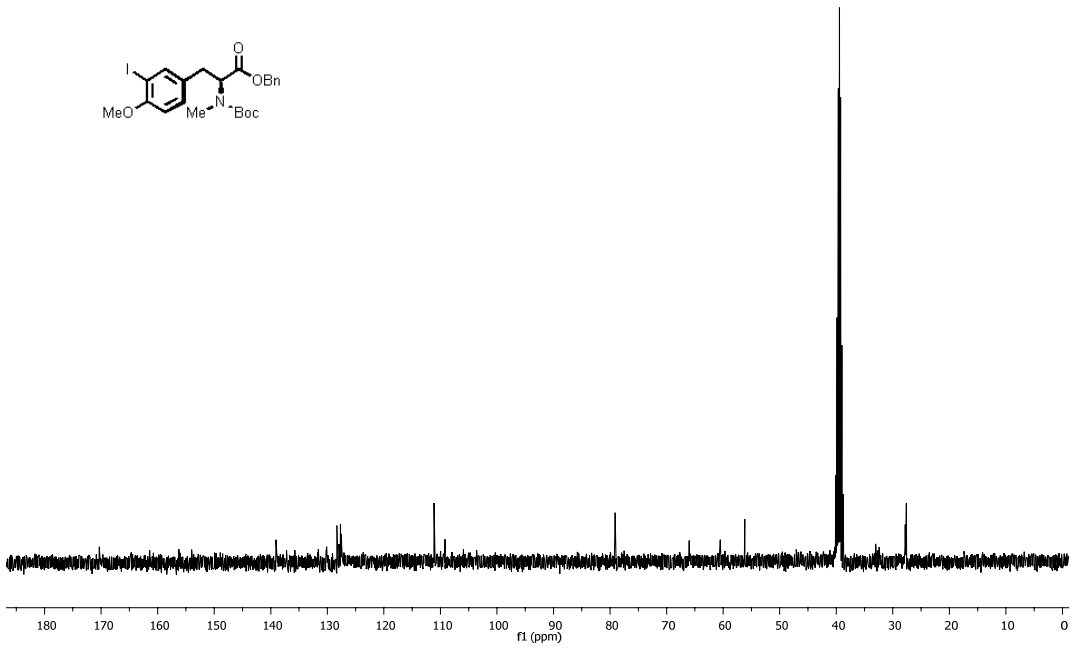

Spectrum 15 ^{13}C NMR tyrosine **169** in DMSO-d_6

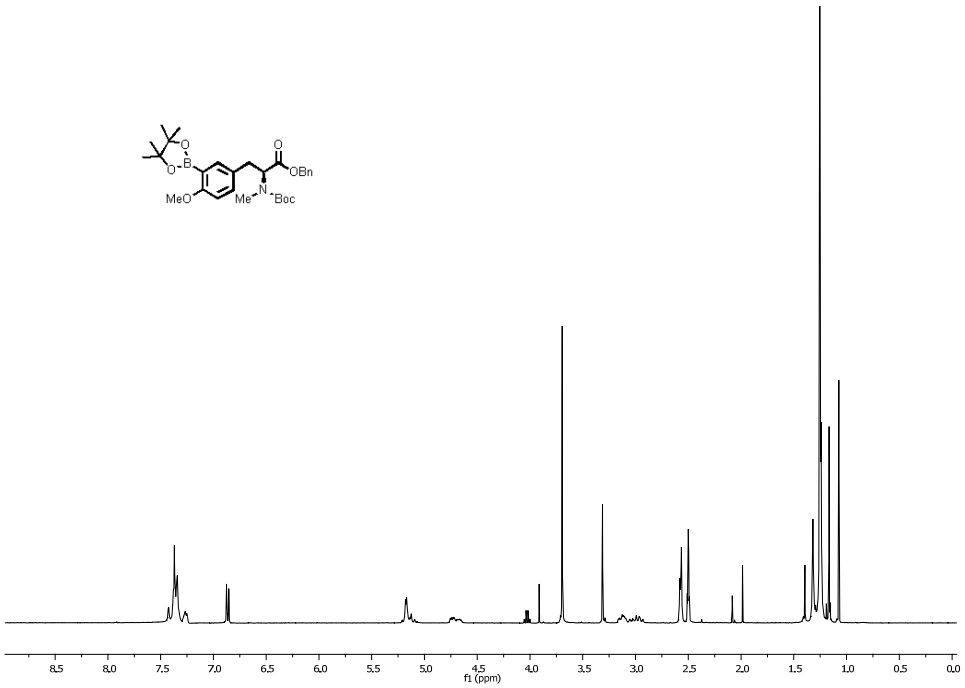

Spectrum 16 ^{13}C NMR tyrosine **170** in DMSO-d_6

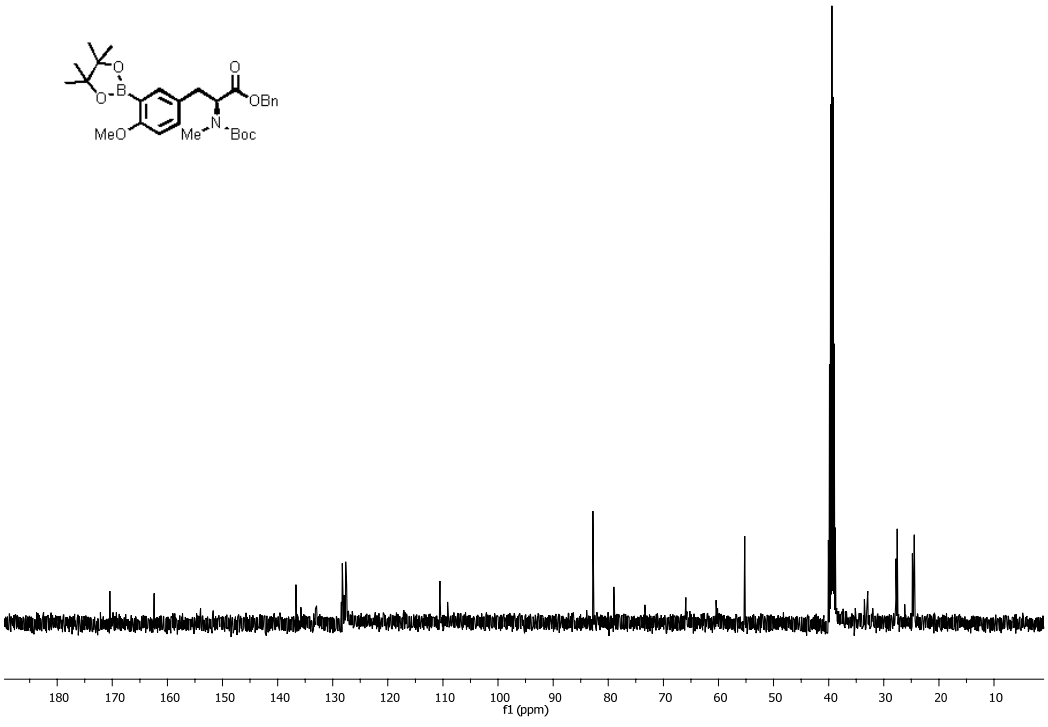

Spectrum 17 ^{13}C NMR tyrosine **170** in DMSO-d_6

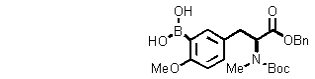

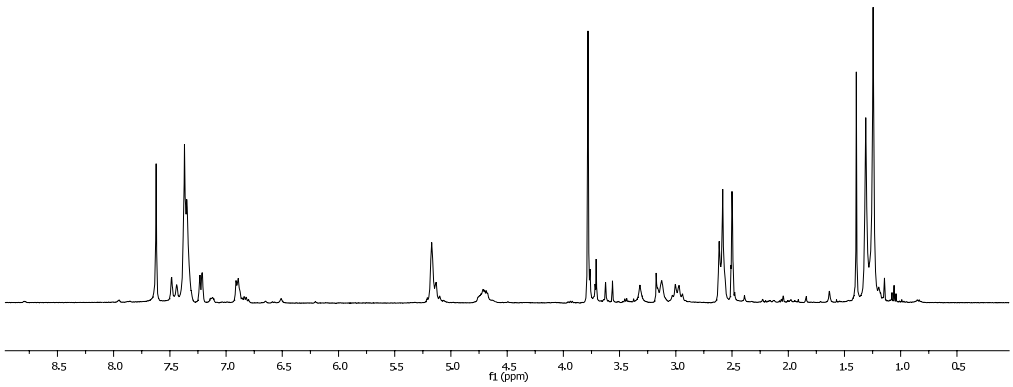

Spectrum 18 ^{1}H NMR tyrosine **128** in DMSO-d_6

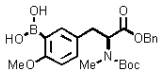

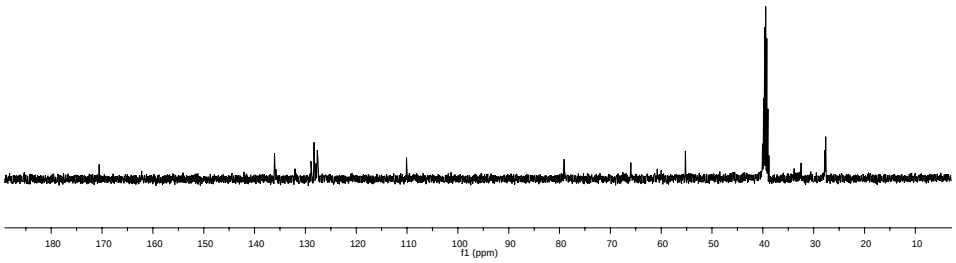

Spectrum 19 ^{13}C NMR tyrosine **128** in DMSO-d_6

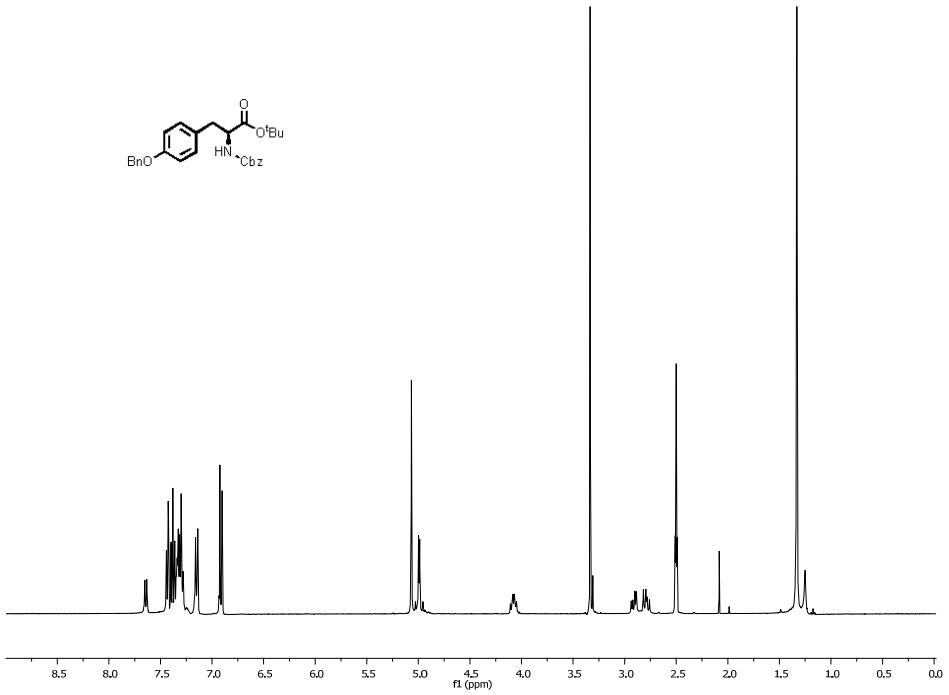

Spectrum 20 ^{1}H NMR tyrosine **188** in DMSO-d_6

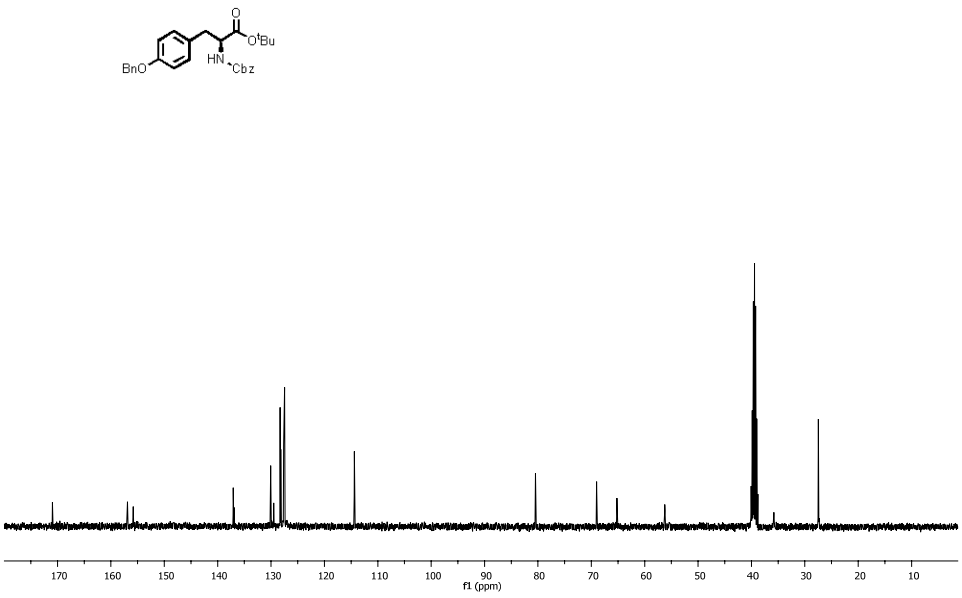

Spectrum 21 ^{13}C NMR tyrosine **188** in DMSO-d_6.

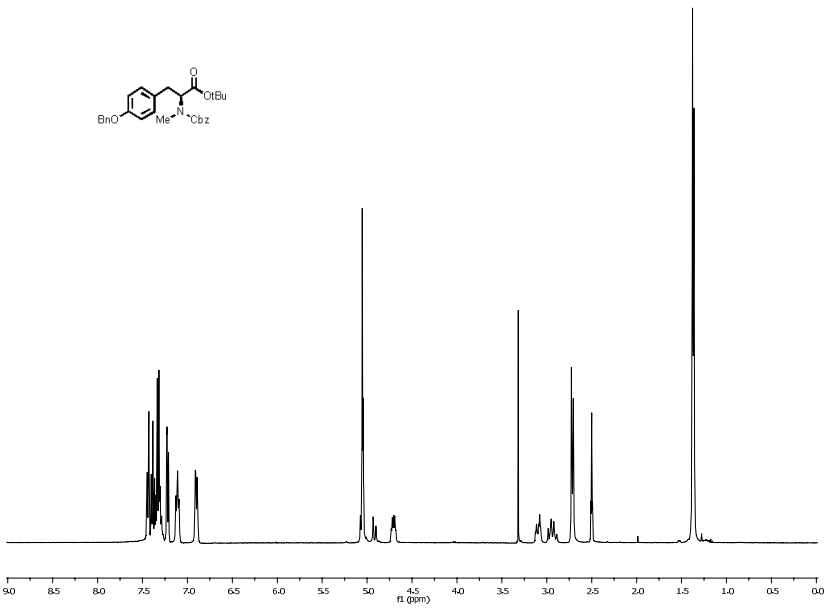

Spectrum 22 ^{1}H NMR tyrosine **189** in DMSO-d_6

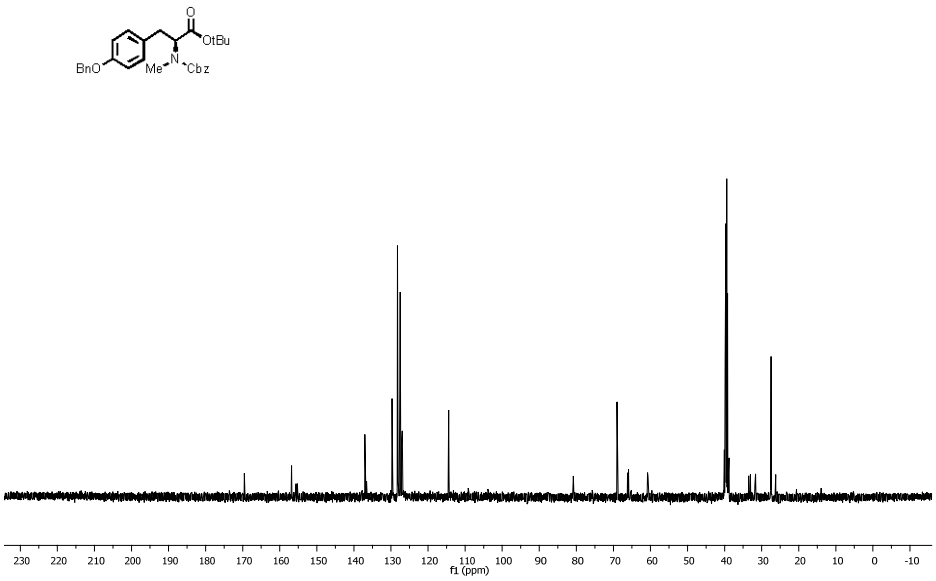

Spectrum 23 ^{1}H NMR tyrosine **189** in DMSO-d_6.

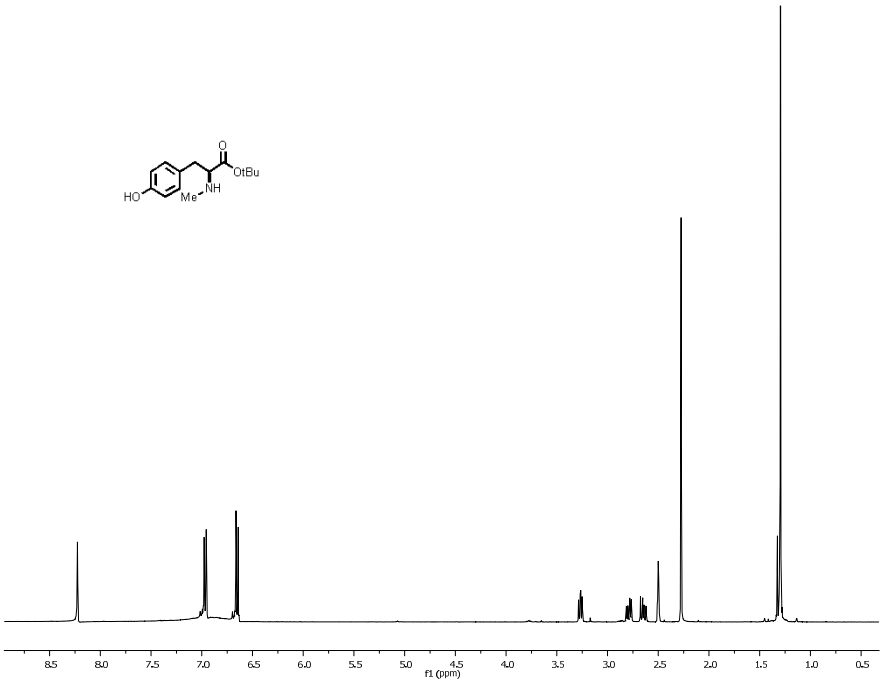

Spectrum 24 ^{1}H NMR tyrosine **190** in DMSO-d_6.

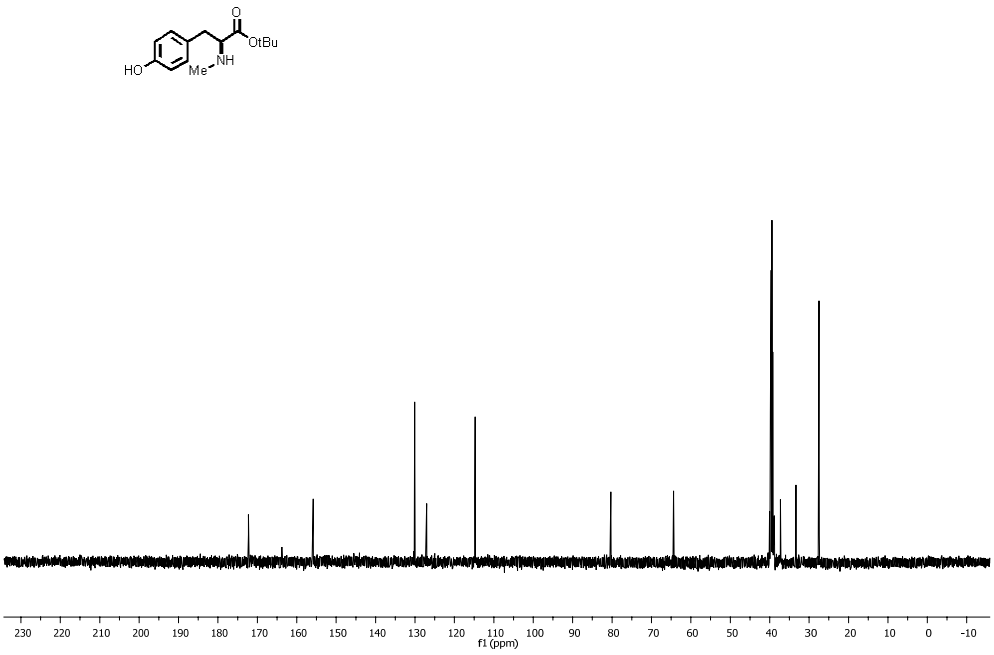

Spectrum 25 ^{1}H tyrosine NMR tyrosine **190** in DMSO-d_6.

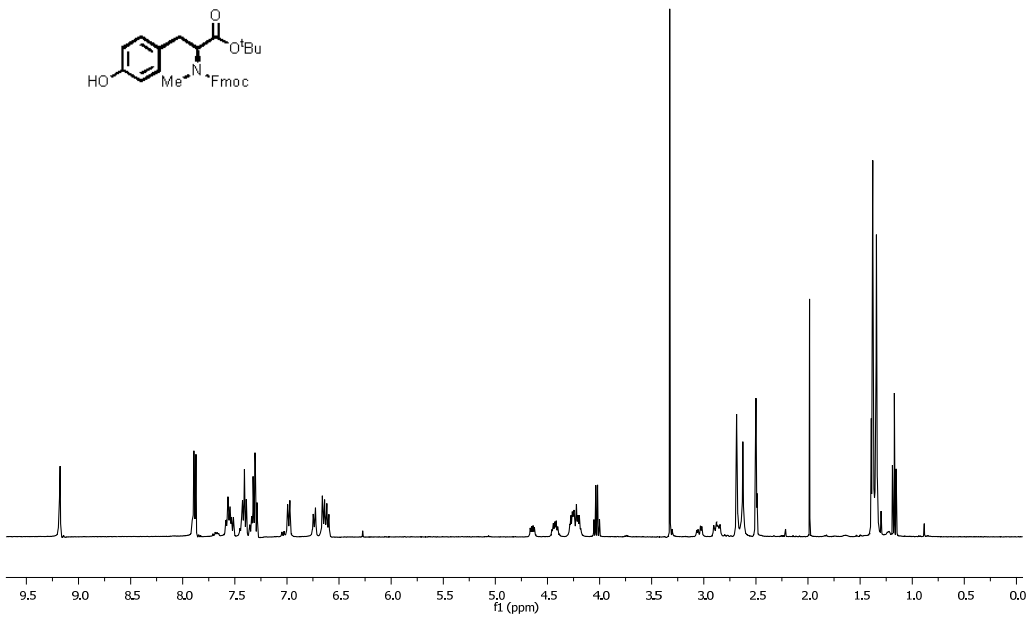

Spectrum 26 ^{1}H NMR tyrosine **129** in DMSO-d_6.

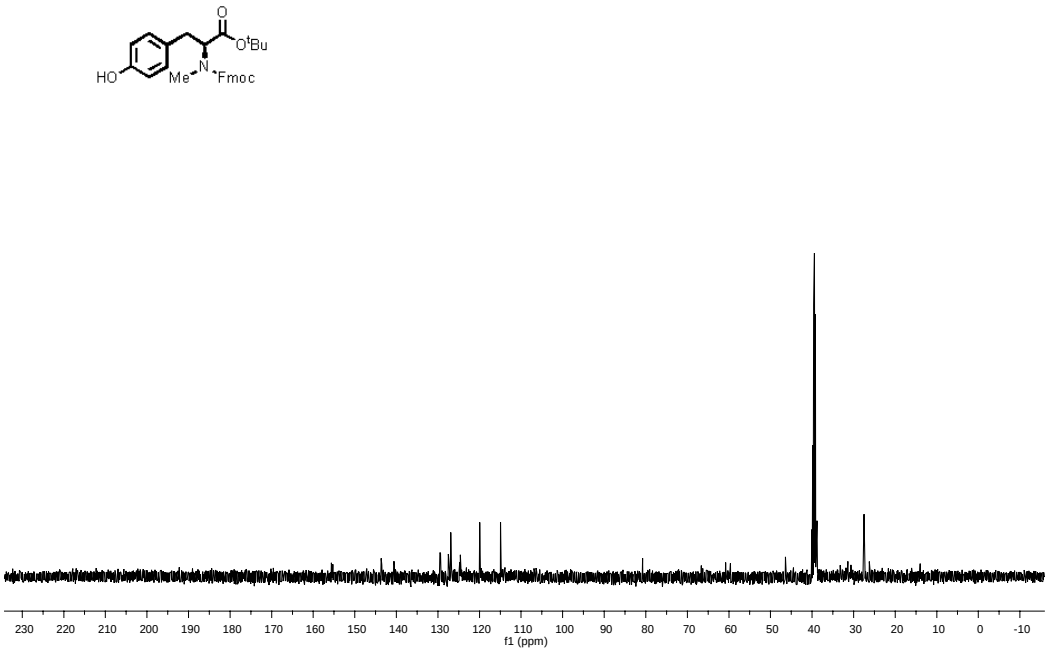

Spectrum 27 ^{13}C NMR tyrosine **129** in DMSO-d_6.

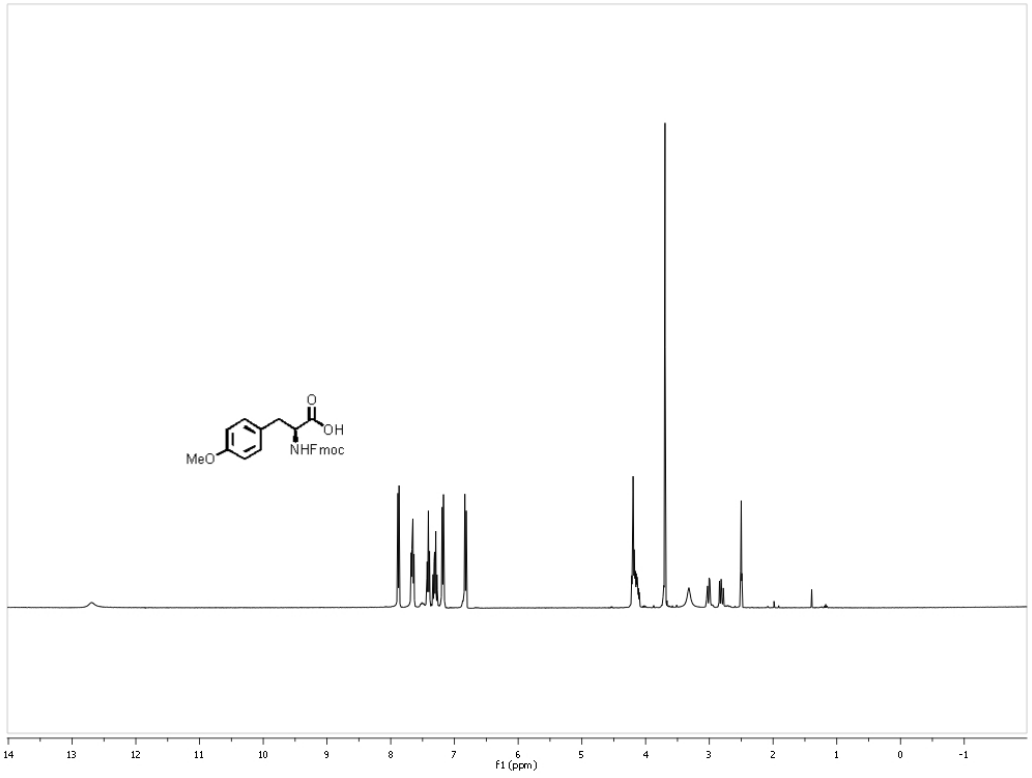

Spectrum 28 ^{1}H NMR tyrosine **161** in DMSO-d_6.

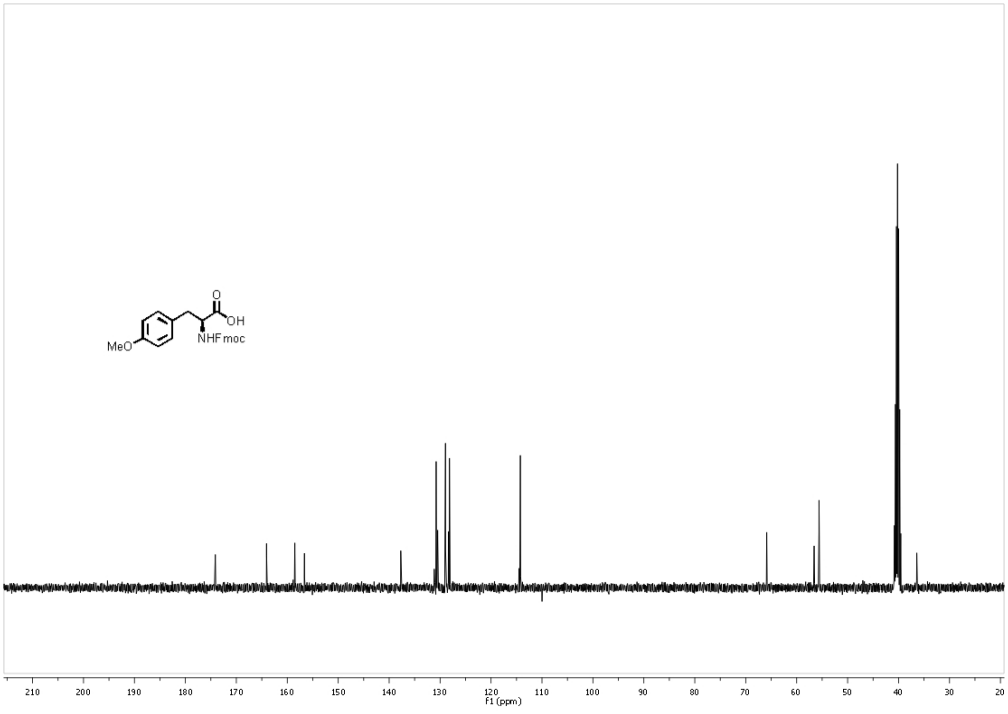

Spectrum 29 ^{13}C NMR tyrosine **161** in DMSO-d_6.

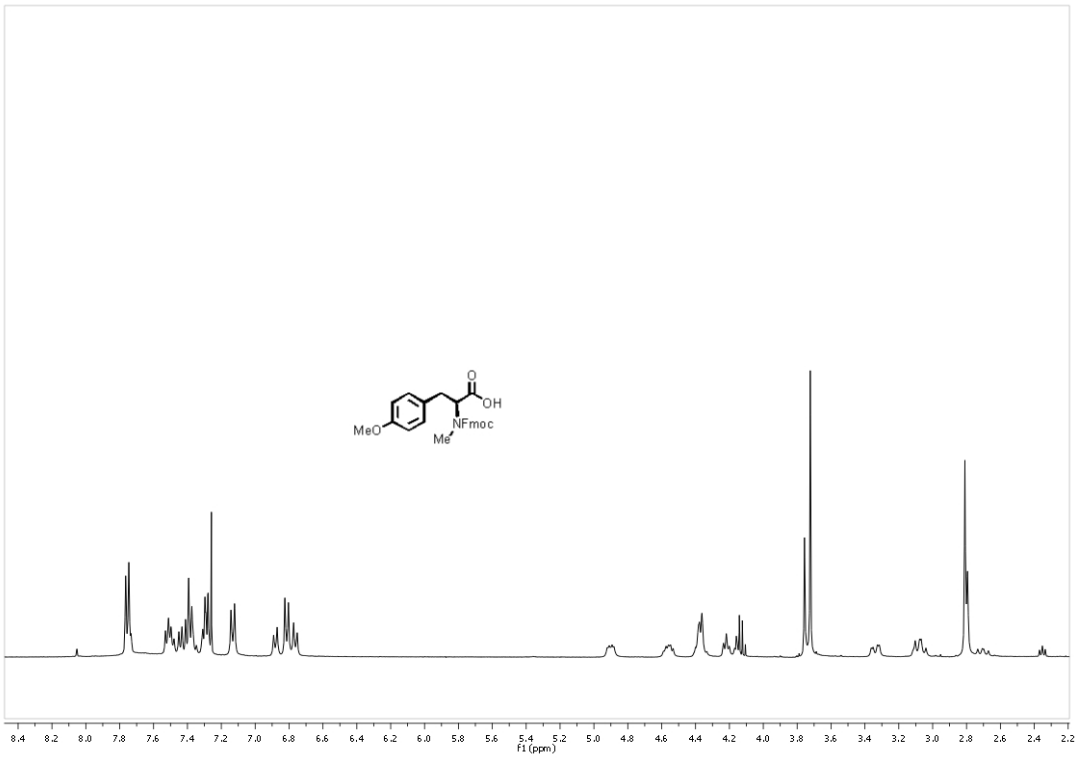

Spectrum 30 ^{1}H NMR tyrosine **126** in DMSO-d_6.

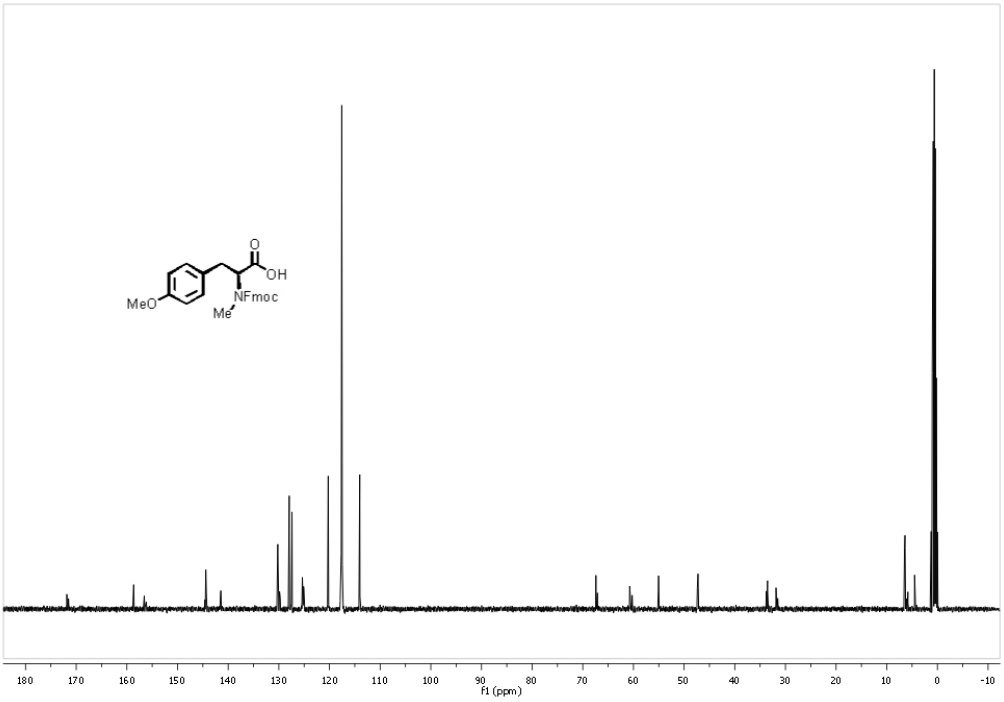

Spectrum 31 ^{13}C NMR tyrosine **126** in DMSO-d_6.

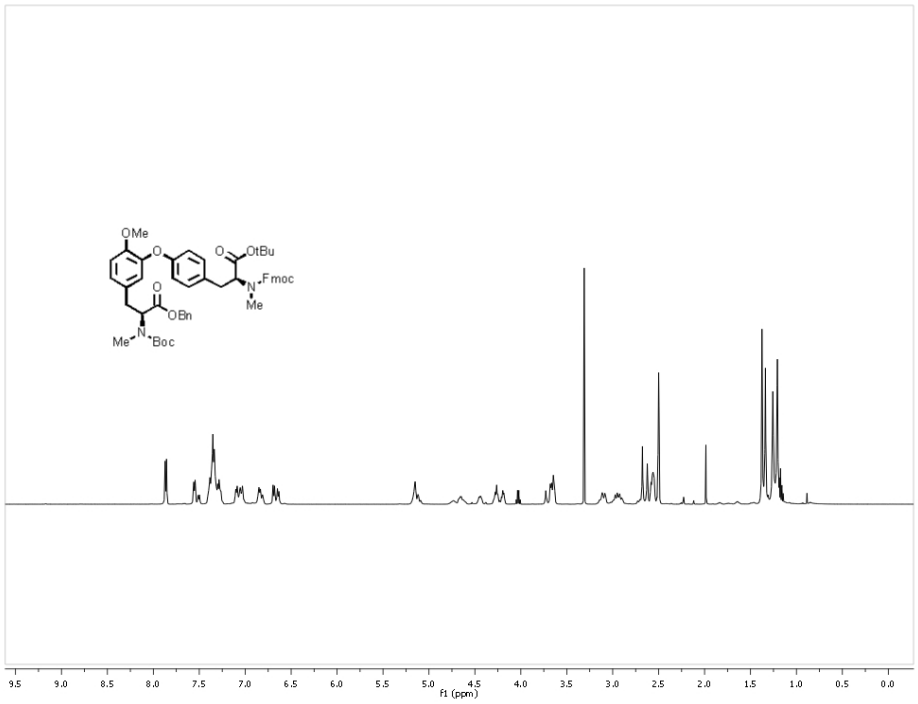

Spectrum 32 ^{1}H tyrosine **125** in DMSO-d_6.

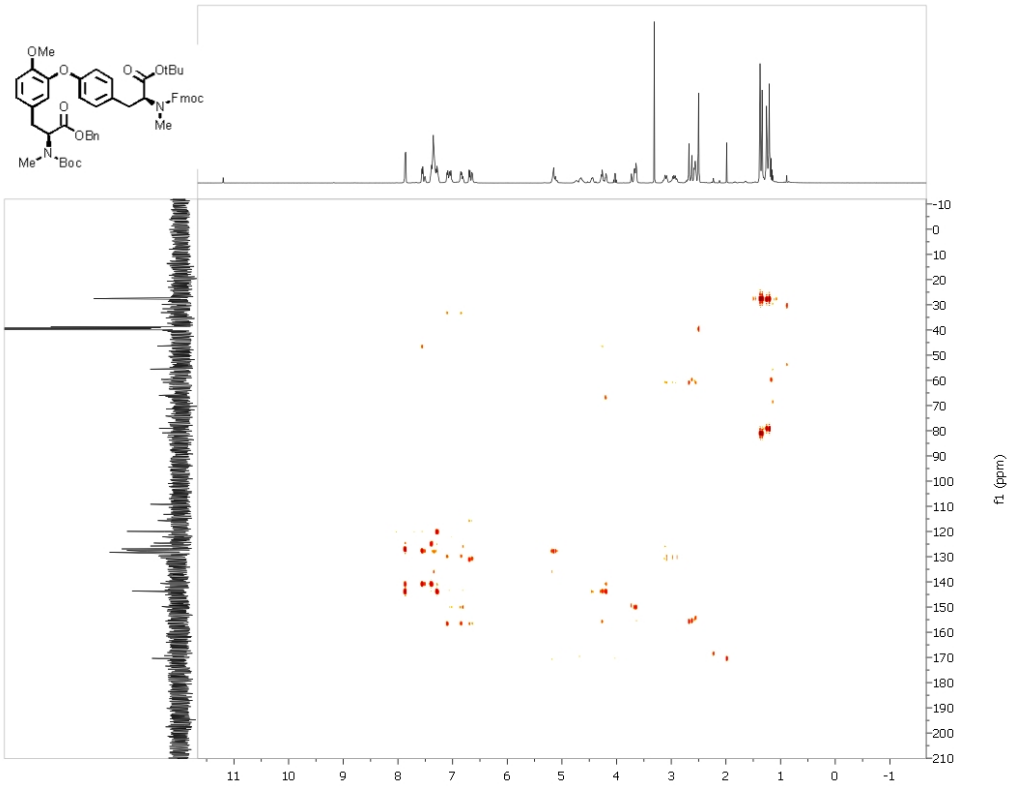

Spectrum 33 HMBC isodityrosine **125** in DMSO-d_6.

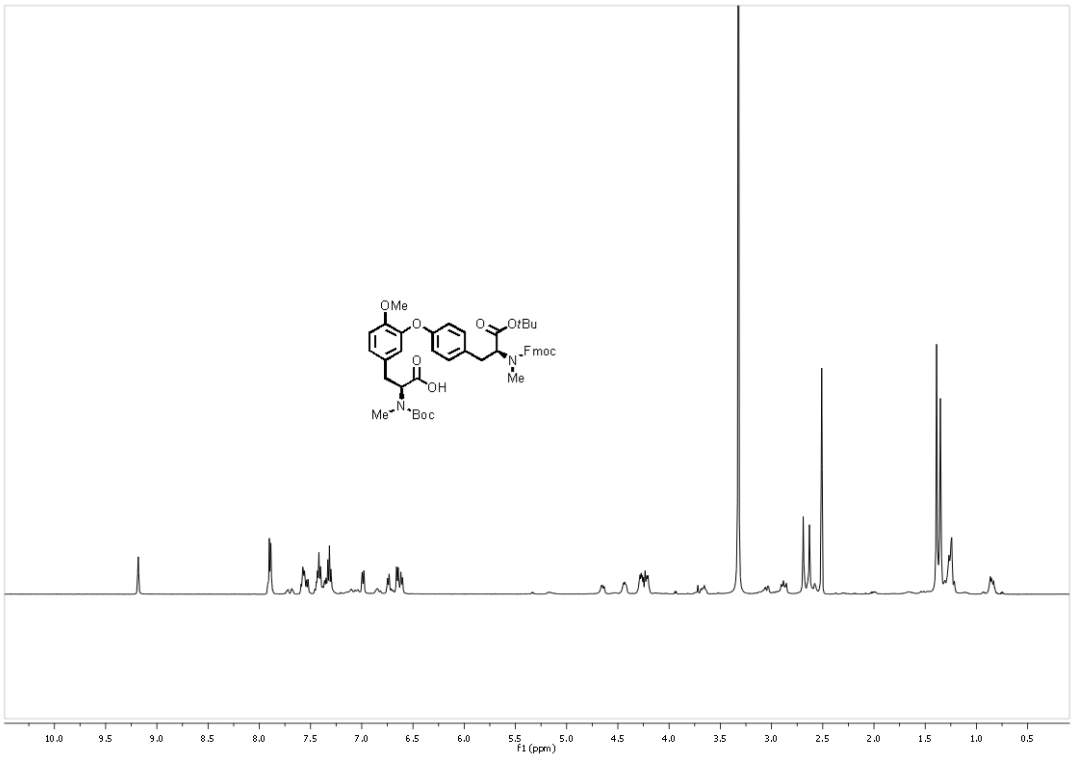

Spectrum 34 ^{1}H isodityrosine acid **127** in DMSO-d_6.

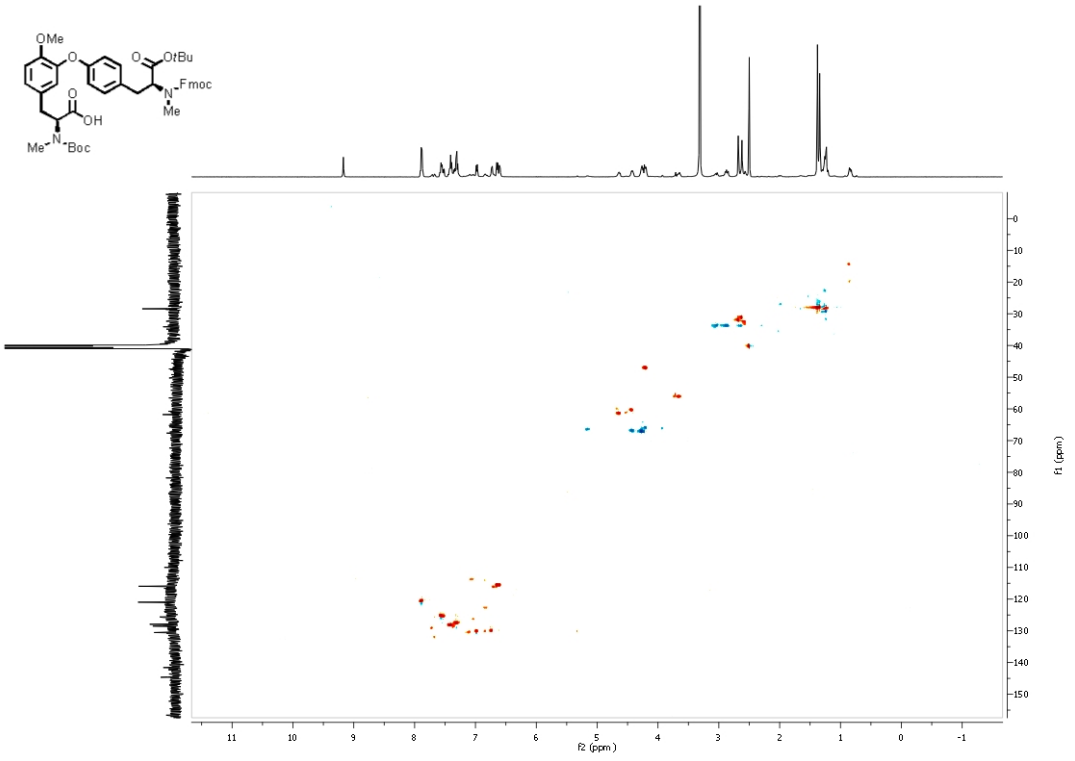

Spectrum 35 HSQC isodiytrosine acid **127** in DMSO-d_6.

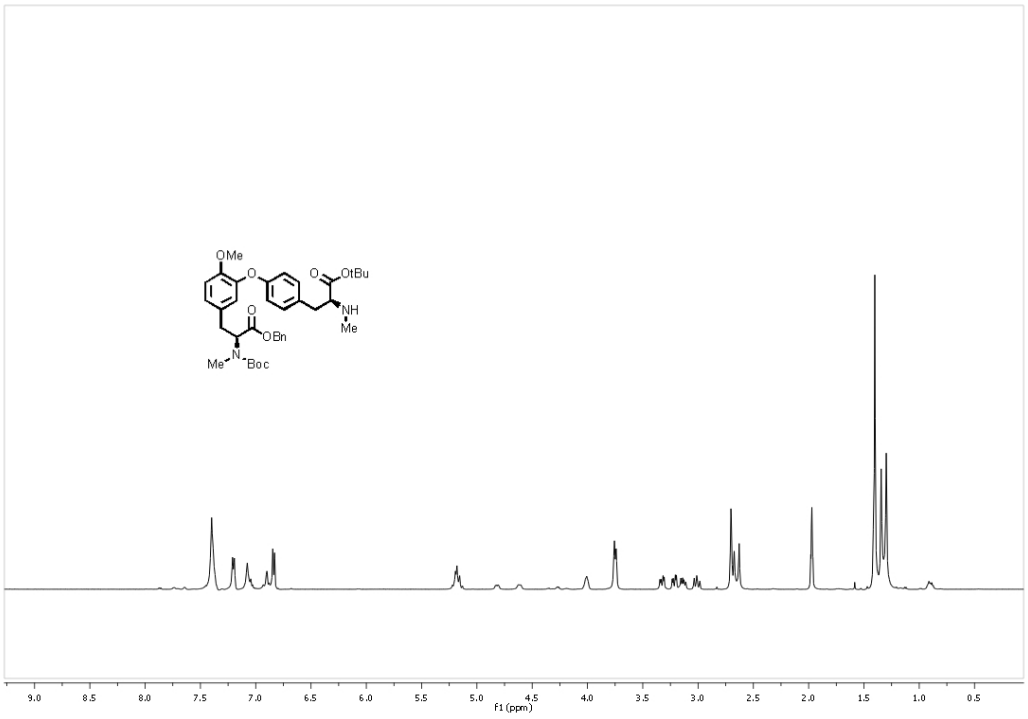

Spectrum 36 ^{13}C tyrosine **121** in MeCN-d_3.

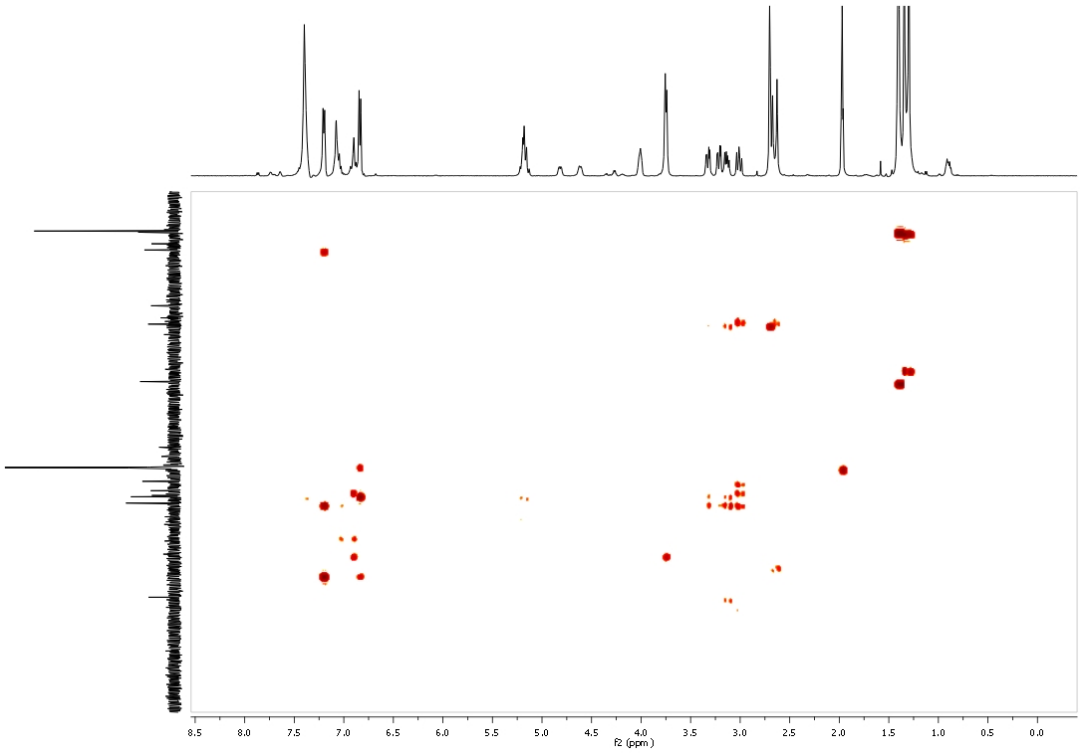

Spectrum 37 HMBC tyrosine **121** in MeCN-d_3.

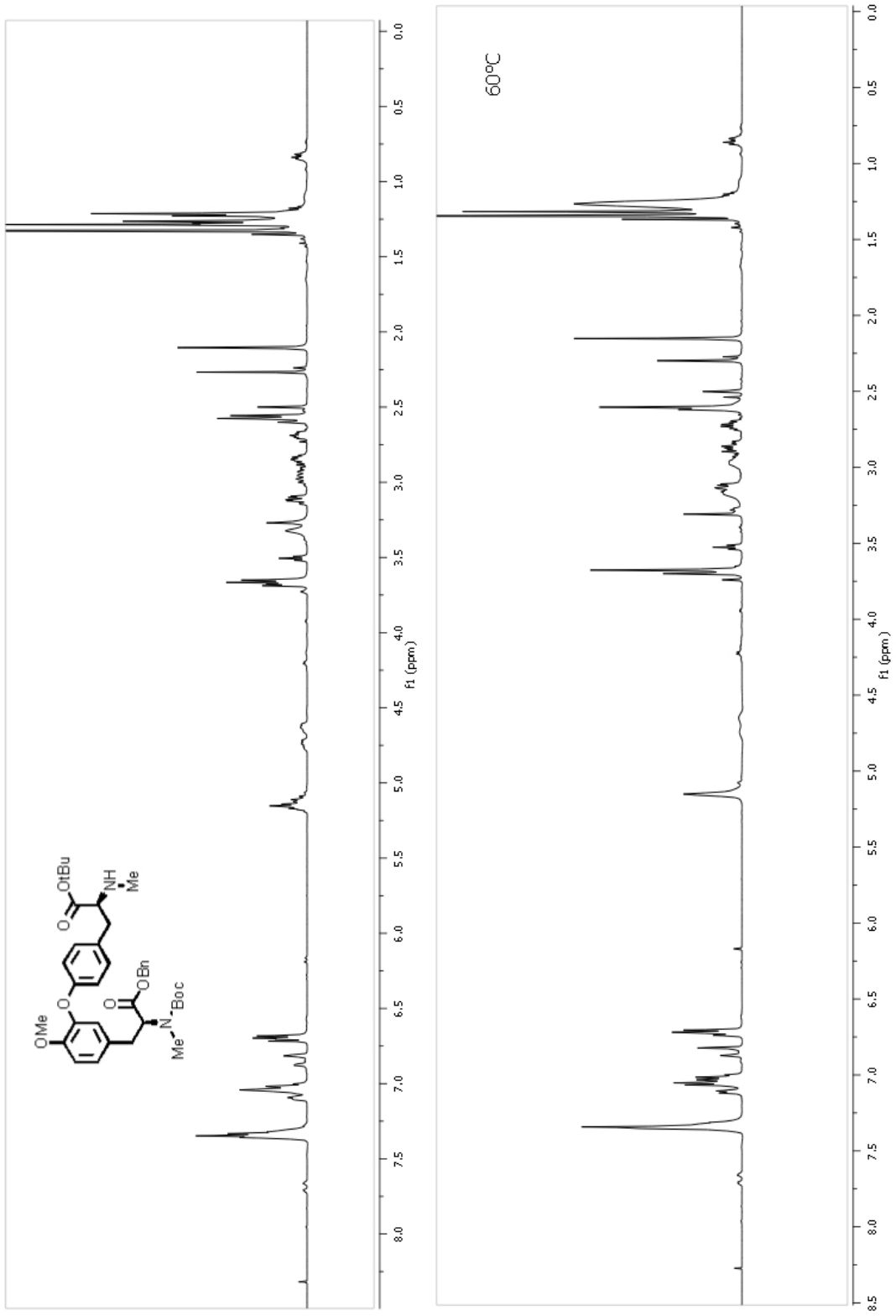

Spectrum 38 ^{13}C isodityrosine **121** in MeCN-d_3. Upper: 25 °C; Lower: 60 °C recorded.

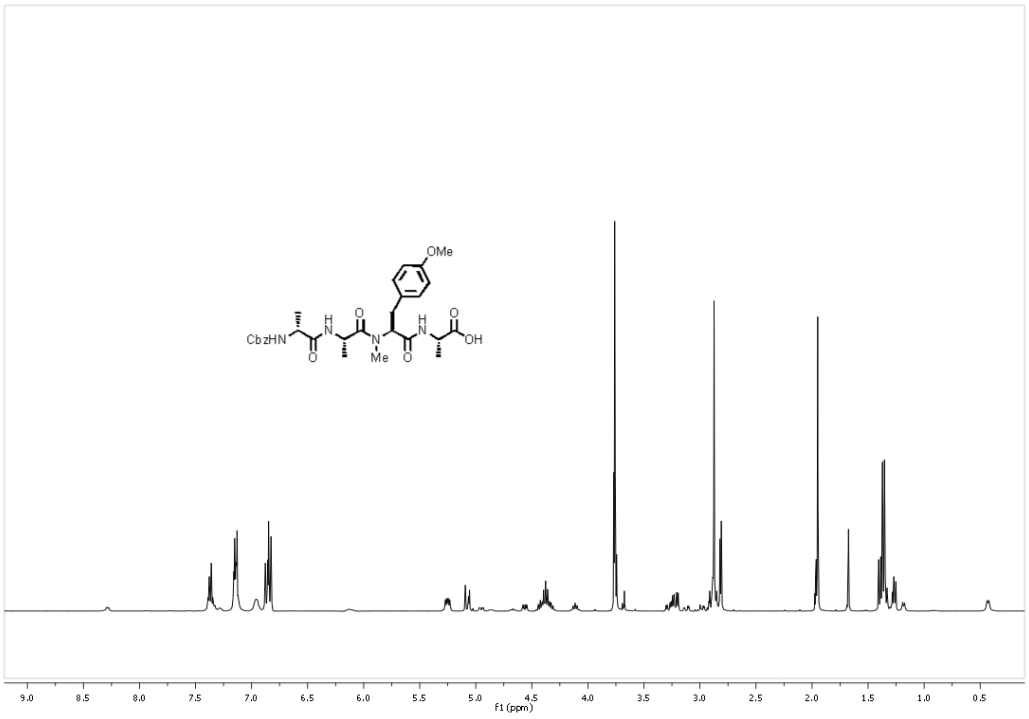

Spectrum 39 ^{1}H tetrapeptide **197** in MeCN-d_3.

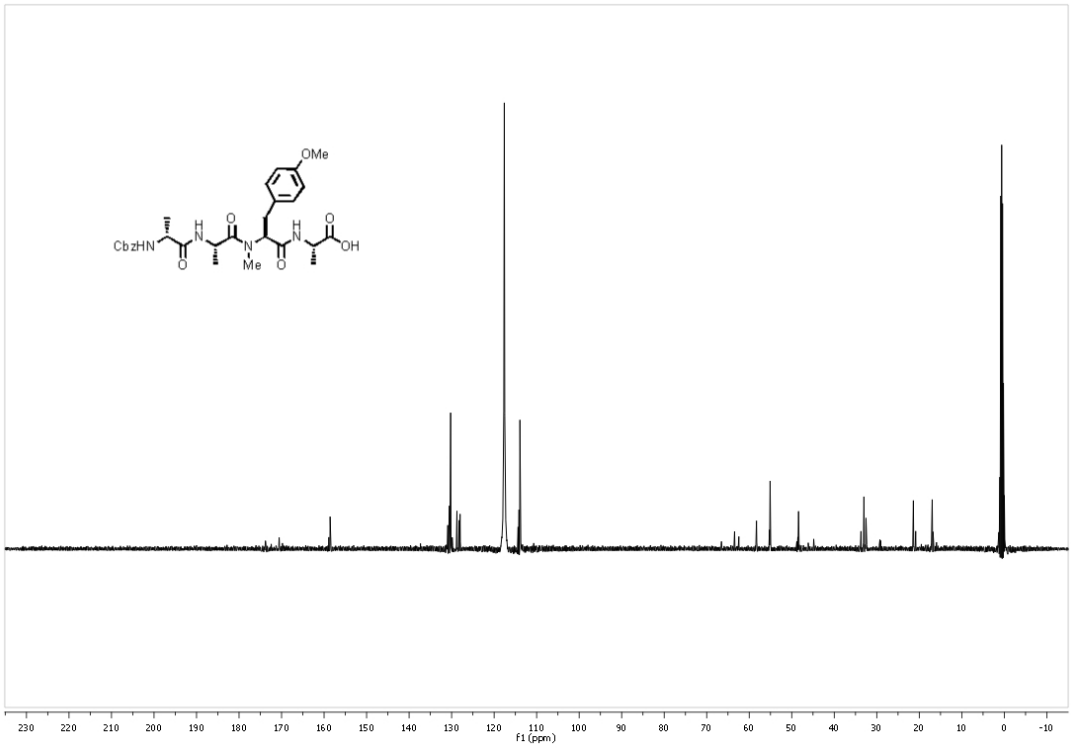

Spectrum 40 ^{13}C tetrapeptide **197** in MeCN-d_3.

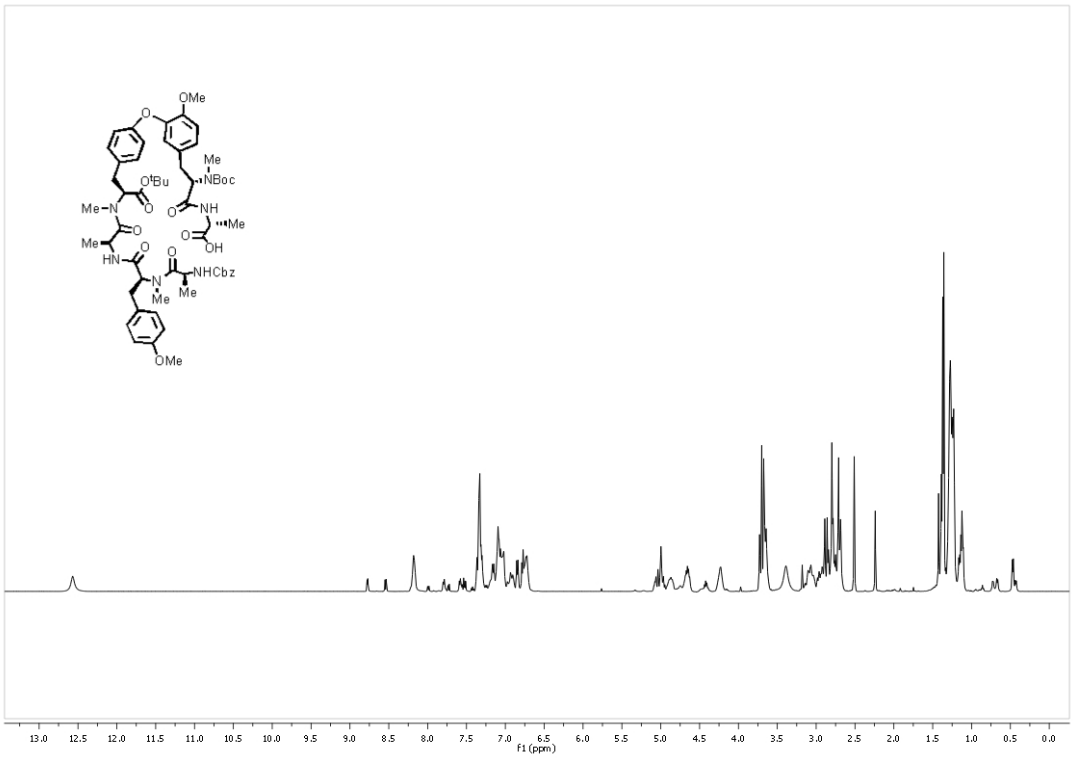

Spectrum 41 ^{1}H hexapeptide **211** in DMSO-d_6.

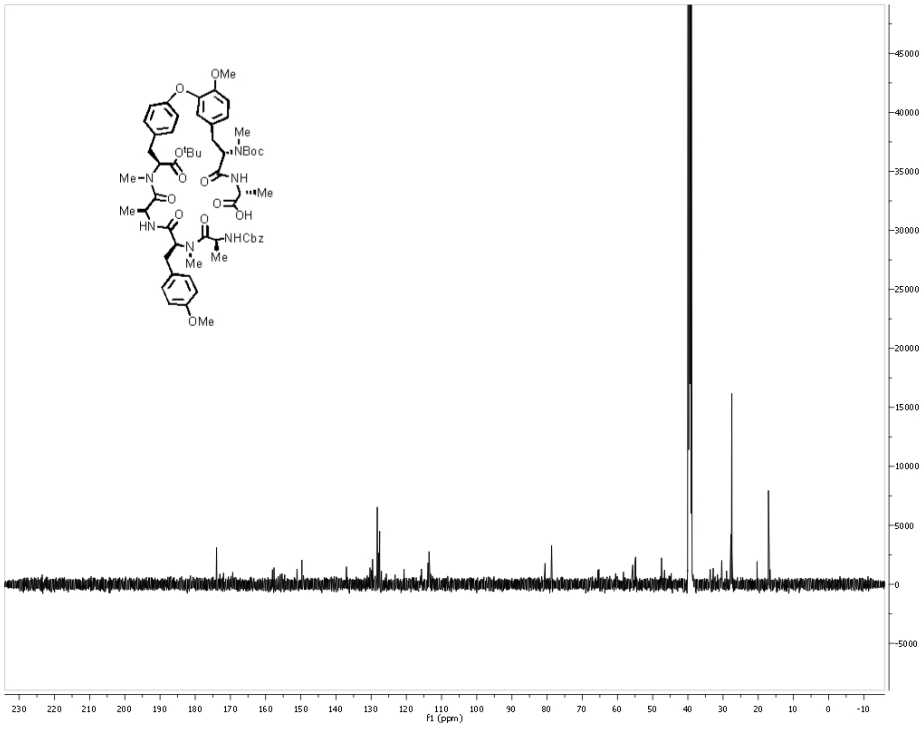

Spectrum 42 ^{13}C NMR of hexapeptide **211** in DMSO-d_6.

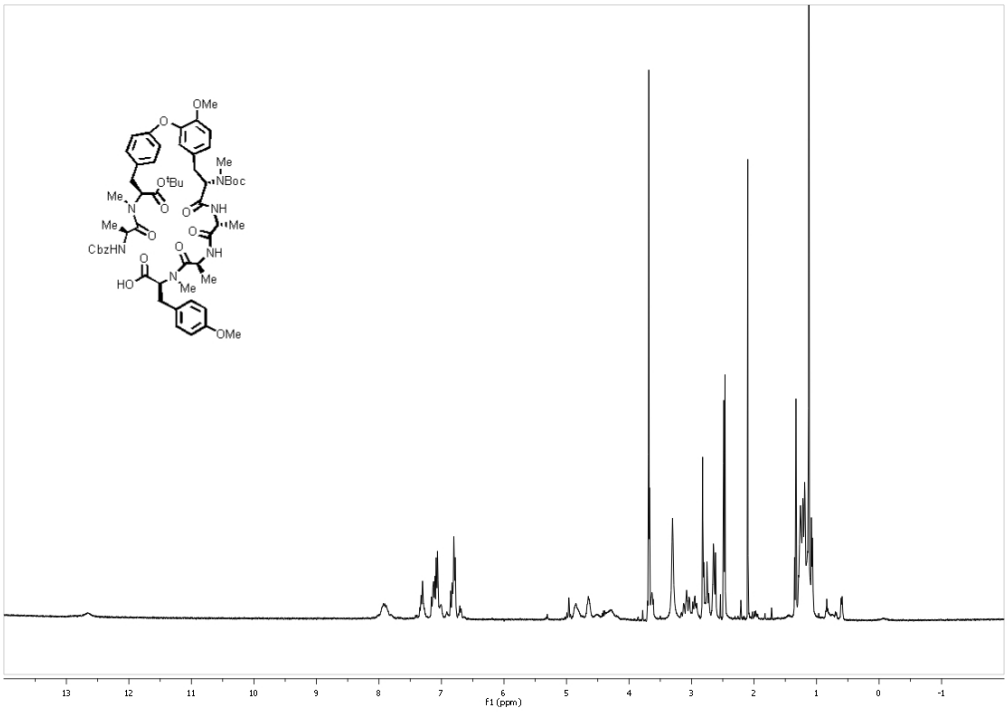

Spectrum 43 ^{1}H NMR of hexapeptide **213** in MeCN-d_3.

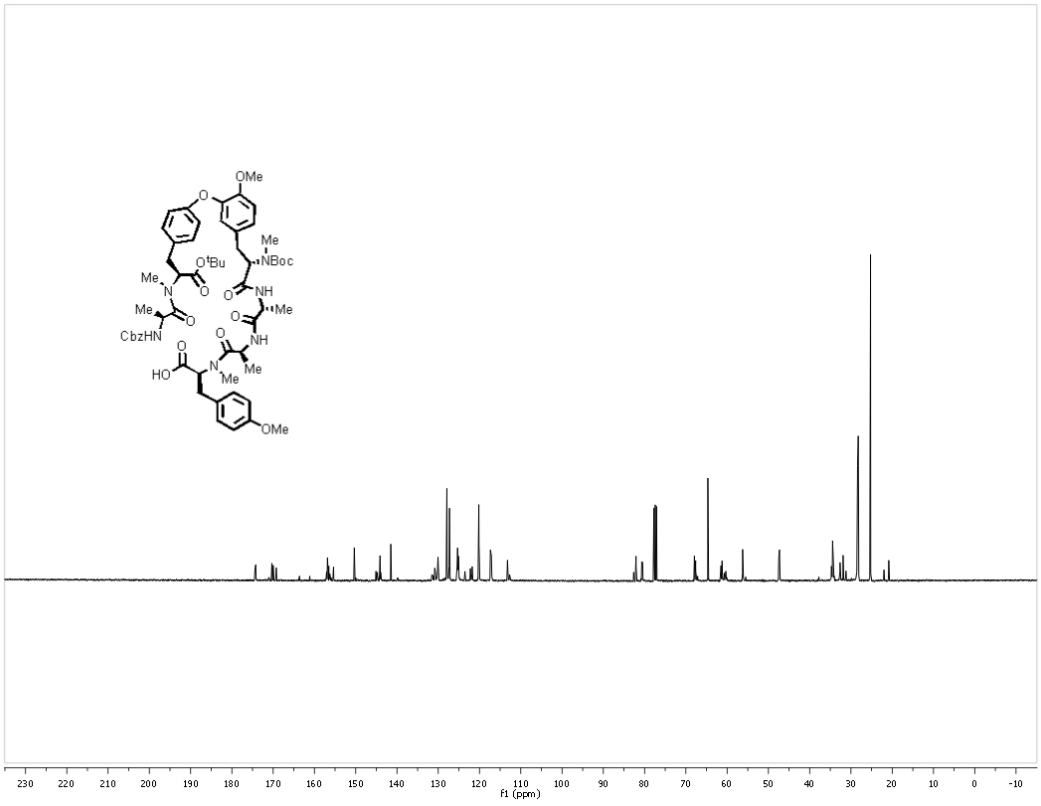

Spectrum 44 ^{13}C NMR of hexapeptide **213** in $CDCl_3$.

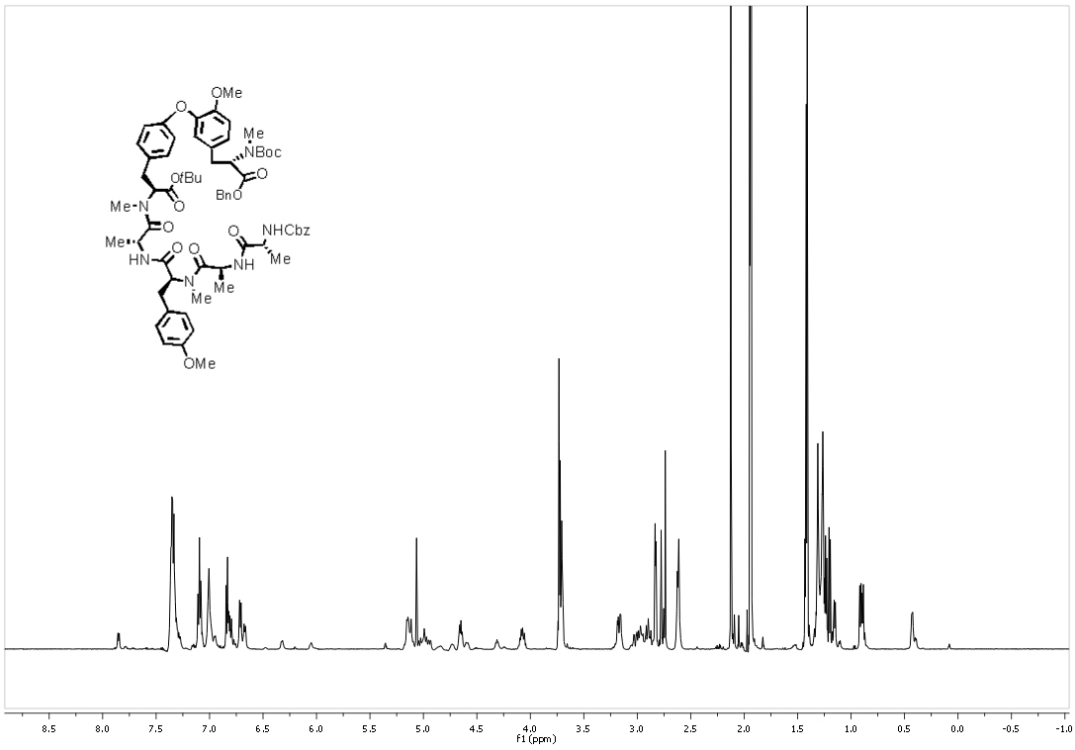

Spectrum 45 ^{1}H NMR of hexapeptide **206** in MeCN-d_3.

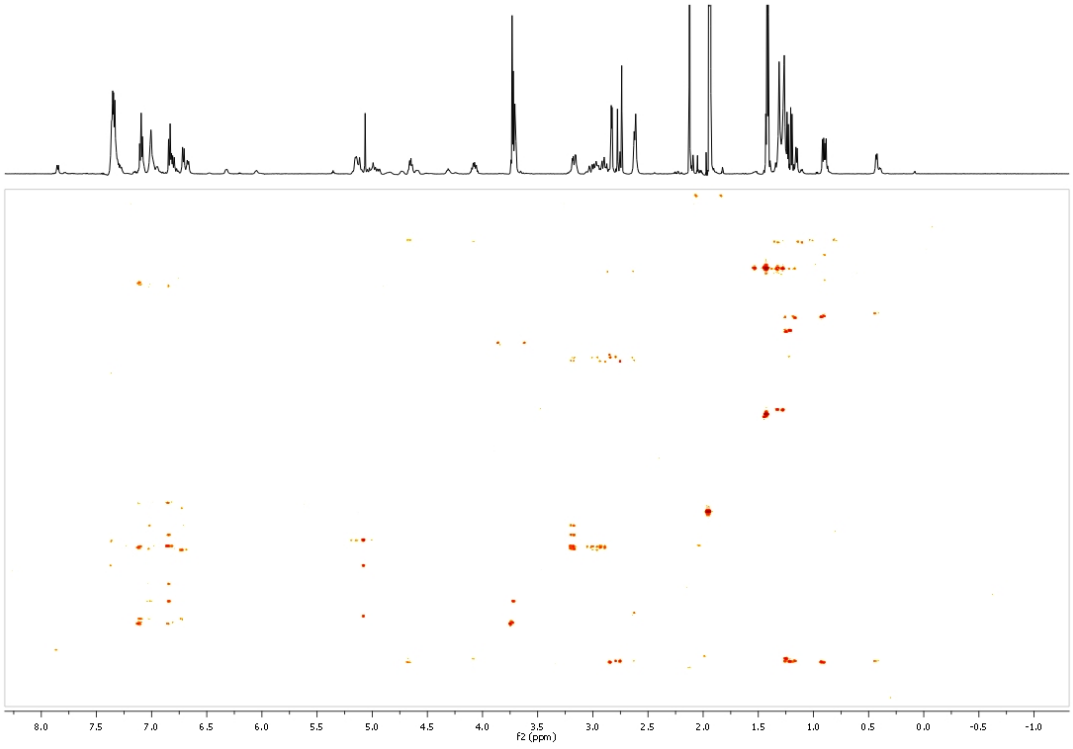

Spectrum 46 HMBC of hexapeptide **206** in MeCN-d_3.

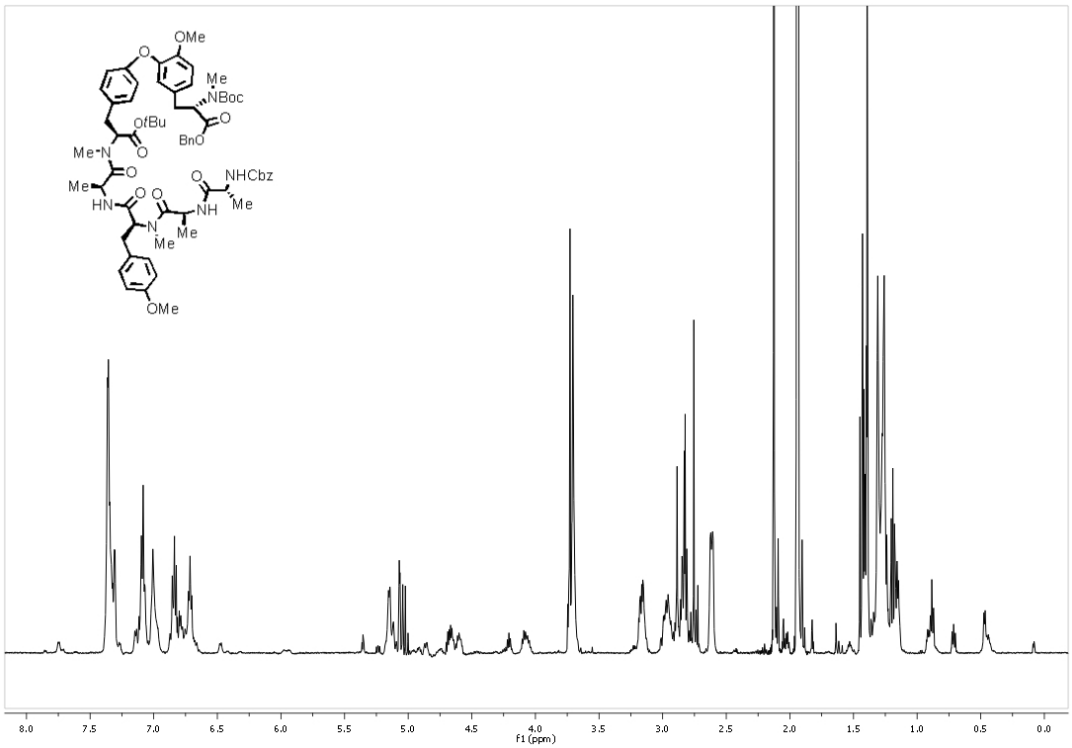

Spectrum 47 ^{1}H NMR of hexapeptide **205** in MeCN-d_3.

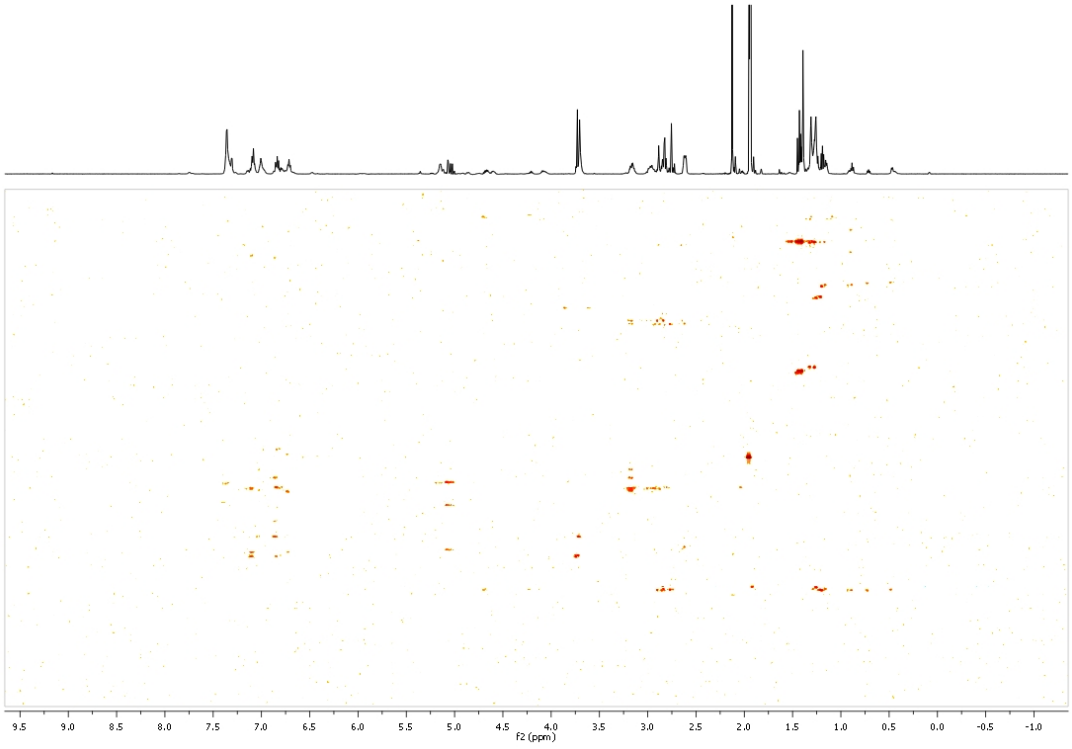

Spectrum 48 HMBC of hexapeptide **205** in MeCN-d_3.

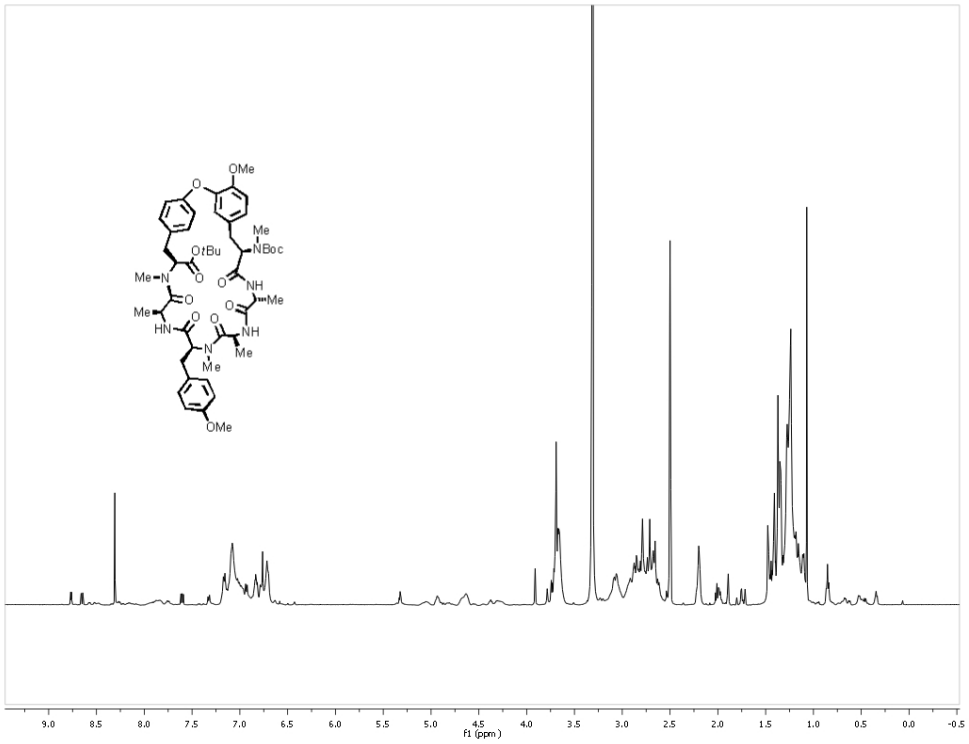

Spectrum 49 ^{1}H NMR of cyclohexapeptide **119** in MeCN-d_3.

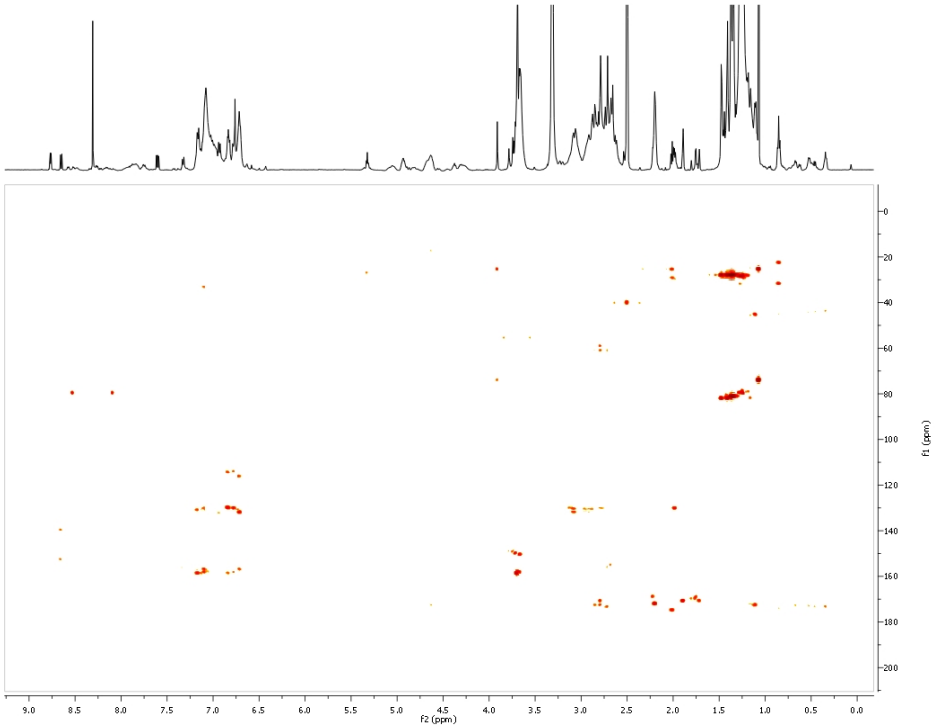

Spectrum 50 HMBC of cyclohexapeptide **119** in MeCN-d_3.

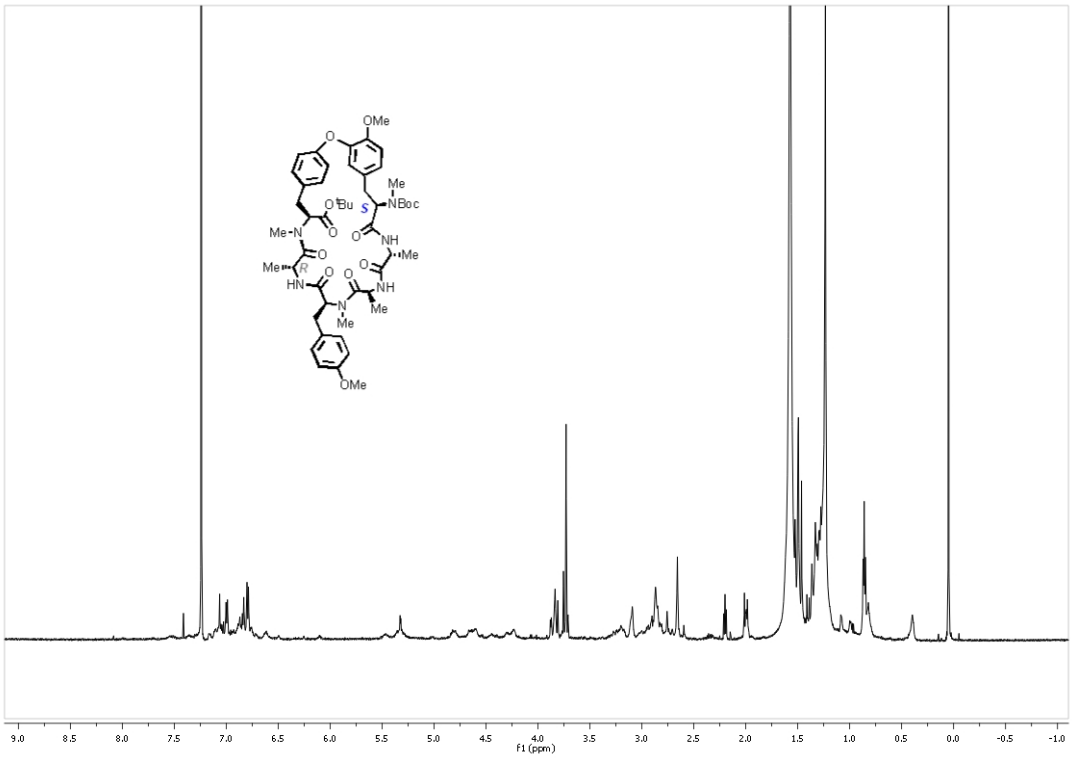

Spectrum 51 ^{1}H NMR of cyclohexapeptide **235** in DMSO-d_6.

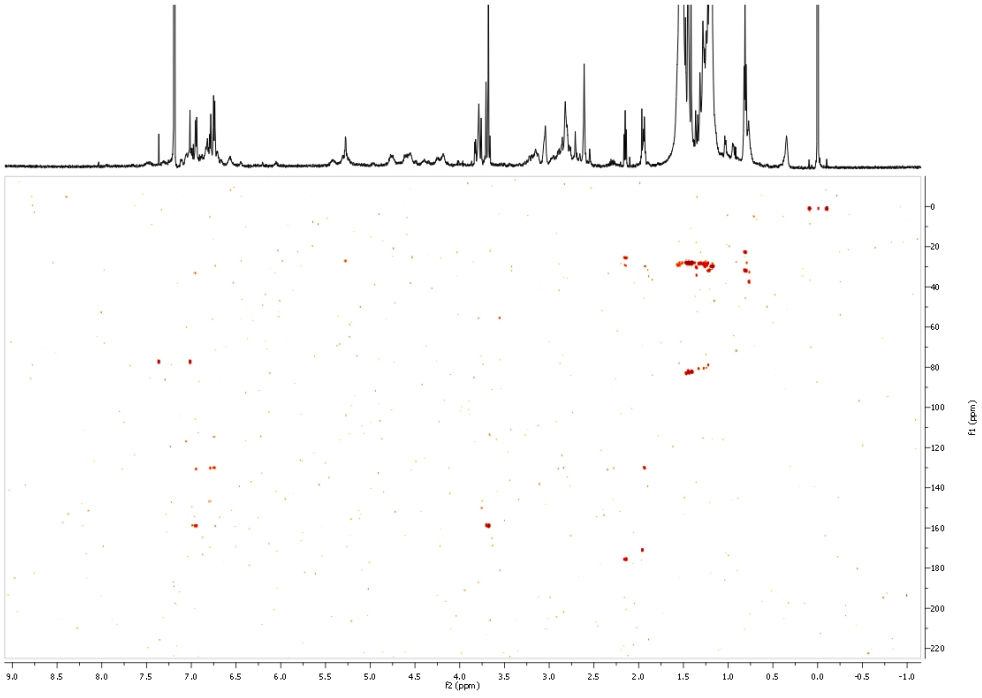

Spectrum 52 HMBC of cyclohexapeptide **235** in DMSO-d_6.

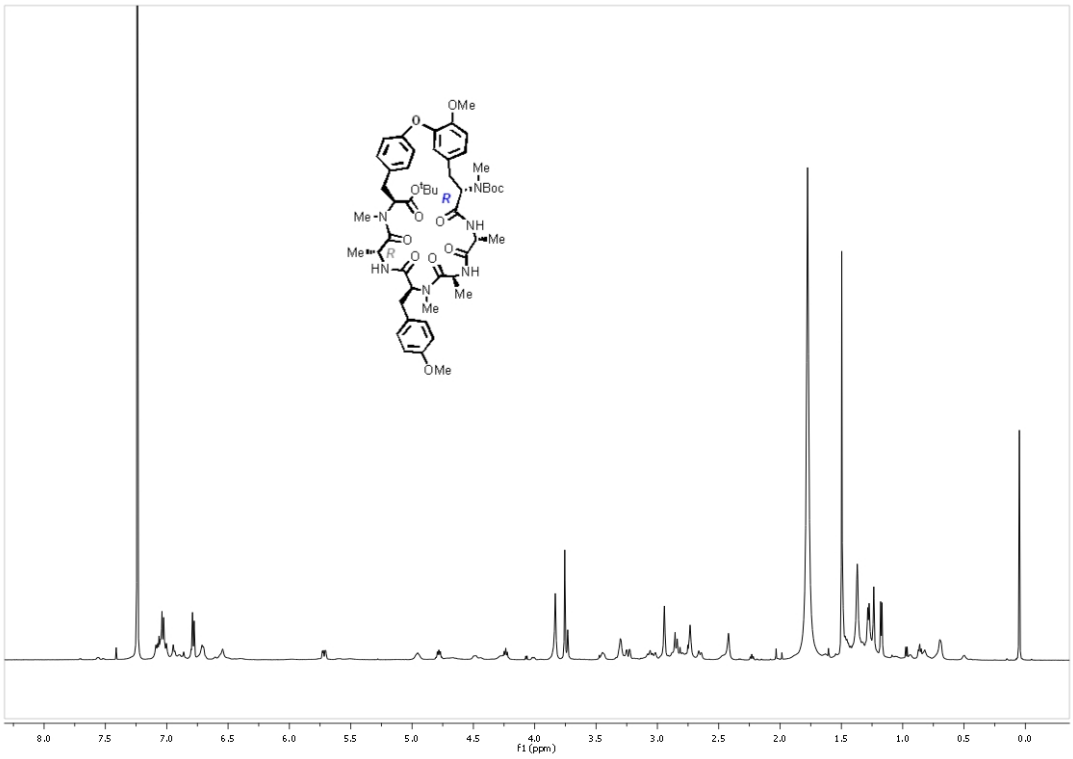

Spectrum 53 ^{1}H NMR of cyclohexapeptide **236** in DMSO-d_6.

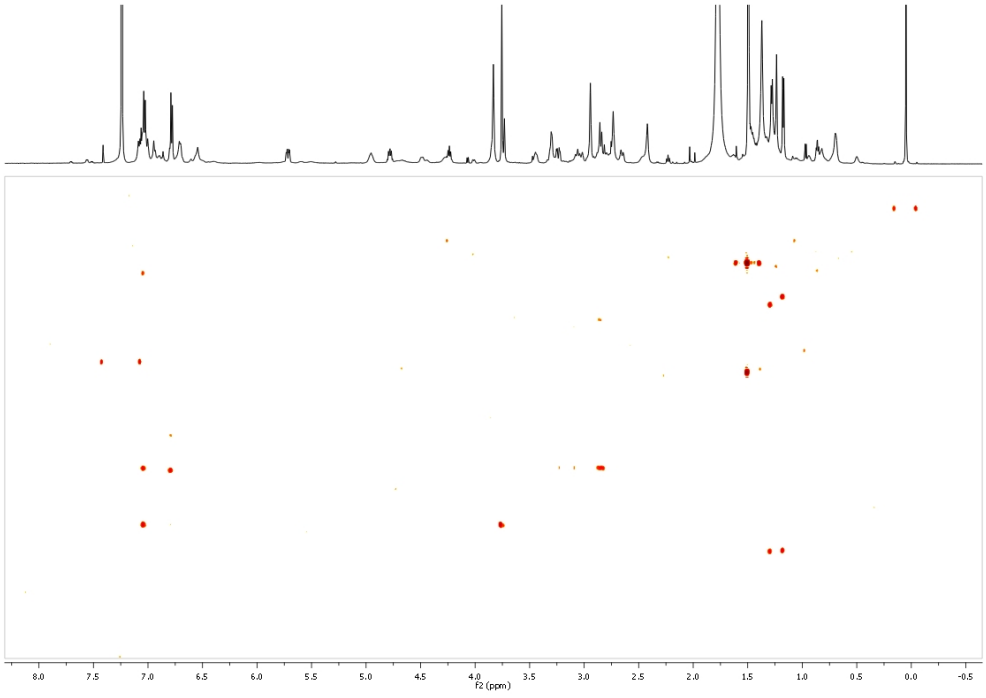

Spectrum 54 HMBC NMR of cyclohexapeptide **236** in DMSO-d_6.

12. Acknowledgements

I would like to take this opportunity to thank all the people that have accompanied me for four and half years during my doctoral research. I would not have been able to learn and enjoy the scientific research that much without their encouragement and support.

First of all, I would like to thank my project supervisor Dr. Hans-Dieter Arndt for offering me this interesting project and for his continuous guidance and support during my work.

I would like to heartily thank my first reviewer Prof. Dr. Herbert Waldmann providing me the opportunity to work at AKW. It was an honor to belong to his group and have his unlimited supports.

I am particularly grateful for the International Max Planck Research School Chemical Biology (IMPRS-CB) for the financial support. Therefore, I would like to thank our former director Prof. Dr. Dr. h.c. Rolf K. H. Kinne and current director Prof. Dr. Martin Engelhard (also as my second reviewer) and many thanks to exceptional coordinators of the school Dr. Jutta Roeter and Dr. Waltraud Hofmann-Goody for their patience and helpful guidance during my PhD research.

I am incredibly thankful to the people who made used the analytical facilities in Max-Planck-Institut and Technische Universität in Dortmund: Dr. Petra Jannig, Dipl. Ing. Evelyne Mertel and Dipl. Ing. Andreas Broeckmeyer (LCMS, HRMS and MS-MS) and Dr. Wolf Hiller, Herr. Bernhard Griewel (2D and temperature dependent NMR measurements).

I would like to thank to hard worker bachelor students Dania Kendziora and Stephan Klopiers. I wish to thank also our competent technicians Sasi Travaham, Elke Simon for their help.

It was a pleasure to collaborate with skillful biologists. I would like to particularly thank Sascha Baumann (Transcription/Translation initiation assay) and Bernhard Ellinger (cell proliferation and related studies) for their immense contribution.

I wish to transmit my special thanks to Dr. Stefan Wetzel for his work on molecular modelling calculations and the helpful discussions.

I would like to thank Dr. Gemma Triola, Dr. Jacqui Young, Anouk Stigter, Patrick Loos for their help for correcting my thesis. A special thanks to Dr. Gemma Triola for her extensive patience and helps.

I would like to thank to my laboratory colleagues and AK Arndt group members, Sascha Baumann, Kirtikumar Jadhav, Dr. Roman Lichtenecker, Patrick Loos, Dr. Jinyong Lu, Dr. Matthias Riedrich, Sebastian Schoof, for the pleasant atmosphere.
I am also grateful for my office colleagues, Nancy, Anouk, Stefan, Robin, Patrick, Nici for daily nice atmosphere and their support and understandings during my writing.
I would particularly like to thank Dr. Gemma Triola, Dr. Marta Rodriguez, Dr. Jacqui Young, Anouk Stigter, Dr. Jinyong Lu, Patrick Loos for the creative and helpful discussions.
A special thanks goes to my friends who comfort my life in abroad and gave their precious times for every moment that I have asked for. Very important thanks to Gemma, Yekbun, Özde, Eric, Marta, Ester, Ana, Esther, Belen, Jacqui, Anouk, Nancy, Maelle, Maarten, Daniel Gotlieb, Jinyong, Bart, Patrick, *Familie* Toborek and Thelen.
At last but not least, I would like to thank to my parents for giving me their continuous support and their love. I wish to thank to my brother for his presence and being a part of me. My foremost thanks to my joa who made my life complete.

13. Declaration/Eidesstattliche Erklärung

Hiermit versichere ich an Eides statt, dass ich die vorliegende Arbeit selbständig und nur mit den angegeben Hifsmitteln angefertigt habe.

I hereby declare that I performed the work presented independently and did not use any other but indicated aids.

Dortmund, Novembre 2009

Bahar Kilitoglu